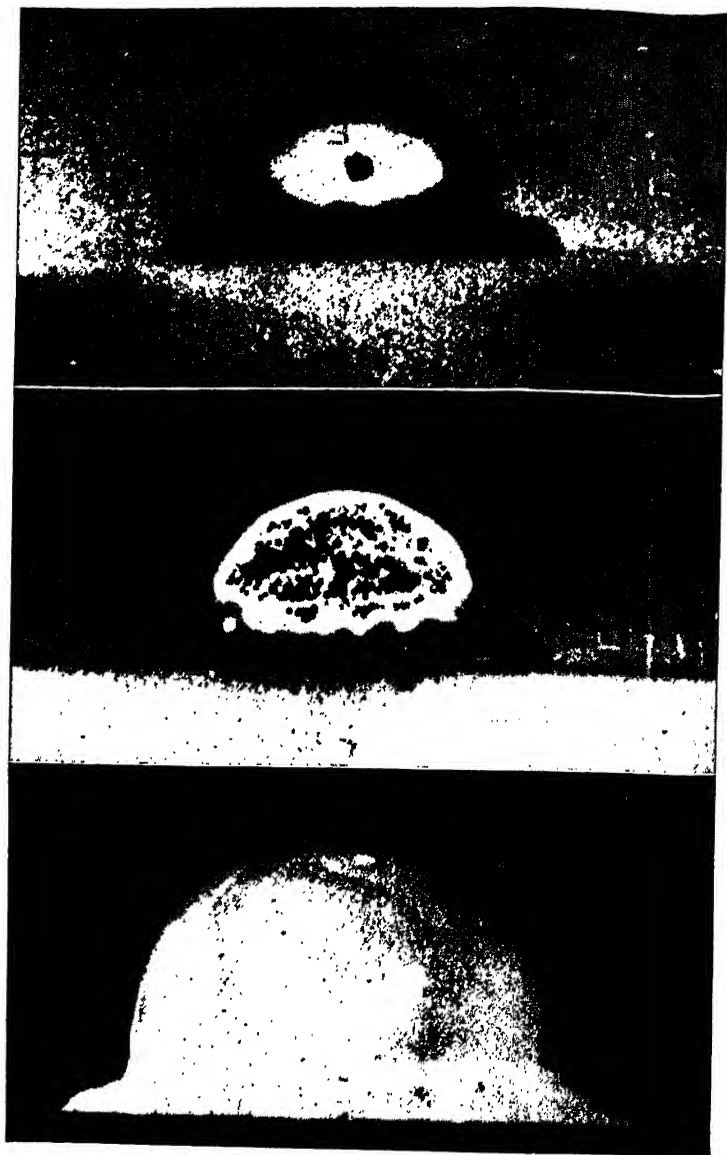


# Introduction to ATOMIC PHYSICS



*U. S. Army-Acme*

Photos of the initial test of the atomic bomb in New Mexico on July 16, 1945, taken at a range of six miles. *Top:* Start of the explosion — a small cloud which later rose to a height of 40,000 feet. *Center:* The cloud, multi-colored, grows bigger. (According to observers the black areas were brighter than the sun.) *Bottom:* The cloud in a later stage of development.

(From Henry DeWolf Smyth, *Atomic Energy for Military Purposes*, 1945, Princeton University Press.)

Introduction to

# ATOMIC PHYSICS

Revised and Enlarged

HENRY SEMAT, Ph.D.

Associate Professor of Physics, The City  
College, College of the City of New York

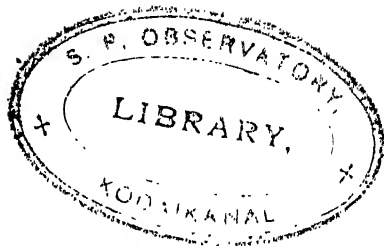
RINEHART & COMPANY, INC.  
PUBLISHERS NEW YORK

*First Printing, June, 1946*  
*Second Printing, November, 1946*  
*Third Printing, June, 1947*  
*Fourth Printing, December, 1947*  
*Fifth Printing, December, 1948*

COPYRIGHT, 1939, 1946, BY HENRY SEMAT  
PRINTED IN THE UNITED STATES OF AMERICA

*ALL RIGHTS RESERVED*

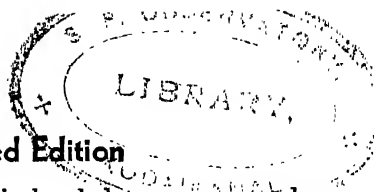




To

RAY K. SEMAT





## Preface to the Revised Edition

The friendly reception accorded this book has encouraged me to revise it. The first edition was published in 1939 just as the formal military phase of World War II was about to begin. Under normal conditions, one could expect tremendous advances in the fundamental aspects of atomic physics in a period of seven years, particularly after the brilliant new discoveries that had been made in the seven years preceding 1939. That period saw the discovery of three new fundamental particles — the neutron, the positron, and the meson. It also saw the discovery of several new phenomena such as induced radioactivity, the materialization of energy by the transformation of a photon into two charged particles, and its converse, the annihilation of matter by the combination of positrons and electrons to form photons. During this period work was begun on the production of transuranic elements which finally culminated in the discovery of nuclear fission.

This brilliant period ended with the beginning of the military phase of World War II when scientists became almost exclusively concerned with applying ideas and concepts already known to particular problems of military importance. Undoubtedly some work was done on fundamental problems, but most of it is still shrouded in the secrecy of military security. Part of this secrecy was rent in dramatic fashion by the explosions of the atomic bombs over Hiroshima and Nagasaki.

With the end of the military phase of the war, scientists left their wartime tasks and returned to their experimental laboratories. Many baffling problems, particularly in nuclear physics still await solution. Large quantities of a new element, plutonium, and many new radioactive isotopes of the more common elements have been produced as a result of the outstanding work of the atomic bomb project. These should be available in the near future for use in the solution of problems in nuclear physics and in the other sciences as well.

As is to be expected, the major changes in this revision have been made in the section on The Nucleus. Not only have the data been corrected and brought up to date, but many of the topics

have been given more extensive treatment — the production of transuranic elements, the fission of nuclei, and nuclear isomers. Several new topics have been added — the discovery of new elements, sources of nuclear energy, and the measurement of nuclear magnetic moments, for example.

The betatron, one of the outstanding developments of recent years, will undoubtedly play a very important role in the solution of many problems in nuclear physics. Chapter 3 describes the principle of its operation; Chapter 9, some of the work in which X rays from it were used to produce photofission of nuclei.

Several of the old diagrams have been redrawn and many new diagrams and photographs have been added to improve the effectiveness of this book.

I have been very fortunate in receiving many suggestions from physicists who have used the first edition of this book. I want to thank all these and also Professor E. F. Barker of the University of Michigan for reading the entire manuscript and making many helpful suggestions; Professor Paul Kirkpatrick of Stanford University, Professor Robert L. Weber of The Pennsylvania State College, Professor Hans Mueller of the Massachusetts Institute of Technology, and Dr. John R. Platt and Dr. Edson R. Peck of Northwestern University for many helpful criticisms and suggestions; my colleagues at The City College, Dr. Dixon Callihan and Dr. Lawrence A. Wills, for stimulating discussions and helpful criticisms; Professor J. M. B. Kellogg of Columbia University and Dr. Sidney Millman, of the Bell Telephone Laboratories, for permitting me to read their paper on the "Radio-frequency Spectra of Atoms and Molecules" prior to its publication; finally, my wife, Ray K. Semat, for the laborious task of typing the manuscript.

IL. S.

*The City College*  
*January, 1946.*

## Preface to the First Edition

This book represents the content of a one-semester course of three hours per week which I have been giving for the past decade to science students who have had one year of general college physics and a course in the calculus. Originally called an *Introduction to Modern Physics*, the material was used in mimeographed form for several years, beginning in 1931. Although the emphasis was on atomic physics, such topics as electromagnetic theory and the special theory of relativity were also included in the original mimeographed book. But with the tremendous growth within recent years of nuclear physics, it was found necessary to omit some topics in order to stay within the limits of a one-semester course. The choice of topics and their arrangement give a connected presentation of the experimental basis of our present ideas concerning the structure of the atom and the nature of its constituent particles.

The order chosen is one which I have found to be teachable and reasonable. After a short introductory chapter which reviews those fundamental concepts of electricity and magnetism essential to the study of atomic physics, the second chapter introduces the atom and presents the experimental evidence leading up to Rutherford's nuclear theory of the structure of the atom. In this chapter the properties of the electron are developed, methods of measuring atomic masses with the mass spectrograph are discussed, and the subject of radioactivity is introduced in such a manner that it leads directly to Rutherford's nuclear theory based on the experiments on the scattering of alpha particles. In Chapter III the structure of the atom is further investigated through its interaction with electromagnetic radiation, leading to the Zeeman effect, photoelectric effect, and a study of X rays and gamma radiation. In its interaction with matter, radiation is shown to possess both wave and particle aspects. The wave and particle concepts of both radiation and matter are then developed in greater detail in Chapter IV. The foregoing concepts are then applied to the extranuclear structure, first to the case of hydrogen in Chapter V, and then to the more complex atoms in Chapter VI. Since both optical and X-ray spectra have contributed immensely to our

knowledge of atomic structure, these topics are considered in some detail, both from the point of view of the simpler vector model of the atom and from that of wave mechanics, but the treatment, while extensive, has been kept as simple as possible. In Chapter VII the subject of nuclear physics is treated extensively and brought up to date (May, 1939). Experiments on natural radioactivity, artificial disintegration, and artificial or induced radioactivity are described and typical nuclear reactions are given, finally leading up to the modern theories of nuclear disintegration. The numerical data presented in this chapter have been carefully checked and represent, in my opinion, the most recent authoritative data.

References to other books for more extended study are given at the end of each chapter. Each teacher, of course, can amplify the list of references to suit his particular needs. These particular books were chosen because they are usually available in most libraries and because they are not too difficult for the type of student for whom this book is written. It is for these reasons that there are no references to individual papers representing original research in this text. At the end of each chapter there is a list of problems based upon the material in the text. Many of these problems contain numerical data, and their solutions should acquaint the student with the order of magnitude of the quantities dealt with in atomic physics.

I am indebted to several publishers for permission to reproduce some of the figures used in the text, and also to many physicists who so kindly sent original photographs to be reproduced in this book.

To my colleagues, Dr. Walter H. Zinn, Professor Mark W. Zemansky, and Mr. H. H. Goldsmith, who read sections of the text and suggested many important changes, I owe a debt of gratitude. Dr. Dixon Callihan, who has been associated with me in giving the course in Atomic Physics and who read the complete manuscript several times, made many important contributions as a result of his experience with it as a text. Finally, for the laborious tasks of typing the manuscript and assisting in the correction of the proof, not the least of my thanks go to Ray K. Semat.

H. S.

*The City College*  
*May, 1939.*

## Table of Contents

Preface to the Revised Edition . . . . .	vii
Preface to the First Edition . . . . .	ix

### PART I: FOUNDATIONS OF ATOMIC PHYSICS

1. Elements of Electricity and Magnetism . . . . .	3
2. Elementary Charged Particles . . . . .	23
3. Electromagnetic Radiation . . . . .	86
4. Waves and Particles . . . . .	149

### PART II: THE EXTRANUCLEAR STRUCTURE OF THE ATOM

5. The Hydrogen Atom . . . . .	183
6. Atomic Spectra and Electron Distribution . . . . .	212

### PART III: THE NUCLEUS

7. Natural Radioactivity . . . . .	277
8. Disintegration of Nuclei . . . . .	298
9. Nuclear Energy . . . . .	357

### APPENDIXES

I. Values of Some Physical Constants . . . . .	379
II. Table of Atomic Weights . . . . .	380
III. Periodic Table of the Elements . . . . .	382
IV. Table of Isotopic Masses . . . . .	384
V. Table of Stable Isotopes . . . . .	385
VI. Displacement Equation for Brownian Motion . . . . .	389
VII. Path of an Alpha Particle in a Coulomb Field of Force . . . . .	392
VIII. Derivation of the Equations for the Compton Effect . . . . .	397
IX. Evaluation of $\int p_r dr = n_r h$ . . . . .	401
Index . . . . .	405





# Part I

## FOUNDATIONS OF ATOMIC PHYSICS



# 1

# Elements of Electricity and Magnetism

## 1. Introduction

The decade from 1895 to 1905 may be termed the beginning of modern physics. During this period, J. J. Thomson succeeded in demonstrating the existence of the electron, a fundamental unit of negative electricity having very small mass. Becquerel discovered the phenomenon of natural radioactivity and Röntgen discovered X rays. To these discoveries must be added the bold hypothesis put forth by Planck, that radiant energy, in its interaction with matter, behaves as though it consists of corpuscles or quanta of energy. This led to the development of the quantum theory of radiation and ultimately to quantum mechanics. It was also during this period that Einstein re-examined the fundamental concepts of physics and was led to the development of the special theory of relativity.

It is the aim of this book to present the important experimental data upon which are based our present ideas of the structure of the atom. An atom is to be regarded not as a static structure composed of particles in fixed positions, but rather as a dynamic structure changing in response to outside agencies, affecting them and, in turn, being affected by them. It is by examining the phenomena that occur during these changes that we get our information concerning the structure of the atom as well as an insight into the nature of those quantities which produce or are the result of these changes.

Accumulation of experimental data, particularly from the study of electrochemistry and the discharge of electricity through gases, indicates clearly that the atom is essentially electrical in nature. It will therefore be of value to discuss briefly those fundamental concepts of electricity and magnetism which have been found essential in studying the structure of the atom.

## 2. Coulomb's Law of Force between Electric Charges

If a glass rod is rubbed with a piece of silk, both the glass and the silk become electrified. When two glass rods which have been rubbed with silk are placed near each other, a force of repulsion will be found to exist between them. In a similar manner, if two rubber rods which have been rubbed with wool or cat's fur are placed near each other, there will be a force of repulsion between them. But if one of these rubber rods is brought near one of the electrified glass rods, a force of attraction is found to exist between them. All other electrified bodies can be compared with such glass and rubber rods. Those electrified bodies which repel the glass rod are said to be positively charged or charged with positive electricity, while those bodies which repel the rubber rod are said to be negatively charged or charged with negative electricity. This arbitrary sign convention is adhered to throughout the realm of physics including the atomic domain. The ultimate determination of the sign of any electric charge must rest on a comparison with the charge on a glass rod which has been rubbed with silk or that on a rubber rod which has been rubbed with wool.

Coulomb (1789) made a study of the quantitative law of force between charged bodies. He found that the force between two charged bodies, whose dimensions are small in comparison with the distance between them, is given by

$$F = \frac{q_1 q_2}{kr^2}, \quad (1)$$

where  $q_1$  is the magnitude of the electric charge on one body,  $q_2$  the magnitude of the charge on the second body, and  $r$  is the distance between them. The force  $F$  between the two charges also depends upon the nature of the medium between them; this is expressed by the factor  $k$ , called the *dielectric constant*, or the *specific inductive capacity* of the medium. The numerical value of  $k$  depends not only upon the nature of the medium but also upon the system of units used in expressing the other quantities in equation (1). In the electrostatic system of units,  $k$  is set equal to unity when the charges are placed in a vacuum,  $F$  is measured in dynes, and  $r$  in centimeters. The charge  $q$  is then said to be expressed in electrostatic units (e.s.u.). The definition of a unit charge now follows directly from equation (1): a unit charge (1 e.s.u.) is a charge

which, when placed in a vacuum one centimeter away from a like equal charge, will repel it with a force of one dyne. The electrostatic unit of charge is very small; hence, in the practical system of electrical units, a much larger charge is taken as the unit and is called a coulomb. A coulomb is equivalent to  $3 \times 10^9$  e.s.u. of charge.

In the system of units defined above, the dielectric constant  $k$  is a pure numerical constant. For nonconductors or insulators,  $k$  is generally greater than unity.

### 3. Intensity of the Electric Field

The fact that a charged body will experience a force when placed at any point in the neighborhood of another body containing a charge  $Q$  suggests the idea that an *electric field* exists in the space around the charge  $Q$ . This electric field may be explored by placing a very small positive charge  $q$  at different points and measuring the force  $F$  experienced by it at each point. The *intensity of the electric field*  $E$  at any point  $P$  is defined as the ratio of this force  $F$  to the magnitude of the small positive charge  $q$  placed at this point, that is,

$$E = \frac{F}{q}. \quad (2)$$

The test charge  $q$  must be sufficiently small so that the electric field is not materially altered by the introduction of this test charge. If  $F$  is measured in dynes and  $q$  in e.s.u. of charge, then  $E$  is expressed in dynes per e.s.u. of charge.

The intensity of the electric field  $E$  at any point is a vector quantity whose direction is that of the force experienced by a *positive* charge placed at that point. A negative charge placed in an electric field will experience a force whose direction is opposite to that of the electric field.

The intensity of the electric field can be evaluated mathematically in many cases. For example, the intensity of the electric field in the space around a point charge  $Q$  can be found by imagining a small positive charge  $q$  placed at any point  $P$  a distance  $r$  from the point charge  $Q$ . The force  $F$  experienced by this positive charge  $q$  is, from Coulomb's law,

$$F = \frac{Qq}{kr^2}. \quad (3)$$

Substituting this value of  $F$  in equation (2), we get

$$E = \frac{Q}{kr^2} \quad (4)$$

for the intensity of the electric field  $E$  at a distance  $r$  from the charge  $Q$ .

There is a convenient method for mapping the electric field in any region of space to show at a glance its magnitude and direction. If the intensity of the electric field is known at any point,

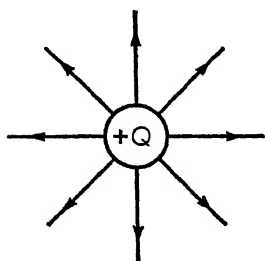


FIG. 1. — Radial electric field around a small charge.

we can imagine a unit area drawn perpendicular to the direction of the electric field at this point and a sufficient number of lines drawn perpendicularly through this unit area so that the number of lines per unit area will represent the magnitude of the intensity of the electric field at this point, and the direction of these lines will represent the direction of this electric field. For example, the electric field around a point charge  $Q$  is radial, as shown in Figure 1. It can be shown

that if one line of force per square centimeter is to represent an intensity of one dyne per e.s.u. of charge, then  $4\pi Q$  lines will have to be drawn radiating from the point charge  $Q$ . If the electric field is uniform throughout a given region of space, that is, if the intensity of the electric field has the same value throughout this region, then it would be represented by a series of parallel, equally spaced lines as shown in Figure 2.

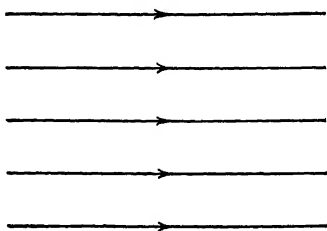


FIG. 2. — A uniform electric field.

#### 4. Potential

The potential at any point in the neighborhood of a positive charge  $q$  is defined as the work done in bringing a unit positive charge from infinity to this point against the forces of the electric field. The work done in bringing the unit charge into the field of the charge  $q$  will result in an increase in the energy of the system. Since a unit positive charge anywhere in the field is acted upon by a force numerically equal to the electric intensity,  $E$ , the work

done in moving this charge through a distance  $dr$  opposite to the direction of the field is

$$dV = - E dr. \quad (5)$$

If the space around the charge  $q$  is a vacuum, then

$$E = \frac{q}{r^2};$$

hence, the work done in bringing this unit charge from infinity to a point  $A$  distant  $a$  from the charge  $q$  is

$$V_A = - \int_{\infty}^a \frac{q}{r^2} dr = \frac{q}{a}, \quad (6)$$

where  $V_A$  is the potential at point  $A$ . The potential at a point infinitely far away from  $A$  is thus chosen as the zero from which potentials at other points are measured.

If the unit charge is brought to any other point  $B$  distant  $b$  from the charge  $q$ , then the potential at  $B$  is

$$V_B = \frac{q}{b}.$$

The difference of potential between the points  $A$  and  $B$  is

$$V = V_B - V_A = \frac{q}{b} - \frac{q}{a}, \quad (7)$$

where  $V$  represents the work done in bringing the unit charge from  $A$  to  $B$ , Figure 3. It will be noted that the difference of potential between two points does not depend upon the path traversed in taking the unit charge from one point to the other nor upon the potential arbitrarily chosen as zero. If the space surrounding the two points is not a vacuum, but has a dielectric constant  $k$  which does not change along the path of integration, then the right-hand member of equation (7) must be divided by  $k$ .

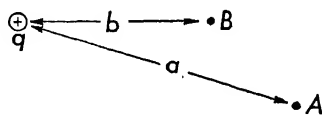


FIG. 3.

In most work in electricity, the potential of the earth is taken as the zero level of potential; the potential of any other point is then referred to that of the earth, and may be either higher or lower than ground potential.

The work done in adding a small charge  $dq$  to a body at some potential  $V$  is, by definition,

$$dW = Vdq,$$

and the total work done in adding a quantity of charge  $q$  to the body is

$$W = \int_0^q Vdq. \quad (8)$$

In order to evaluate equation (8), it is necessary to know the relationship between the potential of the body and the charge on it. Such a relationship is given by the equation

$$C = \frac{q}{V} \quad (9)$$

where  $C$  is the *capacitance* of the body; the capacitance of a body is a constant determined by its geometrical configuration and the nature of the dielectric medium surrounding it. The work done in charging a body may now be evaluated with the aid of equation (9), yielding

$$W = \frac{1}{2} \frac{q^2}{C} = \frac{1}{2} qV = \frac{1}{2} CV^2. \quad (10)$$

If the electric field in any region is uniform, the electric intensity  $E$  is constant throughout this region; the difference of potential  $V$ , that is, the work done in carrying a unit positive charge through a distance  $s$  parallel to this field is

$$V = \int_0^s E dr = Es. \quad (11)$$

A very convenient way of obtaining a comparatively uniform electric field is to use a capacitor consisting of two large parallel plates a small distance  $s$  apart. If the plates are kept at a difference of potential  $V$  by means of a battery, the electric intensity of the field between the plates will be

$$E = \frac{V}{s}. \quad (12)$$

The electric field will be uniform except at the edges of the plates.

In the electrostatic system of units, no special names are as-



signed to the various electrical quantities. Since the definitions of these quantities are based on the c.g.s. system of units, the difference of potential between two points represents the number of ergs of work required to transfer one electrostatic unit of charge from one point to the other. In the practical system of units, the difference of potential is expressed in volts, and represents the number of joules of work required to transfer a coulomb of electricity from a point of lower potential to one at a higher potential. Since a joule is  $10^7$  ergs and a coulomb is equivalent to  $3 \times 10^9$  e.s. units of charge, the unit for difference of potential in the electrostatic system is 300 times as big as the volt.

## 5. Coulomb's Law of Force between Magnetic Poles

Permanent magnets have been known and used for centuries. If a thin steel rod which has been magnetized is suspended so that it can swing freely about a vertical axis, the steel rod will come to rest in a very definite position. If there are no other magnetic materials in the immediate neighborhood, the rod will set itself in an approximately north-south position. The end which points north is called the north-seeking pole, or, more briefly, the north pole of the magnet; the other end is called the south pole of the magnet. If the north pole of another magnet is brought near the north pole of the first magnet, a force of repulsion will be found to exist between them; similarly for the south poles of the two magnets. But if opposite poles are brought near one another, there will be a force of attraction between them.

Coulomb investigated the law of force between magnetic poles and found that the force is proportional to the strengths of the magnetic poles, and inversely proportional to the square of the distance between them, or in the form of an equation, Coulomb's law states that

$$F = \frac{p_1 p_2}{\mu r^2}, \quad (13)$$

where  $F$  is the force between the two poles,  $r$  is the distance between them, and  $p_1$  and  $p_2$  represent the strengths of the poles.  $\mu$  is a constant of proportionality depending upon the units used and the nature of the medium between the poles.  $\mu$  is called the *permeability* of the medium. If the magnets are placed in a vac-

uum, and  $F$  is measured in dynes and  $r$  in centimeters, then  $\mu$  can be set equal to unity. The definition of a magnetic pole of unit strength now follows directly from equation (13). A unit magnetic pole, or a pole of unit strength, is one which when placed in a vacuum one centimeter away from a like equal pole, will repel it with a force of one dyne. The north and south poles of any one magnet are of equal strength.

## 6. Intensity of the Magnetic Field

The fact that a magnet will exert forces on other magnets suggests the idea that a *magnetic field* exists in the space around the magnet. This magnetic field may be explored by placing the north pole of a long thin magnet at any point in the field and measuring the force experienced by it. The *intensity of the magnetic field*  $H$  at any point  $P$  is defined as the ratio of the force  $F$  to the magnitude of the pole strength  $p$  of this exploring magnet which is placed at this point, that is,

$$H = \frac{F}{p}. \quad (14)$$

The strength of the exploring pole must be sufficiently small so that the magnetic field is not materially altered by the introduction of this pole. If  $F$  is measured in dynes and  $p$  in unit poles, then  $H$  is expressed in *oersteds*.

The intensity of the magnetic field  $H$  is a vector quantity whose direction at any point in space is that of the force experienced by the north pole of a magnet placed at that point. The south pole of a magnet, when placed in a magnetic field, will experience a force whose direction is opposite to that of the magnetic field at that point.

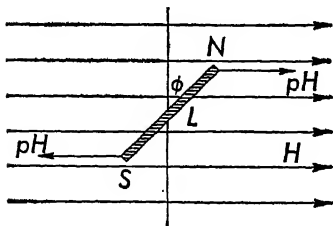


FIG. 4. — Couple acting on a bar magnet placed in a uniform magnetic field.

The magnetic field may be mapped in a manner analogous to that of the electric field. The number of *magnetic lines of force* drawn perpen-

dicularly through a unit area at any point in space represents the intensity of the magnetic field at this point and the direction of these lines represents the direction of this magnetic

field. If the magnetic field is uniform throughout a given region of space then it would be represented by a series of parallel, equally spaced lines as shown in Figure 4. Such a field can be closely approximated experimentally, and has been used extensively in atomic investigations.

## 7. Magnetic Moment of a Magnet

A bar magnet whose diameter is small in comparison with its length can be specified by two quantities, its length  $L$  and the strength of either pole  $p$ . The product of the pole strength of a magnet and the length of a magnet is known as the magnetic moment,  $M$ , of the magnet; thus

$$M = pL. \quad (15)$$

If such a small bar magnet is placed in a uniform magnetic field of strength  $H$ , as shown in Figure 4, each pole will experience a force  $pH$ . The two forces on the poles of the magnet constitute a couple. The moment,  $T$ , of this couple is

$$T = pH \cdot L \cos \phi = MH \cos \phi, \quad (16)$$

where  $\phi$  is the angle between the magnet and a line perpendicular to the direction of the magnetic field  $H$ . The amount of work done,  $dW$ , in rotating this magnet through an angle  $d\phi$  is

$$dW = MH \cos \phi d\phi.$$

If the magnet rotates through  $90^\circ$  from a position perpendicular to the field to one parallel to the field, the work done by the field will be

$$W = MH \int_0^{\frac{\pi}{2}} \cos \phi d\phi = MH. \quad (17)$$

Any magnetic substance may be considered as made up of a very large number of very small elementary magnets. When the substance is unmagnetized, these elementary magnets are oriented at random, but when an external magnetic field is applied to this substance, each elementary magnet experiences a couple tending to orient it parallel to the direction of the magnetic field. The degree of orientation of these elementary magnets determines the strength of the poles of a magnetized substance. It is thus clear

that work must be done to orient the elementary magnets and hence to magnetize a substance.

## 8. Energy in Electric and Magnetic Fields

It has been shown that work must be done to charge bodies electrically, and also to magnetize substances. A body which has been charged may be considered to possess more energy in virtue of the work done in charging it. One point of view is to consider this energy as residing in the electric field around this charged body. Similarly, the work done in magnetizing a substance may be considered as having been transformed into the energy which resides in the magnetic field surrounding the magnetized substance. Adopting this point of view, we may easily calculate the energy per unit volume in the electric field.

Consider, for example, a parallel plate capacitor consisting of two large metal plates separated by an insulating material whose dielectric constant is  $k$ . If  $q$  is the charge on either plate,  $V$  the difference of potential between the plates, and  $C$  the capacitance of the capacitor, the work done in charging this capacitor is

$$W = \frac{1}{2}qV = \frac{1}{2}CV^2. \quad (10)$$

The capacitance of a parallel plate capacitor may also be expressed as

$$C = \frac{kA}{4\pi s}, \quad (18)$$

where  $A$  is the area of either plate and  $s$  is the thickness of the insulating material between the plates. Since the electric field between the plates is uniform except for end effects, which may be neglected, the electric intensity anywhere in the space between the plates is simply

$$E = \frac{V}{s}. \quad (12)$$

With the aid of the above equations, the work  $W$  can be expressed as

$$W = \frac{kE^2sA}{8\pi}. \quad (19)$$

Assuming that the energy resides in the electric field between the

plates of the capacitor in the volume  $sA$ , the energy per unit volume in the electric field between the plates is

$$\frac{kE^2}{8\pi}. \quad (20)$$

No generality is lost in deriving the above expression for the special case of a uniform electric field, for if the field is not uniform, we can consider a very small region of the field which is practically uniform and deduce the same result.

In a similar manner, the energy per unit volume in a magnetic field can be shown to be

$$\frac{\mu H^2}{8\pi}, \quad (21)$$

where  $\mu$  is the permeability of the medium and  $H$  is the intensity of the magnetic field.

## 9. The Electric Current

The motion of a group of electric charges constitutes an electric current. The magnitude of the electric current,  $i$ , is the time rate of flow of charges through a given surface  $S$ . Thus

$$i = \frac{dq}{dt}. \quad (22)$$

If  $q$  is expressed in c.s.u. and  $t$  in seconds, then  $i$  is the e.s.u. of current. The practical unit of current is the ampere which is  $3 \times 10^9$  times as big as the c.s.u. of current.

## 10. Magnetic Effect of an Electric Current

Oersted (1820) discovered that a magnetic field exists in the neighborhood of a wire carrying current. Experiments with small magnets or iron filings show that the magnetic field in the neighborhood of a straight wire carrying current is circular in a plane at right angles to the wire with the wire as the center of these circles.

II. A. Rowland (1876) performed a famous experiment to show the equivalence of a moving charge and an electric current in so far as the magnetic effect was concerned. He used an ebonite disk having metallic sectors distributed near its rim. The metallic sectors were charged electrically, then the disk was rotated very rapidly. A magnetic needle near the disk was deflected by the

magnetic field set up by the moving charges. When the direction of rotation of the disk was reversed, the deflection of the magnetic needle was also reversed. More recently (1929), R. C. Tolman, using a charged cylinder, showed that as far as the magnetic effect is concerned, an oscillating charge is equivalent to an alternating current.

The quantitative relationship between the intensity of the magnetic field at any point in space and the current in the wire was established empirically as a result of the experiments of Biot and Savart (1820), with long straight wires carrying current. If we consider a small section  $ds$  of a wire carrying current  $i$ , then the intensity of the magnetic field at any point  $P$  distant  $r$  from this current element is given by the expression

$$dH = \frac{kids \sin \theta}{r^2}, \quad (23)$$

where  $dH$  is the magnetic field intensity at point  $P$ ,  $\theta$  is the angle between  $r$  and the current in the element  $ds$ , and  $k$  is a constant of proportionality. The direction of the magnetic field at point  $P$  is perpendicular to the plane containing  $r$  and  $ds$  and is given by the usual right-hand rule. Thus, in Figure 5, the magnetic field at  $P$  is directed into the paper away from the reader.

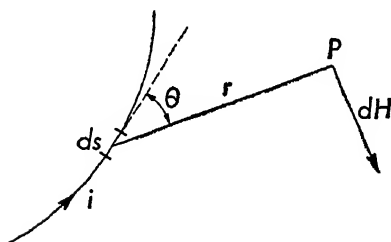


FIG. 5. — The magnetic field intensity at  $P$  is directed into the paper.

The magnetic field due to a current provides one of the best methods for measuring the magnitude of the current. Instead of utilizing our previous definition of the electric current and then evaluating the constant  $k$ , a new unit of current may be defined in terms of its magnetic effect. This is equivalent to replacing  $ki$  by a new symbol,  $i_m$ , to be defined by means of equation (23), which now takes the form

$$dH = \frac{i_m ds \sin \theta}{r^2}. \quad (24)$$

As an aid in defining this new unit of current, let us calculate the magnetic field intensity,  $H$ , produced by a current  $i_m$  flowing in a circular wire of radius  $r$ . The magnetic field intensity at the

center of the circle due to the current flowing in a small element of wire  $ds$ , is, from equation (24),

$$dH_c = \frac{i_m ds}{r^2},$$

since the angle  $\theta$  between  $ds$  and  $r$  is equal to  $\pi/2$ . Now, from Figure 6,

$$ds = r d\phi,$$

so that the magnetic field intensity at the center of the circle due to the entire circuit is

$$H_c = \int_0^{2\pi} \frac{i_m d\phi}{r} = \frac{2\pi i_m}{r}. \quad (25)$$

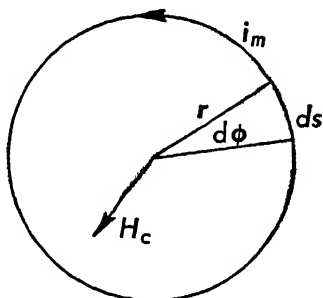


FIG. 6. — The magnetic field at the center of the circle is directed outward from the paper.

The magnetic field at the center is perpendicular to the plane of the circle; if the current is in a counterclockwise direction, the magnetic field will be directed out of the plane toward the observer. The new unit of current, known as the electromagnetic unit of current, can now be defined with the aid of equation (25). The unit current, in c.m.u., is that current, which, flowing in the arc of a circle one centimeter in length, the radius of the circle being one centimeter, produces a magnetic field of unit intensity at the center of the circle. The practical unit of current, the ampere, is 1/10 of the c.m. unit of current. If a current  $i_m$  flows in this circle of unit radius, the magnetic field intensity at the center of the circle is

$$H_1 = 2\pi i_m. \quad (26)$$

If there are  $n$  turns of wire close together in a circle of radius  $r$ , each turn carrying current  $i_m$ , the intensity of the magnetic field at the center of the circle is

$$H_n = \frac{2\pi n i_m}{r}. \quad (27)$$

The magnitude of a current may be expressed in either electrostatic units or electromagnetic units. Experiments show that the electromagnetic unit of current is about  $3 \times 10^{10}$  times larger than the electrostatic unit of current. The most recent determination

of this ratio by Rosa and Dorsey (1907) gave the value as  $2.9979 \times 10^{10}$ . Furthermore, a comparison of the dimensions of these two units of current shows that the ratio is not a dimensionless constant, but that it has the dimensions of a velocity. This ratio will be denoted by the letter  $c$  where  $c = 2.9979 \times 10^{10}$  cm/sec. Thus, to convert current from the electromagnetic units to electrostatic units, we use the relationship

$$i_s = ci_m. \quad (28)$$

Within the limits of experimental error,  $c$  is equal to the velocity of light in a vacuum. This result was of great importance in enabling Maxwell (1865) to establish the electromagnetic theory of light.

All electric and magnetic quantities can be expressed either in e.m. units or e.s. units. The ratio of the two units for any quantity always involves the constant  $c$  or  $c^2$ . For example, to convert a charge  $q_m$  expressed in e.m.u. to one  $q_s$  expressed in e.s.u., we use the equation

$$q_s = cq_m. \quad (29)$$

## 11. Force on a Wire Carrying Current in a Magnetic Field

Consider some point  $A$  in the neighborhood of a wire carrying current and imagine that the north pole of a long thin magnet of strength  $p$  be situated at this point. The intensity of the magnetic field at  $A$  due to any current element  $ids$  is given by

$$dH = \frac{ids \sin \theta}{r^2},$$

where  $i$  is expressed in e.m.u.,  $r$  is the distance of the current element from  $A$ , and  $\theta$  is the angle between  $ids$  and  $r$ . The north pole of the magnet will thus experience a force due to this current element given by

$$dF = pdH = \frac{pids \sin \theta}{r^2}. \quad (30)$$

Assuming Newton's third law, that to every action there is an equal and opposite reaction, the current element will experience an equal force in the opposite direction. Equation (30) may be



written in a more useful form if we note that the quantity

$$\frac{p}{r^2} = H_p \quad (31)$$

is merely the intensity of the magnetic field at the current element due to the north pole at  $A$ . Thus the current element experiences a force given by

$$dF = H_p ids \sin \theta. \quad (32)$$

This force is at right angles to both  $H_p$  and  $ids$ . In the particular case of a straight wire of length  $L$  carrying current  $i$  placed in a uniform magnetic field  $H$  perpendicular to the current, the force  $F$  on the wire is, from equation (32),

$$F = HiL. \quad (33)$$

Rowland's experiment showed that, as far as the magnetic effect is concerned, a moving charge is equivalent to a current. Suppose we have a motion of charges in any given direction with uniform velocity  $v$ . Let  $n$  be the number of charges per unit volume moving in a tube of uniform cross-sectional area  $A$ . If the magnitude of each charge in e.m.u. is  $e$ , then the current in any

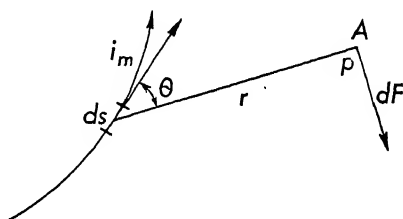


FIG. 7. — The force on the north magnetic pole  $p$  at point  $A$  is directed into the paper.

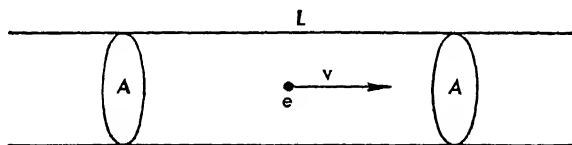


FIG. 8.

section of the tube is  $i = nAev$ . If this tube is in a uniform magnetic field of intensity  $H$  perpendicular to the direction of motion, the force on the charges in a length  $L$  will be

$$F = HnevL = Hqv, \quad (34)$$

where  $q$  is the charge in a length  $L$ . The force is perpendicular to both  $H$  and  $v$ . A single particle bearing a charge  $q$  and moving with a velocity  $v$  in a direction perpendicular to a magnetic field of

intensity  $H$  will also experience a force  $F = Hqv$ : this force will be perpendicular to both  $H$  and  $v$ .

## 12. Magnetic Moment of a Plane Circuit Carrying Current

Any plane circuit carrying current  $i$ , when placed in a uniform magnetic field of strength  $H$ , will experience a torque,  $T$ , given by

$$T = iAH \cos \phi, \quad (35)$$

where  $\phi$  is the angle between the plane of the circuit and the direction of the magnetic field. This torque will be a maximum when the plane of the circuit is parallel to the field, and will be zero when the plane circuit is at right angles to the field. If left free to rotate, a plane circuit will always set itself at right angles to the direction of the external magnetic field. This follows directly from the application of equation (32) to each element of the plane circuit. It is left as an exercise for the student to carry out this calculation for some simple geometrical figure such as a rectangle or a circle.

By comparing equation (35) with equation (16) it is seen that a plane circuit carrying current may be assigned a magnetic moment  $M$  given by

$$M = iA, \quad (36)$$

where  $i$  is expressed in e.m.u.

## 13. Electromagnetic Induction

Michael Faraday in England and Joseph Henry in the United States discovered the phenomenon of electromagnetic induction at about the same time, in 1831. They found that whenever the magnetic field around a circuit is changed, an electromotive force is induced in this circuit. The magnetic field may be changed in any number of ways, for example by moving a permanent magnet relative to the circuit, or by bringing another circuit carrying current near the first one, or by varying the current in a neighboring circuit, or by varying the current within the circuit under investigation. It is found experimentally that the magnitude of the electromotive force induced in any circuit is proportional to the time rate of change of the magnetic field around the circuit.

The relationship between the induced electromotive force and the changing magnetic field can best be put in quantitative form

by considering the changes in the total *magnetic flux* through the circuit. If we consider any small area  $dA$  in a region of permeability  $\mu$  in which there is a magnetic field of intensity  $H$ , the magnetic flux  $d\Phi$  through this small area is defined by the equation

$$d\Phi = \mu H_n dA \quad (37)$$

in which  $H_n$  is the component of the magnetic field intensity perpendicular to the element of area  $dA$ . The total magnetic flux  $\Phi$  through the area  $A$  enclosed by any circuit is then

$$\Phi = \int_0^A \mu H_n dA. \quad (38)$$

In the particular case in which the magnetic field intensity is uniform and perpendicular to the area  $A$ , the total magnetic flux is simply

$$\Phi = \mu HA. \quad (39)$$

The *magnetic flux density*, denoted by  $B$ , is defined by the equation

$$B = \mu H. \quad (40)$$

In the particular case in which the field is uniform and perpendicular to the area  $A$ , the flux is

$$\Phi = BA. \quad (41)$$

In the electromagnetic system of units  $H$ , as we know, is measured in *oersteds*: the magnetic flux density  $B$  is measured in *gausses*. In this system of units an oersted and a gauss are the same dimensionally since  $\mu$  is simply a number. The total magnetic flux  $\Phi$  is measured in *maxwells*: thus a gauss is also a maxwell per square centimeter.

Applied to any plane coil consisting of a single turn enclosing an area  $A$ , Faraday's law states that the induced electromotive force  $V$  in this circuit is equal to the time rate of change of the magnetic flux through the coil or

$$V = - \frac{d\Phi}{dt}. \quad (42)$$

The minus sign is used to indicate that the direction of the induced electromotive force is such as to give rise to a current which, by its magnetic effect, will oppose the change inducing the current. This

is a consequence of the principle of conservation of energy and was first formulated by Lenz (1834).

In equation (42) all quantities are expressed in c.g.s. electromagnetic units. If  $V$  is to be expressed in volts when  $\Phi$  is in maxwells and  $t$  in seconds, then the equation takes the form

$$V = -10^{-8} \frac{d\Phi}{dt}. \quad (43)$$

If the coil through which the flux is changing consists of  $n$  turns each enclosing the same area  $A$ , then the e.m.f. induced in the coil is  $n$  times that induced in one turn.

Equation (42) is perfectly general and is independent of the material of which the coil is made. Thus an e.m.f. will be induced in any closed path surrounding a changing magnetic field whether this closed path consists of a conductor or is merely an imaginary closed path in free space. An induced electromotive force in any closed path implies the existence of an electric field  $E$  which is tangent to the path at every point, that is,

$$V = \int_0^s E ds \quad (44)$$

where  $s$  is measured along the closed path.

The phenomenon of electromagnetic induction is the basis for many of our most practical devices such as the electromagnetic generator, the transformer, the induction coil, and the electric motor.

## REFERENCES

- PAGE, L., and N. I. ADAMS, *Principles of Electricity*. New York: D. Van Nostrand Company, Inc., 1931, Chaps. I, II, IV, VII, VIII.
- RICHTMYER, F. K., and E. H. KENNARD, *Introduction to Modern Physics*. New York: McGraw-Hill Book Company, Inc., 1942, Chaps. I, II.
- STARLING, S. G., *Electricity and Magnetism*. New York: Longmans, Green & Company, 1934, Chaps. I, III, V, IX, X, XIII.

## PROBLEMS

1. (a) Show that the intensity of the magnetic field at any point distant  $r$  from a very long straight wire carrying current  $i$ , is

$$H = \frac{2i}{r}.$$

(b) Calculate the intensity of the magnetic field at a distance of 10 cm from a very long straight wire carrying a current of 4 amperes.

*Ans.* 0.08 oersteds.

2. (a) Show that the potential of an isolated sphere of radius  $R$  is equal to  $q/R$ , where  $q$  is the charge on the sphere. (b) Using the result of part (a), show that the capacitance of an isolated sphere in a vacuum is equal to its radius.

3. A capacitor, consisting of two parallel plates each of area  $80 \text{ cm}^2$  separated a distance of 5 mm, has a difference of potential of 300 volts maintained between its plates by means of a battery. Calculate (a) the intensity of the field between the plates, and (b) the energy per unit volume in this field. (c) A very small oil drop carrying a charge of  $32 \times 10^{-19}$  coulombs is introduced between the plates. Calculate the force acting on this oil drop.

*Ans.* (a) 600 volts per cm or 2 dynes per c.s.u. of charge.

(b)  $\frac{1}{2\pi}$  ergs per  $\text{cm}^3$ .

(c)  $1.92 \times 10^{-8}$  dynes.

4. (a) A rectangular loop of wire of length  $L$  and width  $b$  is placed in a uniform magnetic field of strength  $H$  with its plane parallel to the direction of the magnetic field. Show that when a current  $i$  is sent through the wire, the loop of wire will experience a torque equal to  $iLbH$ , where  $i$  is in c.m.u. (b) A galvanometer coil consists of 600 turns of very fine wire wound on a rectangular frame 4 cm long and 1 cm wide, and is hung by means of a gold wire in a magnetic field of 500 oersteds. What is the torque on the galvanometer coil when a current of  $10^{-8}$  amperes flows through each turn?

*Ans.*  $12 \times 10^{-4}$  dyne cm.

5. With the aid of equation (32), calculate the torque on a circular coil of wire of radius  $R$  carrying current  $i$  in a uniform magnetic field of strength  $H$  parallel to the plane of the coil. Compare this result with equation (35).

6. A circular coil of wire of 30 cm radius contains 750 turns wound

close together. Determine the intensity of the magnetic field at the center of the coil when the current in the coil is 5 amperes.

*Ans.* 78.5 oersteds.

7. A stream of alpha particles, each carrying a charge of  $3.2 \times 10^{-19}$  coulombs is sent through a uniform magnetic field of 30,000 oersteds. The velocity of each particle is  $1.52 \times 10^9$  cm/sec and is at right angles to the direction of the magnetic field. Determine the force on each alpha particle.

*Ans.*  $14.6 \times 10^{-7}$  dynes.

8. A thin bar magnet 12 cm long has a pole strength of 500 unit poles. It is placed in a uniform magnetic field of 200 oersteds intensity with the length of the magnet, that is, its axis, at right angles to the direction of the magnetic field. (a) Calculate the torque on the magnet in this position. (b) Determine the work done by the field in rotating the magnet so that its axis is parallel to the field.

*Ans.* (a)  $12 \times 10^5$  dyne cm.

(b)  $12 \times 10^5$  ergs.

9. A coil of fine wire of 8 cm radius has 500 turns. The magnetic field through the coil is increased from zero to 12,000 gaussses in 0.2 second. Determine the average value of the induced electromotive force in this coil.

*Ans.* 60.4 volts.

# 2 Elementary Charged Particles

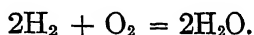
## 14. Introduction: Atomic Weights

The concept of atoms was introduced into chemistry as a hypothesis by Dalton (1802), to explain the formation of compounds from simpler substances called elements. The atoms of any one element were assumed to be identical in all their properties including weight. Dalton also formulated the law of multiple proportions which states that if two elements combine in more than one proportion to form different compounds, the weights of one of the elements which unite with identical amounts of the second element are in the ratio of integral numbers. For example, 16 grams of oxygen combine with 12 grams of carbon to form carbon monoxide, CO, while 32 grams of oxygen can also combine with 12 grams of carbon to form another compound, carbon dioxide, CO<sub>2</sub>. Shortly afterward, the law of definite proportions was established. This law states that, in any compound, the proportion by weight of the constituent elements is a constant. For example, when mercuric oxide is decomposed, for every 16 grams of oxygen liberated, 200.6 grams of mercury are liberated. When oxygen and mercury are combined to form mercuric oxide, their proportions by weight are always in the ratio of 16 to 200.6.

Many of the elements and compounds were studied in the gaseous state: it was found that the volumes of the elements and compounds involved in a reaction, in which both the initial and final constituents were gases, were connected by very simple relationships. To explain the behavior of gases, Avogadro (1811) put forth the bold hypothesis that equal volumes of different gases, under the same conditions of temperature and pressure, contain equal numbers of molecules. Ampère supported this hypothesis and pointed out that, if correct, it should lead to "a method for determining the relative masses of the atoms and the proportions according to which they enter into combination."

In the combination of hydrogen and oxygen to form water vapor, it is found that when measured at the same temperature and pressure, two volumes of hydrogen and one volume of oxygen

combine to form two volumes of water vapor. The interpretation of this result on the basis of Avogadro's hypothesis is that two molecules of hydrogen and one molecule of oxygen combine to form two molecules of water vapor. The chemical equation expressing this result is



This equation also states that, in the free state, hydrogen and oxygen molecules are composed of two atoms each, and water vapor molecules consist of three atoms, two hydrogen atoms and one oxygen atom. From a determination of the combining weights it has been found that 16 grams of oxygen combine with 2.016 grams of hydrogen to form 18.016 grams of water vapor. Since one atom of oxygen combines with two atoms of hydrogen to form water vapor, the relative atomic weights of oxygen and hydrogen are in the ratio of 16 to 1.008. The *chemical system of atomic weights* adopts as a standard 16.00 for the atomic weight of oxygen. The atomic weights of all the other elements are then stated in terms of  $\text{O} = 16.00$  as the standard.

Since a molecule of oxygen in the free state contains two atoms, the molecular weight of oxygen is 32.00. The molecular weight of hydrogen,  $\text{H}_2$ , is 2.016. A quantity of any substance whose mass, in grams, is numerically equal to its molecular weight, is called a *mole*. The volume occupied by a mole of any gas is called a gram molecular volume. At  $0^\circ \text{C}$  and 76 cm. pressure the *gram molecular volume* of any gas is 22.4 liters. On the basis of Avogadro's hypothesis, every mole of a substance contains the same number of molecules. The number, usually referred to as *Avogadro's number*, will be denoted by the letter  $N$ .

From the above discussion, it is readily seen that, in the case of an element, a mass in grams equal numerically to its atomic weight must contain  $N$  atoms. For example, 16 grams of oxygen contain  $N/2$  molecules and hence contain  $N$  atoms. Similarly for any other diatomic molecule. For a monatomic molecule such as helium or neon, it is obvious, of course, that there are  $N$  atoms in a gram-atomic weight of the element. Hence, if Avogadro's number  $N$  can be determined, the mass in grams of any atom will be known. Since we are evidently dealing with large numbers of atoms, the atomic mass determined in this manner may be only an average



value. It has been found that in many cases the masses of the atoms of an element are not all identical (§ 22).

Avogadro's number  $N$  can be determined by several methods. Two of these methods will be discussed in this chapter. One method is based upon a study of electrolysis, and the other is based upon a study of the Brownian motion of particles suspended in a fluid.

## 15. Electrolysis

Solutions of acids, bases, and salts are known to be conductors of electricity. The conductivity of these solutions is due to the presence of *ions* in the solution. An ion is an atom or a group of atoms charged electrically. On the modern theory of the structure of the atom (§ 35), an atom consists of a positively charged *nucleus* surrounded by a number of negatively charged particles called *electrons*. In the neutral atom, the sum of all the electronic charges is equal, numerically, to the positive charge of the nucleus. An atom is said to be ionized if the total electronic charge is not equal numerically to the positive charge of the nucleus; similarly, a group of atoms is said to be ionized if the total electronic charge differs numerically from the total positive charge of their nuclei. If there is a deficiency of electrons, the ion is positively charged and if there is an excess of electrons, it is negatively charged. It has been found empirically that the charge on any ion can be expressed in terms of integral multiples of a fundamental quantity of electricity which has been shown to be equivalent to the charge of an electron (§ 19). If the charge on an ion is equivalent to one electron, it is said to have a valence of unity; if the charge on an ion is equivalent to two electrons, it has a valence of two, and so on.

As a typical example of electrolysis, let us consider a chemical cell containing a solution of silver nitrate,  $\text{AgNO}_3$ , a silver anode connected to the positive terminal of a battery, and a copper cathode connected to the negative terminal of the battery, as shown in Figure 9. The silver nitrate in the solution

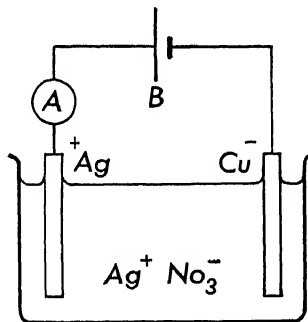


FIG. 9.

is dissociated into silver ions,  $\text{Ag}^+$ , and nitrate ions,  $\text{NO}_3^-$ . Under the action of the electric field between the electrodes, the  $\text{Ag}^+$  ions migrate toward the cathode, and the  $\text{NO}_3^-$  ions migrate toward the anode. If the chemical cell is examined after the current has been flowing in the circuit for some definite time, it will be found that a mass  $M$  of metallic silver  $\text{Ag}$  has been deposited on the cathode and an equal mass  $M$  of metallic silver has been removed from the anode, leaving the concentration of the solution unchanged. A simplified analysis of the action of this cell is as follows: when a silver ion,  $\text{Ag}^+$ , reaches the cathode, it acquires an electron from it, thus forming a neutral atom which adheres to the cathode. At the anode a silver atom breaks up into a silver ion and an electron; the ion,  $\text{Ag}^+$ , goes into solution to replace the one which was removed, while the electron is forced through the external part of the circuit. Thus an atom is removed from the anode for each atom deposited on the cathode. The silver ions are transferred through the solution and the electrons are transferred through the external metallic portions of the circuit.

The behavior of electrolytic cells can be summarized in terms of two laws first formulated by Faraday. The first law states that the quantity of any substance liberated from the solution depends only upon the total charge passing through the circuit, or

$$M = kQ, \quad (1)$$

where  $M$  is the mass of the material liberated at one electrode,  $Q$  is the quantity of charge transferred, and  $k$  is a factor of proportionality called the *electrochemical equivalent* of the substance. From this equation, it is evident that  $k$  is the mass liberated per unit charge transferred, usually expressed in grams per coulomb.

Faraday's second law states that for any substance the mass liberated by the transfer of a quantity of electricity  $Q$  is proportional to the *chemical equivalent* of the substance, or

$$M = Q \frac{A}{v} \frac{1}{F}, \quad (2)$$

where  $A/v$ , the ratio of the atomic weight to the valence of the element, is the chemical equivalent of the element, and  $F$  is a constant of proportionality known as the *Faraday constant*.

From equations (1) and (2), it will be noted that

$$F = \frac{A}{kv}.$$

The value of  $F$  can be determined from the results of the experiments on electrolysis. For the case of silver, where  $k = 0.0011180$  grams per coulomb,  $A = 107.88$  grams per gram-atomic weight, and  $v$  is unity, we get

$$F = \frac{107.88}{0.0011180} = 96,500 \text{ coulombs/gm-at wt.}$$

Thus the transfer of 96,500 coulombs of charge will deposit a gram-atomic weight of a monovalent element.

Since the valence of silver is unity, for every atom of silver deposited on the cathode, a charge equivalent to one electron has been transferred through the solution. If  $e$  is the charge of one electron, then  $Ne$  is the total charge transferred when one gram-atomic weight of silver is deposited on the cathode. Or

$$F = Ne = 96,500 \text{ coulombs/gm-at wt.} \quad (3)$$

If the charge of an electron can be determined independently, then Avogadro's number,  $N$ , can be calculated from the above equation. The first accurate determination of the charge of an electron was made by Millikan (§ 19), who found the value of the charge to be  $e = 4.770 \times 10^{-10}$  e.s.u. or  $1.592 \times 10^{-10}$  coulombs. Using this value of  $e$ , we get for Avogadro's number  $N = 6.06 \times 10^{23}$  atoms in a gram-atomic weight of an element. More recent experiments (§ 57) indicate that the value of  $e$  is probably  $4.80 \times 10^{-10}$  e.s.u., or  $1.60 \times 10^{-10}$  coulombs, which makes  $N = 6.028 \times 10^{23}$ .

Of course, if Avogadro's number  $N$  could be determined independently with the same degree of precision as the electronic charge  $e$ , it would be a check on the determination of  $e$  as well as additional confirmation of Avogadro's hypothesis. The first direct determination of Avogadro's number was made by Perrin in 1908 in an investigation of the motion and distribution of very small particles suspended in a fluid.

## 16. Brownian Motion

If fine particles suspended in a fluid are examined in the field of a microscope, it will be observed that they are in constant hap-

hazard motion. This random motion continues indefinitely and is found to depend upon several factors such as the size of the particles, the viscosity of the fluid in which they are immersed, and the temperature of the system. The motion of these particles was first observed by Brown in 1827. Many observers recognized that these particles behave in the same way that molecules of an ideal gas are supposed to behave. The random motion of these particles may be likened to the thermal motion of gas molecules.

The explanation of the Brownian motion, first given by Einstein and Smoluchowski, is based on the assumption that the particles in suspension are continually bombarded by the molecules of the fluid and that this bombardment produces an unbalanced force which accelerates the particle. The motion of the particle through the fluid is opposed by another force due to the viscosity of the fluid. From this theory the distribution of particles in a field of force and their displacement in the course of time can be calculated. Perrin performed these two different types of experiments on Brownian motion, one on the vertical distribution of the particles in the fluid, the other on the displacement of the particles in a given time interval.

## 17. Vertical Distribution of Particles

If the particles suspended in a fluid behave like large-sized gas molecules, then their distribution in the vertical direction should be similar to the distribution of the air in the atmosphere; that is, the density of particles should be greatest at the bottom of the fluid and should decrease exponentially with increasing height. Consider a cylinder of gas of cross-sectional area  $A$  and height  $h$ . If  $\rho$  is the density of the gas, then the mass of gas in a small cylindrical element of height  $dh$  is  $\rho A dh$ , and its weight is  $\rho A g dh$ , where  $g$  is the acceleration due to gravity. The weight of this gas is balanced by the upward force due to the difference in pressure on the two circular surfaces of the cylinder. If  $dp$  is this difference in pressure, then the upward force is  $A dp$ , from which

$$dp = - \rho g dh.$$

The minus sign indicates that as the height increases the pressure decreases. Now  $\rho = M/v$ , where  $M$  is the mass of a mole of the

gas and  $v$  is its volume, so that

$$dp = - \frac{M}{v} g dh.$$

The general gas law, for one mole of a gas, is

$$pv = RT,$$

where  $T$  is the absolute temperature of the gas and  $R$  is the universal gas constant. Eliminating  $v$  from the last two equations, we get

$$dp = - \frac{Mpgdh}{RT},$$

or

$$\frac{dp}{p} = - \frac{Mgdh}{RT}.$$

Integrating this equation assuming the temperature to be the same throughout the gas, we get

$$\log p = - \frac{Mgh}{RT} + \log C.$$

Let  $p = p_0$  when  $h = 0$ , then  $\log C = \log p_0$ . Hence

$$p = p_0 e^{-\frac{Mgh}{RT}}.$$

Since the pressure is directly proportional to the density or the number of molecules per unit volume, this equation can be written as

$$n = n_0 e^{-\frac{Mgh}{RT}}, \quad (4)$$

where  $n$  is the number of molecules per unit volume at a height  $h$  above the reference plane, and  $n_0$  is the number of molecules per unit volume at the reference plane. This is the well-known law of atmospheres. If  $n_0$  represents the number of molecules per unit volume at the surface of the earth, then  $n$  gives the number of molecules per unit volume at any height  $h$  above the earth's surface.

The law of atmospheres may be put in a more useful form if we replace the mass  $M$  of a mole of gas by  $Nm$ , where  $m$  is the mass

of a molecule and  $N$  is Avogadro's number. It then becomes

$$n = n_0 e^{-\frac{Nmg h}{RT}}. \quad (5)$$

In applying this law to the determination of the distribution of particles suspended in a fluid, the buoyant force due to the fluid must be taken into consideration. If  $\rho$  is the density of the substance and  $\rho_0$  the density of the fluid, then the effective weight of a particle of this substance is  $mg \left(1 - \frac{\rho_0}{\rho}\right)$  so that the number of particles per unit volume at any height  $h$  above the reference plane is given by

$$n = n_0 e^{-\frac{Nmg \left(1 - \frac{\rho_0}{\rho}\right) h}{RT}}. \quad (6)$$

For particles showing observable Brownian motion,  $h$  is so small that the entire exponent becomes very small in comparison with 1 and the exponential factor may be expanded in a series of which the first two terms are

$$\frac{n}{n_0} = 1 - \frac{Nmg}{RT} \left(1 - \frac{\rho_0}{\rho}\right) h. \quad (7)$$

The higher powers in this series may be neglected.

Perrin prepared emulsions from gamboge and mastic and with the aid of a centrifuge obtained particles of nearly uniform size. In order to be able to apply equation (7) it is necessary to determine both the density and the volume of the grains in the emulsion. The density was determined in three ways: (a) by the specific gravity bottle method, (b) by measuring the density of the fused mass remaining after the water was boiled off, and (c) by adding potassium bromide to the emulsion until the density of the fluid was equal to that of the particles and then determining the density of the solution.

The sizes of the particles were determined in several ways. One method was to allow a drop of very dilute emulsion to evaporate from a cover glass. It was found that the particles arranged themselves neatly in rows. The sizes of the particles could then be determined by counting the number of particles in a row of known length or the number in a known area. Another method

was to time the rate of fall of one of the particles through the fluid, and then calculate the size of the particle with the aid of Stokes' law for the velocity of spherical particles falling through a viscous medium.

The experimental determination of the number of particles at any level in the emulsion was made by placing a drop of emulsion in a glass cell about 0.1 mm deep covered by a microscope cover glass to give a plane surface, as shown in Figure 10. To prevent evaporation, the edges of the cover glass were treated with paraffin. Under a high-power microscope, the grains in a

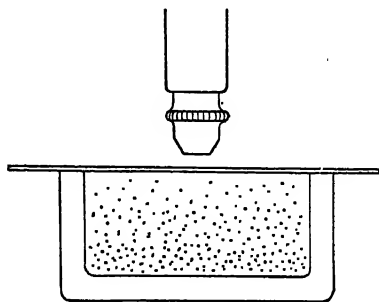


FIG. 10. — Perrin's method of observing the vertical distribution of particles in a fluid.

very thin horizontal section, about 0.001 mm in thickness, were sharply defined. Raising or lowering of the microscope made the grains in other sectional layers visible. The method of observation consisted in narrowing the field of view so that not more than five or six particles were visible at any one time. A shutter, placed in the path of light illuminating the emulsion, opened at regular intervals, and the number of grains observed on each such occasion was noted. About two hundred observations were made at one level and then the microscope was moved vertically through a known distance and a similar set of observations was made. In this way the ratio  $n/n_0$  was determined. Perrin also used the photographic method, taking photographs of the emulsion at equidistant levels and then counting the number of images of grains appearing on the photographic plate.

Many experiments were performed under a variety of conditions of temperature, using grains of different sizes suspended in several different liquids. As a result of these experiments Perrin obtained a value for Avogadro's number  $N = 6.88 \times 10^{23}$ . When this was combined with the results of the experiments on electrolysis, the value of the charge of an electron was determined as

$$e = 4.25 \times 10^{-10} \text{ c.s.u.}$$

## 18. Displacement of Particles in Brownian Motion

The second type of experiment performed by Perrin for the determination of Avogadro's number consisted in observing one of the particles in suspension and measuring the displacement of this particle in a given time interval. The fundamental assumption used in the derivation of the equation for the displacement of such a particle is that the particles suspended in a fluid have a mean kinetic energy equal to the mean kinetic energy of gas molecules at the same temperature. The displacement equation, derived first by Einstein in 1905 (see Appendix VI), is

$$\overline{x^2} = \frac{2RT}{NK} t, \quad (8)$$

where  $x$  is the displacement of the particle in the  $x$  direction in a given time interval  $t$ , and  $\overline{x^2}$  is the average of the squares of the displacements of the particle in the  $x$  direction in equal time intervals  $t$ .  $K$  is a factor of proportionality determined by the viscosity of the medium.

Perrin tested Einstein's equation in several ways. He used grains of mastic and gamboge in various solutions and at various temperatures. The displacements were determined by plotting the position of the particle after fixed time intervals. A typical trajectory is shown in Figure 11. The positions of the particle are represented by dots and the lines joining the dots represent the displacements in the given time interval, say 30 sec. The  $x$  component of each of these displacements can be obtained by projecting them on the  $x$  axis;  $\overline{x^2}$  is then obtained by squaring and averaging the squares of these displacements.

For the determination of  $N$  by the displacement method, the microscope was focused at a given level and the first particle that appeared in the center of the field of view was followed for a little while, the positions being noted at given time intervals. The emulsion was then displaced laterally and again the trajectory of the first particle that appeared in the center was traced. From a measurement of 1500 displacements of gamboge particles of  $0.367 \times 10^{-4}$  cm radius, Perrin obtained for the value of Avogadro's number  $N = 6.88 \times 10^{23}$ . As a result of many determinations of  $N$  under different experimental conditions, Perrin adopted

$$N = 6.85 \times 10^{23}$$



as the best value for Avogadro's number, yielding the value

$$e = 4.2 \times 10^{-10} \text{ e.s.u.}$$

for the electronic charge.

Later work by Millikan and Fletcher on Brownian motion in a gaseous medium such as air yielded the value  $N = 6.03 \times 10^{23}$ ,

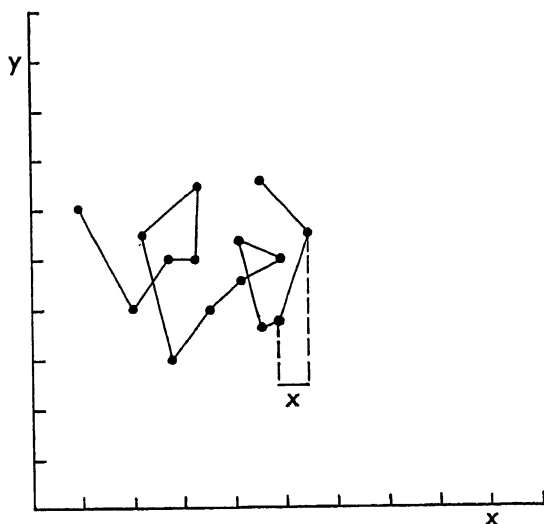


FIG. 11. — Trajectory of a particle in Brownian motion. Each line connecting two dots represents the displacement of the particle in a fixed time interval.

while Westgren (1915), working with colloidal gold, silver, and selenium particles, obtained the value  $N = 6.05 \times 10^{23}$ . Avogadro's hypothesis was thus confirmed experimentally about a century after it was formulated.

R. T. Birge, who has been making a very exhaustive and critical study of the experimental determinations of the different fundamental physical constants, considers recent determinations of the Avogadro number to be among the most reliable of any of the physical constants. One method which has attained great precision and has yielded generally consistent results is the determination of the Avogadro number from measurements of the densities of crystals and their structure as determined by X-ray analysis (see § 58). From weighted averages of measurements on five different varieties of crystals, Birge arrives at the following value

for the Avogadro number:

$$N = 6.02338 \times 10^{23} \text{ per mole}$$

on the chemical scale of atomic weights.

When the above value is combined with the value of the Faraday

$$F = 96487.7 \text{ coulombs per gram-atomic weight,}$$

the value of the electronic charge becomes

$$e = 4.8021 \times 10^{-10} \text{ e.s.u. of charge.}$$

## 19. Determination of the Charge of an Electron

The earliest experiments on the determination of the electronic charge were performed by Townsend (1897) and J. J. Thomson (1898). Their method consisted in allowing water vapor to condense on ions thus forming a cloud, and then determining the charge carried by the cloud. The number of individual droplets in the cloud was then computed by weighing the water condensed from the cloud and dividing it by the average weight of a single droplet. The latter was determined by measuring the rate of fall of these droplets through air, assuming Stokes' law to hold. On the assumption that each droplet was condensed on a single ion carrying charge  $e$ , they obtained values for  $e$  of the order of  $3 \times 10^{-10}$  e.s.u.

A very important by-product of this type of investigation was the discovery by C. T. R. Wilson (1897) of a method for producing these clouds. If air, saturated with water vapor and ionized by some agency, is expanded suddenly, the air is cooled and the water vapor condenses on the ions in the air.

H. A. Wilson (1903) made a decided improvement in the method for determining the electronic charge by forming clouds between two capacitor plates which could be connected to the terminals of a battery. The experimental procedure was first to determine the rate of fall of the top surface of the cloud under the influence of gravity alone, and then to produce a second cloud and charge the capacitor plates so that the droplets would be urged downward by both gravity and the force due to the electric field. The numerical results for the electronic charge were about the

same as those obtained by Townsend and Thomson. All of these experiments suffered from the fact that the weight of a drop of water did not remain constant during the time of observation. Further, the exact number of ions on which each drop was condensed was not known.

Millikan, while repeating the experiments of H. A. Wilson, found that single drops of water could be held stationary between

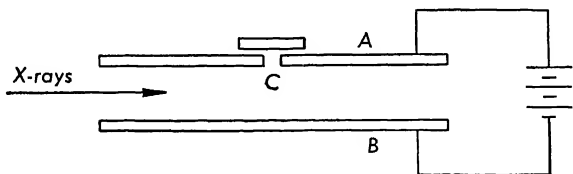


FIG. 12.

the two plates of the capacitor by adjusting the voltage between the plates so that the weight of the drop could be balanced by the force due to the electric field between the plates. While working with these "balanced drops" he noticed that occasionally the drop would start moving up or down in the electric field. This drop had evidently captured an ion, positive in one case, negative in the other case. This made it possible to determine the charge carried by an ion irrespective of the original charge carried by the drop of water. To avoid the errors due to evaporation Millikan decided to use drops of oil instead of water.

The apparatus consisted essentially of two brass plates A and B about 22 cm in diameter and about 1.5 cm apart, see Figure 12. These plates were placed in a large metal box to avoid air currents. In this experiment small drops of oil are sprayed into the box by means of an atomizer. After a while one of these drops drifts through the pinhole C in the top of plate A and can then be observed with the aid of a telescope. Indirect illumination of the drop is provided by a lamp on the side. When there is no electric field between the plates, the forces acting on the oil drop are its weight  $mg$  and a resisting force due to the viscosity of the medium. This resisting force is proportional to the velocity of the oil drop. Equilibrium will be reached when the velocity of the drop reaches such a value that the resisting force becomes equal to the weight. The oil drop will then continue to move downward with uniform

velocity. Calling this value of the velocity  $v_1$ , we can write

$$mg = Kv_1, \quad (9)$$

where  $K$  is a factor of proportionality. For very small drops, this value of the velocity is reached very quickly. If the capacitor plates are now connected to the battery so that plate  $A$  is positive, the velocity of the oil drop will be changed suddenly. This change is due to the fact that the oil drop is charged when it comes from the atomizer. If  $q$  represents the charge on the oil drop, then the force on it due to the electric field is

$$F = \frac{V}{d}q, \quad (10)$$

where  $V$  is the difference of potential between the plates and  $d$  is the distance between the plates. If the charge on the oil drop is negative, then the force due to the electric field will be upward and the new velocity  $v_2$  will be given by

$$F - mg = Kv_2 \quad (11)$$

where  $v_2$  is considered positive in the upward direction. Combining equations (10) and (11), we get

$$\frac{V}{d}q - mg = Kv_2. \quad (12)$$

In Millikan's experiment the air between the capacitor plates was ionized by various methods such as allowing X rays or the radiations from radioactive substances to pass through it. The oil drop occasionally acquired an additional ion, either positive or negative, and its velocity in the electric field was observed to change. Or it may have lost an ion in its passage through the ionized air. If  $v_3$  represents its new velocity after the acquisition of an ion of charge  $q_n$ , then from equation (12)

$$\frac{V}{d}(q + q_n) - mg = Kv_3. \quad (13)$$

Solving equations (12) and (13) for  $q_n$ , we get

$$q_n = \frac{d}{V}K(v_3 - v_2). \quad (14)$$

The experiment consists in determining  $q_n$ , the charges on the

ions captured or lost by the oil drop during the time of observation, which, in some cases, lasted for several hours. The velocity of the oil drop was measured by timing the passage of its image between two cross hairs in the telescope a known distance apart. The difference of potential  $V$  was of the order of several thousand volts. The only quantity left to be evaluated in the determination of  $q_n$  is the factor  $K$ . If Stokes' law for the velocity of spheres falling through a viscous medium holds, then  $K = 6\pi\eta a$  where  $\eta$  is the coefficient of viscosity of the air and  $a$  is the radius of the oil drop. A series of experiments was performed to verify the accuracy of Stokes' law. It was found that for very small drops, Stokes' law had to be modified, the correction being given with sufficient accuracy if  $K$  is written

$$K = \frac{6\pi\eta a}{1 + \frac{b}{pa}}, \quad (15)$$

where  $p$  is the pressure of the air in centimeters of mercury and  $b$  is an empirically determined constant. The value of the coefficient of viscosity was determined in another series of experiments, and the value used by Millikan is  $\eta = 0.0001825$  c.g.s. units.

From many determinations of  $q_n$ , it was found that  $q_n$  could always be represented by

$$q_n = ne, \quad (16)$$

where  $n$  is an integer and  $e$  represents the elementary charge equivalent to that of an electron. The value of the charge of an electron from Millikan's work (1917) is

$$e = 4.770 \times 10^{-10} \text{ e.s.u.}$$

It must be emphasized that the value of  $e$  is the same for both positive and negative charges since  $q_n$ , the ionic charge captured or lost by the oil drop, could be either positive or negative, depending on chance.

Later experimental evidence, particularly from the study of X-ray wave lengths (§ 58), indicated that this value of  $e$  was too small. Shiba, in 1932, pointed out that the error in Millikan's determination of  $e$  was probably due to an error in the determination of  $\eta$ . Many experiments have since been performed for the

redetermination of this constant. The weighted average of seven different determinations of the coefficient of viscosity of air at  $23^{\circ}\text{C}$  is

$$\eta = 1832.5 \times 10^{-7} \text{ c.g.s. units.}$$

When this value of  $\eta$  is used with Millikan's measurements, the value of the electronic charge becomes

$$e = 4.8071 \times 10^{-10} \text{ e.s.u. of charge.}$$

An interesting modification of Millikan's oil drop experiment was recently devised by Hopper and Laby (1941). In this experiment the oil drop was allowed to fall through a horizontal electric

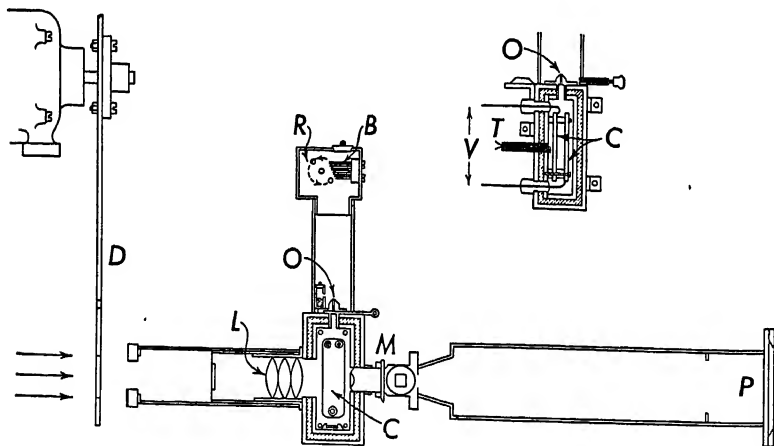


FIG. 13. — Apparatus used by Hopper and Laby for determining the electronic charge. *B* is a steel wire brush, *R* a rotating bar, *O* opening for oil drops, *C* capacitor plates; *D* rotating metal disk, *L* condenser lens system, *M* microscope objective, *P* photographic plate, *T* thermocouple, and *V* leads for applying voltage to capacitor plates.

field between two vertical plates. Under the action of its weight  $mg$  and the force due to the horizontal electric field, the oil drop moves at an angle to the vertical. Because of the resistance provided by the viscosity of the air, the oil drop quickly reaches the limiting velocity  $v$  at an angle  $\theta$  to the vertical. It then continues to travel in a straight line with this uniform velocity  $v$ . For an oil drop of radius  $5 \times 10^{-4}$  cm, calculations show that it takes less than 0.003 seconds to reach within 1 part in 10,000 of its terminal velocity.

Hopper and Laby found that the most effective method for producing oil drops of the proper size was to place a drop of oil on the wires of a fine steel brush; a rotating bar, see Figure 13, first pushes the wires of the brush back and then suddenly releases them, producing a copious supply of oil drops of about the desired range of sizes. Drops of castor oil and apiezon oil were used in this experiment. These drops were produced in a box which was mounted vertically on a well-insulated copper box containing the vertical plates of the capacitor. The tube connecting these two boxes was fitted with a tap which served to separate drops of different sizes, to protect the air in the copper box from external disturbances, and to allow the drops to enter so that they are in focus as they fall past the microscope objective. The temperature of the air in the copper box was controlled by means of a thermostat; the temperature was kept constant and slightly above room temperature. The drops were illuminated intermittently at intervals of 0.04 second, each flash lasting for  $1/1500$  second. This was accomplished by allowing light from an arc to pass through a slot cut near the edge of a disk; this disk was rotated by means of a synchronous motor at a speed of 25 revolutions per second. A shutter in front of the condenser lens was kept open for two seconds, during which time the oil drops between the capacitor plates were illuminated fifty times and their images were recorded on the photographic plate.

In this experiment a drop is first allowed to fall between the two vertical plates without an electric field and the successive positions of the drop are photographed at intervals of 0.04 second. The horizontal electric field is then applied and the successive positions of the drop are again photographed at intervals of 0.04 second. With no electric field on, the oil drop falls with uniform vertical velocity  $v_y$  given by

$$mg = Kv_y.$$

With the electric field on, the oil drop moves with uniform velocity  $v$  at an angle  $\theta$  to the vertical. The horizontal component of this velocity  $v_x$  is given by

$$v_x = v \sin \theta. \quad (17)$$

The force due to the electric field is balanced by the horizontal

component of the resisting force so that

$$\frac{V}{d} ne = K v_x \quad (17a)$$

where  $V$  is the difference of potential between the plates,  $d$  the distance between them, and  $ne$  the charge on the oil drop. From equations (17) and (17a), we get

$$ne = \frac{d}{V} K v \sin \theta. \quad (18)$$

Figure 14 is a typical plate showing the paths of both deflected and undeflected oil drops. The velocities  $v_y$  and  $v$  can be calcu-

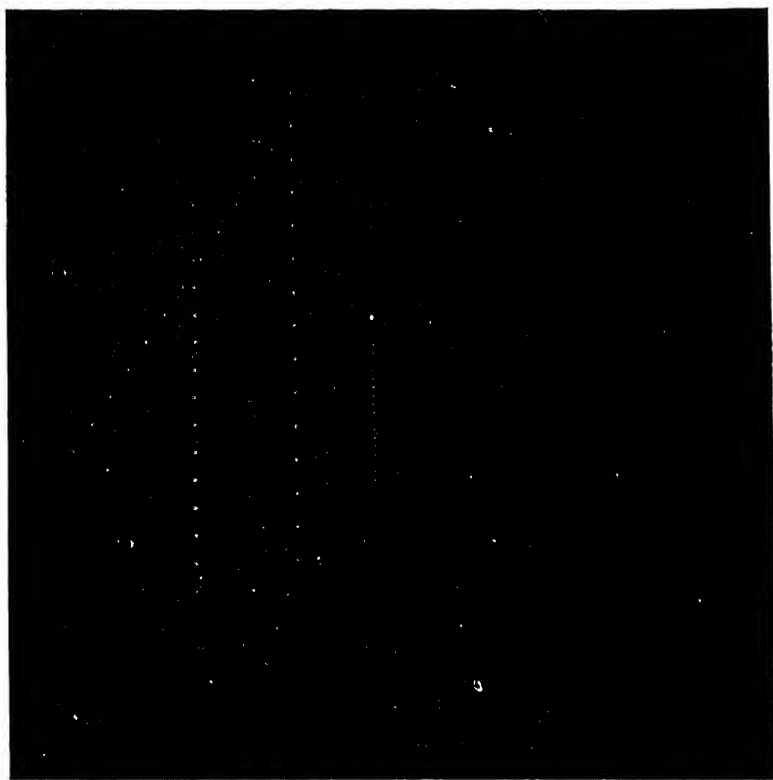


FIG. 14. — Photograph of deflected and undeflected paths of oil drops.

lated by measuring the distances between the images of the oil drop, and the angle  $\theta$  can be measured from the plate. Hence the



total charge  $ne$  carried by the oil drop can be computed. This is another way in which this experiment differs from Millikan's experiment. The values of  $n$  in this experiment were rather large, from about 40 to 300. The larger the oil drop used, the larger was the value of  $n$ .

Hopper and Laby did not measure the viscosity of the air in this experiment. Instead, they calculated the weighted mean of nine previously determined values and adopted  $\eta = 1830 \times 10^{-7}$  c.g.s. units for the viscosity of air at  $23^\circ \text{C}$ . With this value of  $\eta$  they obtained the value  $e = 4.802 \times 10^{-10}$  e.s.u. for the value of the electronic charge.

Using the method of least squares averaging instead of arithmetical averaging of the differences in the positions of the oil drops, and the value  $\eta = 1832.5 \times 10^{-7}$ , R. T. Birge recalculated the value of  $e$  from Hopper and Laby's measurements, and obtained  $e = 4.8137 \times 10^{-10}$  c.g.s. units for the electronic charge.

In this book we shall adopt the values

$$e = 4.802 \times 10^{-10} \text{ e.s.u.}$$

for the electronic charge,

$$N = 6.0234 \times 10^{23} \text{ per mole}$$

for the Avogadro number,

and  $F = 96487.7$  coulombs per gram-atomic weight

for the Faraday constant on the chemical atomic weight scale.

## 20. Electric Discharge through Gases

The phenomenon of the discharge of electricity through gases has been known for many years and has been utilized for the study of many problems connected with atomic structure. In its simplest form a discharge tube, Figure 15, consists of a long glass tube which has a circular electrode sealed into each end. A smaller side tube is sealed into it so that the pressure of the gas in the tube may be controlled by connecting it to a pumping system.

Let us consider the phenomena when there is air in the tube. Electrode  $A$  is connected to the positive side of a source of high potential such as an induction coil, and electrode  $C$  is connected to the negative side. When the pressure of the air inside the tube

is reduced to a few millimeters of mercury, the electric discharge fills the entire space between the electrodes with a pink or reddish glow. If the light from this tube is examined with a spectroscope, it will be found to consist of a series of lines characteristic of the

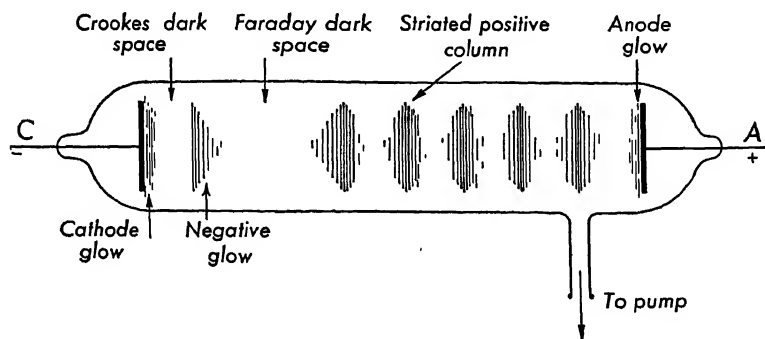


FIG. 15. — Appearance of the electrical discharge when the pressure of the air in the tube is about 0.1 mm of mercury.

gases within the tube. This type of discharge is frequently used in studying the spectra of various substances which can be obtained in the form of a gas or vapor.

When the pressure of the air within the tube is reduced to about 0.1 mm, the appearance of the discharge is approximately as follows: there is a bluish velvety glow around the cathode *C*, called the cathode glow; then a dark space, called the Crookes dark space, then the negative glow, followed by the Faraday dark space, and then, filling the rest of the tube up to the anode, is the striated positive column, and just around the anode is the anode glow.

The electric field is not uniform along the length of the tube but varies widely as we pass from one electrode to the other. The field is most intense in the Crookes dark space. The width of this dark space depends upon the pressure. As the pressure is reduced, this dark space widens out until at a pressure of about 0.001 mm, it fills the entire tube. At this pressure the positive column and negative glow have disappeared.

The phenomena observed in the discharge tube may be explained qualitatively by assuming that neutral molecules or atoms are ionized by collisions with ions or free electrons, and also that positive ions recombine with free electrons or with negative ions

to form neutral atoms or molecules. Under the action of the electric field, the positive ions are accelerated toward the cathode, while the negative ions and electrons are accelerated toward the anode, and thus acquire considerable kinetic energy. A charged particle will lose some of its energy in a collision with a neutral atom or molecule if this collision results in the ionization of the neutral particle, since, in the process of ionization, work must be done to separate the positive from the negative charges. On the other hand, energy will be released when an electron and an ion recombine to form a neutral atom or molecule. Some of this energy may be emitted in the form of light characteristic of the gas in the tube.

When the pressure of the gas is comparatively low, about 0.001 mm of mercury, the mean free path of the ions and atoms is very large, so that an ion or electron makes very few collisions in traversing the length of the tube. The positive ions, for example, will thus have a great deal of kinetic energy when they strike the cathode. The result of this bombardment of the cathode by the positive ions is that the cathode emits particles called *cathode rays*. These cathode rays travel away from the cathode in practically straight lines perpendicular to the surface of the cathode since the direction of motion is determined almost exclusively by the very intense field in the immediate neighborhood of the cathode.

These cathode rays can be deflected by electric and magnetic fields, and the direction of the deflection shows that they are negatively charged. Certain substances such as glass and zinc sulphide emit fluorescent radiations when bombarded by cathode rays. Cathode rays will also affect a photographic plate. These effects may be used to detect and measure the cathode rays.

## 21. Determination of $e/m$ for Cathode Rays

J. J. Thomson (1897) first successfully determined the nature of the cathode rays and showed that they are *electrons*; he was also the first to measure the ratio of the charge of the cathode ray to its mass, denoted by the symbol  $e/m$ .

A typical cathode ray tube, Figure 16, consists of a circular disk  $C$  as cathode, and a cylindrical anode  $A$  with a small circular hole bored through it along the axis of the cylinder. Two parallel plates of length  $L$  separated a distance  $d$  are placed behind the

anode and a zinc sulphide screen is placed at the end of the tube. A gas discharge is maintained between the anode and the cathode by means of some source of high potential. Most of the cathode rays coming from  $C$  strike the anode. Some cathode rays, how-

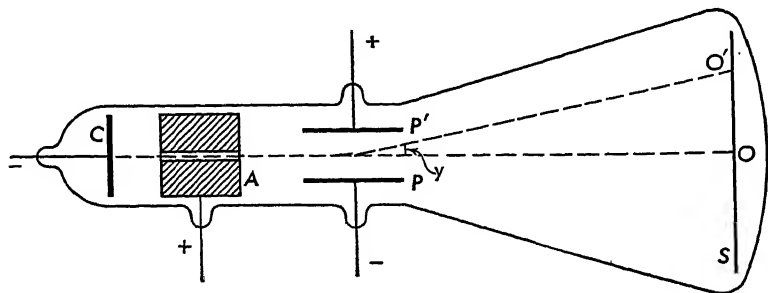


FIG. 16. — A typical cathode ray tube.

ever, pass through the hole in the anode and proceed with uniform velocity  $v$  until they strike the fluorescent screen  $S$  at  $O$ , producing a bright spot.

If a difference of potential  $V$  is applied between the plates  $PP'$ , then the cathode rays will be deflected upward toward the positive plate by a force  $F$ , given by

$$F = \frac{V}{d}e = ma, \quad (19)$$

in which  $e$  is the charge on a cathode ray, and  $m$  is its mass. Since the electric field between the plates is uniform, the path of the cathode rays will be parabolic in the region between the plates. After they leave this space, they will continue with uniform rectilinear motion until they strike the screen at  $O'$ . To determine  $e/m$ , the acceleration of the particle must be measured. This can be done indirectly by noting that the amount of the deflection  $y$  parallel to the electric field between the plates is given by

$$y = \frac{1}{2}at^2, \quad (20)$$

and that the time  $t$  during which the particle is accelerated is given by

$$t = \frac{L}{v},$$

where  $L$  is the length of the plates and  $v$  is the velocity of the rays

parallel to the plates. The velocity of the cathode rays can be found very simply with the aid of a magnetic field applied at right angles to the electric field and acting over the same length of path  $L$ . This magnetic field may be supplied by an electromagnet having its  $N$  pole on the side toward the reader and its  $S$  pole on the side of the tube away from the reader. If the intensity of the magnetic field is  $H$ , the cathode ray will experience an additional force  $F_1$  given by

$$F_1 = Hev. \quad (21)$$

The direction of the deflection due to the magnetic field will be downward; this field can be adjusted so that the cathode rays are not deviated from their original path, as is evidenced by the return of the fluorescent spot to point  $O$ . This will occur when the forces due to the electric and magnetic fields are equal, in which case

$$\frac{V}{d}e = Hev, \quad (22)$$

from which

$$v = \frac{V}{dH}. \quad (23)$$

The expression for  $e/m$  thus becomes

$$\frac{e}{m} = 2 \frac{V}{dH^2 L^2} y. \quad (24)$$

All the quantities on the right-hand side of the equation are measurable quantities. The deflection  $y$  at the end of the path in the electric field is proportional to the distance  $OO'$  which is measured on the fluorescent screen.

A consistent set of units must be used for all the quantities in equations (19) to (24). If  $e$ ,  $V$ , and  $H$  are expressed in the e.m. system of units, and the other quantities in c.g.s. units, the value of  $e/m$  will be expressed in e.m.u. of charge per gram. The present accepted value of  $e/m$  determined by the above method is

$$\frac{e}{m} = 1.7592 \times 10^7 \text{ e.m.u./gm.} \quad (25)$$

Measurements of  $e/m$  with electrons from other sources (for

example, electrons emitted by hot filaments and electrons ejected from metallic plates by the action of light) all yield the same value within the limits of experimental error. The value given above is the weighted average of many such determinations.

The mass of an electron may now be computed using the above value of  $e/m$  and the known value of  $e$ . Using  $e = 1.602 \times 10^{-20}$  e.m.u., we find the mass of an electron to be

$$m = 9.106 \times 10^{-28} \text{ gm.}$$

It is interesting to compare the mass of an electron with that of the hydrogen atom, the lightest atom known. The mass of a hydrogen atom can be determined from its atomic weight, which is 1.00813, and the Avogadro number  $N = 6.0234 \times 10^{23}$ . This yields for the mass of a hydrogen atom  $M = 1.674 \times 10^{-24}$  gm. The ratio of the mass of a hydrogen atom to that of an electron is

$$\frac{M}{m} = 1838.$$

## 22. Isotopes

One of the hypotheses introduced by Dalton into atomic theory was that all of the atoms of any one element were identical in all respects, including that of mass. On this basis, the numbers representing the weights of the elements would give the relative masses of the atoms of these elements. Others, however, suggested that the atoms of any one element need not be identical in mass, that the numbers representing the chemical atomic weights are only average values of the different weights of the atoms of the particular element. The basis of this suggestion was the hope that the weights of all atoms could be expressed by integral numbers. Prout (1815) first formulated this idea in his hypothesis that the atoms of all the elements are made up of hydrogen atoms. If this hypothesis were correct, the weights of all the atoms would be expressed as integers with that of hydrogen as unity. Careful determinations of atomic weights, however, showed that the atomic weights of many elements were not integral numbers relative to that of hydrogen. In the latter half of the nineteenth century Prout's hypothesis had been discarded in favor of Dalton's hypothesis. But with the discovery of radioactivity at the end of the

nineteenth century and the study of the radioactive elements produced in the process of natural radioactive disintegration (§ 108), sufficient experimental evidence was presented to support the suggestion that the atoms of an element need not be identical in mass, and renewed efforts were made to determine whether atomic masses could be represented by whole numbers. Several groups of elements having identical properties but different atomic weights are formed in the process of radioactive disintegration. This means that the elements within any one group must occupy the same place in the periodic table of the elements (Appendix III). Soddy suggested the name *isotopes* for the elements occupying the same place in the periodic table.

The search for isotopes among the nonradioactive elements was begun by J. J. Thomson about 1910. The first element successfully investigated was neon. It is the lightest element whose atomic weight, 20.2, differs appreciably from an integral number. The method used was the determination of the ratio of the charge to the mass of the positive ions formed in an electrical discharge tube containing neon gas.

### 23. Positive-Ray Analysis

In Thomson's method of positive-ray analysis, positive ions are formed in the space between the anode *A* and the cathode *C*

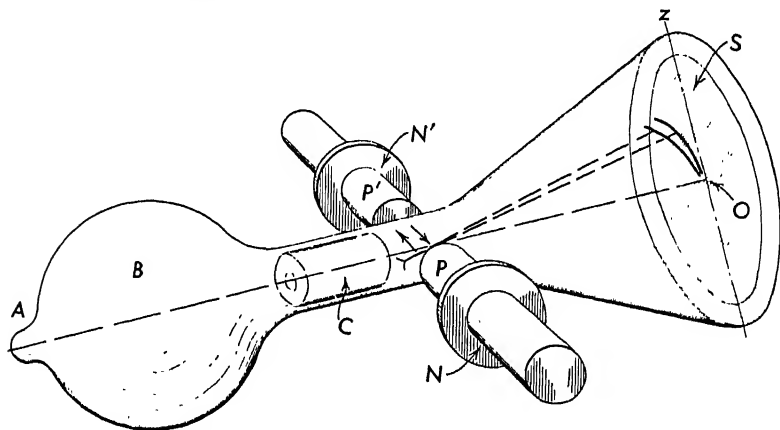


FIG. 17. — J. J. Thomson's positive ray tube.

of the tube *B*, Figure 17, operated at a voltage of about 50,000 volts. The cathode consists of a long cylinder about 7 cm long

with a hole about a millimeter in diameter along the axis of the cylinder. Those positive ions which travel along the axis of the tube pass through the hole in the cathode and emerge as a very narrow beam of positive ions. When there is no electric or magnetic field acting on these ions, they strike the fluorescent screen or photographic plate  $S$  at point  $O$ .

In analyzing the beam, both electric and magnetic fields are used. The pole pieces  $PP'$  of an electromagnet are placed outside the tube just behind the cathode. These pole pieces are insulated from the rest of the electromagnet by means of thin mica sheets  $NN'$ , so that the pole pieces can be used as the plates of a capacitor by connecting them to a battery. The electric and magnetic fields are parallel and act simultaneously on the beam of positive ions passing through them.

Assume that the beam moves in the  $x$  direction and that the electric and magnetic fields are in the positive  $y$  direction. Because of the action of the electric field alone, the positive ions will be accelerated in the  $y$  direction by a force

$$F_y = YE = Ma_y, \quad (26)$$

where  $Y$  is the electric field intensity due to the difference of potential across the capacitor plates,  $E$  the charge carried by the positive ion,  $M$  its mass, and  $a_y$  its acceleration in the  $y$  direction. The deflection of the ion in the  $y$  direction will be

$$y = \frac{1}{2}a_y t^2 = \frac{1}{2} \frac{YE}{M} \frac{L^2}{v^2}, \quad (27)$$

where  $L$  is the length of the capacitor plates and  $v$  is the original velocity of the ion in the  $x$  direction.

The force on an ion due to the magnetic field is perpendicular to both  $H$  and  $v$ , and for small deflections this force may be considered as accelerating the ion in the  $z$  direction. This force is

$$F_z = HEv = Ma_z, \quad (28)$$

where  $H$  is the intensity of the magnetic field and  $a_z$  is the acceleration of the ion in the  $z$  direction. The deflection in the  $z$  direction is given by

$$z = \frac{1}{2}a_z t^2 = \frac{1}{2} \frac{HE}{M} \frac{L^2}{v}. \quad (29)$$



It will be noticed that the deflection produced by the magnetic field varies inversely as the first power of the velocity while the deflection produced by the electric field varies inversely as the second power of the velocity. Eliminating  $v$  from the equations (27) and (29), we get

$$z^2 = \frac{L^2 H^2}{2 Y} \frac{E}{M} y = C \frac{E}{M} y, \quad (30)$$

which is the equation of a parabola, since  $C = \frac{L^2 H^2}{2 Y}$  is a constant in any one experiment. All positive ions with the same value of  $E/M$  will form a single parabola; those moving with the greatest velocity will be deflected least and will be closest to the origin, which is the original undeflected position  $O$ . If the direction of the magnetic field be reversed during one half of the exposure, the negative half of the parabola will be obtained and thus give a convenient method for determining the position of the  $y$  axis on the photographic plate.

The first element to be analyzed by the parabola method was neon of atomic weight 20.2. Two parabolas were identified as due to two isotopes of neon of atomic weights 20 and 22 respectively,

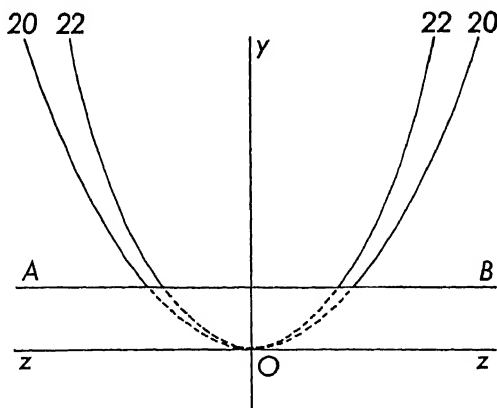


FIG. 18. — Graph showing the two parabolas of the neon isotopes. The points of intersection of the line  $AB$  with the parabolas represent the positions of the ions of maximum energy; all other ions reach points above  $AB$ .

Figure 18. Several other elements were analyzed by this method. While the parabola method was capable of showing the existence of isotopes, it was not sufficiently accurate for the precise determina-

tion of the masses of these isotopes. Aston redesigned the instrument so that it became an instrument of precision for the determination of the masses of isotopes and their relative abundance in a given sample of material. This instrument has received the name of mass spectrograph. Mass spectrographs of somewhat different designs were developed by Dempster, Bainbridge, and other experimenters.

## 24. Aston's Mass Spectrograph

Aston's method is an improvement on J. J. Thomson's method in that all positive ions of the same mass fall on a single line on the photographic plate instead of being spread out into a parabola.

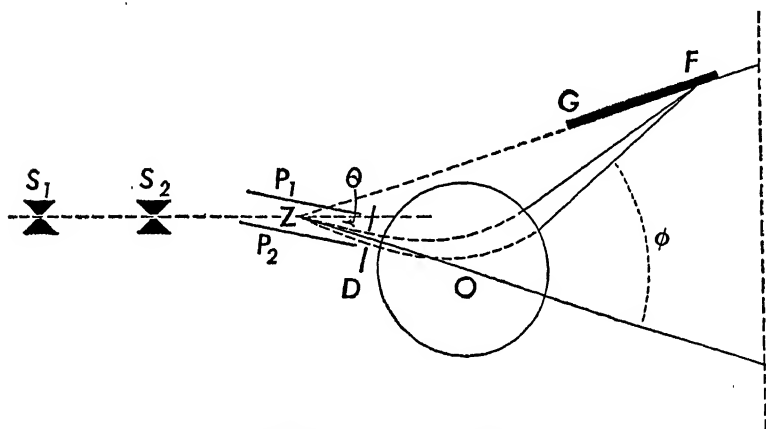


FIG. 19. — Diagram of Aston's mass spectrograph.

The stream of positive ions coming through the hole in the cathode of the discharge tube passes through two defining slits  $S_1$  and  $S_2$ , Figure 19, and then into the electric field between the capacitor plates  $P_1 P_2$ . The deflections of the ions depend upon their *energies*. Those of kinetic energy  $\frac{1}{2} Mv^2$  and charge  $E$  are deflected parallel to the electric field  $Y$  between the plates by an amount

$$d_1 = \frac{1}{2} \frac{YE}{M} \frac{L^2}{v^2}, \quad (31)$$

where  $L$  is the length of the path between the plates. The diaphragm  $D$  is placed behind the plates so as to permit only those ions which have been deflected through the same distance  $d_1$  to pass through its opening. This narrow bundle of rays which has

been deflected through a small angle  $\theta$  is allowed to pass through the diaphragm  $D$  into the magnetic field  $H$  at right angles to the plane of the paper. This magnetic field is produced by a large electromagnet, the position of the pole pieces being indicated by the large circle in the diagram. This magnetic field deflects the ions in a direction opposite to that due to the electric field by an amount

$$d_2 = \frac{b^2}{2v} \frac{HE}{M} \quad (32)$$

where  $b$  is the length of the path in the magnetic field.

Those positive ions which pass through the diaphragm  $D$  have a small range of energies depending upon the size of the slit in the diaphragm and the position of this slit. As shown by equation (31), the ions with smaller energies are deflected downward more than the ions of larger energies; that is, the deflection in the electric field is inversely proportional to the square of the velocity of the ion. The magnetic field is directed so as to deflect the particles upward, and the amount of this deflection varies inversely as the first power of the velocity of the ions as shown by equation (32). The paths of the slow-moving ions will therefore intersect those of the faster-moving ions at some point  $F$  which is determined by the geometry of the apparatus. Thus ions having the same value of  $E/M$  but slightly different energies are brought to a single focus on the photographic plate  $GF$ . Other ions having the same range of energies but a different value of  $E/M$  are brought to a focus at a different point on the photographic plate. It can be shown that these foci for different values of  $E/M$  lie along a line  $ZF$  passing through the center  $Z$  of the plates of the capacitor and that the angle between  $ZF$  and the original path of the ions is equal to  $\theta$ . The photographic plate is placed along this line to detect the positive ions.

Each line on the photographic plate represents a definite value of  $E/M$ . Several different methods are used for the determination of the masses. In general, substances whose masses are accurately known are mixed with elements whose isotopes are to be determined. The positions of the lines representing the known masses are then used as reference points in measuring the masses of the isotopes. Aston's mass spectrometer has been used not only for

the discovery of isotopes of elements but also for the precise determination of their atomic masses. The importance and significance of these results will become apparent as we proceed with our study of atomic physics.

## 25. Dempster's Mass Spectrograph

Dempster's mass spectrograph differs from that of Aston in that the positive ions all acquire practically the same energy be-

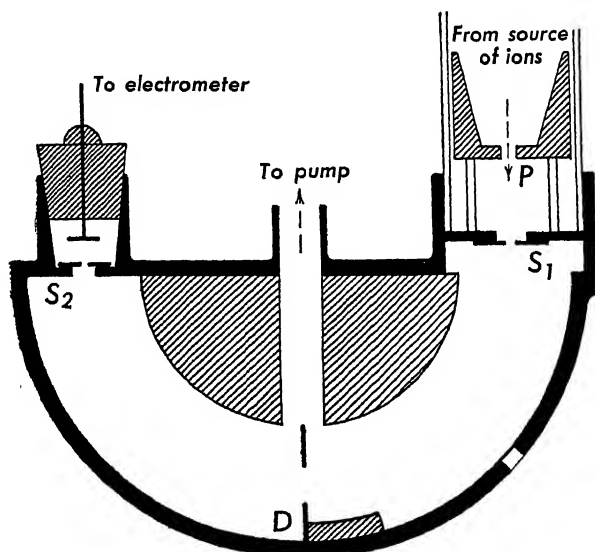


FIG. 20. — Diagram of Dempster's mass spectrograph.

fore entering the magnetic field. The magnetic field is large enough and the path through it long enough to deflect these ions through  $180^\circ$ . The source of positive ions is usually a salt containing the element to be investigated. This salt is deposited on the anode. When the anode is heated by an electric current, or by the bombardment of electrons from a filament, positive ions are liberated from the anode. In later work with metallic elements, the metal itself was vaporized and the vapor then ionized by bombardment with electrons. The positive ions pass through a hole in an iron plate  $P$ , Figure 20, and are accelerated to the slit  $S_1$  by a difference of potential  $V$  between  $P$  and  $S_1$ . The energy acquired by the ions in going from  $P$  to  $S_1$  is

$$VE = \frac{1}{2}Mv^2. \quad (33)$$

The ions entering through  $S_1$  are bent in the form of a semicircle by a magnetic field  $H$  perpendicular to the plane of the paper, and focused upon the second slit  $S_2$ . The radius  $R$  of the semi-circular path traversed by these ions is given by

$$HEv = \frac{Mv^2}{R}. \quad (34)$$

The value of  $E/M$  for the ions which reach  $S_2$  is then given by

$$\frac{E}{M} = \frac{2V}{H^2 R^2}. \quad (35)$$

The ions which pass through  $S_2$  are detected and measured by the charge deposited on the plate connected to the electrometer.

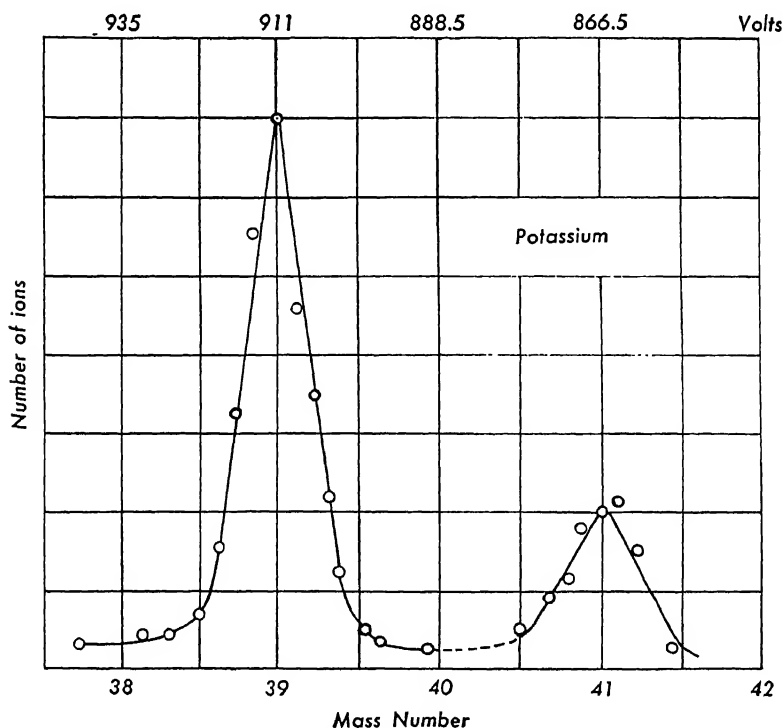


FIG. 21. — Curve obtained by Dempster showing two of the isotopes of potassium of mass numbers 39 and 41.

One of the advantages of this instrument is that even though the beam of ions which enters the slit  $S_1$  is slightly divergent, the effect of the magnetic field is to reconverge the beam after deflect-

ing it through  $180^\circ$ . It can be shown that if a divergent beam of ions is sent perpendicularly through a magnetic field in such a way that the central part of the beam enters and leaves the magnetic field normal to the edges of the pole pieces producing the magnetic field, then the beam of ions will be brought to a focus on a line which extends from the source through the center of curvature of the central beam. The magnetic field thus acts as a *lens* and forms an image of the slit through which the ions pass.

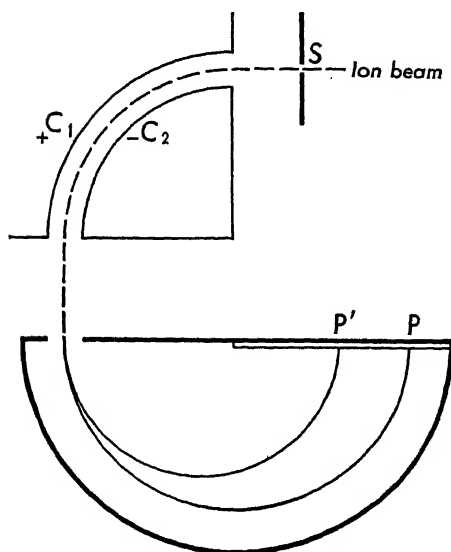


FIG. 22. — Dempster's new mass spectrograph utilizing cylindrical capacitor plates.

measured by the electrometer for different values of the potential  $V$ . A typical curve giving the results of the experiment on potassium is shown in Figure 21. The two peaks correspond to two isotopes of potassium of mass numbers 39 and 41.

In practice, the magnetic field is kept at a constant value and the difference of potential  $V$  between  $P$  and  $S_1$  is varied. The number of ions passing through  $S_2$  is then



FIG. 23. — A photograph of the isotopes of ytterbium obtained with Dempster's new mass spectrograph. The mass numbers of the isotopes can be obtained from the number scale printed above the lines. (Reprinted from a photograph supplied to the author by Professor A. J. Dempster.)

Recently Dempster redesigned his mass spectrograph so that the positive ions coming through the slit  $S$  pass through a radial electric field between two cylindrical capacitor plates  $C_1$  and  $C_2$ , Figure 22, and then enter the magnetic field perpendicular to the

plane of the diagram. The ions are recorded on a photographic plate  $PP'$ . The advantage of this arrangement is that ions of the same mass but of slightly different velocities are focused at the same place on the photographic plate. A typical mass spectrogram obtained with this apparatus is illustrated in Figure 23, which shows the different isotopes of the element ytterbium.

## 26. Bainbridge's Mass Spectrograph

In the mass spectrograph designed by Bainbridge, the positive ions pass through the narrow slits  $S_1$  and  $S_2$  and then into a *velocity selector* so that the ions coming through  $S_3$  are homogeneous in

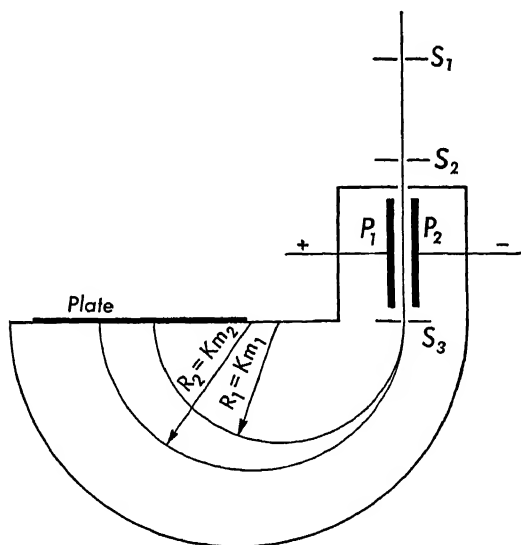


FIG. 24. — Bainbridge's mass spectrograph utilizing a velocity selector.

velocity but not in energy. The velocity selector consists of a set of capacitor plates  $P_1P_2$ , Figure 24, connected to a battery and a magnetic field perpendicular to the plane of the paper. The electric and magnetic fields acting on the ions moving between the plates will permit those ions to pass through which satisfy the condition that

$$v = \frac{V}{dH}, \quad (23)$$

where  $v$  is the velocity of the ions,  $V/d$  the intensity of the electric

field between the plates, and  $H$  the intensity of the magnetic field in this region. The ions which pass through slit  $S_3$  are now acted upon by a second magnetic field  $H_1$  perpendicular to the plane of the paper. The force acting on each ion is given by

$$H_1 E v = \frac{M v^2}{R},$$

from which

$$M = \frac{H_1 E}{v} R = K R. \quad (36)$$

The ions travel in a circular path for  $180^\circ$  and then strike a photographic plate. Since the ions all have the same velocity, the masses of the ions are directly proportional to the radius  $R$  of the circular path. Thus the mass scale of this instrument is linear.

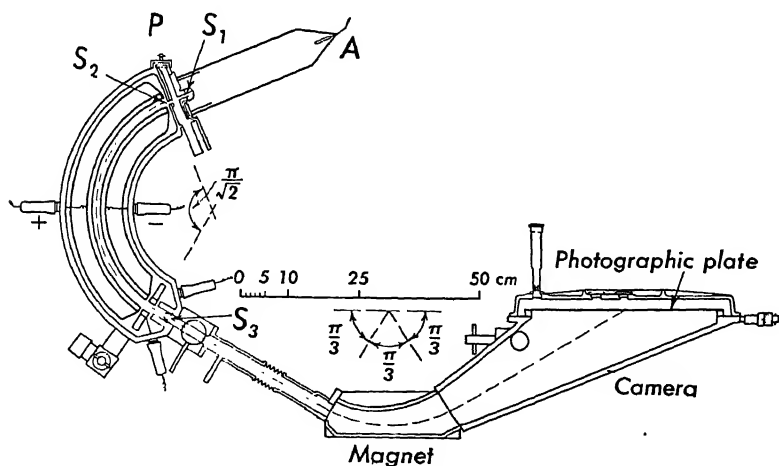


FIG. 25. — The mass spectrograph developed by Bainbridge and Jordan.

A mass spectrograph of high precision and resolving power has recently been developed by Bainbridge and Jordan. In this apparatus a beam of ions from the gas discharge tube  $A$ , Figure 25, passes through a narrow slit  $S_1$  at the end of the tube, and enters a radial electric field through a second slit,  $S_2$ . The ions are bent through an angle of  $\pi/\sqrt{2}$  radians by the radial electric field and emerge through the slit  $S_3$ . They then continue in straight lines until they reach the magnetic field where they are bent through an angle of  $\pi/3$  radians, after which they travel in straight lines



to the photographic plate. In this arrangement of electric and magnetic fields, ions with the same value of  $E/M$  and a distribution of velocities within a certain range are focused at a single

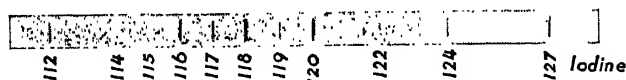


FIG. 26. — A photograph of the ten isotopes of tin obtained by Bainbridge and Jordan. The mass numbers of the isotopes are given in the figure. (From a photograph supplied by Bainbridge and Jordan.)

place on the photographic plate. The mass scale is linear over a large portion of the plate.

The mass spectrogram of tin, Figure 26, showing its ten isotopes, is typical of the results obtained with this instrument. The relative abundance of the different isotopes can be obtained from measurements of the densities of the different lines. An indication of the resolving power of the instrument can be obtained from Figure [27, which shows the separation of the ions CO and  $N_2$ , whose masses differ by 1 part in 2500. Figure 28 shows the separation between the ion of deuterium,  $H_2^2$ , and the molecular hydrogen ion,  $H_2^1$ , whose masses are 2.01473 and 2.01626, respectively.

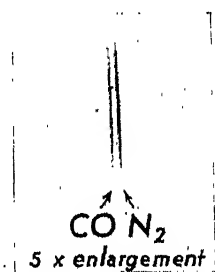


FIG. 27. — Photograph obtained with the Bainbridge and Jordan mass spectrograph showing the separation of the ions CO and  $N_2$ . Enlarged 5X. (From a photograph supplied by Bainbridge and Jordan.)

## 27. Isotopic Masses and Nuclear Constitution

As the result of the investigations with the mass spectrograph, it has been established that about 280 different isotopes occur in nature. The atomic weights of these isotopes differ very little from whole numbers. The range of atomic weights runs from 1 to 238. The number of isotopes per element varies from one for elements fluorine and gold, to ten for the element tin. Since there are about 92 different elements, there are, on the average, about 3 isotopes per element. A table of known stable isotopes and their relative abundance is given in Appendix V.

It is now well established from experiments on the scattering of alpha particles (§ 35), and from the study of X-ray spectra

(§ 101), that an atom consists of a very small nucleus with a net positive charge, surrounded by a sufficient number of electrons so that the normal atom is electrically neutral. The results of these experiments lead to the conclusion that the charge of the nucleus

of an atom can be represented by  $Ze$ , where  $e$  is numerically equal to the charge of an electron but positive in sign, and  $Z$  is an integer. There are also  $Z$  electrons outside the nucleus of a neutral atom. The number  $Z$  is called the *atomic number* of the element. The atomic number  $Z$  ranges in value from 1 to 94 for elements occurring in nature.

The isotopes of any one element all have the same atomic number  $Z$  but have different atomic weights. One conclusion from this fact is that the isotopes of any element have exactly the same number of extranuclear electrons. The chemical properties of an element must therefore be ascribed to the arrangement and action of the electrons outside the nucleus. Differences in atomic weights among isotopes of the same element must therefore be due to differences in nuclear structure.

The fact that the atomic weights of all isotopes are nearly integers indicates that nuclei are made up of particles of unit atomic weight, with the unit of weight equal to one sixteenth the weight of the nucleus of oxygen of atomic weight 16.00. It will be convenient to introduce the term *mass number* for the integer nearest the value of the atomic weight of the isotope.

At present two particles of nuclear size and of mass nearly unity are known. These are the *proton* and the *neutron*. The proton is the positively charged nucleus of the hydrogen atom of

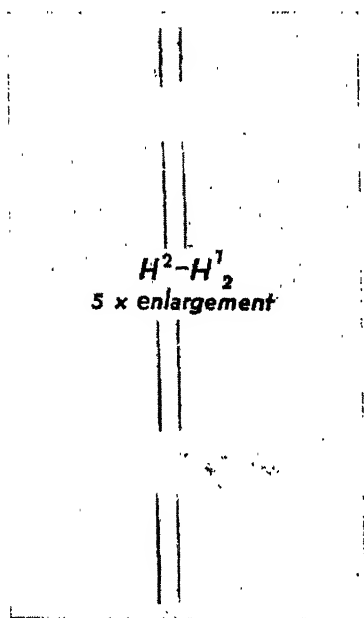


FIG. 28. — Photograph obtained with the Bainbridge and Jordan mass spectrograph showing the separation of the ions of deuterium,  $H^2$  and molecular hydrogen  $H^1_2$ . (From a photograph supplied by Bainbridge and Jordan.)

mass number 1. This hydrogen atom consists of a positively charged nucleus, called the proton, and an electron outside the nucleus. Since the mass of the hydrogen atom is about 1840 times the mass of the electron, practically the entire mass of the hydrogen atom is due to the proton. The mass of the proton on our scale of atomic mass units is 1.00756. The other nuclear particle of unit mass was discovered experimentally in 1932 by Chadwick as a result of experiments on artificial disintegration (§ 117). The neutron has no electric charge and its mass is 1.00893.

Prior to the discovery of the neutron, the nucleus was supposed to be made up of protons and electrons. With the tremendous amount of new experimental data on nuclear phenomena which have become available in the past few years, it became necessary to discard this hypothesis in favor of one in which the nucleus consists of protons and neutrons. There are several arguments against the existence of electrons in the nucleus. Some of these arguments will be presented in the appropriate places in the text.

On the hypothesis that a nucleus of an atom consists of protons and neutrons, the mass number  $A$  represents the total number of particles in the nucleus. The atomic number  $Z$  is the number of protons in the nucleus, and  $A - Z$  is the number of neutrons in the nucleus. The isotopes of any one element differ only in the number of neutrons in the various nuclei. The convention adopted for representing this information can be illustrated with a typical case such as oxygen. The atomic number of oxygen is 8; there are three known stable isotopes of oxygen of mass numbers 16, 17, and 18. These are represented by the symbols  ${}_8\text{O}^{16}$ ,  ${}_8\text{O}^{17}$ , and  ${}_8\text{O}^{18}$ , respectively, the atomic number being written as a subscript on the lower left-hand side of the chemical symbol of the element, and the mass number as a superscript on the upper right-hand side of the chemical symbol.

The results of the measurements of the atomic masses of the isotopes can be presented most conveniently by considering the deviations of the atomic masses from the whole-number rule. The *mass defect* of an atom is defined as

$$\Delta = M - A \quad (37)$$

where  $\Delta$  is the mass defect,  $M$  the atomic mass of the isotope, and

$A$  its mass number. Aston introduced the term *packing fraction* defined by the relation

$$P = \frac{\Delta}{A} = \frac{M - A}{A}, \quad (38)$$

where  $P$  is the packing fraction, or the mass defect per elementary particle in the nucleus.

When the packing fraction is plotted against the mass number, Figure 29, a curve is obtained with several interesting features.

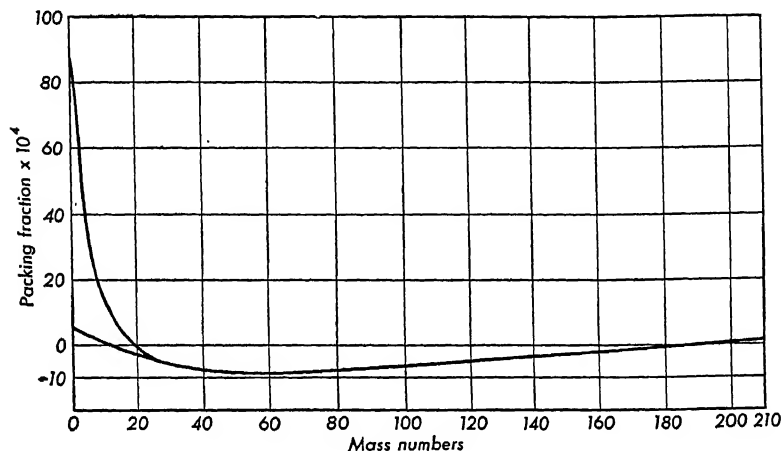


FIG. 29. — The “packing fraction” curve.

The packing fractions have small negative values for the elements whose mass numbers lie between 20 and 200; they have positive values for mass numbers greater than 200 and also for mass numbers less than 20. For most of the lighter elements the packing fractions have very large positive values; the only exceptions are the elements  ${}^4_2\text{He}$ ,  ${}^{12}_6\text{C}$ , and  ${}^{16}_8\text{O}$ . The packing fraction of  ${}^{16}_8\text{O}$  is, of course, zero by definition.

## 28. Mass and Energy

It might at first be supposed that the mass of a nucleus should be the sum of the masses of its constituent particles. A survey of the data, however, shows that the mass of a nucleus is, in general, less than the sum of the masses of its constituent particles in the free state. To account for this difference in mass, use is made of the *principle of equivalence of mass and energy*, a principle first de-

veloped by Einstein in his theory of relativity. Einstein's principle states that a mass  $m$  is equivalent to an amount of energy  $\mathcal{E}$ , and the equation relating these quantities is

$$\mathcal{E} = mc^2, \quad (39)$$

where  $c$  is the speed of light. If  $\Delta m$  is the decrease in mass when a number of particles combine to form the nucleus of an atom, then this principle states that an amount of energy

$$\Delta \mathcal{E} = \Delta mc^2 \quad (40)$$

is released in this process. This amount of energy represents the *binding energy* of the particles in the nucleus; if the binding energy is large, the nucleus is stable.

While the unit of energy in the c.g.s. system is the erg, other units of energy have been found to be more convenient in atomic physics. Since mass and energy are equivalent, the atomic unit of mass (a.m.u.), which is one sixteenth of the mass of one atom of  ${}_8\text{O}^{16}$ , is frequently used as a unit of energy in nuclear physics. Using the relationship  $\mathcal{E} = mc^2$ , we get

$$1 \text{ a.m.u.} = 1.49 \times 10^{-3} \text{ ergs.} \quad (41)$$

Another convenient energy unit is the *electron volt*, which is the kinetic energy an electron acquires when it is accelerated in an electric field produced by a difference of potential of one volt. Since the work done upon an electron by a difference of potential  $V$  is  $Ve$ ,

$$1 \text{ electron volt} = 1 \text{ ev} = 1.60 \times 10^{-12} \text{ ergs.} \quad (42)$$

Other convenient units are

$$1 \text{ kev} = 1000 \text{ ev}$$

$$1 \text{ Mev} = 10^6 \text{ ev.}$$

The conversion factor for a.m.u. to Mev is

$$1 \text{ a.m.u.} = 931.8 \text{ Mev.} \quad (43)$$

The mass of an electron, for example, is frequently expressed in terms of its energy equivalent in electron volts. Since its mass is

$$m = 9.11 \times 10^{-28} \text{ gm}$$

its energy in ergs is from equation (39)

$$\mathcal{E} = 8.18 \times 10^{-7} \text{ ergs}$$

which is equivalent to

$$\mathcal{E} = 0.515 \text{ Mev.} \quad (44)$$

The energy of an electron at rest, in a.m.u. is

$$\mathcal{E} = 0.00055 \text{ a.m.u.} \quad (45)$$

To illustrate the relationship between mass and energy and the meaning of binding energy of a nucleus, let us consider the isotope of lithium of mass number 7. Since its atomic number is 3, the lithium nucleus is composed of 3 protons and 4 neutrons. The masses of these particles, including one electron with each proton and three electrons with the lithium nucleus, are

$$\begin{aligned} 4_0n^1 &= 4 \times 1.00893 = 4.03572 \\ 3_1H^1 &= 3 \times 1.00813 = 3.02439 \\ 4_0n^1 + 3_1H^1 &= \underline{7.06011} \\ {}_3Li^7 &= \underline{7.01816} \\ \Delta m &= 0.04195 \text{ a.m.u.} = 39.09 \text{ Mev.} \end{aligned}$$

In subtracting, the masses of the electrons cancel out. The difference in mass between these particles in the free state and in the nucleus of lithium is 0.04195 a.m.u., or the binding energy of the  ${}_3Li^7$  nucleus is 39.09 Mev. The nucleus of  ${}_3Li^7$  thus has a very stable structure. In any attempt to disrupt this nucleus, energy will have to be supplied from some external source.

It may be noted that the use of atomic masses rather than nuclear masses in calculations of nuclear energy changes is correct in all cases except the one in which a nuclear transformation takes place with the emission of a positron (§ 120).

## 29. Discovery of Natural Radioactivity

The discovery of radioactivity by Henri Becquerel in 1896, shortly after the discovery of X rays by Röntgen in 1895, marked the beginning of the modern approach to the study of the structure of the atom. Becquerel was interested in determining whether there was any relationship between the phosphorescence of certain salts after irradiation by ordinary light and the fluorescence of the

glass of an X-ray tube which was emitting X rays. One of the salts used was the double sulphate of uranium and potassium. He wrapped a photographic plate in very thick black paper, placed a crystal of the uranium salt on it and exposed the whole thing to sunlight. When the plate was developed, a silhouette of the phosphorescent substance appeared in black on the negative, showing that radiations came from the uranium salt. He then varied this experiment by placing a coin, or a metallic screen pierced with an open-work design, between the uranium salt and the photographic plate, and, on developing the plate, found the image of each of these objects on the negative.

In attempting to repeat the above experiments, Becquerel ran into some cloudy weather; he put all the materials away in a drawer and waited for a sunny day. A few days later, he developed this photographic plate and found that the dark silhouettes again appeared with great intensity, even though the salt had not been exposed to much sunlight. To make certain that this activity goes on without the aid of an external source of light, he built a light-tight box and performed a series of experiments with the photographic plate at the bottom of the box. In one experiment uranium salt crystals were put directly on the photographic plate; he obtained very dark silhouettes of the crystals. In another experiment he put a piece of aluminum between the salt crystals and the photographic plate; he again obtained silhouettes, but these were slightly less intense than those obtained without the aluminum plate. He then concluded that the active radiations came from the uranium salt and that the external light had no influence whatever on this activity.

Becquerel then proceeded to experiment with different compounds of uranium, both in crystalline form and in solutions, and found that radiations were emitted by all of them, whether they did or did not phosphoresce. He was thus led to the conclusion that it was the element uranium which was responsible for these radiations. He confirmed this conclusion by repeating the above experiments with some commercial powdered uranium. Further experiments showed that the radiations from uranium would also cause the discharge of electrically charged bodies. Shortly thereafter, Rutherford investigated the penetrating power of the radiations from uranium and showed that they were of two types, a

very soft radiation easily absorbed in matter which Rutherford called *alpha rays*, and a more penetrating type of radiation which he called *beta rays*. It is apparent now that the radiation which affected the photographic plate in Becquerel's experiment consisted of beta rays.

The method used by Rutherford in studying these radiations was an electrical method based upon the ionization produced by the radiation in its passage through a gas. The ionization currents so produced can be used for quantitative measurements. Using such a method, Mme Curie showed that the activity of any uranium salt was directly proportional to the quantity of uranium in the salt, thus demonstrating that radioactivity is an atomic phenomenon.

M. and Mme Curie subjected uranium pitchblende to a systematic chemical analysis, and, using an electrical method, measured the activity of the different elements obtained from the pitchblende. In 1898 they succeeded in discovering two new radioactive elements, polonium and radium. Radium was precipitated in the form of radium chloride. The activity of radium was found to be more than a million times that of a similar quantity of uranium. In 1910, Mme Curie and Debierne obtained pure radium metal by means of electrolysis of the fused salt. The atomic weight of radium as determined by Honigschmidt is 225.97. Radium fits in at the end of the second group in the periodic table; it is chemically similar to calcium, strontium, and barium. Many more radioactive substances have been discovered since then, thus filling many of the gaps which existed in the periodic table prior to the discovery of radioactivity.

### 30. Radiation Emitted by Radioactive Substances

In addition to the alpha and beta rays, naturally radioactive substances emit a third type of radiation called *gamma rays*. The existence of these three distinct types of radiation can be demonstrated very simply. A small quantity of some radioactive salt is placed at the bottom of a long narrow groove in a lead block, Figure 30. A fairly parallel beam will come from the radioactive material *R* through the slit *S*. Rays going in all other directions will be absorbed by the lead. This lead block is placed in an airtight chamber and a photographic plate *P* is placed a short distance



above it. To avoid absorption of the rays, the air is pumped out of the chamber. A strong magnetic field is applied at right angles to the plane of the paper.

After a reasonable exposure, three distinct lines will be found on the photographic plate. If the magnetic field is directed away from the reader, the positively charged particles or alpha rays will be deflected to the left in the figure, the negatively charged particles or beta rays will be deflected to the right, and the neutral rays or gamma rays will not be deviated at all.

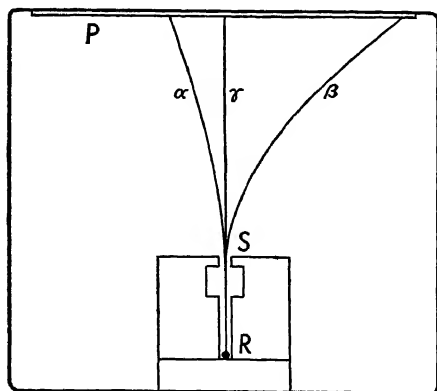


FIG. 30. — Paths of the rays from a radioactive substance *R* in a magnetic field perpendicular to the plane of the paper. The magnetic field is directed into the paper.

### 31. Beta Rays and the Variation of Mass with Velocity

The above qualitative experiment shows that beta rays are negatively charged particles. The speeds with which beta rays are expelled from radioactive substances can be found by allowing these particles to pass through electric and magnetic fields. The results of these experiments show that the beta rays from any one radioactive element have speeds which vary over a large range of values. In general these speeds are very great, some as high as 0.9995 times the speed of light (for beta rays from mesothorium 2).

One of the predictions of Einstein's special theory of relativity is that the mass of a particle should vary with its velocity according to the equation

$$m = \frac{m_0}{\sqrt{1 - \frac{v^2}{c^2}}}, \quad (46)$$

where  $m_0$  is the mass of the particle when at rest,  $m$  its mass when it is moving with velocity  $v$ , and  $c$  the velocity of light. The fast-moving beta rays provide convenient particles for testing this relationship. Kaufmann, Bucherer, and others performed a series

of experiments on the determination of  $e/m$  of beta rays of different speeds. Assuming, as a consequence of the laws of electrodynamics, that the total charge on a particle is conserved, then any variation in the value of  $e/m$  with the speed of the particle should be due to the variation in mass according to the equation

$$\frac{e}{m} = \frac{e}{m_0} \sqrt{1 - \frac{v^2}{c^2}}. \quad (47)$$

In Bucherer's experiment, a small grain of radium fluoride  $R$  was placed between two parallel circular disks  $AB$  at their centers, Figure 31. The spacing between the disks was about 0.25 mm.

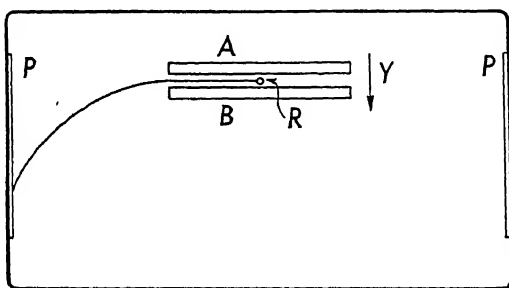


FIG. 31. — Diagram of the apparatus used in Bucherer's experiment. The magnetic field is perpendicular to the paper and directed toward the reader.

A photographic film  $P$  was bent in a cylindrical form concentric with the disks  $AB$ . This apparatus was placed in a vacuum chamber. An electric field  $Y$  was maintained between the plates by means of a battery. The whole apparatus was placed in a uniform magnetic field of strength  $H$  parallel to the planes of the disks. The beta particles coming out radially from the source  $R$  experienced a force  $Ye$  due to the electric field, and a force  $Hev \sin \theta$ , due to the magnetic field, where  $\theta$  is the angle between  $v$  and  $H$ . If the resultant force on a beta particle was not zero, it was deflected either up or down and could not escape from the narrow space between the disks. If, however, the force on any of the beta rays due to the magnetic field was equal and opposite to that due to the electric field, then these particles traveled radially from  $R$  and struck the photographic film  $P$ . For these beta particles

$$Hev \sin \theta = Ye, \quad (48)$$

from which

$$\sin \theta = \frac{Y}{Hv}. \quad (49)$$

Since both  $Y$  and  $H$  are in e.m. units, the ratio  $Y/H$  has the dimensions of a velocity. In Bucherer's experiment, the ratio  $Y/H$  was made equal to  $\frac{1}{2}c$ . On the basis of the relativity theory the velocity of a beta particle cannot exceed the velocity of light, hence by setting  $v = c$ , we obtain the limiting value of  $\sin \theta$ , which is  $\frac{1}{2}$ , so that  $\theta = 30^\circ$  or  $150^\circ$ . Only those beta particles which were projected initially at angles with the magnetic field lying between  $30^\circ$  and  $150^\circ$  could get to the photographic film.

After leaving the region between the disks, the beta particles continued traveling in the magnetic field until they reached the film. In general these particles moved in helical paths, but those coming out perpendicular to the magnetic field moved in circles of radius  $r$  given by

$$Hev = mv^2/r \quad (50)$$

from which  $e/m$  could be calculated. Putting this value of  $e/m$  in equation (47) should give the constant value  $e/m_0$  for all values of  $v$ . A typical set of Bucherer's experimental results is given in the following table:

TABLE I

$v/c$	$e/m_0 \frac{\text{c.m.u.}}{\text{gm}}$
0.3173	$1.752 \times 10^7$
0.3787	1.761
0.4281	1.760
0.5154	1.763
0.6870	1.767

These values of  $e/m_0$  are constant within the limits of experimental error. The results are thus in good agreement with equation (46) derived on the basis of the special theory of relativity.

### 32. Determination of $E/M$ for Alpha Particles

One of the best determinations of the ratio of the charge  $E$  to the mass  $M$  of the alpha rays was made by Rutherford and Robinson using the alpha particles emitted by the gas radon ( $Z = 86$ ), and two of its products of disintegration, radium A and radium C. In the apparatus sketched in Figure 32, the alpha particles coming

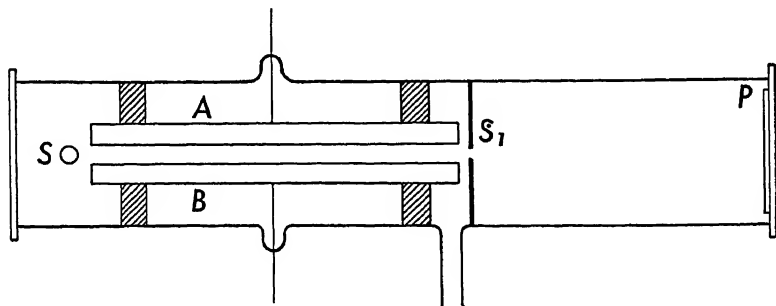


FIG. 32. — Diagram of the apparatus used by Rutherford and Robinson for the determination of  $E/M$  for alpha particles.

from the radioactive materials contained in the thin-walled glass tube  $S$  pass between two silvered glass plates  $A$  and  $B$ , then through a narrow slit  $S_1$ , and strike the photographic plate  $P$  placed about 50 cm from the slit. The photographic plate was wrapped in aluminum leaf to protect it from light and from the glow of the source  $S$ . A difference of potential of about 2000 volts was maintained between the plates. If  $V$  is the difference of potential between the plates,  $d$  the distance between them, and  $L$  the length of the plates, then the deflection  $y$  due to the electric field is given by

$$y = \frac{1}{2} \frac{V}{d} \frac{E}{M} \frac{L^2}{v^2}, \quad (51)$$

where  $v$  is the velocity of the alpha particle.

The photographic plate was then removed, a new plate was substituted, and the alpha particles were subjected to the action of a magnetic field of strength  $H$  perpendicular to the plane of the paper. The deflection due to the magnetic field is given by

$$y' = \frac{1}{2} \frac{HE}{M} \frac{L^2}{v}. \quad (52)$$

An enlargement of the photograph obtained by the electrostatic deflection method is shown in Figure 33. Three distinct lines are visible on each side of the central line. The central line

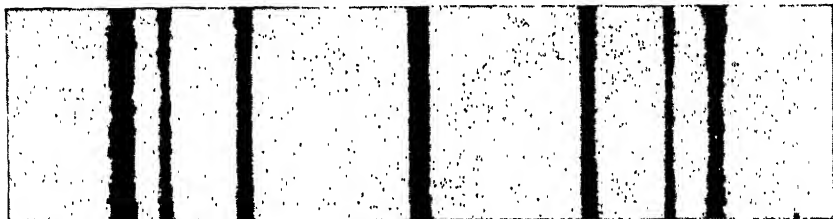


FIG. 33. — Lines on the photographic plate obtained by the electrostatic deflection of the alpha particles. (From Rutherford, Chadwick, and Ellis, *Radiations from Radioactive Substances*. By permission of The Macmillan Company, publishers.)

is due to the action of the alpha particles before the field is applied. Lines on both sides of the central line are produced by reversing the electric field. The outermost lines are due to the alpha particles of radon, the next pair of lines to the alpha particles of radium A and the innermost pair to those from radium C. An enlargement of the photograph obtained in the magnetic deflection experiment is shown in Figure 34.



FIG. 34. — Lines on the photographic plate obtained by the magnetic deflection of the alpha particles. (From Rutherford, Chadwick, and Ellis, *Radiations from Radioactive Substances*. By permission of The Macmillan Company, publishers.)

From the electrostatic deflection experiment the quantity  $Mv^2/E$  was determined, and the quantity  $Mv/E$  was determined from the magnetic deflection experiment. By combining the results of these two experiments, the value of  $E/M$  for the alpha particles was computed. The best value was determined from the measurements of the alpha particles of radium C and yielded

$$\frac{E}{M} = 4820 \frac{\text{e.m.u.}}{\text{gm}}.$$

### 33. Nature of the Alpha Particles

The value of  $E/M$  for alpha particles having been accurately determined, a measurement of either  $E$  or  $M$  independently would give sufficient evidence as to the nature of these particles. One method of determining  $E$  is to count the number of alpha particles,  $N$ , emitted by some radioactive substance in a given time interval, and then determine the charge  $NE$  carried by these particles. Two methods frequently used for counting alpha particles are (a) the scintillation method, and (b) the Geiger counter method.

In the scintillation method, alpha particles strike a screen containing a thin layer of powdered zinc sulphide. The energy of the alpha particle is transformed into energy of fluorescent radiation

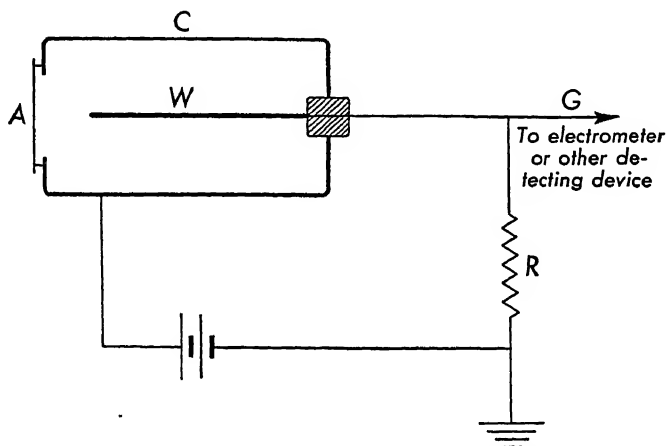


FIG. 35. — Diagram of a Geiger point counter.

by the small crystals of zinc sulphide. This radiation is in the visible region of the spectrum. Each alpha particle which strikes the screen produces a single scintillation. These scintillations may be viewed with a microscope and the number of alpha particles appearing in the field of view may be counted.

One type of counter known as a Geiger point counter consists essentially of a cylinder  $C$  and a fine wire  $W$  mounted parallel to the axis of the cylinder and insulated from it, Figure 35. The cylinder contains a gas such as air or argon at a pressure of about 5–12 cm of mercury. A difference of potential slightly less than that necessary to produce a discharge through the gas is main-

tained between the wire and the cylinder wall. Alpha particles can enter the Geiger counter through the aperture  $A$ , which is usually covered with a thin sheet of mica, glass, or aluminum. An alpha particle ionizes the gas along its path; these ions are accelerated by the electric field and produce more ions by collision with neutral atoms and molecules so that the ionization current builds up very rapidly. A very high resistance is connected between the wire and ground so that the energy due to the ionization current is rapidly dissipated. The effect is thus the production of a very large current lasting for a very short interval of time. This momentary current registers as a "kick" in an electrometer connected at  $G$ . This momentary current may be amplified so that it is capable of operating a loud-speaker, or a mechanical counter. By the proper choice of the value of the resistance  $R$ , the time constant of the circuit may be made sufficiently small so that each alpha particle which enters the chamber produces a momentary electrical surge which is recorded.

By counting the number of alpha particles entering the aperture  $A$  from any source placed a convenient distance away, the total number of alpha particles emitted by the source in a given time may be computed. Using this method Rutherford and Geiger found that  $3.57 \times 10^{10}$  alpha particles per second are emitted by one gram of radium.

Knowing the rate at which alpha particles are emitted by a given mass of radioactive material, one may measure the charge on the alpha particles by allowing these particles to charge up a plate connected to an electrometer. Using the alpha particles from radium ( $C$ ), Rutherford and Geiger found the charge  $E$  to be  $9.3 \times 10^{-10}$  e.s.u., while Regener, using the alpha particles of polonium, obtained the value  $E = 9.58 \times 10^{-10}$  e.s.u. Within the limits of experimental error, the charge on the alpha particle is equivalent to twice the electronic charge. Using the latter value of  $E$  and the previously determined value of  $E/M$  for computing the mass of the alpha particle, we get

$$M = 6.62 \times 10^{-24} \text{ gm.}$$

Comparing this with the mass of the hydrogen atom, we get

$$\frac{M}{M_H} = \frac{6.62}{1.67} \doteq 4.$$

The mass of the alpha particle is almost four times that of hydrogen, that is, it has the same atomic weight as helium ( $Z = 2$ ). Since the alpha particle carries a charge of  $+2e$  and has a mass equal to that of the helium atom, it is probably the nucleus of a helium atom. To make this identification certain, Rutherford and Royds (1909) carried out a spectroscopic analysis with the aid of alpha particles emitted by radon.

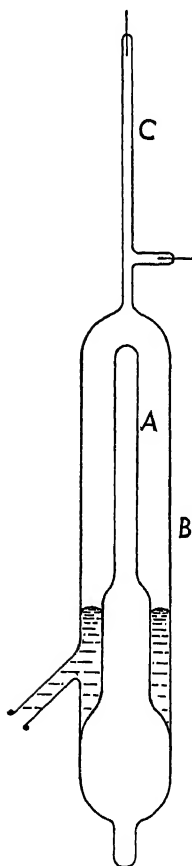


FIG. 36. — Diagram of the tube used to show that alpha particles are helium nuclei.

In this experiment, Figure 36, some radon was put into the thin-walled glass tube *A*. This tube was placed in a thick-walled glass tube *B*, which had sealed on to it a capillary tube *C* with two electrodes sealed into it. Tubes *B* and *C* were pumped out and the system allowed to stand for a few days. The alpha particles emitted by the radon passed through the thin walls of tube *A* and collected in tube *B*. The gases collecting in tube *B* could be compressed and forced into the capillary tube *C* by letting mercury in through a side tube. After six days enough gas was accumulated and forced into *C* so that a high voltage across its electrodes produced an electric discharge through the gas. The light coming from this tube was examined with a spectroscope which clearly showed the spectral lines of helium. Control experiments showed that ordinary helium gas could not penetrate through the thin walls of tube *A*. This spectroscopic evidence proves conclusively that alpha particles are helium nuclei.

### 34. Velocities of the Alpha Particles

The velocities of emission of alpha particles can be measured by allowing them to pass through a magnetic field perpendicular to the direction of motion. In the magnetic spectrograph, Figure 37, used by Rosenblum, the radioactive material *R* is deposited on a fine wire, and the alpha rays coming through the narrow slit *S* are bent in a circular path by the magnetic field *H* perpen-



dicular to the plane of the figure. After traversing a semicircle, the alpha rays of any one velocity are focused on the photographic plate  $P$ . The air in the chamber is pumped out to avoid loss of velocity by the alpha particles. The radius of the circle is given by the expression

$$HEv = \frac{Mv^2}{r},$$

where the radius of the circle,  $r$ , is half the distance from the slit to the trace on the photographic plate, and  $v$  is the velocity of the alpha particle. The magnetic field intensity in this

experiment was about 36,000 oersteds. Rutherford and his co-workers used a similar apparatus but substituted an ionization chamber for the photographic plate.

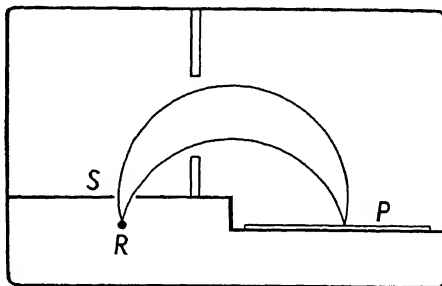


FIG. 37. — Magnetic spectrograph used for measuring the velocities of alpha particles. The magnetic field is perpendicular to the plane of the paper and directed toward the reader.

TABLE II

VELOCITIES OF ALPHA PARTICLES FROM DIFFERENT ELEMENTS	
Element	Velocity
Radon	$1.625 \times 10^9$ cm/sec.
Radium A	1.699 "
Polonium	1.597 "
Actinium A	1.882 "
Radium $\alpha_0$	1.517 "
$\alpha_1$	1.488 "
Radium C' $\alpha_0$	1.628 "
$\alpha_1$	1.619 "
Thorium C' $\alpha_1$	1.711 "
$\alpha_2$	1.705 "
$\alpha_3$	1.665 "
$\alpha_4$	1.645 "
$\alpha_5$	1.642 "

The results of the experiments on the velocities of emission of alpha particles show that these velocities are of the order of  $10^9$  cm/sec. In many cases the velocity spectrum consists of only a single line, that is, all the alpha particles emitted from this type of element have exactly the same velocity. In another large group of elements, the velocity spectrum consists of two or more lines very close together. In a few cases there are several groups of lines covering a comparatively large velocity range. A few of the results of these measurements are given in Table II.

### 35. Rutherford's Nuclear Theory of the Atom

Rutherford, in 1911, proposed a nuclear theory for the structure of the atom. He was led to this theory by the results of an experiment by Geiger and Marsden on the scattering of alpha particles by matter. They observed that some of the alpha particles were scattered through angles greater than  $90^\circ$ , that is, they emerged on the side of incidence. To explain such large-angle scattering of fast-moving alpha particles, Rutherford assumed that there was an intense electric field within the atom and that the alpha particle was deflected by a single atom. To provide such an intense electric field, Rutherford assumed that the entire positive charge of the atom was concentrated in a very small nucleus and that the electrons occupied the space outside the nucleus.

In developing the theory of the scattering of alpha particles by atomic nuclei, Rutherford assumed that both the nucleus and the alpha particle behaved as point charges, that Coulomb's law was valid for such small distances, and that Newtonian mechanics was applicable. To test this theory, he instituted a series of experiments on the scattering of alpha particles by thin films of matter. These experiments were performed by Geiger and Marsden in 1913 and repeated with greater accuracy by Chadwick in 1920. They verified Rutherford's nuclear theory of the structure of the atom and showed that the charge on the nucleus of an atom is  $Ze$ , where  $Z$  is the atomic number of the element and  $e$  is the electronic charge.

### 36. Single Scattering of Alpha Particles by Thin Foils

Consider a nucleus of charge  $Ze$  stationary at point  $C$ , and an alpha particle of mass  $M$  and charge  $E$  approaching it along the

line  $AB$ , Figure 38. The original velocity of the alpha particle in the direction of  $AB$  is  $V$ . There will be a force of repulsion between the two charges given by Coulomb's law

$$F = \frac{ZeE}{r^2}, \quad (53)$$

where  $r$  is the distance between the alpha particle and the nucleus. Because of this force of repulsion, the alpha particle will be de-

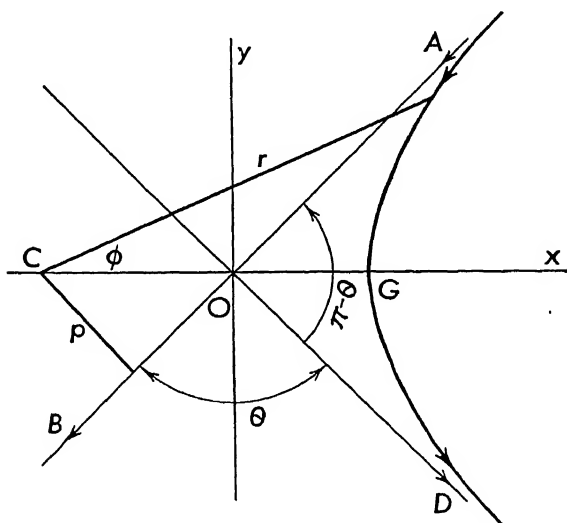


FIG. 38. — The hyperbolic path of an alpha particle in the field of force of a nucleus.

flected from its original direction, and will move in a hyperbolic path with the nucleus at the focus on the convex side of this branch of the hyperbola. When it leaves the region close to the nucleus, the alpha particle will be moving in the direction of  $OD$ , making an angle  $\theta$  with its original direction of motion,  $AB$ . It can be shown (see Appendix VII) that the angle of deflection,  $\theta$ , is given by

$$\cot \frac{\theta}{2} = \frac{MV^2}{ZeE} p, \quad (54)$$

where  $p$  is the distance from the nucleus at  $C$  to the original line of motion  $AB$ . In the actual experiments on the scattering of alpha particles, a large number of particles were directed against a thin metallic foil. It is therefore necessary to calculate the number of

alpha particles scattered through a given angle  $\theta$ , or, what amounts to the same thing, the probability that an alpha particle will be deflected through this angle  $\theta$ . We shall assume that the foil is so thin that the alpha particles suffer no loss in velocity in passing through it.

Suppose that a stream of alpha particles is directed normally on a thin foil of matter of thickness  $t$  containing  $n$  atoms per unit volume. The number of atoms per unit area of this foil, and also the number of nuclei per unit area of foil, is  $nt \times 1 \text{ cm}^2$ . Any alpha particle whose initial velocity would bring it within a distance  $p$  of a nucleus will be deflected through an angle equal to or greater than  $\theta$ , where  $\theta$  is given by equation (54). To determine the probability that an alpha particle would come within this distance, imagine a circle of radius  $p$  drawn around each nucleus, then the area occupied by all such circles in a unit area of foil is  $\pi p^2 nt$ . The probability that an alpha particle would come within this distance  $p$  of a nucleus is the ratio of the area  $\pi p^2 nt$  to unit area. Since every alpha particle which would come within a distance  $p$  of a nucleus will be deflected through an angle equal to or greater than  $\theta$ , the probability that an alpha particle will be deflected through such an angle, or the fraction of the total number of alpha particles which will be deflected through an angle equal to or greater than  $\theta$ , is given by

$$f = \pi p^2 nt = \pi nt \left( \frac{ZeE}{MV^2} \right)^2 \cot^2 \frac{\theta}{2}, \quad (55)$$

using the value of  $p$  from equation (54).

The probability that the original direction of motion of an alpha particle would fall between the radii  $p$  and  $p + dp$ , or the probability that an alpha particle would be deflected through an angle lying between  $\theta$  and  $\theta + d\theta$  is

$$df = 2\pi p n t d p$$

or

$$df = \pi nt \left( \frac{ZeE}{MV^2} \right)^2 \cot \frac{\theta}{2} \csc^2 \frac{\theta}{2} d\theta. \quad (56)$$

In the experiments on the scattering of alpha particles, the scattered particles were detected by the scintillations produced on a fluorescent screen. To compare results for different angles of

scattering, it is necessary to know the number of alpha particles falling on unit area of the fluorescent screen. To determine this number, consider a stream of alpha particles which are incident normally on the thin foil

$T$  as shown in Figure 39.

The alpha particles which are scattered through an angle  $\theta$  will travel along the elements of a cone of semivertex angle  $\theta$ . Similarly, the alpha particles

which are scattered through an angle  $\theta + d\theta$  will travel along the elements of a cone of semivertex angle  $\theta + d\theta$ . If the fluorescent screen is to be placed at right angles to the direction of motion of the scattered particles, its shape must be that of a zone of a sphere of radius  $r$  and width  $rd\theta$ . Since the radius of this zone is  $r \sin \theta$ , an element of area  $dA$  of the fluorescent screen formed in this way is

$$\begin{aligned} dA &= 2\pi r \sin \theta \cdot r d\theta = 2\pi r^2 \sin \theta d\theta \\ &= 4\pi r^2 \sin \frac{\theta}{2} \cos \frac{\theta}{2} d\theta. \end{aligned} \quad (57)$$

If  $Q$  is the total number of alpha particles incident on the foil, then the number striking unit area of the screen is, from equations (56) and (57),

$$\begin{aligned} N &= Q \frac{\pi n t \left( \frac{ZeE}{MV^2} \right)^2 \cot \frac{\theta}{2} \csc^2 \frac{\theta}{2} d\theta}{4\pi r^2 \sin \frac{\theta}{2} \cos \frac{\theta}{2} d\theta} \\ &= \frac{Q n t (Ze)^2 E^2}{4r^2 (MV^2)^2 \sin^4 \frac{\theta}{2}}. \end{aligned} \quad (58)$$

A study of equation (58) shows that if Rutherford's nuclear theory of the atom is correct, then the number of alpha particles falling on unit area of a screen at a distance  $r$  from the point of scattering must be proportional to

(a) the reciprocal of  $\sin^4 \theta/2$ ,

- (b) the thickness  $t$  of the scattering material,
- (c) the reciprocal of the square of initial energy of the particle or  $1/(\frac{1}{2}MV^2)^2$ ,
- (d) the square of the nuclear charge, or  $(Ze)^2$ .

### 37. Experimental Verification of Rutherford's Nuclear Theory of the Atom

Each of the above deductions was tested and verified experimentally in a series of experiments carried out in Rutherford's laboratory. The angular distribution of the alpha particles scattered by a thin foil  $F$ , Figure 40, was measured by Geiger and

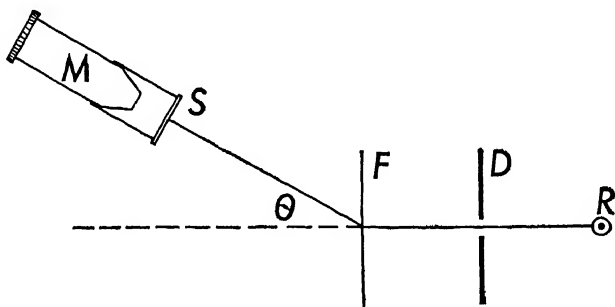


FIG. 40.

Marsden. The alpha particles from a radon source  $R$  passed through a diaphragm  $D$  and were scattered by the thin foil  $F$ . The alpha particles which were scattered through an angle  $\theta$  struck a zinc sulphide screen  $S$  and the scintillations were viewed through the microscope  $M$ . The microscope and screen were rotated about an axis passing through the center of the foil  $F$ , and the number of particles striking the screen in a given time was measured at different angles over a range of angles from  $5^\circ$  to  $150^\circ$ . Gold and silver foils were used in the experiment. Some of the results are given in Table III for gold as the scattering element. If the number of particles,  $N$ , scattered per unit time through an angle  $\theta$  is proportional to the reciprocal of  $\sin^4 \theta/2$ , then the product  $N \times \sin^4 \theta/2$  should be a constant. The last column in Table III lists the values of these products; these values are approximately constant and lie within the limits of error of the experiment.

To test the dependence of scattering on the thickness of the

foil, the angle of scattering was kept at about  $25^\circ$  and foils of different thicknesses and also of different materials were used. The alpha-particle source was radium (B + C). The results of the

TABLE III

SCATTERING OF ALPHA PARTICLES FROM GOLD FOIL			
Angle of Deflection $\theta$	$\frac{1}{\sin^4 \frac{\theta}{2}}$	Number of Scintillations in Unit Time $N$	$N \times \sin^4 \frac{\theta}{2}$
$150^\circ$	1.15	33.1	28.8
$135^\circ$	1.38	43.0	31.2
$120^\circ$	1.79	51.9	29.0
$105^\circ$	2.53	69.5	27.5
$75^\circ$	7.25	211	29.1
$60^\circ$	16.0	477	29.8
$45^\circ$	46.6	1435	30.8
$30^\circ$	223	7800	35.0
$15^\circ$	3445	132,000	38.4

experiments are shown in Figure 41, in which the number of particles per minute,  $N$ , scattered through an angle of  $25^\circ$ , is plotted as ordinates, and the thickness,  $t$ , of the scattering foil of a given material is plotted as abscissae. It is seen that for any one element, the number of particles scattered per minute is directly proportional to the thickness of the scattering foil. In the graph, the thickness of each foil is expressed in terms of an equivalent length of air path, that is, a thickness of air path which produces the same loss in energy of the alpha particle traversing it as that produced by the material under investigation.

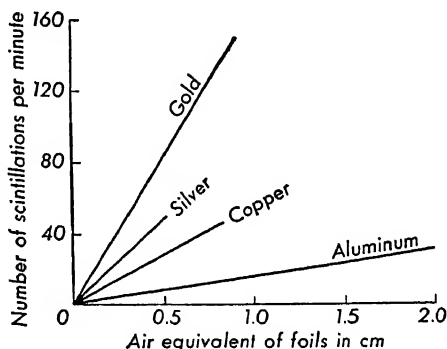


FIG. 41. — Curves showing that the number of alpha particles scattered through a given angle is directly proportional to the thickness of the scattering foil. Each curve is the result of an independent set of measurements.

In another series of observations, the velocity of the incident alpha particle was changed by placing absorbing screens of mica between the source and the scattering foil. The velocities of the alpha particles were determined empirically by first finding the range  $R$  of the alpha particles in air (§ 110), and then applying Geiger's rule that

$$R = aV^3 \quad (59)$$

where  $a$  is a constant. The results of the experiment are shown in Table IV.

TABLE IV

VARIATION OF SCATTERING WITH VELOCITY			
Range of Alpha Particles	Relative Values of $\frac{1}{V^4}$	Number of Scintillations in Unit Time $N$	$NV^4$
5.5	1.0	24.7	25
4.76	1.20	29.0	24
4.05	1.50	33.4	22
3.32	1.91	44	23
2.51	2.84	81	28
1.84	4.32	101	23
1.04	9.22	255	28

If the number of particles scattered through an angle  $\theta$  is inversely proportional to the square of the energy of the particles, then the product  $NV^4$  should be constant. The values of this product over a wide range of velocities are given in the last column of Table IV. These values are considered constant within the limits of error of the experiment.

The experiments of Geiger and Marsden have been interpreted as establishing the essential correctness of Rutherford's nuclear theory of the atom. However, these experiments were not sufficiently accurate to provide a reliable determination of the atomic number  $Z$ . It was not until 1920 that Chadwick succeeded in measuring the nuclear charge directly. In the meantime, Bohr had adopted Rutherford's nuclear hypothesis in his brilliant work



on atomic spectra, and Moseley, from his work on X-ray spectra, was able to determine the nuclear charge and showed that it was equal to  $Ze$ .

### 38. Direct Determination of the Nuclear Charge

In Chadwick's experiment, alpha particles from the source  $R$ , Figure 42, were scattered by a thin foil  $AA'$  which was made in the form of an annular ring. The alpha particles which were scattered

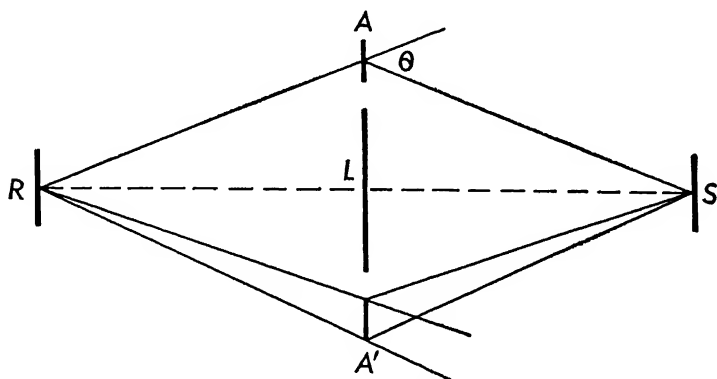


FIG. 42. Diagram of the arrangement used by Chadwick in his experiments on the scattering of alpha particles.

through an angle  $\theta$  were counted by the scintillations they produced on the zinc sulphide screen placed at  $S$  on the axis of the cone  $RAA'$  such that  $RA = AS$ . The total number of alpha particles falling on the foil  $AA'$  could be determined by counting the number reaching  $S$  directly from  $R$ , since the areas of the screen  $S$  and the foil  $AA'$  were known. When the scattered rays were investigated, the direct rays from  $R$  were cut off by means of the lead plate  $L$ . Account was taken of the fact that the annular ring was of finite width. The results of Chadwick's experiments using platinum, silver, and copper foils are tabulated below:

TABLE V

Element	Nuclear Charge $Ze$	Atomic Number $Z$
Cu	29.3e	29
Ag	46.3e	47
Pt	77.4e	78

Within the limits of experimental error, these results are in agreement with Rutherford's nuclear theory of the atom and provide the only direct measurement of the nuclear charge.

### 39. Nuclear Sizes

The results of the scattering experiments may be used to calculate the distance of approach of the alpha particle to the nucleus ( $GC$  in Figure 38). This distance of approach is smallest when the scattering angle  $\theta$  is greatest. In some of the experiments, the scattering angle observed was as big as  $150^\circ$ . In the case of gold, the distance of closest approach corresponding to a scattering angle of  $150^\circ$  is about  $3.2 \times 10^{-12}$  cm. For silver this distance is about  $2 \times 10^{-12}$  cm.

Considering the process of scattering as a type of collision between two particles, the alpha particle and the nucleus, the distance of closest approach gives an upper limit to the size of the nucleus. Thus the radius of the gold nucleus is less than  $3.2 \times 10^{-12}$  cm. Data on the size of the atom indicate that the radius of an atom is about  $10^{-8}$  cm. The nucleus thus occupies an extremely small part of the atom.

## REFERENCES

### *Brownian motion*

MILLIKAN, R. A., *Electrons + and -*. Chicago: University of Chicago Press, 1935, Chap. VII.

PERRIN, J., *Atoms*. New York: D. Van Nostrand Company, Inc., 1917, Chaps. III, IV.

### *Electronic charge*

MILLIKAN, R. A., *Electrons + and -*. Chicago: University of Chicago Press, 1935, Chaps. IV, V.

### *Isotopes*

ASTON, F. W., *Mass Spectra and Isotopes*. New York: Longmans, Green & Company, 1933.

RICHTMYER, F. K., and E. H. KENNARD, *Introduction to Modern Physics*. New York: McGraw-Hill Book Company, Inc., 1942, Chap. XI.

STRANATHAN, J. D., *The Particles of Modern Physics*. Philadelphia: The Blakiston Company, 1942, Chap. V.

*Radioactivity*

RUTHERFORD, E., J. CHADWICK, and C. D. ELLIS, *Radiations from Radio-active Substances*. London: Cambridge University Press, 1930, Chaps. II, VIII.

*Relativity*

BORN, M., *Einstein's Theory of Relativity*. London: Methuen & Company, Ltd., 1924, Chaps. V, VI.

EINSTEIN, A., *Relativity*. London: Methuen & Company, Ltd., 1931, Chaps. I–XVI.

RICHTMYER, F. K., and E. H. KENNARD, *Introduction to Modern Physics*. New York: McGraw-Hill Book Company, Inc., 1942, Chap. IV.

TOLMAN, R. C., *The Relativity of Motion*. Berkeley: University of California Press, 1917, Chaps. I–IV.

## PROBLEMS

1. The following data were recorded during a performance of an oil drop experiment:

plate distance	1.60 cm
distance of fall	1.021 cm
potential difference	5085 volts
viscosity of air	$1.824 \times 10^{-4}$ gm/cm sec
density of oil	0.92 gm/cm <sup>3</sup>
radius of oil drop	$2.76 \times 10^{-4}$ cm
average time of fall	11.88 sec
successive times of rise	22.37 sec
	34.80 sec
	29.25 sec
	19.70 sec
	42.30 sec

Calculate the successive changes in charge on the oil drop and obtain an average value of  $e$  from these data. Assume  $b/pa = 0.03$ .

2. The following are the important dimensions of a cathode ray tube:

distance from anode to screen	33.0 cm
length of plates	7.8 cm
distance between plates	2.4 cm

The plates are placed close to the anode.

(a) In the balance method of determining  $e/m$ , the voltage across the plates was 2800 volts and the magnetic field was 8.20 oersteds. When

only the magnetic field was on, the deflection on the fluorescent screen was 2.40 cm. Calculate  $e/m$ .

(b) With the same tube but using the magnetic deflection only, when the accelerating potential between the anode and cathode was 32,500 volts, a magnetic field of 5.6 oersteds produced a displacement of 2.10 cm on the fluorescent screen. Calculate the value of  $e/m$ .

3. Given the following data on the masses of isotopes:

$${}_3\text{Li}^7 = 7.01816$$

$${}_3\text{Li}^6 = 6.01692$$

$${}_0n^1 = 1.00893$$

Calculate the binding energy of a neutron in a  ${}_3\text{Li}^7$  nucleus. Express the result in both a.m.u. and Mev.

*Ans.* 0.00769 a.m.u. or 7.17 Mev.

4. An electron emitted from a heated filament is accelerated to the anode by a difference of potential of 300 volts between the filament and the anode. Calculate (a) its kinetic energy in ergs, (b) the velocity of the electron when it reaches the anode.

*Ans.* (a)  $4.8 \times 10^{-10}$  erg.

(b)  $1.03 \times 10^9$  cm/sec.

5. An electron moving with a kinetic energy of 5000 ev, enters a uniform magnetic field of 200 oersteds perpendicular to its direction of motion. Determine the radius of the path of this electron.

*Ans.* 1.20 cm.

6. Singly charged lithium ions of mass numbers 6 and 7, liberated from a heated anode, are accelerated by means of a difference of potential of 400 volts between the anode and the cathode and then pass through a hole in the cathode into a uniform magnetic field perpendicular to their direction of motion. If the intensity of this magnetic field is 800 oersteds, determine the radii of the paths of these ions.

*Ans.* 8.83 cm and 9.54 cm.

7. (a) Show that the path of an alpha particle in the electrostatic deflection experiment performed by Rutherford for the determination of  $E/M$  (§ 32) is a parabola given by

$$y = x \tan \alpha - \frac{1}{2} \left( \frac{V}{d} \frac{E}{M} \right) \frac{x^2}{v_0^2 \cos^2 \alpha}$$

where  $\alpha$  is the angle which the initial velocity  $v_0$  makes with the line joining the source  $S$  and the slit  $S_1$ , and  $V$  is the difference of potential between the plates.

(b) Show that only those alpha particles which are directed initially at an angle  $\alpha$  given by

$$\sin 2\alpha = \frac{V}{d} \frac{E}{M} \frac{L}{v_0^2}$$

will get through the slit  $S_1$ .  $L$  is the distance from  $S$  to  $S_1$ .

(c) Using the data supplied in this chapter, calculate the value of the angle  $\alpha$  in this experiment for the alpha particles from radon. The distance between the plates is 4 mm and the length of each plate is 35 cm.

*Ans.*  $\alpha = 55$  minutes.

8. Alpha particles from polonium are directed normally against a thin sheet of gold of thickness  $10^{-5}$  cm. The density of gold is  $19.32$  gm/cm<sup>3</sup>. Determine the fraction of the incident alpha particles scattered through angles greater than  $90^\circ$ .

*Ans.*  $8.5 \times 10^{-6}$ .

9. One method of actually determining masses of isotopes with a mass spectrograph is to take a series of *doublets*, that is, ions differing slightly in mass (see Figure 27), and then determining the difference between their masses. Three such doublet measurements are given below:

$$\text{H}_2^1 - \text{H}^2 = 1.53 \times 10^{-3} \text{ a.m.u.}$$

$$\text{H}_3^2 - \frac{1}{2}\text{C}^{12} = 42.19 \times 10^{-3} \text{ a.m.u.}$$

$$\text{C}^{12}\text{H}_4^1 - \text{O}^{16} = 36.49 \times 10^{-3} \text{ a.m.u.}$$

The term  $\frac{1}{2}\text{C}$  means that the carbon was doubly ionized while the others were all singly ionized. From the above data determine the masses of the isotopes  $\text{H}^1$ ,  $\text{H}^2$ , and  $\text{C}^{12}$ .

*Ans.*  $\text{H}^1 = 1.00813$ .

$\text{H}^2 = 2.01473$ .

$\text{C}^{12} = 12.00398$ .

# 3

## Electromagnetic Radiation

### 40. Early Theories of the Nature of Light

Ever since the days of Newton and Huygens — that is, since the latter part of the seventeenth century — there have been two fundamentally different theories concerning the nature of light. Newton proposed a corpuscular theory of light without specifying definitely the nature of these corpuscles; Huygens proposed a wave theory to explain exactly the same phenomena that were explained by Newton on his corpuscular theory. In one important case, the velocity of light in material media, deductions from these two theories led to divergent results. On the basis of Newton's corpuscular theory, light should travel faster in the denser medium, while on the basis of the wave theory, light should travel slower in the denser medium. It was not until the middle of the nineteenth century that the velocity of light in a dense medium, water, was determined by Foucault and Fizeau, and found to be less than that in a vacuum. By this time, the wave theory had become fairly well established, mainly because of the work of Young, Fresnel, and Arago on the phenomena of interference and diffraction of light. Further, the polarization of light by reflection, and by double refraction through crystals, could be explained on the assumption that light waves were transverse waves. The wave theory of light was the only one which could explain satisfactorily all the optical phenomena then known.

### 41. Maxwell's Electromagnetic Theory of Light

Although the wave theory of light was definitely established, the nature of the waves remained a puzzle. It was at first thought that these waves were similar to the transverse waves which are propagated through an elastic solid. A luminiferous ether, filling all of space and having some of the properties of an elastic solid, was postulated as the medium through which light waves were propagated. Maxwell, in his work on electricity and magnetism (1864), showed that a disturbance consisting of transverse electric

and magnetic fields should be propagated through the ether with the speed of light. Hertz (1887) succeeded in producing electromagnetic waves by means of an oscillatory current and showed the correctness of Maxwell's theory. Modern wireless telegraphy and radio are practical developments based upon the work of Maxwell and Hertz.

Serious difficulties arose in connection with the properties of the luminiferous ether through which these waves were assumed to be propagated. Einstein's theory of relativity (1905) finally resolved these difficulties by showing that such an ether was not necessary for the propagation of electromagnetic waves. As a consequence of this theory, light waves are now regarded as electromagnetic oscillations, consisting of variations in the intensities of transverse electric and magnetic fields, each of which may exist in free space, that is, space completely devoid of matter.

On the basis of classical electrodynamics, it is shown that an accelerated charge radiates energy in the form of electromagnetic waves. This electromagnetic wave consists of an electric field of intensity  $Y$  and a magnetic field of intensity  $H$  always at right angles to each other. The magnitudes of these electric and magnetic intensities at a distance  $r$  from a charge  $e$  are given by

$$Y = H = \frac{ae}{rc^2} \sin \phi, \quad (1)$$

where  $a$  is the acceleration of the charge and  $\phi$  is the angle between  $r$  and the direction of the acceleration, Figure 43.  $Y$  and  $H$  are numerically equal when  $Y$  is expressed in e.s.u. and  $H$  is expressed in e.m.u. Equation (1) holds only when the velocity of the charge is much smaller than the velocity of light. The electric and magnetic fields are always at right angles to the direction of propagation and move through space with the velocity of light.

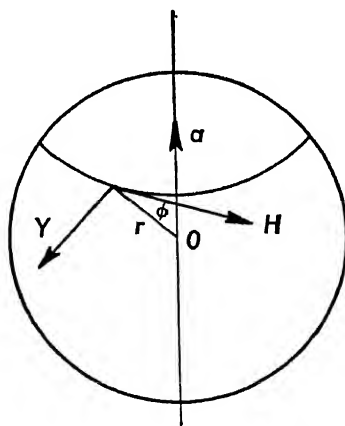


FIG. 43. -  $Y$  and  $H$  are tangent to the surface of the sphere.

It has been shown that the energy per unit volume in an elec-

tric field in free space is equal to  $Y^2/8\pi$ , and that the energy per unit volume in a magnetic field in free space is equal to  $H^2/8\pi$ . The energy per unit volume,  $w$ , in the electromagnetic wave is, therefore,

$$w = \frac{Y^2}{8\pi} + \frac{H^2}{8\pi} = \frac{Y^2}{4\pi}. \quad (2)$$

Since this energy is propagated with velocity  $c$ , the amount of energy,  $I$ , which flows in one second through unit area perpendicular to the direction of propagation is

$$I = \frac{cY^2}{4\pi}. \quad (3)$$

$I$  represents the instantaneous value of the intensity of the electromagnetic wave at any point in space. It will be noted, by referring to equation (1), that the intensity of the electromagnetic wave produced by a charge which is accelerated along the axis is a maximum in a direction at right angles to the acceleration, and is zero in a direction parallel to the acceleration.

The rate at which energy is radiated from an accelerated charge

can be calculated by integrating the intensity  $I$  over the surface of a sphere of radius  $r$  containing the accelerated charge at its center, Figure 44. Consider a small element of surface area included between two small circles of radii  $r \sin \phi$  and  $r \sin (\phi + d\phi)$ , and of area

$$dA = 2\pi r \sin \phi \cdot r d\phi.$$

The amount of energy,  $dS$ , which passes through this element of surface in one second is

$$dS = IdA = \frac{cY^2}{4\pi} \cdot 2\pi r^2 \sin \phi d\phi.$$

Substituting the value of  $Y$  from equation (1), and integrating over the whole surface, we get

$$S = \int_0^A IdA = \frac{1}{2} \frac{a^2 e^2}{c^3} \int_0^\pi \sin^3 \phi d\phi,$$

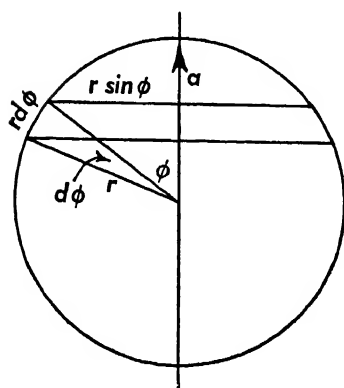


FIG. 44.



yielding

$$S = \frac{2}{3} \frac{a^2 e^2}{c^3}. \quad (4)$$

$S$  represents the rate at which energy is radiated from the accelerated charge; it depends upon the square of the acceleration and also upon the square of the charge. It is thus independent of the direction of the acceleration and of the sign of the charge.

The simplest type of electromagnetic wave is a plane wave in which the electric field intensity is in one direction only, say the  $y$  direction, which vibrates with a single frequency, and which has a single wave length  $\lambda$ . Such a wave is called a *linearly polarized monochromatic* electromagnetic wave; the direction of polarization is taken as the direction of vibration of the vector representing the electric field intensity. In the example above the direction of polarization is the  $y$  direction. Since an electromagnetic wave is a transverse wave, its direction of propagation is at right angles to the direction of vibration of the electric vector which represents the intensity of the electric field. Such a linearly polarized electromagnetic wave traveling, say, in the  $x$  direction can be represented by the following two equations:

$$Y = Y_0 \sin \frac{2\pi}{\lambda}(x - ct) \quad (5a)$$

$$H = H_0 \sin \frac{2\pi}{\lambda}(x - ct), \quad (5b)$$

where  $Y$  is the electric intensity at any point in the path of the wave at any instant of time,  $H$  is the intensity of the magnetic field at the same point at the same time, but always at right angles to the electric vector  $Y$ . Both  $Y$  and  $H$  are in a plane at right angles to the direction of propagation. In Figure 45,  $Y$  is chosen parallel to the  $y$  axis and  $H$  parallel to the  $z$  axis.  $Y_0$  and  $H_0$  are the amplitudes of the electric and magnetic intensities, respectively. This plane wave is propagated in the  $x$  direction with the velocity  $c$ .

The average intensity of the wave is the average value of the energy flowing through unit area in unit time. Since the rate at which electromagnetic energy flows through unit area is given by

$I = c \frac{Y^2}{4\pi}$  the average intensity can be obtained by averaging  $I$

over a convenient interval of time, say half a period, yielding

$$I_{av} = \frac{1}{T} \int_0^T I dt = \frac{2}{T} \int_0^{\frac{T}{2}} \frac{c}{4\pi} Y_0^2 \sin^2 \frac{2\pi}{\lambda} (x - ct) dt,$$

or

$$I_{av} = \frac{cY_0^2}{8\pi}. \quad (6)$$

The average intensity of the electromagnetic wave is thus proportional to the square of the amplitude of the electric intensity which, of course, is equal to the square of the amplitude of the magnetic intensity.

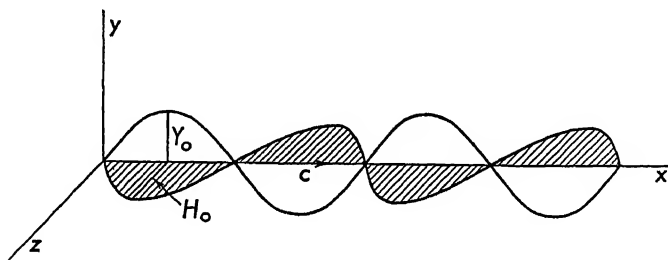


FIG. 45. — Graph showing the values of the intensities of the electric and magnetic fields in a plane electromagnetic wave at a given instant of time.

In the case of light, a plane electromagnetic wave can be produced very simply by placing a small source of light at the focus of a converging lens or mirror and producing a parallel beam, that is, one in which the wave front is a plane. A linearly polarized plane wave can be obtained by passing a plane parallel beam of light through a Nicol prism, or by reflecting the parallel beam from a glass plate set at the polarizing angle, or by passing the parallel beam of light through a sheet of polaroid. Again the direction of polarization is the direction of vibration of the electric vector representing the intensity of the electric field of the light wave.

A Nicol prism may also be used as an analyzer to determine whether the beam is polarized. The Nicol prism is rotated about the beam of light as an axis, and, if a position of the prism can be found in which no light can pass through it, the beam is said to be linearly polarized. The direction of vibration of the electric vector

is then easily determined since the Nicol prism does not transmit light in which the direction of vibration is parallel to the long diagonal of the face of the prism.

An interesting and important type of polarization is produced when a linearly polarized beam of light is allowed to pass through a thin sheet of some doubly refracting crystal such as mica. If the linearly polarized monochromatic beam of light is incident on the thin sheet of mica with its direction of vibration at  $45^\circ$  to the axis of the crystal, then the electric vector will be resolved into two components at right angles to one another which travel through the crystal with different velocities. For a certain value of the thickness of the crystal one beam will emerge a quarter of a period behind the other, or they will be out of phase by a quarter of a wave length. Such a crystal is called a quarter-wave plate. The vibrations of the electric vectors in the two beams are at right angles to one another and they differ in phase by a quarter of a period. Thus when one component is a maximum the other component is zero, yielding a resultant vector which describes a circle. Such a beam is said to be *circularly* polarized. The direction of rotation of the circularly polarized beam may be either clockwise or counterclockwise, depending upon the nature of the crystal and upon the angle between the electric vector of the incident beam and the crystal axis, i.e., whether the angle is  $+45^\circ$  or  $-45^\circ$ . When the circularly polarized beam is passed through a second quarter-wave plate with its axis parallel to the first one, the beam becomes linearly polarized again.

## 42. The Zeeman Effect

It is known that the light emitted by any element consists of sharp lines of definite wave lengths, and hence of definite frequencies, characteristic of the element. The light evidently comes from the atoms of the element and, on the classical theory, is due to the periodic motions of the charges within the atom. Since moving charges are affected by electric and magnetic fields, it should be possible to produce changes in the emitted light by subjecting the source of radiation to electric and magnetic fields. Faraday attempted to find such an effect by placing a sodium flame in a strong magnetic field but failed to detect any change in the character of the light. Zeeman (1896), with apparatus of greater re-

solving power, succeeded in producing this effect and in determining the nature of the charge emitting the light.

To produce the Zeeman effect, the source of light, such as a sodium flame or a mercury arc, is placed between the poles of a powerful electromagnet. The light coming from the source is examined by means of a spectroscope of high resolving power. The light may be viewed in a direction perpendicular to the magnetic field, or parallel to the magnetic field; to make the latter possible, a hole is drilled in one of the pole pieces along the axis of the magnet. If one of the intense lines in the spectrum of the element is focused in the spectroscope, then, when the magnetic field is applied, it is found that this line splits into several component lines. Furthermore, although the original line was unpolarized, each of the component lines is polarized. In the simpler *normal* Zeeman effect, there are three components when the light is viewed perpendicular to the direction of the magnetic field and only two components when the light is viewed parallel to the magnetic field. In the more complex or *anomalous* Zeeman effect, the line is split into many more components. Consideration of the anomalous Zeeman effect will be left to a later chapter (Chapter 6), since the classical theory is unable to account for this anomalous effect.

In the normal Zeeman effect, when the light is viewed in a direction perpendicular to the direction of the magnetic field, three component lines are observed, one in the same position as the original line, and two components separated by equal distances on either side of this central line, Figure 46. By means of an analyzer such as a Nicol prism it can be shown that the outer components are polarized at right angles to the undisplaced component. The direction of vibration of the electric vector in the outer components is perpendicular to the magnetic field, and in the inner component the electric vector is parallel to the magnetic field. When the light is viewed parallel to the magnetic field, there is no undisplaced line; only the two outer components are present in the same positions as in the perpendicular case. These two components are circularly polarized in opposite directions.

The classical explanation of the normal Zeeman effect is based on Lorentz's electron theory. Assume that an electron in the atom is moving in a circular orbit of radius  $r$ , Figure 47, under the

action of some central force  $F_0$ . Then from Newton's second law of motion

$$F_0 = \frac{mv_0^2}{r} = m\omega_0^2 r \quad (7)$$

where  $v_0$  is its linear velocity in the orbit and  $\omega_0$  is its angular

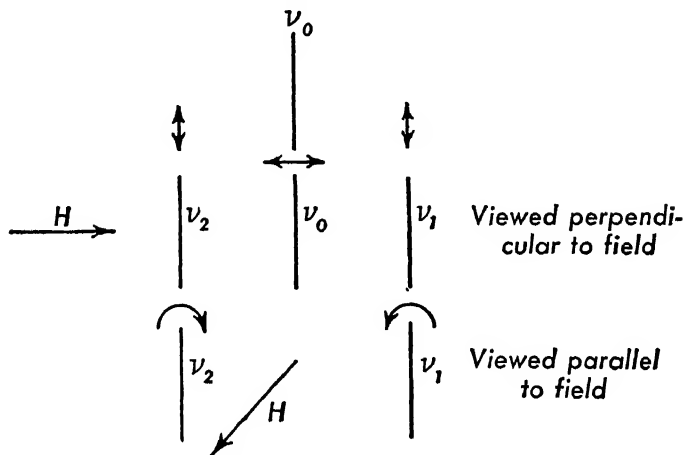


FIG. 46. — The normal Zeeman effect showing the splitting of a spectral line when the source of light is in a magnetic field.

velocity. If an external magnetic field is applied which is perpendicular to the plane of the orbit of the electron, two effects will be produced. During the time that the magnetic field is being established, there will be an electric field tangent to the orbit because of the e.m.f. produced by the changing magnetic flux through it. At the same time there will be an additional force on the electron which will be perpendicular to the direction of the magnetic field and to the velocity of the electron, that is, the force will be radial. A simple analysis shows that if the tangential electric field is such as to cause an increase in the velocity of the electron, the radial force will be directed toward the center, thus providing the additional force needed to keep it moving in the same orbit

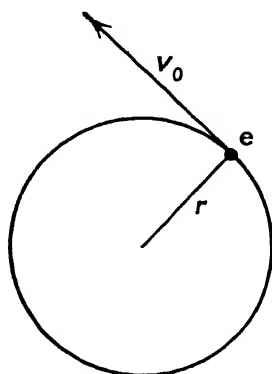


FIG. 47.

with this higher velocity. Conversely, if the tangential electric field is such as to decrease the velocity of the electron, then the radial force due to the magnetic field will be directed away from the center, thus decreasing the centripetal force to the amount needed to keep the electron moving in the same circular orbit at the smaller velocity. The simplified analysis given above is a special case of a very famous theorem due to Larmor which will be discussed in greater detail in Chapter 6.

Suppose that the velocity of the electron has been increased to  $v_1$  by the application of the magnetic field of intensity  $H$ , then the force  $F_H$  due to the magnetic field is

$$F_H = Hev_1 = H e \omega_1 r$$

where

$$v_1 = \omega_1 r.$$

Since this force is directed toward the center, the total force acting radially is

$$F_0 + F_H = m\omega_1^2 r.$$

Substituting the values for  $F_0$  and  $F_H$ , we get

$$m_0\omega_0^2 r + He\omega_1 r = m\omega_1^2 r. \quad (8)$$

Solving equation (8) for  $\omega_1$ , we get

$$\omega_1 = \frac{\frac{eH}{m} \pm \sqrt{\left(\frac{eH}{m}\right)^2 + 4\omega_0^2}}{2}.$$

It can be shown that  $\left(\frac{eH}{m}\right)^2 \ll 4\omega_0^2$ ;

therefore we can write  $\omega_1 = \omega_0 + \frac{eH}{2m}$ . (9)

Only the positive sign is retained since the effect of the magnetic field is small and can produce only a slight change in the magnitude of the angular velocity. If the charge should be rotating in the opposite direction, its angular velocity will be decreased by the amount  $eH/2m$ , so that, in general, its angular velocity will be

$$\omega = \omega_0 \pm \frac{eH}{2m}. \quad (10)$$

This equation may be put in terms of the frequency of rotation

with the aid of the equations

$$\omega = 2\pi\nu$$

$$\omega_0 = 2\pi\nu_0,$$

where  $\nu$  is the frequency corresponding to the angular velocity  $\omega$ . Equation (10) then becomes

$$\nu = \nu_0 \pm \frac{eH}{4\pi m}. \quad (11)$$

The quantity  $eH/4\pi m$ , where  $e$  is in electromagnetic units, is called the normal Zeeman separation in a magnetic field of intensity  $H$ . The quantity  $e/m$  can thus be determined from a measurement of the normal Zeeman separation of a single spectrum line. Most recent determinations of  $e/m$  from measurements of the Zeeman effect yield

$$\frac{e}{m} = 1.757 \times 10^7 \frac{\text{c.m.u.}}{\text{gm}},$$

which is practically identical with the value of  $e/m$  obtained for electrons by means of electric and magnetic deflection experiments.

To compare prediction with experimental observation, consider the direction of the magnetic field  $H$  as that of the positive  $x$  axis; the current in the electromagnet producing this field can be represented as circular in the  $Y-Z$  plane, as shown in Figure 48. In the actual source of light, the atoms will have all possible orientations. Since light is a transverse wave motion, only those components of the acceleration of the electron which are perpendicular to the line of sight will be effective in sending radiation in this direction. Those electrons moving in orbits parallel to the  $Y-Z$  plane will have their frequencies increased or decreased by an amount  $eH/4\pi m$ . Any uniform circular motion can be resolved into two simple harmonic vibrations at right angles to one another and differing in time phase by a quarter of a period. If the light coming from these electrons is viewed along the  $z$  axis, only the  $y$  component of the vibration will be observed and the frequencies will be

$$\nu_1 = \nu_0 + \frac{eH}{4\pi m} \quad (12)$$

and

$$\nu_2 = \nu_0 - \frac{eH}{4\pi m}. \quad (13)$$

Since only the  $y$  component of the acceleration is effective in sending light in this direction, these components will be linearly polarized with the direction of vibration perpendicular to the magnetic

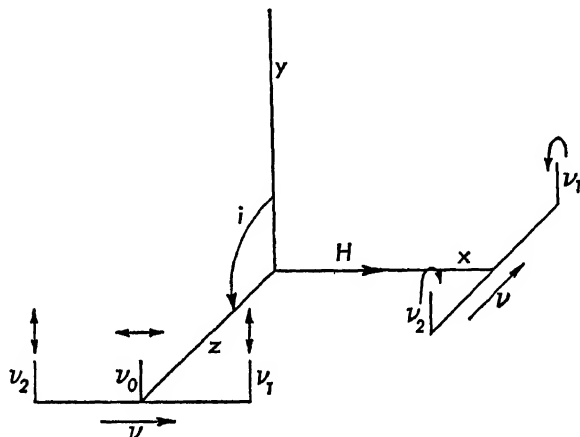


FIG. 48. — The direction of vibration of the components of a spectral line exhibiting the normal Zeeman effect in relation to the direction of the current producing the magnetic field.

field. If the light is viewed along the  $x$  axis, both the  $y$  and  $z$  vibrations will be effective in sending out radiations and the two component lines will be circularly polarized. Experiment shows that the higher frequency component is circularly polarized in the same direction as that of the current in the electromagnet. An analysis of the direction of the force due to the magnetic field shows that only a negative charge rotating in the same direction as that of the polarization can have its frequency increased by the magnetic field, Figure 48. The component of lower frequency is circularly polarized in the opposite direction and again must be due to a negative charge rotating in this direction. Thus it appears that the light emitted by an atom originates in negatively charged particles for which the value of  $e/m$  is identical with that observed for electrons.

To explain the presence of the undeviated component of frequency  $\nu_0$ , consider those vibrations which are parallel to the  $x$



axis. Since the motion of the electron is parallel to the direction of the magnetic field, there will be no additional force acting on it and its frequency will be unchanged. This component will therefore be observed when the light is viewed perpendicular to the magnetic field; the light of frequency  $\nu_0$  will be linearly polarized with the direction of vibration parallel to the direction of the magnetic field. This component will not be observed when the source is viewed parallel to the magnetic field since no light can be emitted parallel to the direction of motion of the charge.

### 43. Photoelectric Effect

The photoelectric effect was first observed by Hertz in his work on the production of electromagnetic waves. Hertz noted that the air in the spark gap became a better conductor when it was illuminated by ultraviolet light from an arc lamp. Hallwachs (1888) found that when ultraviolet light was incident on a negatively charged zinc surface, the surface lost its charge rapidly. If the surface was positively charged, there was no loss of charge under the action of the light. A neutral surface became positively charged when illuminated by ultraviolet light. It is evident that only negative charges are emitted by the surface because of the action of the ultraviolet light. Measurements of  $e/m$  for these negative charges by the usual electric and magnetic deflection methods show that these charges are electrons.

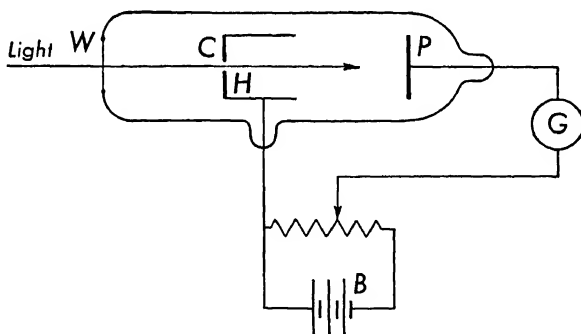


FIG. 49. — Experimental arrangement for measuring the photoelectric current.

A typical arrangement for the study of the photoelectric effect is shown in Figure 49. A glass tube has a quartz window  $W$  sealed on to it to permit ultraviolet light to enter the tube.  $P$  is the

photoelectric surface to be investigated and  $C$  is a hollow cylinder to collect the electrons emitted by  $P$ . A small hole in the base of the cylinder permits light to reach the plate  $P$ . In this type of work it is very important that the surface of the plate  $P$  be as clean as possible. Not only must the air be pumped out of the tube, but the entire tube must be baked during the pumping operation to get rid of as much gas as possible if the results of the experiment are to have any quantitative significance. Further, to insure that no electrons come from the cylinder  $C$  because of the action of scattered light,  $C$  is usually coated with copper oxide or some other substance which is comparatively insensitive photoelectrically. However, when  $C$  and  $P$  are made of different materials, it is found that a *contact* difference of potential exists between them. This contact difference of potential may be of the order of one or two volts. If the contact difference of potential between  $C$  and  $P$  is such as to make  $C$  negative with respect to  $P$ , then the motion of the electrons will be opposed by this contact potential difference. In all photoelectric experiments correction must be made for this contact difference of potential, and in the discussion which follows, the values of the potential difference between  $C$  and  $P$  have been corrected for the contact difference of potential.

When light from some source such as a quartz mercury arc lamp is incident on the plate  $P$ , the electrons emitted by the plate are collected by the cylinder  $C$ . A difference of potential is maintained between  $P$  and  $C$  by means of a potentiometer arrangement, and the photoelectric current is measured by a sensitive galvanometer  $G$ . The photoelectric current is found to depend upon two factors: (a) the intensity of the incident light, (b) the wave lengths of the incident beam. To determine the effect of each of these factors, monochromatic light of known wave length must be used. There are two points of interest in the photoelectric effect: one is the velocity with which the electrons are emitted by the surface, and the other is the number of electrons emitted under known conditions.

#### 44. Velocity of the Photoelectrons

If monochromatic light of wave length  $\lambda$  and intensity  $I$  is incident upon the surface  $P$ , the electrons emitted from the surface

will be acted upon by the electric field between the plate  $P$  and the collecting cylinder  $C$ . With a potentiometer arrangement, the electric field can be varied by varying the difference of potential between  $P$  and  $C$ . If  $C$  is made positive with respect to the plate, the electrons will be accelerated toward  $C$ ; if  $C$  is made negative,

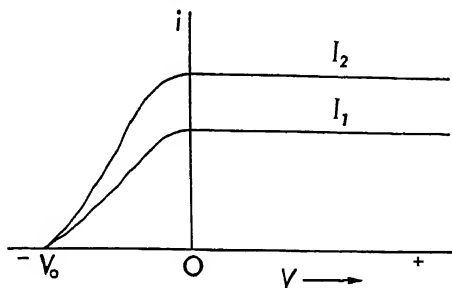


FIG. 50. — Curves of the photoelectric current produced by a monochromatic beam of light.

the electrons will be retarded. The current, as registered by the galvanometer, is proportional to the number of electrons per second reaching the cylinder. If the photoelectric current  $i$  is plotted against the difference of potential  $V$  between  $C$  and  $P$ , Figure 50, it is found that for all positive values of  $V$  the current is constant, but as  $C$  is made negative with respect to  $P$ , the current decreases rapidly and becomes zero at some value  $V_0$ . If the intensity of the monochromatic beam of light is increased from  $I_1$  to  $I_2$ , and the experiment is repeated, the photoelectric current is increased in the same ratio for all positive values of  $V$ . As  $V$  is made negative, the photoelectric current decreases sharply and reaches zero at the same value of the voltage  $V_0$ .  $V_0$  is called the *stopping potential* for this particular wave length  $\lambda$ .

There are two results of great importance that have been obtained in this experiment. The direct proportionality between the maximum current and the intensity of the light indicates that the number of electrons per second emitted by the surface  $P$  is directly proportional to the intensity of the incident beam of light. The fact that the stopping potential  $V_0$  is independent of the intensity of the beam can be interpreted only by assuming that the kinetic energy of the electrons emitted by the surface does not exceed a certain maximum value give by

$$V_0 e = \frac{1}{2} m v_{\max}^2. \quad (14)$$

Those electrons which leave the surface with kinetic energies less than the maximum are stopped by smaller values of the potential difference. This explains the decrease in the current when the potential difference between  $C$  and  $P$  is made negative.

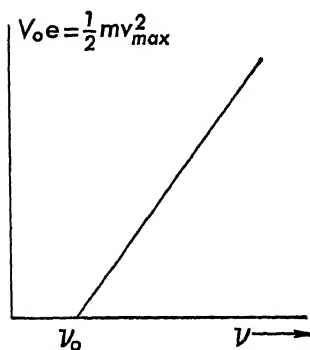


FIG. 51. — Dependence of the stopping potential on the frequency of the incident radiation.

The dependence of the stopping potential on the wave length of the light was investigated by Millikan (1916) in a series of very careful experiments using sodium and potassium as the photoelectric surfaces. The surfaces were illuminated by light of different wave lengths. The stopping potential,  $V_0$ , was determined for each particular wave length. The results of Millikan's experiments can best be represented in a graph, Figure 51, in which  $V_0e$  is plotted against the frequency,  $\nu$ , of the light incident upon the given surface. The curve is a straight line given by the equation

$$V_0e = \frac{1}{2}mv_{\max}^2 = h(\nu - \nu_0) = h\nu - h\nu_0, \quad (15)$$

where  $h$  is the slope of the line and  $\nu_0$  is the smallest frequency which can cause the emission of an electron from the surface. The frequency  $\nu_0$  is known as the *threshold frequency* and depends upon the nature of the surface. The slope  $h$ , however, is a constant which is independent of the nature of the surface. This constant  $h$  is known as the *Planck constant* and plays an exceedingly important role in atomic phenomena. The value of the Planck constant  $h$  determined photoelectrically depends upon the value of the electronic charge. Using the early value  $e = 4.77 \times 10^{-10}$  e.s.u., Millikan found that  $h = 6.55 \times 10^{-27}$  erg seconds. If the present value  $e = 4.802 \times 10^{-10}$  e.s.u. were used, the value of  $h$  would become  $6.59 \times 10^{-27}$  erg seconds. More recent determinations of this constant, particularly from measurements of the short wave length limit of the continuous X-ray spectrum, have yielded more precise values for the Planck constant. The present accepted value is

$$h = 6.624 \times 10^{-27} \text{ erg sec.}$$

## 45. Einstein's Photoelectric Equation

The direct dependence of the energy of the photoelectron upon the frequency of the incident light cannot be explained by the electromagnetic wave theory of light. On this classical theory there should be a relationship between the intensity of the incident light and the energy of the photoelectron. The intensity of an electromagnetic wave depends upon the square of the amplitude of the electric vector and is independent of the frequency of the light. To explain the photoelectric effect, Einstein (1905) made use of the concept of a *quantum of energy*, a concept which was first introduced into physics by Planck (1900), in order to explain the distribution of energy among the various wave lengths in the radiation from a "black body" at temperature  $T$ . According to Planck's theory, whenever radiation is emitted or absorbed by such a body, the energy is emitted or absorbed in whole *quanta*, where a *quantum of energy* is given by

$$\mathcal{E} = h\nu \quad (16)$$

in which  $\nu$  is the frequency of the radiation and  $h$  is the Planck constant. Such a quantum of energy has since received the name *photon*. The energy of a quantum or a photon is directly proportional to the frequency of the radiation. In Einstein's explanation of the photoelectric effect, the entire energy of a photon is transferred to a single electron in the metal, and when the electron comes out of the surface of the metal it will have an amount of kinetic energy given by

$$\frac{1}{2}mv^2 = h\nu - p. \quad (17)$$

Equation (17) is known as Einstein's photoelectric equation and is identical with equation (15) if  $p = h\nu_0$ .

The photoelectric effect is not confined to the action of light upon metallic surfaces. It can occur in gases and liquids as well as in solids. The nature of the light effective in producing the photoelectric effect includes the whole range of electromagnetic waves from the very short gamma and X rays, down into the infrared region of wave lengths. The quantity  $p$  should yield valuable information concerning the origin of the photoelectrons. For example, in the case of the surface photoelectric effect in conductors, it was assumed that  $p$  is equal to the work done by the elec-

tron in getting through the surface of the metal. According to the modern theory of electron conduction in metals, however, the conduction electrons have a wide range of energy values while they are inside the metal. This energy range depends only slightly upon the temperature of the metal. If  $W_i$  represents the energy of an electron in the metal and  $W_s$  the work necessary to go through the surface of the metal, then

$$p = W_s - W_i.$$

For the electron which comes through the surface with the maximum kinetic energy,

$$p = W_s - W_m = h\nu_0, \quad (18)$$

and therefore

$$\frac{1}{2}mv_{\max}^2 = h\nu - (W_s - W_m). \quad (19)$$

$W_s$  is called the work function of the particular surface, and  $W_m$ , according to the theory of conduction, is given by

$$W_m = \frac{h^2}{2m} \left( \frac{3n}{8\pi} \right)^{2/3}, \quad (20)$$

where  $h$  is the Planck constant,  $m$  the mass of the electron, and  $n$  the number of free electrons per unit volume. The results of the determinations of the work function  $W_s$  from photoelectric measurements are in agreement with data on thermionic emission of electrons and on the refraction of electrons in crystals.

## 46. Discovery of X Rays

X rays were discovered by Röntgen in 1895. He found that the operation of a cathode ray tube produced fluorescence in a platinum-barium-cyanide screen placed at some distance from the tube. The source of the rays causing this fluorescence was traced to the walls of the cathode ray tube. In further experiments he found that the interposition of various thicknesses of different substances between the screen and the tube reduced the intensity of the fluorescence but did not obliterate it completely. This showed that these "X" rays, as Röntgen called them, had very great penetrating power. It was also found that these rays could blacken a photographic plate and could ionize a gas.

The X rays, or Röntgen rays, traveled in straight lines from the source and were not deflected in passing through electric or magnetic fields. They were thus not charged particles. Röntgen tried to reflect and refract them but without success. Haga and Wind, in 1899, tried to diffract X rays through a narrow aperture. They actually succeeded in getting a diffraction pattern, but the effect was so small that their results were not generally accepted as conclusive. It was not until 1912 that the wave nature of X rays was definitely established by Laue's experiments on the diffraction of X rays by crystals. Barkla's experiments on the polarization of X rays established the fact that these rays were transverse waves similar to light waves.

## 47. Production of X Rays

X rays are produced whenever fast-moving electrons strike a substance. In Röntgen's experiment the cathode rays struck the walls of the tube so that the glass wall became the source of the X rays. The gas-filled type of X-ray tube is a modification of the cathode ray tube. Instead of allowing the cathode rays to strike the walls of the tube, the cup-shaped cathode *C* focuses them onto a metal target, *T*, Figure 52.

The anode, or anticathode, *A*, is usually put in a side tube and connected to the target *T*. The gas pressure in the tube is of the

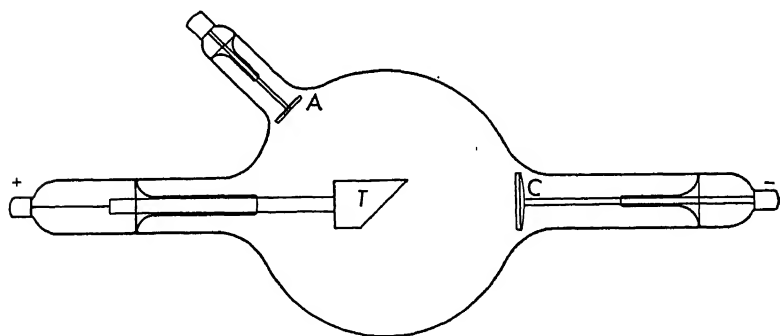


FIG. 52. — Gas-filled type of X-ray tube.

order of 0.001 mm of Hg, and the difference of potential between the cathode and anode is usually of the order of 30,000 to 50,000 volts. The electrons from the cathode are stopped by the target,

which then becomes the source of X rays. These X rays proceed in all directions from the target.

The Coolidge type of X-ray tube is a thermionic tube in which the cathode is a tungsten filament; one common design of a Coolidge tube is shown in Figure 53. When the filament is heated to incandescence by means of a current supplied either by a storage

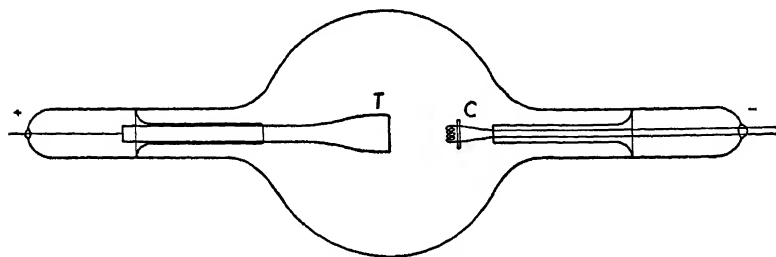


FIG. 53. — Coolidge type of X-ray tube.

battery or by a step-down transformer, electrons are emitted by the filament. These electrons are accelerated to the target by a difference of potential maintained between *C* and *T*. The filament is usually placed inside a metallic cup, not shown in the figure, in order to focus the electrons on to the target. The tube must be highly evacuated so that no electric discharge can take place in the residual gas under normal operating conditions. One great advantage of the Coolidge type of tube is that the emission, and hence the current in the tube, can be controlled by varying the temperature of the filament. In general, the Coolidge tube is more stable in operation than the gas type of tube.

Coolidge X-ray tubes have been designed to operate at voltages which range from a few hundred volts to about one million volts. Various types of high voltage sources are used in operating X-ray tubes. In special cases small lead storage cells have been connected in series to supply voltages from a few hundred volts up to one hundred thousand volts. The most common type of high voltage source is the step-up transformer with its secondary coil well insulated from the primary coil. If the A.C. voltage from the secondary is applied directly across the cathode and the target of the X-ray tube, the tube acts as its own rectifier, that is, current flows in the tube only during that half of the cycle in which the target is positive with respect to the cathode. In those



experiments in which it is necessary to have a constant direct current through the tube, the transformer terminals are connected to a rectifier circuit consisting of two or more high voltage rectifiers together with a large capacitor and inductance coils. The rectified, constant D.C. voltage is then applied to the X-ray tube.

When an X-ray tube is to be operated continuously with comparatively large amounts of power, special arrangements must be made for cooling the target. One common method for doing this is to mount the target material on a hollow copper tube and to circulate water through this tube. Almost any substance can be used as the target of an X-ray tube, depending upon the problem under investigation. The targets of general purpose X-ray tubes usually are made of tungsten or molybdenum because these metals have high melting points.

#### 48. The Betatron

An entirely new type of X-ray tube has recently been developed by D. W. Kerst (1941); this tube is called a *betatron*. In the older type of X-ray tubes, the electrons which strike the target acquire their energy by the application of a high voltage between the filament and the target. In the betatron, the electrons acquire their energy by the action of the force exerted on them by the electric field which accompanies a changing magnetic field. One tube now in operation (1946) accelerates electrons so that they have energies up to 100 Mev when they strike the target and produce X rays. These X rays have been used in nuclear experiments as described in Chapter 8.

In the operation of the betatron, electrons from the heated filament  $F$  are injected into the circular or doughnut-shaped tube by applying a difference of potential between the filament and the plate  $P$ , see Figure 54. The electrons are focused with the aid of the grid  $G$ . When an alternating magnetic field is applied parallel to the axis of the tube, two effects are produced: an electromotive force tangential to the electron orbit is produced by the changing magnetic flux and gives the electrons additional energy; a radial force due to the action of the magnetic field, which is perpendicular to the electron velocity, keeps the electron moving in a circular path. The magnetic flux through the orbit has to be chosen in such a way that the electrons will move in a stable orbit of fixed

radius  $R$ . The electrons make several hundred thousand revolutions in this circular path while the alternating magnetic field is increasing in intensity from zero to a maximum, that is, during a

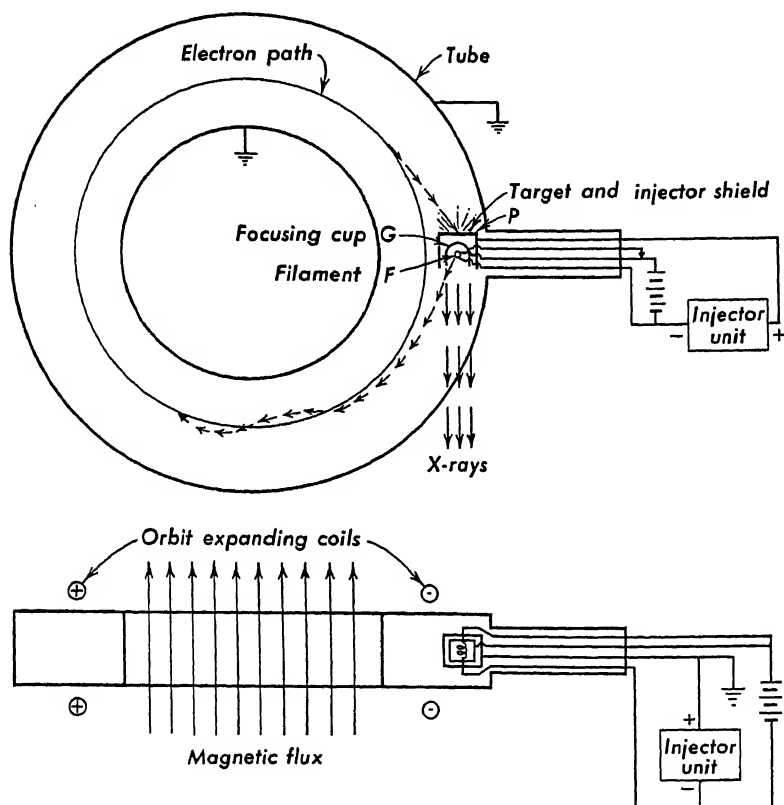


FIG. 54. — Path of an electron in a betatron tube.

quarter of a cycle. With each revolution they gain additional energy. When the electrons have acquired the desired amount of energy, a capacitor is discharged through two coils of wire, one directly above and the other directly below the stable orbit producing a sudden addition to the magnetic flux. This destroys the condition for the stability of this orbit and the electron beam moves out to larger radii until it strikes the back of the injector  $P$  which acts as the X-ray target.

In the operation of the 20 Mev betatron, about 15 to 20 kilovolts are applied to the injector, and electrons are injected into

the tube for only a short time, about 8 microseconds, when the magnetic field just starts increasing. The magnetic field alternates 180 times per second, but the electrons are accelerated during only one quarter of a cycle or  $1/720$  of a second. The tube is kept on

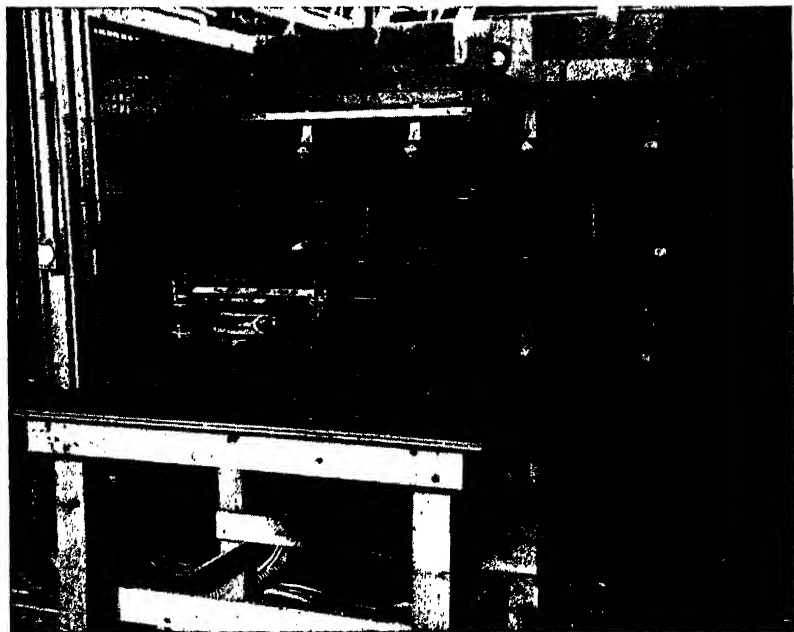


FIG. 55. — Photograph showing the original 2.3 Mev betatron in front of the 20 Mev betatron. Each machine has its doughnut-shaped vacuum tube in place between the poles of the magnet. (From a photograph supplied to the author by Professor D. W. Kerst.)

the vacuum pumps continuously. Figure 55 is a photograph showing both the 2.3 Mev betatron and the 20 Mev betatron with the doughnut-shaped tube between the poles of the electromagnet in each case.

We can think of the circular electron path of fixed radius  $R$  as a circuit, and the e.m.f.  $V$  induced in this circuit by the changing magnetic flux is, according to Faraday's law,

$$V = \frac{d\Phi}{dt}$$

where  $\Phi$  is the instantaneous value of the magnetic flux which is perpendicular to the plane of the circuit. The work done on an

electron of charge  $e$  is therefore

$$Ve = e \frac{d\Phi}{dt}.$$

This work can also be expressed in terms of the tangential force  $F$  which, acting on the electron over a distance  $ds$ , does an amount of work  $dW$  given by

$$dW = F \cdot ds$$

from which

$$F = \frac{dW}{ds}.$$

Thus the tangential force acting on the electron is equal to the work done per unit length of path. Evaluating this for one revolution for which the path length is  $2\pi R$ , we get

$$F = \frac{Ve}{2\pi R} = \frac{e}{2\pi R} \frac{d\Phi}{dt}.$$

Now, from Newton's second law

$$F = \frac{d}{dt}(mv);$$

hence

$$\frac{d}{dt}(mv) = \frac{e}{2\pi R} \frac{d\Phi}{dt}$$

or

$$d(mv) = \frac{e}{2\pi R} d\Phi. \quad (21)$$

Because of the presence of the magnetic flux perpendicular to the plane of the electron orbit, the electron will experience a radial force inward given by

$$Hev = \frac{mv^2}{R}$$

where  $H$  is the value of the magnetic field intensity at the electron orbit of constant radius  $R$ . From the above equation

$$mv = HeR;$$

therefore

$$d(mv) = eR \cdot dH. \quad (22)$$

Comparing equations (21) and (22) we see that

$$\frac{e}{2\pi R} d\Phi = eR dH,$$

from which

$$d\Phi = 2\pi R^2 dH.$$

Integrating this equation between the limits of zero and  $\Phi$  and zero and  $H$  respectively, we get

$$\Phi = 2\pi R^2 H \quad (23)$$

for the instantaneous relationship between the total magnetic flux  $\Phi$  and the intensity of the magnetic field  $H$  at a distance  $R$  from the center. This equation shows that the magnetic flux within the orbit of radius  $R$  is always proportional to the intensity of the magnetic field at the orbit, and, furthermore, that the magnetic flux through the orbit is twice what it would have been if the magnetic field intensity were uniform throughout the orbit at the value  $H$ . This distribution of magnetic flux is obtained in an air gap between specially shaped pole faces of an electromagnet.

Since the magnet and its coils correspond to an inductance, by adding sufficient capacitors we can produce resonance in this circuit at the desired frequency, which in this case is 180 cycles per second for the 20 Mev betatron. The magnetic pole faces of the 20 Mev betatron are 19 inches in diameter and the radius of the equilibrium orbit is 7.5 inches. The magnetic structure weighs about 3.5 tons. The operating power when producing 20 Mev electrons is about 25 kilowatts. The efficiency of X-ray production is very great; about 65 per cent of the electron beam energy is converted into X rays, the rest into heat.

#### 49. Measurement of the Intensity of X Rays

The intensity of a beam of X rays may be measured by any one of its effects, such as the blackening of a photographic plate, the rise in the temperature of a piece of lead which absorbs these rays, or by the ionization produced in a gas or vapor. The photographic effect and the ionization effect are the ones most commonly used in quantitative measurements.

A typical ionization chamber used for measuring the intensity of a beam of X rays is shown in Figure 56. The ionization chamber consists of a metal cylinder  $C$  containing some convenient gas or vapor such as air or methyl bromide, at about atmospheric pressure. A metal rod  $R$ , insulated from the cylinder, runs parallel to the axis of the cylinder. The X-ray beam enters the chamber through a thin window  $W$ , usually made of mica or thin aluminum,

and ionizes the gas in the chamber. A battery  $B$  maintains a difference of potential between  $R$  and  $C$  so that the ions are set in motion toward  $C$  and  $R$  just as soon as they are formed. This ionization current is measured by the electrometer  $E$ . Experiment shows that the ionization current is directly proportional to the intensity of the X-ray beam.

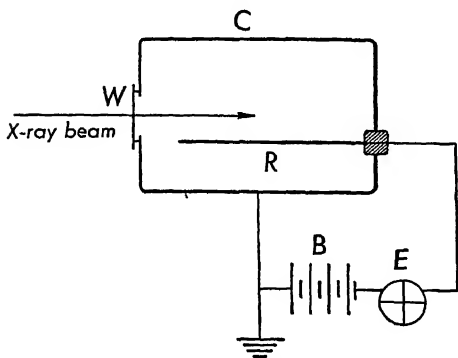


FIG. 56. — Ionization chamber and electrometer for measuring the intensity of X rays.

The intensity of the X rays coming from any tube depends upon two major factors, the element used as the target and the power supplied to the tube. The intensity of the X rays coming from any target is

directly proportional to the atomic number of the element constituting the target. The total energy emitted in the form of X rays is less than 1 per cent of the energy supplied to a tube operating at about 50,000 volts.

## 50. Diffraction of X Rays

The explanation of the origin of X rays on the basis of classical electrodynamics is that X rays are emitted in the form of electromagnetic pulses or groups of waves when the electrons are stopped by the target of an X-ray tube. The existence of a wave motion can be definitely established only by diffraction and interference phenomena. The conditions under which these phenomena occur are well known for waves in the visible region of the spectrum. For example, if yellow light is allowed to pass through a diffraction grating having about 6000 lines to the centimeter, a diffraction pattern is obtained consisting of a central image or undeviated line, then a first-order image which is deviated by about  $20^\circ$  from the original direction, and farther on a second-order image, and so on. An analysis of the action of the grating shows that the spacing between the lines ruled on the grating should be of the order of magnitude of the wave length of the light used. The results of the early experiments on the diffraction of X rays indicated that their

wave lengths were of the order of  $10^{-8}$  or  $10^{-9}$  cm. It occurred to von Laue (1912) that the ordered arrangement of atoms or molecules in crystals fulfilled all the conditions essential for the diffraction of such short wave lengths. The spacing between these atoms or molecules was known to be of the order of  $10^{-8}$  cm. A

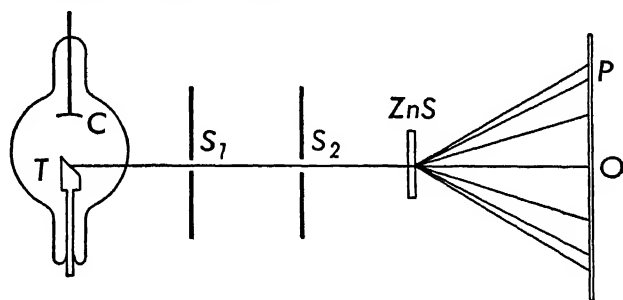


FIG. 57. — Arrangement of apparatus for producing a Laue diffraction pattern. crystal differs from an ordinary diffraction grating in that the diffracting centers in the crystal are not all in one plane; the crystal acts as a space grating rather than as a plane grating.

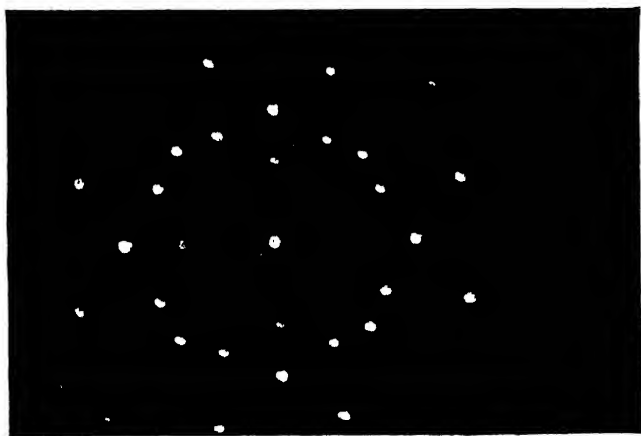


FIG. 58. — Photograph of Laue diffraction pattern of rock salt. (From photograph by J. G. Dash.)

Following von Laue's suggestion, Friedrich and Knipping carried out the following experiment. A narrow pencil of X rays was allowed to pass through a thin crystal of zinc blende ( $\text{ZnS}$ ). The emergent beam fell on a photographic plate  $P$ , Figure 57. The diffraction pattern obtained consisted of the central spot at  $O$  and a series of spots arranged in a definite pattern about  $O$ .

Figure 58 is a photograph of the Laue diffraction pattern obtained by passing a narrow pencil of X rays through a thin crystal of rock salt perpendicular to its *cleavage* planes; these cleavage planes are parallel to a surface along which a crystal can be readily

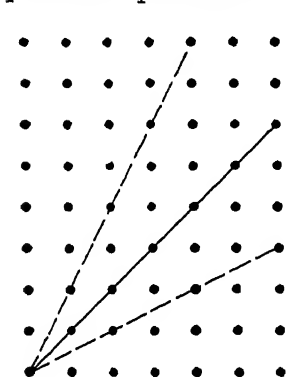


FIG. 59. — Orientation in a crystal of planes which are rich in atoms.

split or broken. From a knowledge of the structure of the crystal, some of the wave lengths in the incident radiation could be computed. A simple interpretation of the diffraction pattern was given by W. L. Bragg. He assumed that the diffraction spots were produced by X rays which were scattered from certain planes within the crystal, which contained large numbers of atoms. That some planes are richer in atoms than others can be seen by considering a two-dimensional array of points, and drawing lines through these points, Figure 59. These lines correspond

to planes in a three-dimensional crystal.

It is easy to derive the condition under which the X rays scattered from a series of atomic planes will produce an intense spot. Consider a series of parallel atomic planes spaced a distance  $d$

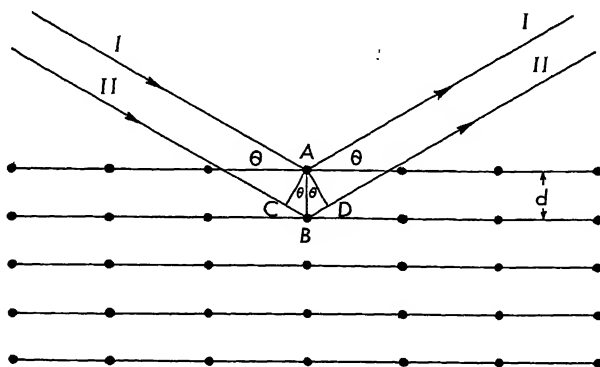


FIG. 60. — "Reflection" of X rays from atomic planes.

apart. Suppose a narrow beam of X rays from some source is incident upon these planes at an angle  $\theta$ , Figure 60. The beam will be scattered in all directions by the atoms in the various atomic planes. Let us consider that portion of the beam which is scat-



tered at an angle  $\theta$  to the atomic planes so that the angle of reflection is equal to the angle of incidence. Consider two rays such as  $I$  and  $II$ , which are scattered by two particles  $A$  and  $B$  in adjacent planes. Ray  $II$  travels a longer path than ray  $I$ ; this difference in path is evidently  $CB + BD$ . In the figure, the spacings are greatly enlarged; actually these two rays are so close together that they produce a single impression on a photographic plate. Whenever the difference in path  $CB + BD$  is a whole wave length,  $\lambda$ , or a whole multiple of the wave length,  $n\lambda$ , then the waves will reinforce each other and produce an intense spot. The condition for reinforcement is thus

$$CB + BD = n\lambda,$$

and from the figure

$$CB = d \sin \theta$$

and

$$BD = d \sin \theta;$$

hence

$$n\lambda = 2d \sin \theta. \quad (24)$$

This is known as Bragg's equation and gives the condition for the *reflection* of X rays from a series of atomic planes. If the distance between atomic planes is known, the wave length of the X rays can be calculated; or the converse, using X rays of known wave lengths, distances between atomic planes can be computed.

In Bragg's equation  $n$  is always an integer. When  $n = 1$ , the difference in path between waves reflected from any two adjacent planes is one wave length. For this case,

$$\lambda = 2d \sin \theta_1$$

gives the condition for the first-order reflection of wave length  $\lambda$  from the crystal. For  $n = 2$ , the equation becomes

$$2\lambda = 2d \sin \theta_2;$$

that is, the second-order reflection of the same wave length will occur at a larger angle of incidence and reflection,  $\theta_2$ .

The analysis used in deriving the Bragg equation can now be used to explain the Laue diffraction pattern. The X rays which

penetrate the crystal are scattered from the different atomic diffraction centers. We can construct sets of parallel atomic planes inside the crystal as shown in Figure 61 and apply the Bragg

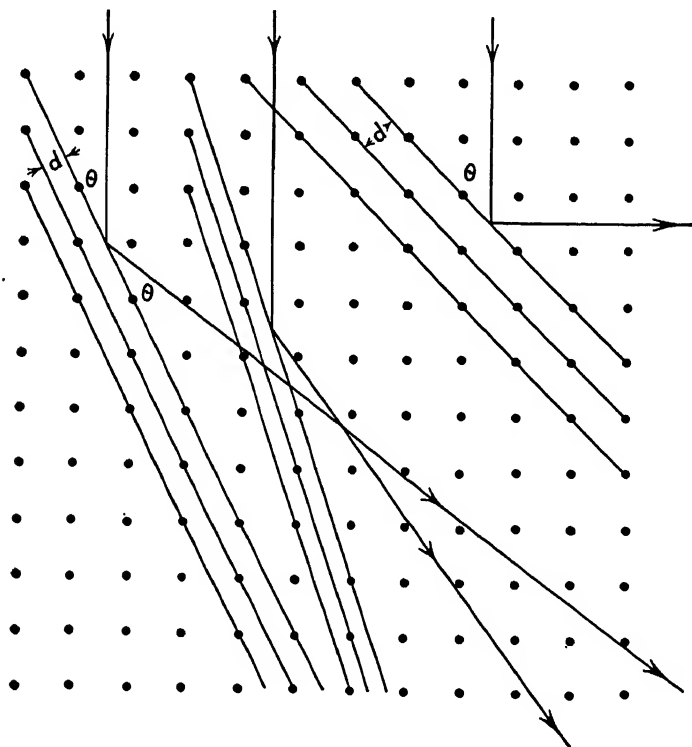


FIG. 61. — Reflection of X rays from sets of atomic planes within a crystal to produce the Laue diffraction pattern.

equation to each set of parallel planes. The value of the incident angle will be different for each set of planes, and each set of parallel planes will have its own particular value for the distance  $d$ , but these distances will be related in a simple way to the distance between planes which are parallel to the cleavage face because of the geometry of the crystal. The X rays scattered from any set of parallel planes will reinforce each other only if the particular wave length which will satisfy the Bragg equation is present in the incident beam. Furthermore, an examination of Figure 61 will show that there are comparatively few sets of parallel planes which are sufficiently rich in atoms to produce intense diffraction

spots. Hence, even if the incident radiation contains a wide range of wave lengths, which is the most common method of producing a Laue pattern, the number of intense diffraction spots produced will be small in spite of the large number of atomic diffraction centers in the crystal.

## 51. Single Crystal X-Ray Spectrometer

The Laue diffraction patterns are very complex and difficult to interpret. Instead of using a crystal as a transmission grating,

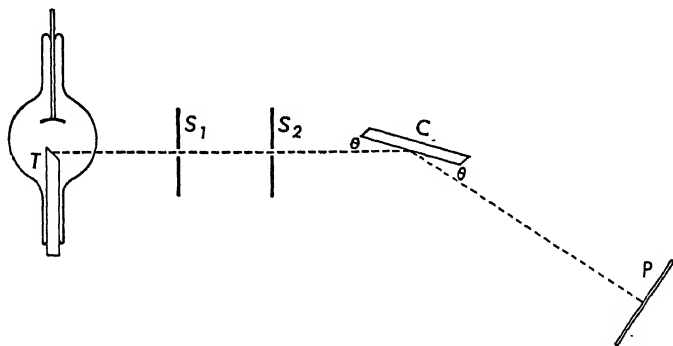


FIG. 62. — Single crystal X-ray spectrometer, with photographic plate.

Bragg set up the crystal as a reflection grating. A typical experimental arrangement is shown in Figure 62. Two lead slits  $S_1$  and  $S_2$  define a narrow beam of X rays coming from the target  $T$ . This beam of X rays strikes the crystal  $C$  at some angle  $\theta$ , and is reflected by it to the photographic plate  $P$ . The crystal  $C$  is mounted on a spectrometer table and can be rotated so that the glancing angle  $\theta$  may be varied.

At each particular setting of the crystal only the particular wave length  $\lambda$  which satisfies Bragg's equation

$$n\lambda = 2d \sin \theta$$

will be reflected to the photographic plate. As the crystal is rotated, other wave lengths will be reflected by the crystal. In this way a spectrum of the incident beam is obtained. The spectrum may consist of several orders. If, in Bragg's equation,  $n\lambda = 2d \sin \theta$ ,  $n$  has the value unity, the spectrum is said to be a first-order spectrum; if  $n = 2$ , a second-order spectrum is obtained, and so on.

In many experiments, the photographic plate is replaced by an ionization chamber which can be rotated about the same axis as the crystal. The ionization chamber is usually used to make accurate measurements of the relative intensities of various wave lengths.

The choice of crystal to be used in an X-ray spectrometer is determined by several factors, such as the range of wave lengths to be examined, the ease with which a good surface can be obtained, and the reflecting power of the crystal. Crystals most commonly used are calcite, quartz, and rock salt. It is obvious that for use in measuring X-ray wave lengths, the distance  $d$  between atomic planes in the crystals must be known from other data. Sufficient data can be obtained from crystallographic studies for some of the simpler crystals, such as rock salt and calcite, for an independent determination of the spacing between atomic planes.

## 52. The Grating Space of Rock Salt Crystals

The distance between atomic planes, or the *grating space* of a crystal, can be calculated when the structure of the crystal is known. Rock salt, one of the best known and one of the simplest of crystals, has the geometrical structure of a simple cube, with ions of sodium and chlorine arranged alternately at the corners of a cube, as shown in Figure 63. The distance between atomic planes can be found by determining the volume of one of these elementary cubes. If  $M$  is the molecular weight of NaCl and  $\rho$  is its density, then the volume of one mole of NaCl is

$$v = \frac{M}{\rho}.$$

Since there are  $2N$  ions or diffracting centers in a mole, the volume associated with each ion will be

$$V = \frac{M}{2\rho N},$$

where  $N$  is Avogadro's number. The distance  $d$  between ions will therefore be

$$d = \sqrt[3]{\frac{M}{2\rho N}}. \quad (25)$$

The molecular weight of sodium chloride is 58.45 and its density is 2.164 gm/cm<sup>3</sup>. Substitution of the value of  $N$  yields  $d = 2.814 \times 10^{-8}$  cm. This was the value known in 1913. The meas-

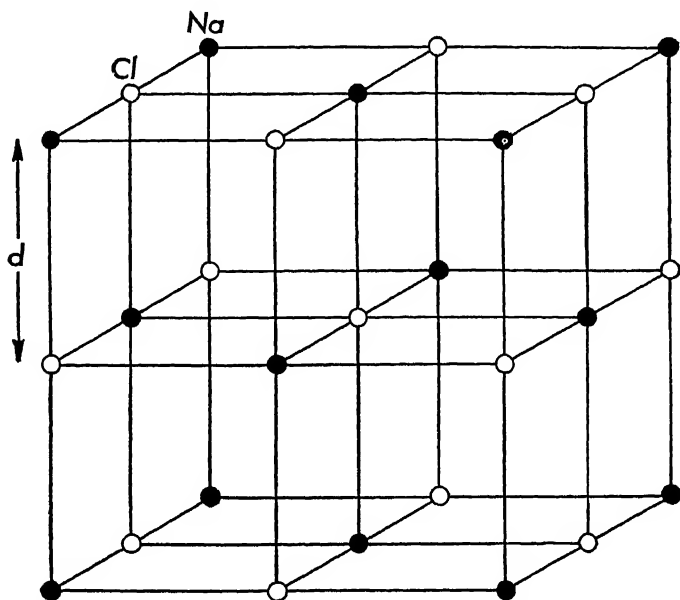


FIG. 63. — Arrangement of sodium ions and chlorine ions in a sodium chloride crystal.

urements of X-ray wave lengths soon achieved very high precision. Siegbahn, from whose laboratory came a great many of the precise determinations of X-ray wave lengths, adopted the value

$$d = 2.81400 \times 10^{-8} \text{ cm at } 18^{\circ}\text{C}$$

for the grating space of rock salt. Large, good, single crystals of rock salt of the type needed for X-ray measurements are not readily available, and when available, have the defect of being hygroscopic; calcite is a much better crystal for such measurements and is more readily obtainable as good, large, single crystals. Careful comparisons between calcite and rock salt crystals made with monochromatic X rays led to the adoption of the value

$$d = 3.02945 \times 10^{-8} \text{ cm at } 18^{\circ}\text{C}$$

for the grating space of calcite. Unless otherwise noted, all X-ray

wave length measurements are based upon the above value for the grating space of calcite. (See § 58.)

### 53. Typical X-Ray Spectra

With a knowledge of the grating space of a crystal and the use of Bragg's equation, it is possible to measure the wave lengths of the X rays emitted by the target of an X-ray tube. When resolved by means of a crystal spectrometer, the heterogeneous beam of X rays from a target is found to consist of two distinct types of spectra:

- (1) A continuous spectrum;
- (2) A sharp line spectrum superposed on the continuous spectrum.

Typical X-ray spectra, obtained by Ulrey, are shown in the curves in Figure 64, in which the intensity of a given wave length is plotted against the wave length in angstrom units. The curve for tungsten shows the continuous spectrum of the X rays coming from the tungsten target of an X-ray tube operated at a voltage of 35 kilovolts. The curve for molybdenum was obtained under similar conditions and shows two sharp lines characteristic of the element molybdenum superposed on the continuous spectrum. These lines are known as the  $K_\alpha$  and  $K_\beta$  lines of molybdenum. To get the  $K_\alpha$  and  $K_\beta$  lines of tungsten, the tube would have to be operated at about 70 kilovolts (§ 103).

### 54. Continuous X-Ray Spectrum

The continuous X-ray spectrum presents several interesting features. It will be noted from Figure 64 that there is a definite short wave-length limit  $\lambda_{\min}$  to the continuous X-ray spectrum independent of the material of the target. Figure 65 shows the distribution of intensity with respect to wave length for different accelerating potentials. When the voltage across the tube is increased, the short wave-length limit  $\lambda_{\min}$ , is shifted toward smaller values. Duane and Hunt showed that the short wave-length limit of the continuous spectrum varies inversely as the voltage across the tube. Put in terms of frequencies,

$$\nu_{\max} = \frac{c}{\lambda_{\min}},$$

and

$$Ve = h\nu_{\max} = \frac{hc}{\lambda_{\min}}, \quad (26)$$

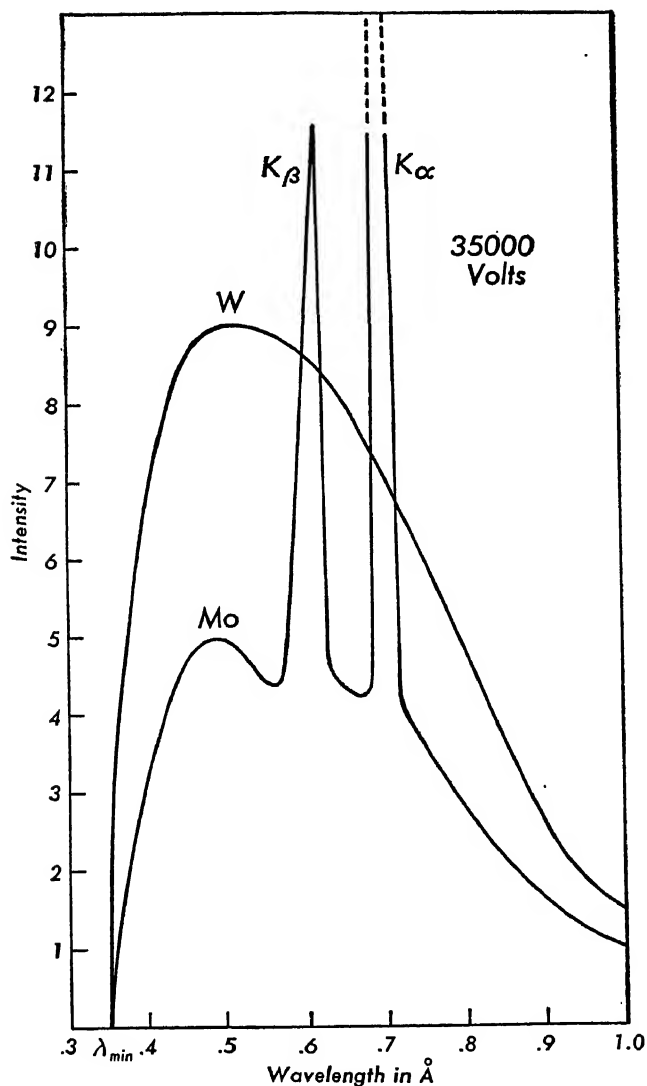


FIG. 64. — Typical X-ray spectra obtained from tungsten and molybdenum targets, respectively.

where  $V$  is the voltage across the tube,  $e$  is the electronic charge, and  $h$  is the Planck constant.  $Ve$  represents the energy with which

an electron strikes the target. Duane and Hunt carried out a series of careful experiments on the determination of the short

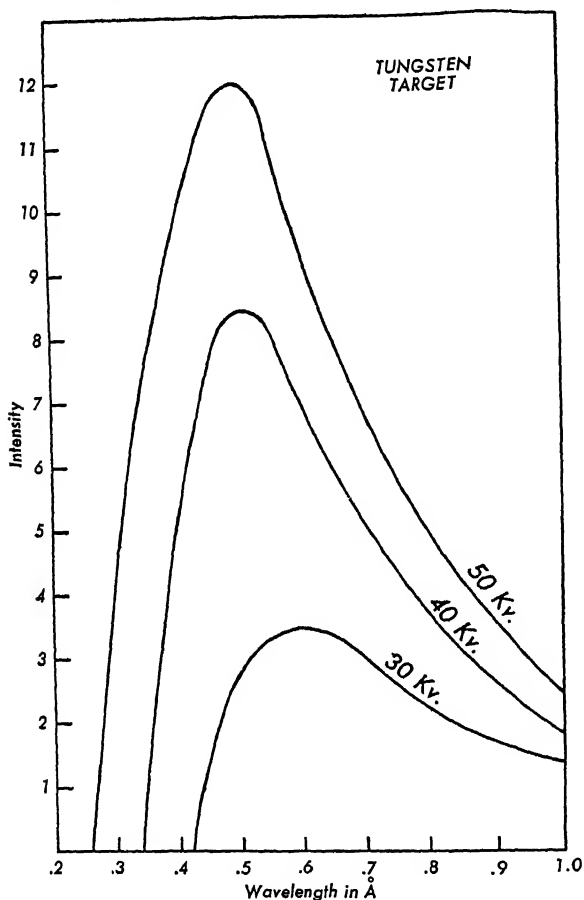


FIG. 65. — The continuous X-ray spectrum from a tungsten target showing the dependence of the short wave-length limit on the voltage across the tube.

wave-length limit of the continuous X-ray spectrum for various voltages across the X-ray tube and determined the value of the Planck constant  $h$  to be

$$h = 6.556 \times 10^{-27} \text{ erg sec.}$$

This is in good agreement with the value of  $h$  determined by means of the photoelectric effect. One may look at this phenomenon as the inverse of the photoelectric effect, since the maximum kinetic



energy of an electron striking the target is

$$\frac{1}{2}mv_{\max}^2 = Ve = h\nu_{\max}. \quad (27)$$

Another method for determining  $h$  by means of X rays is to keep the crystal fixed at some arbitrary angle  $\theta$ , and to increase the voltage across the tube until the wave length corresponding to this angle first appears. The wave length is then determined from Bragg's equation. A typical curve of this type, obtained by Feder, using a rock salt crystal set at  $\theta = 14^\circ 00.5'$ , is shown in Figure 66. The voltage at which the wave length first appeared was 9045 volts. From a series of such experiments Feder obtained the value

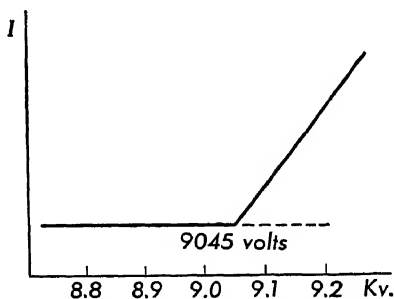


FIG. 66. — Determination of the voltage at which a given X-ray wave length first appears.

$$h = 6.5465 \times 10^{-27} \text{ erg sec.}$$

This X-ray method provides one of the most accurate ways of determining  $h$ , but it must be remembered that the value of the electronic charge  $e$  must be known in order to calculate  $h$ . In the above determinations of  $h$ , Millikan's original value of  $e$  ( $= 4.77 \times 10^{-10}$  c.s.u.) was used.

## 55. Wave Lengths of Gamma Rays

In examining the radiations from radioactive materials, it was found that gamma rays were not affected by electric and magnetic fields. It is now known that gamma rays are short electromagnetic waves of the same nature as X rays, except that they are emitted from the nucleus of the atom. The wave lengths of some of the gamma rays have been measured by X-ray crystal diffraction methods.

Rutherford and Andrade (1914) made use of the Bragg spectrometer for determining the wave lengths of gamma rays from radium B. A narrow beam of gamma rays from the radioactive preparation, *R*, Figure 67, after passing through a fine slit in a lead block, was reflected by the rock salt crystal, *C*, on to the

photographic plate, *P*. By rotating the crystal from  $0^\circ$  to about  $15^\circ$ , a series of sharp lines was obtained corresponding to the gamma-ray wave lengths emitted by radium B. This method has been used for measuring the wave lengths of the gamma rays from many other radioactive substances. The smallest gamma-ray wave length measured with the crystal spectrometer is  $\lambda = 0.016\text{\AA}$ , one of the lines emitted by radium C. In order to produce X rays of the same wave length, the X-ray tube would have to be operated at a difference of potential of 770,000 volts. X-ray tubes capable of being operated at such high voltage have been developed and are now in use in many laboratories.

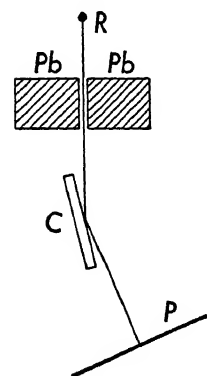


FIG. 67. — Crystal reflection method of determining gamma-ray wave lengths.

## 56. X-Ray Powder Crystal Diffraction

Comparatively few substances are available in the form of large single crystals for use in the Bragg type of spectrometer. Most substances exist as aggregates of very small crystals. Methods have been developed for studying the crystal structure of a substance even though these crystals may be very minute. If the substance is made into a very fine powder, it may be considered as made up of a multitude of very small crystals.

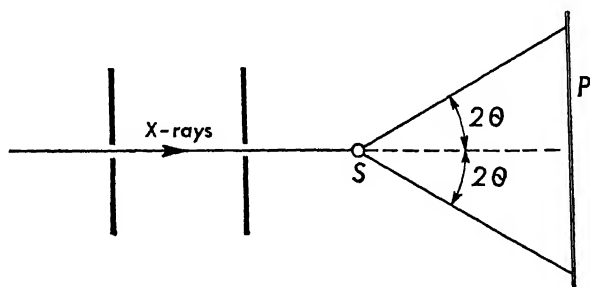


FIG. 68. — Method of obtaining X-ray diffraction patterns using a powder.

Suppose a very narrow pencil of monochromatic X rays of wave length  $\lambda$  is incident on this powder at *S*, Figure 68. Since these small crystals are oriented at random, there undoubtedly will be some crystal oriented at just the right angle to satisfy Bragg's equa-

tion  $n\lambda = 2d \sin \theta$  for this particular wave length  $\lambda$ . The scattered beam will have maximum intensity at an angle  $2\theta$  with respect to the incident beam of X rays, and because of the random orienta-

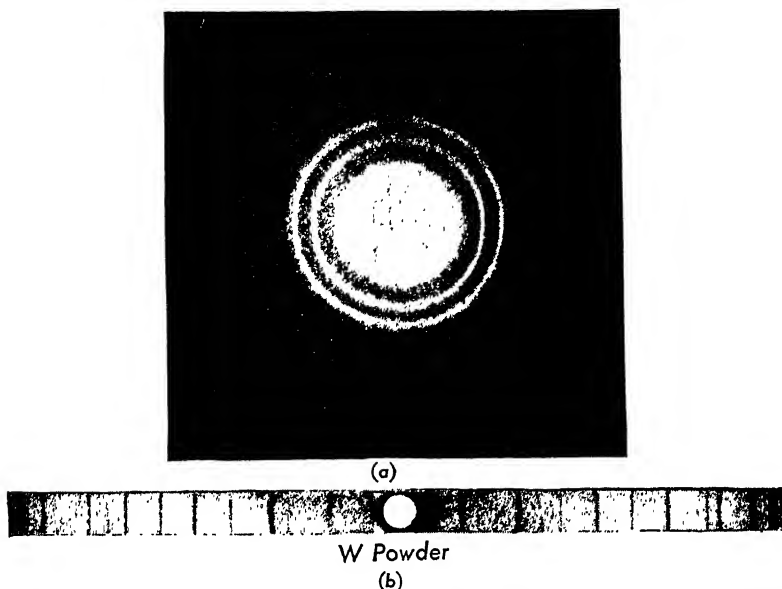


FIG. 69. — (a) X-ray powder diffraction pattern of aluminum. (Reproduced with the permission of A. W. Hull.)

(b) X-ray powder diffraction pattern of tungsten obtained with a film bent in the form of a circle. Radiation from a copper target was used in making this photograph. (From a photograph made by L. L. Wyman and supplied by A. W. Hull.)

tions of the crystals, these maxima will lie on a cone of central angle  $4\theta$ . If the X rays scattered by the powder are incident on a photographic plate placed perpendicular to the incident beam, concentric circles will be registered on it corresponding to the different orders of reflection. Another method is to bend a thin strip of photographic film in the form of a circle with the powder at the center of this circle. Small holes are cut in this film to permit the direct beam of X rays to enter and leave the camera without blackening the photographic film.

Frequently, instead of a monochromatic beam, X rays from a target which emits a few intense characteristic lines are used for these powder photographs. Since the relative intensities of these characteristic lines are known, it is not difficult to determine which circles correspond to the different wave lengths. Typical

powder crystal diffraction patterns are shown in Figure 69. This method of crystal analysis was first developed by Debye and Scherrer and by Hull, and is one of the most valuable aids in studying crystal structure.

## 57. Refraction of X Rays

Several of the early experimenters, including Röntgen and Barkla, tried to find out whether X rays are refracted when they

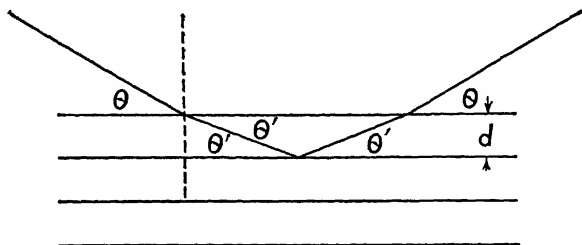


FIG. 70. — Refraction of X rays on penetrating a crystal.

enter a material medium. The phenomenon of refraction, however, was not discovered until 1919, when Stenström observed that Bragg's law  $n\lambda = 2d \sin \theta$  did not yield the same value for  $\lambda$  in the different orders of reflection of a monochromatic beam from a crystal. The explanation of this apparent failure of Bragg's law is that the X rays are refracted when they penetrate the crystal. Because of refraction, the wave length in the crystal is different from that outside. If  $\mu$  is the index of refraction,  $\lambda$  the wave length in a vacuum, and  $\lambda'$  the wave length in the crystal, then

$$\mu = \frac{\lambda}{\lambda'}. \quad (28)$$

Further, the angle of incidence upon the inner crystal planes is not the angle between the incident beam and the surface of the crystal, but is the angle between the refracted ray and the atomic planes in the crystal. The deviations from Bragg's law show that the angle of refraction  $\theta'$  is less than the grazing angle of incidence  $\theta$ ; that is, that the X rays are bent away from the normal upon penetrating into the crystal. This means that the index of refraction for X rays is less than unity. In Figure 70, if  $\theta$  is the angle between the incident ray and the surface of the crystal, and  $\theta'$  the

angle of refraction, then Snell's law of refraction takes the form

$$\mu = \frac{\cos \theta}{\cos \theta'}. \quad (29)$$

The angle  $\theta'$  is not only the angle of refraction, but is also the angle that the ray makes with the atomic planes, so that inside the crystal Bragg's law is

$$n\lambda' = 2d \sin \theta'. \quad (30)$$

However, the angle that is actually measured is the angle  $\theta$ , and the wave length usually desired is the wave length  $\lambda$  in a vacuum. A modified form of Bragg's law containing  $\lambda$ ,  $\theta$ , and  $\mu$  can be obtained by combining equations (28) and (29) with (30). Remembering that

$$\sin \theta' = (1 - \cos^2 \theta')^{1/2}$$

and substituting the values of  $\cos \theta'$  and  $\lambda'$  from equations (28) and (29), we find that equation (30) becomes

$$\frac{n\lambda}{\mu} = 2d \left( 1 - \frac{\cos^2 \theta}{\mu^2} \right)^{1/2}$$

$$n\lambda = 2d(\mu^2 - \cos^2 \theta)^{1/2},$$

$$\text{or} \quad n\lambda = 2d(\mu^2 - 1 + \sin^2 \theta)^{1/2};$$

and by factoring out  $\sin \theta$ , we have

$$n\lambda = 2d \sin \theta \left[ 1 + \frac{\mu^2 - 1}{\sin^2 \theta} \right]^{1/2}. \quad (31)$$

Equation (31) is a modified form of Bragg's law. For purposes of calculation, this equation can be simplified by expanding the quantity in the bracket by means of the binomial theorem; thus

$$\begin{aligned} \left[ 1 + \frac{\mu^2 - 1}{\sin^2 \theta} \right]^{1/2} &= 1 + \frac{1}{2} \frac{\mu^2 - 1}{\sin^2 \theta} + \dots \\ &= 1 + \frac{1}{2} \frac{(\mu + 1)(\mu - 1)}{\sin^2 \theta}. \end{aligned}$$

Experiment shows that  $\mu$  does not differ appreciably from unity, and to a very close approximation  $\mu + 1 = 2$ , so that the bracket

can be written as

$$\left[ 1 + \frac{\mu^2 - 1}{\sin^2 \theta} \right]^{\frac{1}{2}} = 1 - \frac{1 - \mu}{\sin^2 \theta},$$

and the modified form of Bragg's law is then

$$n\lambda = 2d \left[ 1 - \frac{1 - \mu}{\sin^2 \theta} \right] \sin \theta. \quad (32)$$

The more common method of expressing the results is to give the quantity  $\delta = 1 - \mu$ , which shows how the index of refraction differs from unity. For example, the index of refraction of calcite for the wave length  $\lambda = 0.708\text{\AA}$  differs from unity by the amount

$$\delta = 1 - \mu = 1.85 \times 10^{-6}.$$

Two interesting conclusions can be drawn from the fact that the index of refraction of X rays in material media is less than

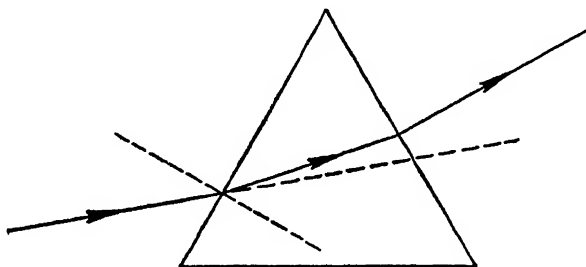


FIG. 71. — Path of a beam of X rays refracted through a prism. The beam is bent away from the normal on entering the prism.

unity. One is that when X rays pass through a prism, the beam will be deviated in a direction opposite to that for ordinary light. The path of an X-ray beam through a prism is shown in Figure 71. The other conclusion is that at a certain critical angle  $\theta_c$ , the X-ray beam should not be refracted into the medium at all but should be totally reflected. At this critical angle of incidence,  $\cos \theta' = 1$  and

$$\mu = \cos \theta_c. \quad (33)$$

For all angles smaller than  $\theta_c$ , there should be no refraction at all, only total reflection of the X-ray beam.

An experimental method for the determination of this critical angle is shown in Figure 72. A narrow beam is obtained by passing the X rays from the target  $T$  through two slits  $S_1$  and  $S_2$ . The

crystal  $C$  reflects a particular wave length  $\lambda$  on to the plane surface  $M$  of the material. If the grazing angle of incidence  $\theta$  is less than the critical angle  $\theta_c$ , the beam will be totally reflected to the

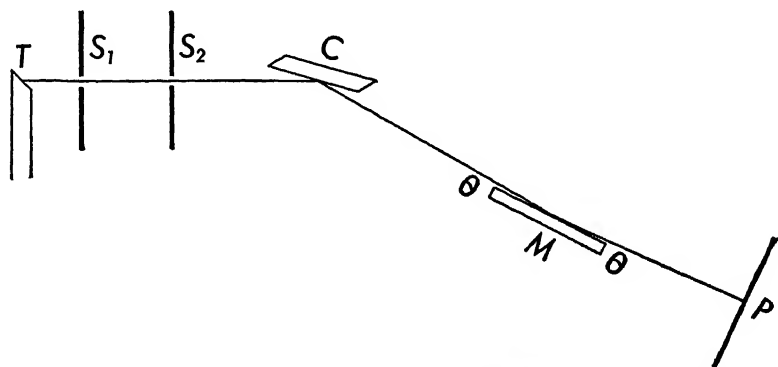


FIG. 72. — Method of reflecting monochromatic X rays from a mirror.

photographic plate  $P$ , and the surface  $M$  will act as a mirror. As the angle of incidence is increased, the beam continues to be reflected until  $\theta = \theta_c$ , after which the beam is refracted into the material medium and the intensity of the reflected beam becomes

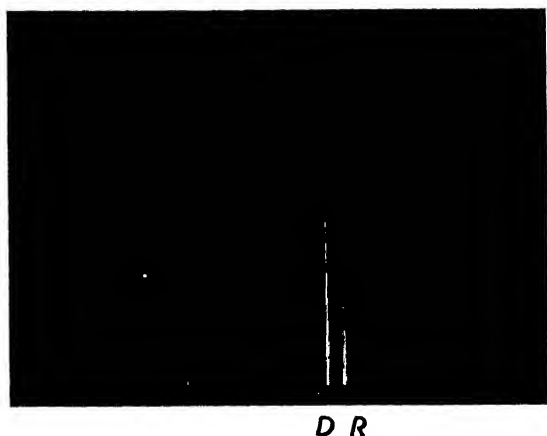


FIG. 73. — Reflection of monochromatic X rays ( $\text{AgK}\gamma$  line) from a palladium mirror near the critical angle.  $D$  is the direct beam and  $R$  is the reflected beam. (From photograph by the author.)

practically zero. A photograph of a beam of X rays reflected from a palladium surface is shown in Figure 73.

According to the classical theory of dispersion, when an elec-

electromagnetic wave of frequency  $\nu$  passes through a substance containing  $n$  electrons per unit volume, the index of refraction of the substance is given by

$$\mu = 1 - \frac{ne^2}{2\pi m\nu^2}, \quad (34)$$

provided that the natural frequency of the electrons is small in comparison with  $\nu$ , and that absorption is negligible. Equation (34) can be rewritten as

$$1 - \mu = \delta = \frac{ne^2}{2\pi m\nu^2}.$$

Setting

$$\nu = \frac{c}{\lambda},$$

we get

$$\delta = \frac{ne^2\lambda^2}{2\pi mc^2}. \quad (35)$$

Now

$$\mu = \cos \theta_c.$$

Since  $\theta_c$  is small,  $\cos \theta_c$  can be expanded in terms of  $\theta_c$ , yielding

$$\cos \theta_c = 1 - \frac{\theta_c^2}{2} + \dots,$$

so that

$$\delta = 1 - \mu = \frac{\theta_c^2}{2}$$

or

$$\theta_c = \sqrt{2\delta} = \sqrt{\frac{ne^2}{\pi mc^2}} \lambda. \quad (36)$$

Measurements of the critical angle show that it is directly proportional to the wave length of the X rays and to the square root of the density of the material except in the neighborhood of an absorption limit (§ 103). This is in good agreement with equation (36). However, the classical theory is inadequate to explain refraction in the neighborhood of an X-ray absorption limit. A quantum theory of dispersion has been developed which predicts results in fair agreement with experimental data. A discussion of the quantum theory of dispersion is beyond the scope of this book.

The index of refraction of a medium for an electromagnetic



wave is defined as

$$\mu = \frac{c}{w}, \quad (37)$$

where  $c$  ( $= 3 \times 10^{10}$  cm/sec) is its velocity in a vacuum, and  $w$  is the velocity of the wave in the medium. Since the index of refraction for X rays is less than unity, its velocity  $w$  in a material medium is greater than  $c$ . At first sight this may appear to be in contradiction to the fundamental postulate of the special theory of relativity which states that electromagnetic waves are always propagated with the same velocity  $c$ . Actually there is no contradiction. On the microscopic point of view, a material body is not a continuous medium but consists of nuclei and electrons separated by distances which are large relative to their sizes. These particles may be imagined to be situated in empty space. The incident wave, in traversing this space, sets the charges into vibration, causing them to emit electromagnetic waves. Two sets of waves, therefore, travel through this space: the incident wave, and the waves produced by the forced vibrations of the electrons. These elementary waves travel through the space with velocity  $c$ . But, through superposition of the elementary waves, a new wave form is produced, which, on the macroscopic (large scale) point of view, consists of a train of waves traveling through the material body with a velocity  $w$  which may be greater or smaller than  $c$ . But the energy carried by the incident wave and the energy radiated by the forced vibrations of the electrons always travel with velocity  $c$ .

The refracted wave thus consists of a train of waves traveling with a velocity  $w$  whose magnitude depends upon the binding forces acting on the electrons. The dielectric constant  $k$  of the material medium is determined by the magnitude of these binding forces, and it can be shown, on the basis of Maxwell's electromagnetic theory of light, that the index of refraction,  $\mu$ , is given by the equation

$$\mu = \sqrt{k} = \frac{c}{w}. \quad (38)$$

It is this equation which is used in deriving the expression for the index of refraction given by equation (34).

## 58. Measurement of X-Ray Wave Lengths by Ruled Gratings

An extremely important application of the total reflection of X rays is in the measurement of X-ray wave lengths using a ruled grating with a known number of lines per millimeter. As long as

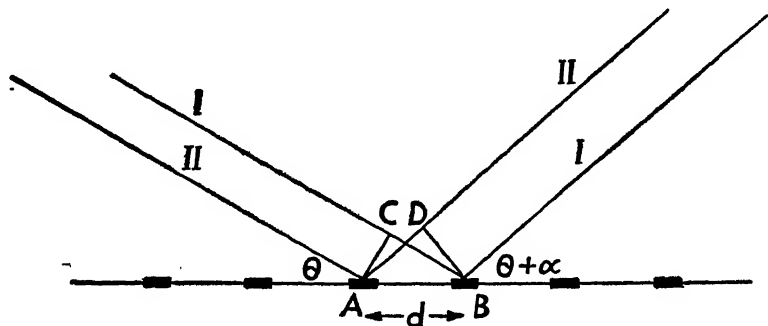


FIG. 74. — Reflection of X rays from a ruled grating.

the grazing angle of incidence  $\theta$  is less than the critical angle  $\theta_c = \sqrt{2\delta}$ , the X-ray beam will be totally reflected from a polished surface. This surface can be made into a diffraction grating by ruling a series of uniformly spaced lines a distance  $d$  apart. The spaces between the rulings will act as diffracting centers producing various orders of diffraction on either side of the regularly reflected line. In Figure 74, if the rays are incident at an angle  $\theta$  to the surface of the ruled grating, an intense maximum will be produced at some other angle  $(\theta + \alpha)$ , provided the difference in path between two adjacent rays is a whole number of wave lengths. The difference in paths between rays I and II is

$$CB - AD = d \cos \theta - d \cos (\theta + \alpha),$$

so that the condition for an intense maximum at this angle of reflection is

$$d [\cos \theta - \cos (\theta + \alpha)] = n\lambda, \quad (39)$$

where  $n$  is an integer and may be either positive or negative. The regular reflection at the angle  $\theta$  is called the zero order; the other orders of reflection are called positive if  $\alpha$  is positive and negative if  $\alpha$  is negative.

Diffraction gratings for X rays have been made of glass, speculum metal, silver, and gold, and the number of lines per milli-

meter has ranged from 50 to 600. Since the grating space  $d$  is accurately known and the angles  $\theta$  and  $(\theta + \alpha)$  can be measured with a high degree of precision, this method can be used as a check on the wave lengths measured with crystal gratings. A comparison of some wave lengths measured by ruled gratings and by crystals is shown in Table VI.

In every case the wave length measured with a ruled grating is greater than that measured with a crystal grating. The possible sources of error in the ruled grating measurements were investigated by many physicists, but in no case could they account for this large discrepancy — about  $\frac{1}{4}$  of 1 per cent. This led to a re-examination of the basis on which crystal grating wave-length measurements depend, namely the grating space  $d$ . It will be re-

TABLE VI

COMPARISON OF WAVE LENGTHS MEASURED BY RULED GRATINGS AND BY CRYSTALS				
Line	$\lambda_g$ by Grating	$\lambda_c$ by Crystal	$\lambda_g - \lambda_c$ in Per Cent	Observer
Mo $L_\alpha$	5.4116 Å	5.3950 Å	+0.31	Cork
Mo $L_\beta$	5.1832	5.1665	+0.33	"
Cu $K_\alpha$	1.54172	1.5387	+0.20	Bearden
Cu $K_{\beta_1}$	1.39225	1.3894	+0.20	"
Cr $K_\alpha$	2.29097	2.2859	+0.22	"
Cr $K_{\beta_1}$	2.08478	2.0806	+0.22	"

called that this distance, for rock salt, is given by the equation

$$d = \sqrt[3]{\frac{M}{2\rho N}}; \quad (25)$$

and for crystals which are not simple cubes, such as calcite and quartz, this equation becomes

$$d = \sqrt[3]{\frac{M}{2\rho N\phi(\beta)}}, \quad (25a)$$

where  $\phi(\beta)$  is a function of the angles of the crystal lattice. The least accurately known constant entering in the computation of  $d$  is Avogadro's number  $N$ . Avogadro's number is computed from

the relationship

$$F = Ne,$$

where  $F$  is the Faraday constant and  $e$  is the electronic charge.  $F$  is very accurately known from many experiments extending over a long period of time. To get agreement between the ruled grating and the crystal grating measurements of X-ray wave lengths, it is necessary to increase the value of  $e$  from Millikan's value  $4.77 \times 10^{-10}$  e.s.u. to about  $4.803 \times 10^{-10}$  e.s.u. As stated in Chapter 2, § 19, redeterminations of the value of the electronic charge have led to the adoption of the value

$$e = 4.802 \times 10^{-10} \text{ e.s.u.}$$

Within recent years improved methods have increased the accuracy of the determinations of the densities of crystals. Chemically pure crystals of NaCl, KCl, and LiF have been prepared artificially, and the grating spaces of these crystals have been determined by measuring the Bragg angle for monochromatic X rays whose wave lengths are known from ruled grating measurements. Using the known molecular weights of these crystals, we can determine values of the Avogadro number with the aid of equation (25). Birge has stated that the Avogadro number determined in this manner, together with the known value of the Faraday constant, leads to the most reliable determination of the electronic charge.

## 59. Absorption of X Rays

When a parallel beam of X rays passes through any material,

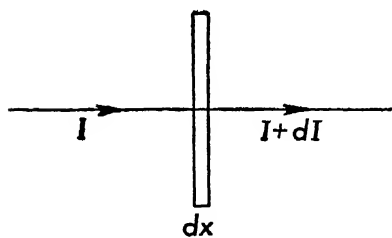


FIG. 75.

the intensity of the emergent beam is less than that of the incident beam. The decrease in intensity of the beam when it traverses a small thickness  $dx$  of the material, Figure 75, depends upon the thickness and upon the intensity  $I$  of the beam, or

$$-dI = \mu I dx$$

where  $-dI$  represents the decrease in intensity of the beam, and  $\mu$  is a factor of proportionality. The above equation can be written

as

$$\frac{dI}{I} = -\mu dx,$$

and upon integration becomes

$$I = I_0 e^{-\mu x}, \quad (40)$$

where  $I_0$  is the initial intensity of the beam, and  $I$  is its intensity after it has traversed a thickness  $x$  of the material.  $\mu$  represents the fraction of the energy removed from the beam per centimeter of path, and is usually referred to as the total absorption coefficient of the material.

There are two ways in which the atoms of a substance can remove the energy from the incident beam. One process is that of scattering in which the electrons of the atoms are set into forced vibrations and then radiate this energy in all directions. The second process is the absorption of some of the energy by the atom, which then radiates a new type of X rays characteristic of the atom. This radiation is called fluorescent radiation and is also emitted in all directions.

The total absorption coefficient  $\mu$  can be written as the sum of two terms

$$\mu = \sigma + \tau, \quad (41)$$

where  $\sigma$  is the scattering coefficient and  $\tau$  is the fluorescent transformation coefficient. These coefficients can be interpreted in a slightly different way by referring to a beam whose cross-sectional area is 1 cm<sup>2</sup>. In this case,  $\mu$  represents the total fraction of the energy removed from the beam by 1 cm<sup>3</sup> of the material,  $\sigma$  represents the fraction of the energy scattered by 1 cm<sup>3</sup>, and  $\tau$  represents the fraction of the energy transformed into fluorescent radiation by this unit volume. The mass absorption coefficient is defined as  $\mu/\rho$  where  $\rho$  is the density of the material. Also

$$\frac{\mu}{\rho} = \frac{\sigma}{\rho} + \frac{\tau}{\rho}. \quad (42)$$

The mass absorption coefficient  $\mu/\rho$  is characteristic of the material and represents the fraction of the energy removed from a beam of unit cross section by one gram of the substance. Similar inter-

pretations hold for the mass scattering coefficient  $\sigma/\rho$  and the mass transformation coefficient  $\tau/\rho$ .

## 60. Scattering of X Rays

When a beam of X rays passes through a substance, the electrons in this substance are set into vibration and radiate X rays in all directions. The radiation emitted by these electrons is called *scattered* or *secondary radiation*. If  $E$  is the electric intensity of the incident wave, the acceleration of the electron will be

$$a = \frac{Ee}{m},$$

where  $e$  is the charge of the electron and  $m$  is its mass. The electric intensity  $E_\phi$  of the scattered wave at a distance  $r$  from this electron is

$$E_\phi = \frac{ea \sin \phi}{rc^2}, \quad (1)$$

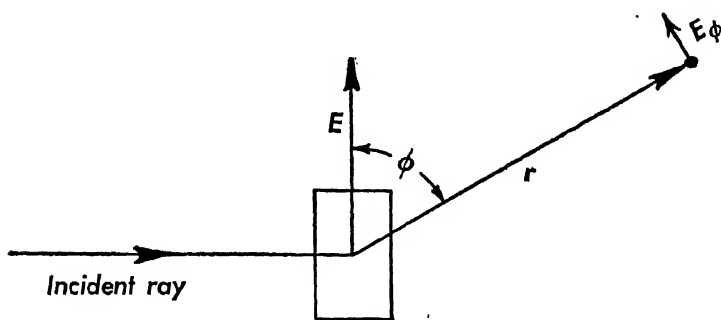


FIG. 76.

where  $\phi$  is the angle between  $E$  and  $r$ , Figure 76. Substituting the value for the acceleration in equation (1), we get

$$E_\phi = \frac{Ee^2}{rmc^2} \sin \phi. \quad (43)$$

Since the intensity of the wave is proportional to the square of the electric vector, the ratio of the intensity  $I$  of the incident radiation to the intensity  $I_\phi$  of the wave sent out along  $r$  is

$$\frac{I_\phi}{I} = \frac{E_\phi^2}{E^2} = \frac{e^4}{r^2 m^2 c^4} \sin^2 \phi. \quad (44)$$

Choose a set of axes so that the incident or primary beam is propagated parallel to the  $x$  axis. The electric intensity  $E$  will then be in a plane parallel to the  $y$ - $z$  plane. Since the position of the  $y$  and  $z$  axes can be chosen arbitrarily in this plane, let the  $y$  axis be

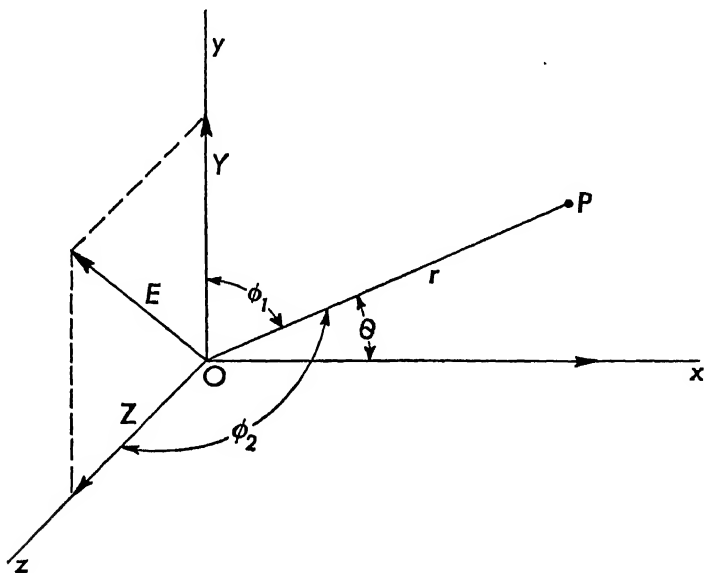


FIG. 77.

taken in the plane determined by the direction of the scattered ray  $OP$  and the primary ray, Figure 77, and let the electron be at the origin of coordinates. The electric vector  $E$  may be resolved into two perpendicular components,  $Y$  and  $Z$ , such that

$$E^2 = Y^2 + Z^2,$$

so that the intensity of the wave is

$$I = I_y + I_z,$$

where  $I_y$  is the intensity of the  $y$  component of the incident wave and  $I_z$  is the intensity of its  $z$  component. Since the primary ray is unpolarized, the intensities of the  $y$  and  $z$  components are equal, yielding

$$I_y = I_z = \frac{I}{2}.$$

Now the intensity,  $I_1$ , of the scattered beam at the point  $P$  due

to the  $y$  component of the incident wave is, from equation (44),

$$I_1 = I_y \frac{e^4 \sin^2 \phi_1}{r^2 m^2 c^4} = \frac{1}{2} I \frac{e^4 \cos^2 \theta}{r^2 m^2 c^4}, \quad (45)$$

where  $\phi_1$  is the angle between  $OP$  and  $Y$ , and  $\theta = \pi/2 - \phi_1$ . Similarly, the intensity,  $I_2$ , of the scattered beam at the point  $P$  due to the  $z$  component of the incident wave is

$$I_2 = I_z \frac{e^4 \sin^2 \phi_2}{r^2 m^2 c^4} = \frac{1}{2} I \frac{e^4}{r^2 m^2 c^4}, \quad (46)$$

where  $\phi_2$  is the angle between  $OP$  and  $Z$ , and is always  $\pi/2$ . The total intensity,  $I_e$ , of the scattered wave at  $P$  due to the energy radiated by a single electron is thus

$$I_e = I_1 + I_2 = I \frac{e^4}{2r^2 m^2 c^4} (1 + \cos^2 \theta). \quad (47)$$

If there are  $n$  electrons per unit volume of material, and if we make the assumption that each electron is effective in scattering the X rays independently of all the other electrons, then the intensity of the scattered wave at point  $P$ , coming from a unit volume of the scatterer, will be given by

$$I_s = nI_e = I \frac{ne^4}{2r^2 m^2 c^4} (1 + \cos^2 \theta). \quad (48)$$

This analysis of the intensity of the scattered X-ray beam leads to three conclusions, each of which can be investigated experimentally. One is that a measurement of the total energy scattered should yield the number of electrons per unit volume effective in scattering, and hence the number of electrons per atom effective in scattering. Another is that when the scattering angle is  $90^\circ$ , the scattered beam should be linearly polarized with the direction of vibration of the electric vector parallel to the  $z$  axis. The third is that equation (48) predicts a definite distribution of intensity of the scattered beam as a function of the angle of scattering with a minimum intensity at  $90^\circ$ .

## 61. Determination of the Number of Electrons per Atom

The rate at which energy is scattered by the electrons in a cubic centimeter of matter can be calculated by integrating  $I_s$  over a large sphere of radius  $r$  with its center at the scatterer. A



convenient element of surface area is one over which  $I_s$  has a constant value and is, from Figure 78,

$$dA = 2\pi r \sin \theta \cdot r d\theta.$$

The amount of energy,  $W_s$ , which is scattered by unit volume in one second is therefore

$$W_s = \int_0^\pi I_s dA$$

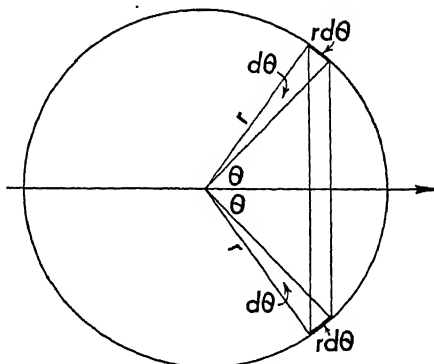


FIG. 78.

$$\begin{aligned} &= \frac{\pi I n e^4}{m^2 c^4} \int_0^\pi (1 + \cos^2 \theta) \sin \theta d\theta \\ &= \frac{8\pi}{3} \frac{n e^4}{m^2 c^4} I. \end{aligned} \quad (49)$$

$$\text{Let} \quad \sigma = \frac{W_s}{I} = \frac{8\pi}{3} \frac{n e^4}{m^2 c^4}. \quad (50)$$

$\sigma$  is called the scattering coefficient of the substance and represents the fraction of the energy removed from the incident beam by the process of scattering when traversing one centimeter of the material. A measurement of  $\sigma$  would make possible an evaluation of the number of electrons effective in scattering. One of the earliest determinations of the scattering coefficient was made by Barkla (1911), and later repeated with greater accuracy by Hewlett, using carbon as the scattering element. Hewlett measured the intensity of the scattered beam over a range of angles  $\theta$  from about 0 to  $\pi$ , thus performing the integration experimentally. The wave length of the incident beam was  $0.71 \text{ \AA}$ . The result obtained for the mass scattering coefficient is  $\sigma/\rho = 0.2$ , where  $\rho$  is the density of carbon. Solving equation (50) for  $n$ , we get

$$n = \sigma \cdot \frac{3m^2 c^4}{8\pi e^4}.$$

Since  $n$  is the number of electrons per cubic centimeter,  $n/\rho$  is the

number of electrons per gram of material and is given by

$$\frac{n}{\rho} = \frac{\sigma}{\rho} \cdot \frac{3m^2c^4}{8\pi e^4}. \quad (51)$$

Putting in the experimentally determined values on the right-hand side of equation (51) yields

$$\frac{n}{\rho} = 3 \times 10^{23} \frac{\text{electrons}}{\text{gram}}.$$

There are  $\frac{6.02 \times 10^{23}}{12} = 5.01 \times 10^{22}$  atoms per gram of carbon.

Therefore the number of electrons per atom effective in scattering is

$$\frac{3 \times 10^{23}}{5 \times 10^{22}} = 6,$$

which is the atomic number of carbon. Hence the number of electrons effective in scattering is equal to the atomic number of the scattering element. This is in excellent agreement with the results of the experiments on the scattering of alpha particles, and is a direct determination of the number of electrons outside the nucleus of the atom.

It must be remarked that such good agreement between the results of the experiments on the scattering of X rays and Thomson's theory has been obtained only with scattering substances of low atomic number and then only with X rays of wave lengths greater than  $0.1\text{\AA}$ . The theory of the scattering of X rays will be discussed further in § 64.

## 62. Polarization of X Rays

This classical theory of scattering predicts that the beam scattered at an angle of  $90^\circ$  should be linearly polarized. This can be seen by a glance at equations (45) and (46). For  $\theta = 90^\circ$ , the intensity due to the  $y$  component of the electric vector will be zero, while the intensity at any point in the  $X$ - $Y$  plane due to the  $z$  component of the electric vector is independent of the angle. Thus in the  $y$  direction the scattered beam will be linearly polarized with the direction of vibration parallel to the  $z$  axis. To detect this polarization another scatterer is used as an analyzer. Barkla was the first to show the polarization of the beam scattered at an angle

of  $90^\circ$ . More recently (1924), Compton and Hagenow repeated this experiment with improved apparatus. Figure 79 shows a diagram of their apparatus. A narrow beam of X rays from a

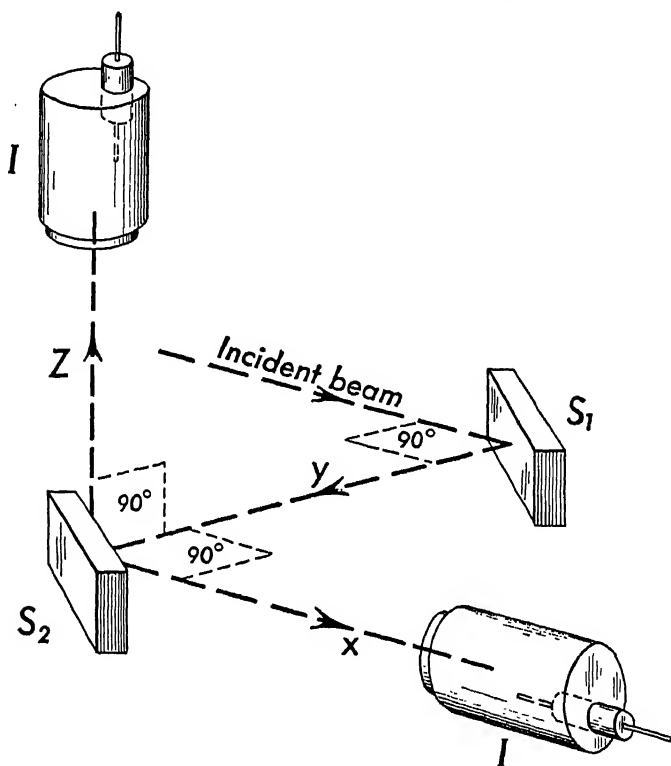


FIG. 79. — Arrangement of apparatus for determining the polarization of X rays scattered through  $90^\circ$ .

tungsten target was scattered by  $S_1$  to a second scatterer placed at  $S_2$  so that the scattered beam made an angle of  $90^\circ$  with the original beam. The scattering materials were blocks of paper, carbon, aluminum, and sulphur. The beam scattered by  $S_2$  was examined in two directions at right angles to one another and perpendicular to the direction  $S_1S_2$ . The intensity in the direction  $S_2-x$  was found to be a maximum, while that in the direction  $S_2-z$  was practically zero within the limits of error of the experiment. This is in complete agreement with the electromagnetic theory, since, if only the  $z$  component of the electric vector is present in the beam scattered from  $S_1$  to  $S_2$ , then the intensity in the direction

$S_z$ - $z$  should be zero for a transverse wave; similarly the beam should have maximum intensity in the direction  $S_z$ - $x$ .

### 63. Intensity of the Scattered X Rays

Many measurements have been made on the distribution of intensity in the scattered X-ray beam as a function of the angle of scattering. For X-ray wave lengths greater than  $0.2\text{\AA}$  the distribution follows the  $(1 + \cos^2 \theta)$  law fairly well except for small angles of scattering, in which cases the intensity of the scattered beam is much greater than that predicted by equation (48). See Figure 80. This large intensity of the scattered beam at small angles can be explained on the assumption that the phase differences of the rays scattered at these angles are small so that the waves scattered by neighboring electrons reinforce each other.

However, for wave lengths much smaller than  $0.2\text{\AA}$ , the intensity falls off rapidly at large angles; the scattering coefficient is much smaller than that predicted by the classical theory. The

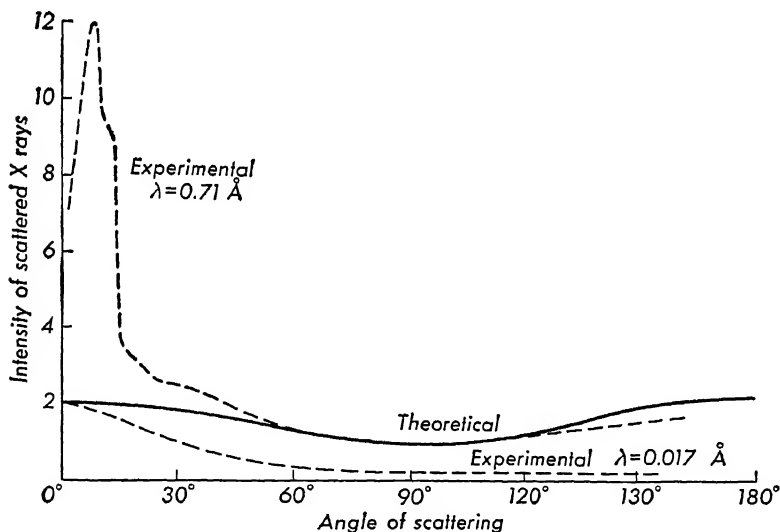


FIG. 80. — A comparison of the theoretical and experimentally determined values of the intensity of the scattered X rays as a function of the angle of scattering.

lowest curve in Figure 80 shows the intensity of the rays scattered by iron; the incident rays were hard gamma rays of wave length  $0.017\text{\AA}$ .

Evidently the classical theory of scattering is not completely

satisfactory. To account for the small intensity of the beam at large angles of scattering, A. H. Compton proposed a quantum theory of scattering, in which the X rays, considered as photons, cause the ejection of electrons from the atom as a result of the scattering process. As will be shown in the next section, the greater the angle of scattering, the greater is the amount of energy removed from the beam by these ejected or *recoil* electrons.

## 64. The Compton Effect

In the experiments on the scattering of X rays by matter, it was noted that for wave lengths of the order of  $1\text{\AA}$ , the experimental results were in good agreement with the classical theory of scattering, but for shorter wave lengths there was great divergence between the classical theory and experimental results. In working with scattered radiation, A. H. Compton (1923) observed that the wave length of the radiation scattered by a block of paraffin, in a direction at right angles to the incident beam, was greater than the wave length of the incident beam. The theory of this effect was given by Compton and also by Debye at about the same time.

Consider the incident radiation as consisting of photons, or quanta, of energy  $h\nu$  traveling in the direction of the primary ray with velocity  $c$ . From the relationship between mass and energy derived from the theory of relativity, a photon of energy  $h\nu$  has a mass given by  $h\nu/c^2$ . Since the momentum of a particle is the product of its mass by its velocity, the momentum of the photon becomes  $h\nu/c$ . Suppose that this photon strikes a comparatively free electron at rest. If we assume that the principles of conservation of energy and conservation of momentum hold during this process, then as a result of this collision, the electron will acquire a velocity  $v$  in a direction making an angle  $\theta$  with the direction of motion of the incident photon, and a photon of energy  $h\nu'$  will be scattered at an angle  $\phi$  with the original direction, Figure 81. From the principle of conservation of energy we get

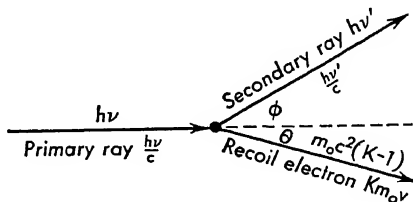


FIG. 81. — The Compton effect.

$$h\nu = h\nu' + m_0c^2(K - 1), \quad (52)$$

where  $m_0c^2(K - 1)$  is the kinetic energy of the electron as derived on the basis of the special theory of relativity, and  $K$  is  $(1 - v^2/c^2)^{-1/2}$ .

Resolving the momentum vectors into two rectangular components, along and at right angles to the direction of the incident photon, and using the principle of conservation of momentum, we get

$$\frac{h\nu}{c} = \frac{h\nu'}{c} \cos \phi + Km_0v \cos \theta; \quad (53)$$

$$0 = \frac{h\nu'}{c} \sin \phi - Km_0v \sin \theta. \quad (54)$$

The solution of these equations (Appendix VIII) yields the following results:

$$\lambda' - \lambda = \frac{h}{m_0c}(1 - \cos \phi), \quad (55)$$

$$\cot \frac{\phi}{2} = -(1 + \alpha) \tan \theta, \quad (56)$$

$$\mathcal{E} = m_0c^2(K - 1) = h\nu \frac{2\alpha \cos^2 \theta}{(1 + \alpha)^2 - \alpha^2 \cos^2 \theta}, \quad (57)$$

where  $\alpha = h\nu/m_0c^2$ ,  $\mathcal{E}$  is the kinetic energy of the recoil electron, and the wave lengths  $\lambda'$  and  $\lambda$  corresponding to the frequencies  $\nu'$  and  $\nu$  have been introduced.

Equation (55) states that the wave length of the ray scattered

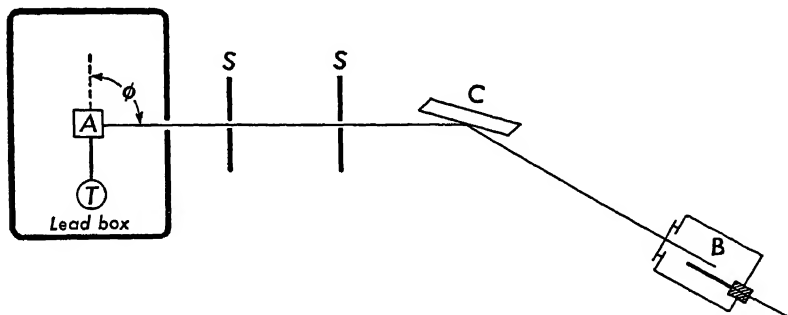


FIG. 82. — Method of determining the wave length of the scattered X rays.

at any angle  $\phi$  should always be greater than the wave length of the incident radiation. Furthermore, this difference in wave

length should not depend upon the nature of the scattering material but should depend only on the angle of scattering.

Equation (56) gives the relationship between the direction of motion of the recoil electron and the scattered photon, while equation (57) gives the kinetic energy of the recoil electron in terms of the energy of the incident photon and the angle  $\theta$ .

A typical experimental arrangement for studying the Compton effect is shown in Figure 82. X rays from some target  $T$ , giving out strong characteristic radiation, are scattered in all directions by the body  $A$ . The radiation scattered in some direction  $\phi$  is then allowed to fall on the crystal  $C$  of an X-ray spectrometer, which analyzes the beam into its component wave lengths. This radiation may be measured with aid of an ionization chamber  $B$ , or with a photographic plate in place of  $B$ .

The results of a typical set of measurements are shown in Figure 83. In this case the  $K_\alpha$  line of molybdenum was scattered by graphite, and measurements were made at scattering angles of  $45^\circ$ ,  $90^\circ$ , and  $135^\circ$ . Each scattered beam is seen to consist of two distinct lines. One line,  $P$ , has a wave length corresponding to the wave length of the incident radiation. The second line,  $M$ , has a longer wave length,  $\lambda'$ , which

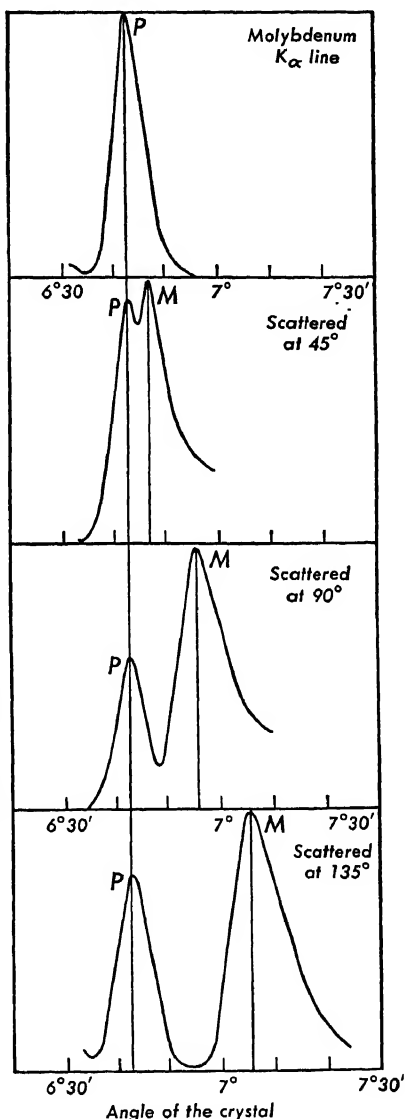


FIG. 83. — Curves showing the displacement of the "modified" line in the Compton effect for three different angles of scattering.

depends upon the angle of scattering. The wave length  $\lambda'$  of this *modified* line is in good agreement with that calculated from equation (55). Similar results were obtained when other substances were used as scatterers. In all cases, the wave length of the modified line was found to depend only upon the angle of scattering and not upon the nature of the scattering substance.

The presence of a line with the same wave length as the incident radiation is not predicted by equation (55). In deriving this equation it was assumed that the electron which took part in the scattering was a "free" electron and that it was ejected from the atom. The unmodified line is due to the interaction between the incident quanta and bound electrons. In this case the bound electrons do not receive energy or momentum from the incident quantum and there is no change in the wave length of the scattered photon. In light atoms, such as Be, C, and Al, the electrons are probably bound more loosely than in the heavier elements. The modified line should be relatively more intense than the unmodified line for light elements, while the reverse should be true for the heavier elements. This has actually been confirmed by the scattering experiments.

In addition to a change in wave length, the theory of the Compton effect predicts that every collision should be accompanied by the ejection of a recoil electron. According to equation (56) these recoil electrons will be ejected at angles  $\theta$  less than  $90^\circ$  and those ejected in the forward direction will have maximum energy. These predictions have been verified experimentally in several ways. The most common method is to photograph the tracks formed by these recoil electrons in a Wilson cloud chamber when X rays pass through the gas in this chamber. In another type of experiment, the maximum energies of the recoil electrons ejected from a thin foil are measured by bending them in circular paths with the aid of a magnetic field, and determining the radii of these paths.

The results of the experiments on the Compton effect leave no doubt that, in its interaction with matter, radiant energy behaves as though it were composed of particles. A similar behavior was observed in the photoelectric effect. It will be shown later that in the processes of emission and absorption light behaves as though it consists of corpuscles. But the phenomena of interference and



diffraction can be explained only on the hypothesis that radiant energy is propagated as a wave motion. We are thus led to the conclusion that radiant energy exhibits a dual character, that of a wave and that of a corpuscle. The relationship between these two concepts, wave and corpuscle, will be examined more fully in the next chapter.

## REFERENCES

### *On polarized light*

WOOD, R. W., *Physical Optics*. New York: The Macmillan Company, 1934, Chap. IX.

### *Zeeman effect*

WOOD, R. W., *Physical Optics*. New York: The Macmillan Company, 1934, Chap. XXI.

### *Electromagnetic theory of light*

HOUSTON, R. A., *A Treatise on Light*. New York: Longmans, Green & Company, 1927, Chap. XXII.

STARLING, S. G., *Electricity and Magnetism*. New York: Longmans, Green & Company, 1934, Chap. XIV.

### *Photoelectric effect*

HUGHES, A. L., and I. DuBRIDGE, *Photoelectric Phenomena*. New York: McGraw-Hill Book Company, 1932, Chap. II.

### *X-ray tubes and equipment*

SIEGBAHN, M., *The Spectroscopy of X-Rays*. New York: Oxford University Press, 1925, Chap. III.

### *X rays*

BRAGG, W. H., and W. L. BRAGG, *X-Rays and Crystal Structure*. London: George Bell & Sons, Ltd., 1923, Chaps. II, III, IV, X.

COMPTON, A. H., and S. K. ALLISON, *X-Rays in Theory and Experiment*. New York: D. Van Nostrand Company, Inc., 1935, Chaps. I-III, IX.

RICHTMYER, F. K., and E. H. KENNARD, *Introduction to Modern Physics*. New York: McGraw-Hill Book Company, Inc., 1942, Chap. X.

SIEGBAHN, M., *The Spectroscopy of X-Rays*. New York: Oxford University Press, 1925, Chaps. I, II, and VII.

## PROBLEMS

1. A Coolidge type of X-ray tube is operated at a voltage of 50 kv. Electrons striking the silver target with maximum kinetic energy are completely stopped in  $10^{-5}$  cm of silver. Assuming that the acceleration is uniform, calculate the rate at which electromagnetic energy is radiated from the electron.

*Ans.* 0.44 erg/sec.

2. A calcium arc is placed between the poles of an electromagnet. The line  $\lambda = 4226.7\text{\AA}$  is found to exhibit the normal Zeeman pattern in a field of 30,000 oersteds. Calculate (a) the difference in frequencies between the displaced and undisplaced components, and (b) the difference in wave lengths between these components.

*Ans.* (a)  $4.2 \times 10^{10} \text{ sec}^{-1}$ .

(b)  $0.25\text{\AA}$ .

3. When a copper surface is illuminated by the radiation of wave length  $\lambda = 2537\text{\AA}$  from a mercury arc, the value of the stopping potential is found to be 0.24 volts.

(a) Calculate the wave length of the threshold value for copper.

(b) On the assumption that there are two free electrons per atom of copper, calculate the value of  $W_m$ .

(c) Using the above values, calculate the work done in taking an electron through the surface of the copper.

*Ans.* (a)  $2665\text{\AA}$ .

(b) 11.2 ev.

(c) 15.8 ev.

4. The photoelectric threshold of tungsten is  $2300\text{\AA}$ . Determine the energy of the electrons ejected from the surface by ultraviolet light of wave length  $1800\text{\AA}$ .

*Ans.* 1.5 ev.

5. Calculate the grating space  $d$  of calcite from the following data: molecular weight  $M = 100.091$ , density  $\rho = 2.71029 \text{ gm/cm}^3$ , and  $\phi(\beta) = 1.09594$ .

*Ans.*  $3.0357 \times 10^{-8} \text{ cm}$ .

6. The radiation from an X-ray tube operated at 40 kv is analyzed with a Bragg X-ray spectrometer using a calcite crystal cut along its cleavage plane. (a) Calculate the short wave-length limit of the X-ray spectrum coming from this tube. (b) What is the smallest angle be-

tween the crystal planes and the X-ray beam at which this wave length can be detected?

*Ans.* (a)  $\lambda = 0.309\text{\AA}$ .

(b)  $\theta = 2^\circ 55.4'$ .

7. Monochromatic X rays are reflected in the first order from a calcite crystal set with its cleavage planes at an angle of  $13^\circ$  with respect to the X-ray beam. These X rays are allowed to fall on a silver mirror at a very small angle to the plane of the mirror. The mirror is then rotated until the critical angle is reached. (a) Calculate the wave length of the X rays incident on the mirror. (b) Calculate the index of refraction of silver for this X-ray beam. (c) Determine the critical angle. The density of silver is  $10.5 \text{ gm per cm}^3$ .

*Ans.* (a)  $1.363\text{\AA}$ .

(b)  $\delta = 1 - \mu = 24 \times 10^{-6}$ .

(c)  $\theta_c = 23.8'$ .

8. A ruled glass surface covered with a thin layer of gold forms a diffraction grating with 200 lines per mm. A very narrow beam of the copper  $K_\alpha$  radiation,  $\lambda = 1.541\text{\AA}$ , is incident upon the grating at an angle of 20 minutes to its surface. (a) Show that for small angles equation (39) can be put in the form

$$n\lambda = d \left( \alpha\theta + \frac{\alpha^2}{2} \right)$$

by expanding the cosine functions.

(b) Calculate the angle between the first-order and the zero-order beams.

*Ans.*  $\alpha = 13.5'$ .

9. The  $K_\alpha$  radiation from a molybdenum target,  $\lambda = 0.708\text{\AA}$ , is scattered from a block of carbon, and the radiation scattered through an angle of  $90^\circ$  is analyzed with a calcite crystal spectrometer. (a) Calculate the change in wave length produced in the scattering process. (b) Determine the angular separation in the first order between the modified and unmodified lines produced by rotating the crystal through the required angle.

*Ans.* (a)  $\lambda' - \lambda = 0.024\text{\AA}$ .

(b)  $27.9 \text{ min.}$

10. (a) Calculate the angle between the direction of motion of the recoil electron and the incident photon in problem 9.

(b) Determine the energy of the recoil electron.

*Ans.* (a)  $\theta = -44^\circ 2'$ .

(b)  $9.37 \times 10^{-10} \text{ erg} = 586 \text{ ev.}$

11. Monochromatic X rays of wave length  $\lambda = 0.124\text{\AA}$  are scattered from a carbon block. (a) Determine the wave length of the X rays scattered through  $180^\circ$ . (b) Determine the maximum kinetic energy of the recoil electrons produced in this scattering process.

*Ans.* (a)  $\lambda' = 0.172\text{\AA}$ .

(b)  $2.813 \times 10^4 \text{ ev.}$

# 4

## Waves and Particles

### 65. Refraction of Particles and Waves on Newtonian Mechanics

In the explanation of the photoelectric effect and the Compton effect, it was found necessary to assume that radiant energy, in its interaction with matter, behaves as though it consists of corpuscles. Newton had also assumed that light consisted of a stream of particles; but on the basis of Newtonian mechanics, it is possible to distinguish between the behavior of particles and waves. As an example, consider the phenomenon of refraction, which occurs whenever a beam, either of waves or of particles, suffers a change in velocity when it goes obliquely from one medium to another. Snell's law of refraction, which is an empirical law, states that

$$\mu = \frac{\sin i}{\sin r}, \quad (1)$$

where  $\mu$  is the relative index of refraction of medium II with respect to medium I,  $i$  is the angle of incidence, and  $r$  is the angle of refraction. Suppose that a beam of particles goes from the medium I in which the velocity of a particle  $v_1$  is characteristic of the medium, into medium II in which it has a new velocity  $v_2$  characteristic of this second medium. To account for the abrupt change in velocity at the boundary of the two media it is necessary to assume the existence of forces which act through very small distances, of the order of magnitude of atomic dimensions. If we resolve the velocity of a particle into two components, one parallel and the other normal to the boundary surface, only the normal component of the velocity will change because of the action of these short-range forces. This will produce a change in direction of the beam of particles as it crosses the boundary.

Referring to Figure 84, let  $AO$  be the direction of the incident beam and  $OD$  that of the refracted beam. Let  $OC$  be a continuation of  $AO$  drawn so that its length is proportional to  $v_1$ .  $OE$  and  $EC$  are then proportional respectively to the normal and parallel components of the velocity  $v_1$ . When the beam goes into the

second medium, only the normal component of the velocity is changed. Draw  $OD$  so that its component parallel to the surface,  $FD$ , is equal to  $EC$ . Then

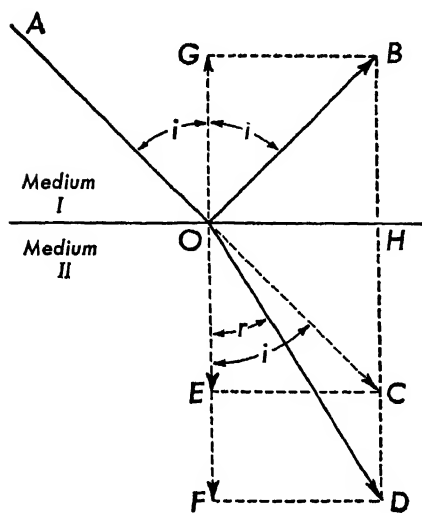


FIG. 84.

$$\mu = \frac{\sin i}{\sin r} = \frac{\frac{EC}{OC}}{\frac{FD}{OD}} = \frac{v_2}{v_1}. \quad (2)$$

As the beam of particles crosses the boundary between the two media, the short-range forces will produce a change in the normal component of the velocity of each particle and hence a change in the energy of each particle. If we assume the principle of conservation of energy to hold in this case, we can write

$$U_1 + \frac{1}{2}m(v_1 \cos i)^2 = U_2 + \frac{1}{2}m(v_2 \cos r)^2 \quad (3)$$

where  $U_1$  is the potential energy of a particle in the first medium and  $U_2$  is the potential energy of the particle in the second medium. Setting

$$U = U_1 - U_2,$$

we can write

$$U + \frac{1}{2}m(v_1 \cos i)^2 = \frac{1}{2}m(v_2 \cos r)^2, \quad (4)$$

where  $U$  is the difference in potential energy of the particle in the two media. If

$$U = -\frac{1}{2}mv_1^2 \cos^2 i,$$

the left-hand side of equation (4) becomes zero and the angle  $r$  becomes  $90^\circ$ . The angle of incidence  $i$  is then the critical angle. If  $U$  is less than  $-\frac{1}{2}m(v_1 \cos i)^2$ , the particle will be totally reflected at the boundary at an angle of reflection equal to the angle of incidence.

From equation (2) we know that

$$v_1 \sin i = v_2 \sin r;$$

hence we can write

$$\frac{1}{2}m(v_1 \sin i)^2 = \frac{1}{2}m(v_2 \sin r)^2. \quad (5)$$

Combining equations (4) and (5), we get

$$U + \frac{1}{2}mv_1^2 = \frac{1}{2}mv_2^2;$$

and solving for  $v_2$ , we get

$$v_2 = \sqrt{v_1^2 + \frac{2U}{m}}.$$

The relative index of refraction  $\mu$  of the two media can therefore be written as

$$\mu = \frac{v_2}{v_1} = \sqrt{1 + \frac{U}{\frac{1}{2}mv_1^2}}. \quad (6)$$

If the relative index of refraction of the two media is measured for a beam of particles and if the kinetic energy of the particles in the first medium is known, then equation (6) can be used to determine the difference in potential energy  $U$  as the particle goes from one medium into the other.

The relative index of refraction of the two media can also be

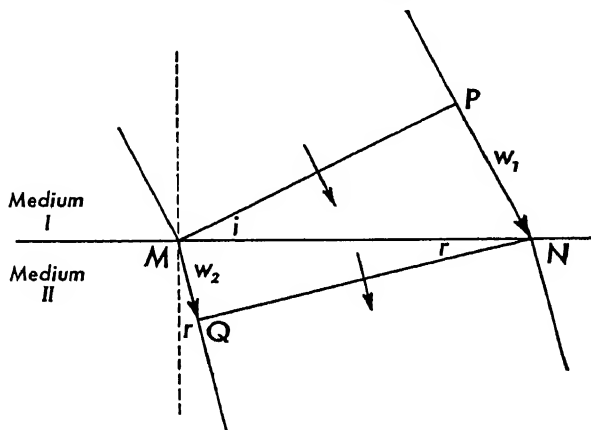


FIG. 85.

expressed in terms of the velocities of the wave in the two media. Referring to Figure 85, let  $MP$  represent a wave front traveling

with velocity  $w_1$  in medium  $I$ , and let  $PN$  be the distance traversed by this wave in unit time.  $QN$  represents the refracted wave front and  $MQ$  is the distance traveled in the second medium during the same unit of time. Evidently

$$\frac{PN}{MQ} = \frac{w_1}{w_2}. \quad (7)$$

Hence

$$\mu = \frac{\sin i}{\sin r} = \frac{\frac{PN}{MN}}{\frac{MQ}{MN}} = \frac{w_1}{w_2}. \quad (8)$$

A comparison of equations (6) and (8) shows that there is a marked difference between the refraction of waves and the refraction of particles; one equation is the reciprocal of the other. It will be recalled that Fizeau and Foucault measured the velocity of light in water and showed it to be less than that in air. Since the index of refraction was known to be greater than unity, the results of these experiments could only be explained on the hypothesis that light is propagated in the form of a wave motion.

## 66. De Broglie's Hypothesis

In order to explain the results of some of the experiments involving the interaction between radiant energy and matter, such as the photoelectric effect and the Compton effect, it was necessary to assign to radiant energy some properties characteristic of particles rather than waves. The amount of energy assigned to such a particle of radiant energy, or photon, is given by

$$\mathcal{E} = h\nu, \quad (9)$$

where  $h$  is the Planck constant and  $\nu$  is the frequency of the radiation. It is important to note that this frequency  $\nu$  is not a directly measurable quantity but must be computed from measurements of the wave length  $\lambda$  of the radiation using the relationship

$$\nu = \frac{c}{\lambda}, \quad (10)$$

where  $c$  is the velocity of light. The wave length  $\lambda$  can be measured only by some experiment which involves interference or diffraction, phenomena characteristic of wave motion. In spite of



the fact that radiation possesses this dual character, it never exhibits both characteristics in any one experiment. In a given experiment it behaves either as a wave or as a corpuscle.

According to an hypothesis introduced by L. de Broglie (1924), this dual character, wave and particle, should not be confined to radiation alone, but should also be exhibited by all the fundamental entities of physics. On this hypothesis, electrons, protons, atoms, and molecules should have some type of wave motion associated with them. De Broglie was led to this hypothesis by considerations based upon the special theory of relativity and upon the quantum theory.

Returning for a moment to a consideration of light of wave length  $\lambda$ , we find that the energy of a photon can be written as

$$\mathcal{E} = \frac{hc}{\lambda} \quad (11)$$

by combining equations (9) and (10). If  $m$  is the mass of the photon, then, on the basis of the special theory of relativity,

$$m = \frac{\mathcal{E}}{c^2} = \frac{h\nu}{c^2}. \quad (12)$$

The momentum  $p$  of this photon is

$$p = mc = \frac{h\nu}{c} = \frac{h}{\lambda}. \quad (13)$$

The quantity  $1/\lambda$  is commonly used by spectroscopists and is known as the *wave number* or the number of waves per centimeter in the monochromatic beam of light. If we let

$$k = \frac{1}{\lambda}, \quad (14)$$

then

$$p = h k. \quad (15)$$

Since momentum is a vector quantity whose magnitude is given by  $p$ , and  $h$  is a scalar quantity,  $k$  may be interpreted as the magnitude of a vector quantity whose direction is that of the direction of propagation of the light waves of length  $\lambda$ .

De Broglie carried these considerations over into the dynamics of a particle. On de Broglie's hypothesis a wave length  $\lambda$  is

associated with each particle and is related to the momentum  $p$  of the particle by the equation

$$p = \frac{h}{\lambda}. \quad (13)$$

If  $m$  is the mass of the particle and  $v$  its velocity, then

$$p = mv, \quad (16)$$

so that

$$\lambda = \frac{h}{mv}. \quad (17)$$

Equation (17) gives the relationship between the wave length  $\lambda$  associated with a particle and the mass  $m$  and velocity  $v$  of the particle. The existence of these waves was demonstrated experimentally by Davisson and Germer (1927) and G. P. Thomson (1928).

## 67. Wave-Particle Parallelism

It is instructive to carry this parallelism between wave and particle a little further. According to the special theory of relativity, the mass of a particle depends upon its velocity as follows:

$$m = \frac{m_0}{\left(1 - \frac{v^2}{c^2}\right)^{\frac{1}{2}}}, \quad (18)$$

where  $m_0$  is the mass of the particle when it is at rest with respect to the observer.  $m_0$  is frequently referred to as the *rest mass* of the particle. The momentum of the particle is

$$p = mv = \frac{m_0 v}{\left(1 - \frac{v^2}{c^2}\right)^{\frac{1}{2}}}. \quad (19)$$

If  $\mathcal{E}$  is the total energy of the particle, then from the principle of equivalence of mass and energy,

$$\mathcal{E} = mc^2. \quad (20)$$

Suppose that the total energy of the particle consists of just two kinds of energy, kinetic energy  $\mathcal{E}_k$  and rest-mass energy  $m_0 c^2$ , then

$$\mathcal{E}_k = mc^2 - m_0 c^2; \quad (21)$$

and substituting the value of  $m$  from equation (18), we get

$$\mathcal{E}_k = m_0 c^2 \left[ \frac{1}{\left(1 - \frac{v^2}{c^2}\right)^{\frac{1}{2}}} - 1 \right] \quad (22)$$

as the expression for the kinetic energy of a particle whose rest mass is  $m_0$  and whose speed is  $v$ . When the speed of a particle is small in comparison with the speed of light, the above expression reduces to the more familiar form  $\frac{1}{2}m_0 v^2$ .

Since the momentum of any particle can be written as

$$p = mv = \frac{\mathcal{E}}{c^2} v, \quad (23)$$

then, by eliminating  $v$  from equations (19) and (23), we get

$$p^2 - \frac{\mathcal{E}^2}{c^2} = -m_0^2 c^2,$$

or

$$m_0^2 = \frac{\mathcal{E}^2}{c^4} - \frac{p^2}{c^2}. \quad (24)$$

If we carry over the quantum relationship between energy and frequency

$$\mathcal{E} = h\nu, \quad (9)$$

and make use of the equation

$$p = \frac{h}{\lambda}, \quad (13)$$

the expression for the rest mass of a particle becomes

$$m_0 = \frac{h}{c} \sqrt{\nu^2 - \frac{1}{\lambda^2}}. \quad (25)$$

Any wave motion of wave length  $\lambda$  has a frequency  $\nu$  associated with it, governed by the equation

$$\nu\lambda = w, \quad (26)$$

where  $w$  is the velocity with which the wave motion is propagated. The velocity of propagation of the wave,  $w$ , can be determined by

substituting in equation (25) the value of  $\nu$  from equation (26) and solving for  $w$ , yielding

$$w = c\sqrt{1 + \frac{m_0^2 c^2}{h^2} \lambda^2}. \quad (27)$$

For any material particle,  $m_0 > 0$ , so that the wave velocity  $w$  associated with this particle is greater than the velocity of light,  $c$ . The relationship between the wave velocity  $w$  and the velocity  $v$  of the particle can be determined from the equations

$$w = \nu\lambda, \quad (26)$$

$$\mathcal{E} = h\nu, \quad (9)$$

and

$$p = \frac{h}{\lambda}, \quad (13)$$

yielding

$$w = \frac{\mathcal{E}}{p} = \frac{c^2}{v},$$

or

$$wv = c^2. \quad (28)$$

For a material particle,  $v$  is always less than  $c$ , so that  $w$  is always greater than  $c$ .

As a special case of de Broglie waves, consider those waves which are propagated with a wave velocity  $w = c$ . This corresponds to the propagation of electromagnetic waves. The velocity of the associated particle, the photon, is therefore also equal to  $c$ . If the value  $w = c$  is substituted in equation (27), we find that the rest mass of the photon  $m_0 = 0$ , that is, there is no such thing as a photon at rest. Photons always move with the velocity  $c$ .

## 68. Electron Diffraction Experiments of Davisson and Germer

De Broglie's hypothesis that material particles should exhibit a dual character, that of a wave and that of a corpuscle, has led to many interesting and far-reaching consequences. The wave length associated with any particle of mass  $m$  moving with velocity

$v$  is

$$\lambda = \frac{h}{mv}, \quad (17)$$

where  $h$  is the Planck constant. If the particle is an electron which has acquired its velocity  $v$  under the action of a difference of potential  $V$ , its kinetic energy, if  $v$  is small in comparison with  $c$ , is

$$\frac{1}{2}mv^2 = Ve, \quad (29)$$

and the wave length associated with it can be expressed as

$$\lambda = \frac{h}{\sqrt{2mVe}}. \quad (30)$$

For a difference of potential of 100 volts, for example,

$$\lambda = 1.22 \times 10^{-8} \text{ cm} = 1.22 \text{ \AA}.$$

This wave length is of the order of magnitude of the distances between atomic planes in crystals. This fact immediately suggests

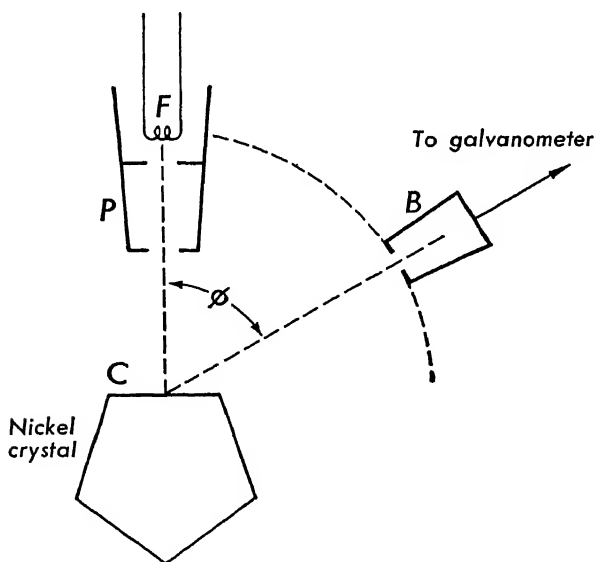


FIG. 86. — Outline of the experimental arrangement in the electron diffraction experiment of Davisson and Germer.

the possibility of showing the existence of these waves by using crystals as diffraction gratings for electrons in a manner analogous

to their use with X rays. Such a series of experiments was first carried out by Davisson and Germer (1927).

The experimental arrangement used by Davisson and Germer

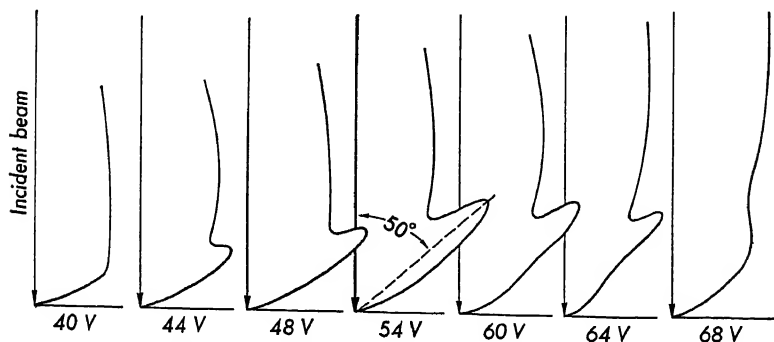


FIG. 87. — Curves, plotted in polar coordinates, showing the intensity of the scattered beam at different angles of scattering. The incident beam in each case is perpendicular to the face of the nickel crystal.

is shown in Figure 86. Electrons from a hot tungsten filament are accelerated by a difference of potential  $V$  between the filament  $F$  and the plate  $P$ . Some of these electrons emerge from a small opening in the plate  $P$  and strike the surface of a nickel crystal at normal incidence. The electrons are scattered in all directions by the atoms in the crystal. The intensity of the electron beam scattered in any given direction is determined by allowing the electrons to enter a chamber or bucket,  $B$ , set in the appropriate position, and then measuring the deflection produced by a galvanometer connected to the bucket. By rotating the bucket  $B$  about the crystal as an axis, the intensity of the scattered beam can be measured as a function of the angle of scattering. The results of one such set of measurements are shown in the set of curves of Figure 87. These curves are plotted in polar coordinates; the length of the radius vector is proportional to the intensity of the scattered beam and the angle between the radius vector and the  $y$  axis is the angle of scattering. The crystal is held in a fixed position throughout this set of measurements. When the difference of potential between  $F$  and  $P$  is 40 volts, the curve is fairly smooth. At 44 volts, a distinct spur appears on the curve at an angle of about 60°. The measurement of the distribution of intensity in the scattered beam is repeated at higher volt-

ages. The length of the spur increases until it reaches a maximum at 54 volts at an angle of  $50^\circ$ , then decreases and disappears completely at 68 volts at an angle of about  $40^\circ$ .

The selective reflection of the "54-volt" electrons at an angle of  $50^\circ$  can be explained as due to the constructive interference,

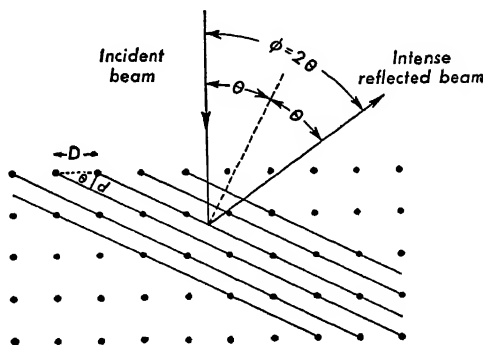


FIG. 88. — Diffraction of electron waves by a crystal.

that is, reinforcement, of the electron waves from the regularly spaced atoms of the nickel crystal. Consider a regular array of atoms such as that shown in Figure 88. Several sets of parallel planes rich in atoms can be drawn through this array in a manner identical with that used in the explanation of the Laue X-ray diffraction patterns. The parallel lines drawn in the figure represent the traces of one such set of planes perpendicular to the plane of the figure. A beam of electrons incident on the crystal will make some angle  $\theta$  with the normal to these planes. If the wave length of the de Broglie waves associated with these electrons is such as to satisfy Bragg's law

$$n\lambda = 2d \cos \theta, \quad (31)$$

then the waves scattered from these planes will have the correct phase relationships to reinforce one another and will produce an intense beam reflected at an equal angle  $\theta$  to the normal. Bragg's equation can be put in a more useful form by noting that the distance  $d$  between atomic planes is related to the distance  $D$  between atoms in the surface layer by the simple equation

$$d = D \sin \theta.$$

Substitution of this value of  $d$  in equation (31) yields

$$n\lambda = 2D \sin \theta \cos \theta = D \sin 2\theta,$$

from which

$$n\lambda = D \sin \phi, \quad (32)$$

where

$$\phi = 2\theta.$$

The angle  $\phi$  would represent the angle between the incident beam and the direction of the most intense part of the scattered beam,

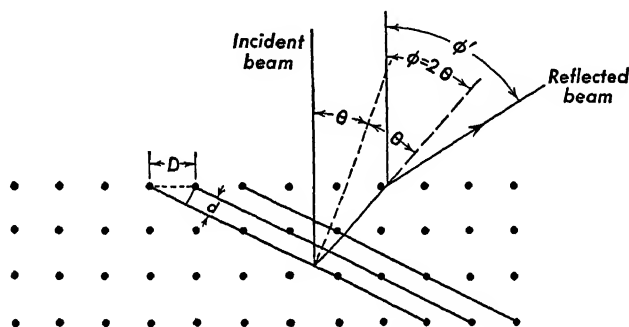


FIG. 89. — Refraction of the electron beam as it emerges from the crystal.

provided the beam was not refracted. But, just as in the case of light and X rays, we should expect the beam of electron waves to be refracted. Referring to Figure 89, we find that the incident beam is not deviated since it enters the crystal normal to the surface, but the emergent beam will leave the surface of the crystal at an angle  $\phi'$  to the normal. If  $\lambda$  is the wave length in a vacuum and  $\lambda'$  the wave length in the crystal, then the index of refraction  $\mu$  is

$$\mu = \frac{\lambda}{\lambda'} = \frac{\sin \phi'}{\sin \phi} = \frac{\sin \phi'}{\sin 2\theta}$$

from which

$$\lambda = \frac{\lambda' \sin \phi'}{\sin 2\theta}.$$

Now, in the crystal

$$n\lambda' = 2d \cos \theta;$$



therefore

$$\lambda = \frac{2d \cos \theta}{n \sin 2\theta} \cdot \sin \phi'$$

or

$$n\lambda = \frac{2d \cos \theta}{2 \sin \theta \cos \theta} \cdot \sin \phi';$$

and since

$$D = \frac{d}{\sin \theta},$$

we have

$$n\lambda = D \sin \phi'. \quad (33)$$

The angle  $\phi'$  represents the angle between incident beam and the direction of the most intense part of the scattered beam, that is, the angle that the spur on the curves of Figure 87 makes with the incident beam. It will be noticed that equation (33) has the same form as the equation for a plane diffraction grating using light at normal incidence, with  $n$  an integer representing the order of the diffraction pattern.

The above equation can be applied directly to the measurements made by Davisson and Germer. For the case of the "54-volt" electron beam,  $\phi' = 50^\circ$  and  $n = 1$ ; from X-ray data  $D$  is known to be  $2.15\text{\AA}$ ; hence

$$\lambda = 2.15\text{\AA} \times \sin 50^\circ = 1.65\text{\AA}.$$

This wave length can be compared with the value obtained by substituting  $V = 54$  volts into equation (30). The latter yields  $\lambda = 1.66\text{\AA}$ . Similar measurements were made with higher energy electrons, and comparable results were obtained in each case. The results of these experiments are in good agreement with de Broglie's hypothesis.

In one variation of this experiment, an oblique angle of incidence was used. An examination of the intensity of the scattered beam showed that there was an intense maximum at an angle of "reflection" equal to the angle of incidence, in accord with Bragg's law of reflection from a crystal grating. In this case the atomic planes producing the diffraction pattern are parallel to the surface.

With the angle of incidence kept fixed, measurements were made of the intensity of the beam reflected at this angle when the energy of the incident electrons was varied. Figure 90, in which the in-

tensity of the reflected beam is plotted against the square root of the voltage between filament and plate, shows a series of maxima almost equally spaced. Each maximum represents a different

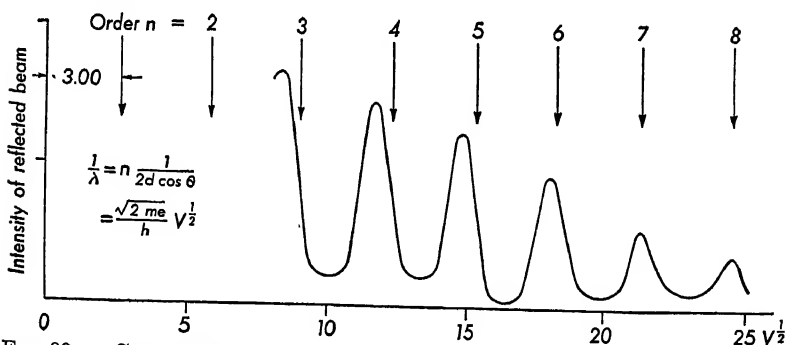


FIG. 90. — Curve obtained when the angle of incidence and the angle of reflection of the electron beam were each kept at  $10^\circ$ , while the energy of the electrons was increased.

order of diffraction. The existence of these maxima follows directly from an application of Bragg's law

$$n\lambda = 2d \cos \theta, \quad (31)$$

where  $\theta$  is now the angle between the incident beam and the normal to the atomic planes. Combining this with equation (30), we have

$$\frac{1}{\lambda} = \frac{\sqrt{2me}}{h} V^{1/2} = \frac{n}{2d \cos \theta}. \quad (34)$$

Whenever the wave length is such as to satisfy Bragg's law, there will be an intense maximum at an angle of reflection equal to the angle of incidence. Since  $\theta$  is kept constant,  $2d \cos \theta$  is also constant; there will therefore be an intense maximum for each new value of  $n$ , the order of diffraction, as  $V$  is changed. From equation (34), the spacings between maxima should all be the same and

proportional to  $\frac{1}{2d \cos \theta}$ . Actually the positions of the maxima

differ slightly from the calculated positions as shown by the positions of the arrows in Figure 90. This discrepancy can be explained as due to the refraction of the electron beam in the crystal, since for the higher voltages the electrons do penetrate the crystal.

The index of refraction  $\mu$  can be calculated with the aid of the modified form of Bragg's law, which is

$$n\lambda = 2d(\mu^2 - \sin^2 \theta)^{1/2}. \quad (35)$$

Values of the index of refraction are plotted against  $V^{1/2}$  in Figure 91. For low-energy electrons  $\mu$  is large and greater than

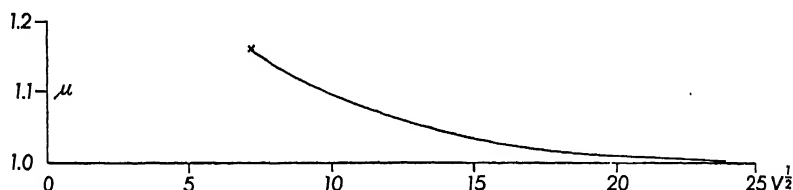


FIG. 91. — The index of refraction of nickel plotted against  $V^{1/2}$ .

unity; at higher energies  $\mu$  decreases and approaches unity. This is in agreement with the equation (6) for the index of refraction of a medium for a beam of particles. By substituting the measured values of  $\mu$  into this equation, we can determine the energy,  $U$ , of the electrons in the nickel crystal. For example, the index of refraction of a 100 ev electron beam, as obtained from Figure 91, is 1.1. Substituting this value in equation (6), we get

$$1.1 = \sqrt{1 + \frac{U}{100 \text{ ev}}}$$

from which

$$U = 21 \text{ ev.}$$

This large value for the potential energy of an electron inside a metal is in agreement with the modern electron theory of metals. (See § 45.)

## 69. Electron Diffraction Experiments of G. P. Thomson

G. P. Thomson (1928) was able to secure electron diffraction patterns by passing a narrow beam of cathode rays through very thin films of matter. The cathode rays were produced in a gas-discharge tube operated at potentials varying from 10,000 to 60,000 volts. The cathode rays, after passing through the thin film  $F$ , were received on a photographic plate at  $P$ , Figure 92. The pattern on the photographic plate consisted of a series of well-defined concentric rings about a central spot, Figure 93. This

pattern is very similar in appearance to X-ray powder diffraction patterns.

Ordinary metals, such as gold, silver, aluminum, are microcrystalline in structure, i.e., they consist of a large number of

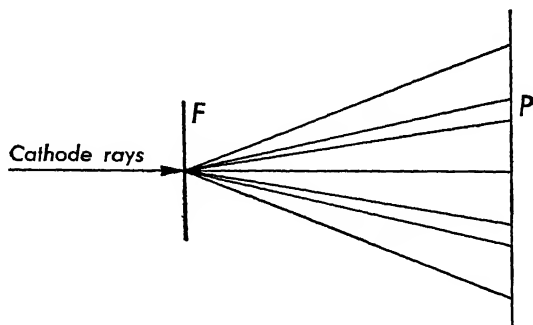


FIG. 92. — Schematic diagram of the electron diffraction experiments of G. P. Thomson.

very small crystals oriented at random. If any wave of length  $\lambda$  is incident upon a thin film of such a microcrystalline substance, a definite circular diffraction pattern will be obtained; the wave

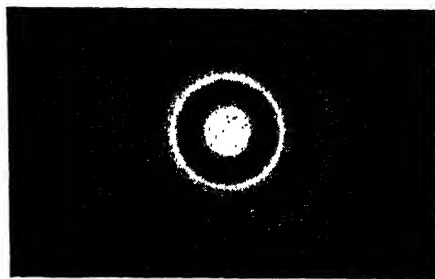


FIG. 93. — Diffraction pattern obtained by passing a beam of electrons through gold foil. (Reproduced from Thomson, *Wave Mechanics of Free Electrons*, Cornell University Press.)

length  $\lambda$  can be determined if the lattice constant,  $d$ , of the microcrystals is known. In Thomson's experiments, a beam of electrons moving with speed  $v$  was used instead of the X-ray beam, and a circular diffraction pattern was obtained. The wave length  $\lambda$  associated with the electron can be calculated with the aid of Bragg's formula, using the value of  $d$  from X-ray data. Actually, Thomson determined the wave length of the electrons from the

de Broglie formula

$$\lambda = \frac{h}{mv},$$

and then calculated the crystal grating constant  $d$ , and compared it with X-ray determinations. The following table gives a few of the results of Thomson's experiments:

TABLE VII

VALUES OF GRATING CONSTANT $d$ IN Å			
Metal	X Ray	Cathode Rays	
Aluminum	4.05	4.06	4.00
Gold	4.06	4.18	3.99
Platinum	3.91		3.88
Lead	4.92		4.99

The results of these experiments confirm de Broglie's hypothesis that there is a wave motion associated with every moving electron.

## 70. Waves Associated with Matter

Since de Broglie's formula applies to any mass particle moving with speed  $v$ , it should be possible to secure diffraction and interference effects with atoms and molecules as well as with electrons. The diffraction of atoms and molecules by crystals was first clearly demonstrated by Stern and his co-workers. In these experiments they investigated the diffraction of hydrogen and helium molecules, using crystals of lithium fluoride and sodium chloride. A stream of molecules from an oven at a known temperature  $T$  was directed against the surface of the crystal at some angle  $\theta$ . The surface of the lithium fluoride crystal in this case behaves in very much the same manner as a "crossed" diffraction grating does in optical experiments, that is, the diffracting centers are at the corners of squares. The incident beam is scattered in all directions, and intensity maxima for any given wave length occur only at those points where the waves from the different diffracting centers meet in phase.

In the case of the molecular beam scattered by the crystal, the points of maximum intensity correspond to regions of maximum pressure of the gas. Hence, Stern used a very sensitive manometer, *M*, Figure 94, to locate the diffraction pattern produced by

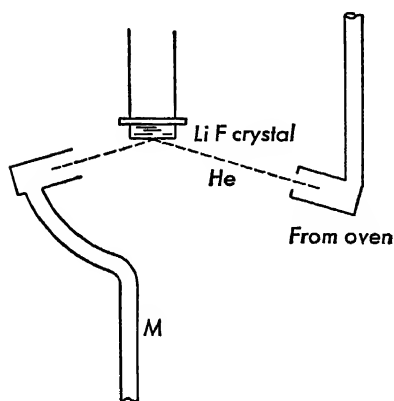


FIG. 94. — Schematic diagram showing the arrangement of apparatus used in the diffraction of atoms and molecules.

the crystal. This manometer could be rotated about an axis at right angles to the face of the crystal and could thus measure the intensity of the scattered molecular beam at various points. Figure 95 is a typical curve showing the diffraction pattern obtained by reflecting helium from the LiF crystal. The intensity maximum at  $0^\circ$  corresponds to the regularly reflected beam in which the angle of reflection is equal to the angle of incidence. Then, as the manometer is rotated on either side

of the reflected beam, the pressure is found to drop to a minimum

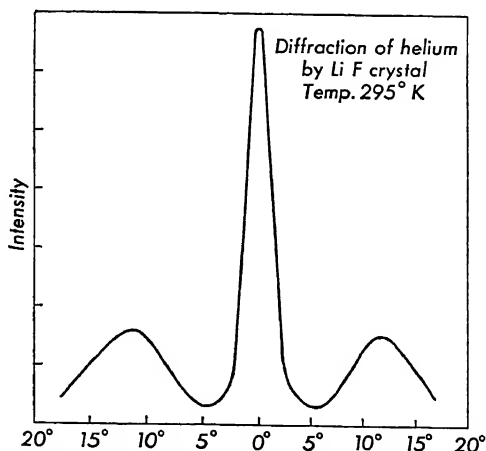


FIG. 95. — The diffraction pattern obtained with helium reflected from a lithium fluoride crystal.

value at about  $5^\circ$  and to rise again to a maximum on either side at  $10^\circ$  from the directly reflected beam. These two maxima cor-

respond to the first-order diffraction patterns obtained with a grating.

The wave length associated with the helium atoms can be calculated, using the known spacing of the atoms in the lithium fluoride crystal and the positions of the first-order diffraction patterns. The wave lengths calculated in this manner are in excellent agreement with those predicted by the de Broglie formula

$$\lambda = \frac{h}{mv},$$

where  $m$  is the mass of the helium atom and  $v$  is the average velocity of the helium atoms calculated from a knowledge of the temperature of the helium in the oven. Many experiments were performed using temperatures varying from 100° abs to 650° abs. Diffraction patterns were obtained in all cases. Similar experiments were performed with hydrogen molecules,  $H_2$ , and the wave lengths obtained were found to be in agreement with de Broglie's hypothesis.

A similar experiment was performed by T. H. Johnson in which a beam of hydrogen atoms was reflected from a lithium fluoride crystal and allowed to strike a plate coated with molybdenum oxide. The oxide was reduced to metallic molybdenum wherever the hydrogen struck the plate, and the pattern thus formed was then photographed. The diffraction patterns obtained agreed with the predictions based upon de Broglie's hypothesis and with the results obtained by Stern.

## 71. Heisenberg's "Uncertainty Principle"

An interesting interpretation of the duality, wave and particle, of both matter and radiant energy has been given by Heisenberg. The concepts of a particle and of a wave have been built up on the basis of experiments performed on a comparatively large scale; these concepts are mental pictures formed on the basis of such experiments. When applied to experiments involving quantities of the order of magnitude of atomic dimensions, these concepts can have the validity of analogies only. The concept of the electron as a particle, for example, was derived from the results of experiments on the motion of the electron through electric and magnetic fields. The problem of particle dynamics is to predict

the position and velocity of the particle at any time  $t$  when its initial position and velocity are known. But the experiments on electron diffraction show that this is not always possible. Electrons starting with the same initial conditions are not all scattered through the same angle by the crystals; the result is a diffraction pattern showing a definite distribution of these electrons with respect to both position and momentum. But a diffraction pattern is the best evidence that we are dealing with a wave phenomenon. To apply the wave concept to a single electron, the electron may be pictured as a small bundle or packet of waves extending over some small region of space  $\Delta s$ . The association of a wave packet with an electron means that the position of the electron at any instant of time  $t$  cannot be specified with any desired degree of accuracy; all that can be said of the electron is that it is somewhere within this group of waves which extends over a small region of space  $\Delta s$ .

Heisenberg's *uncertainty principle* refers to the simultaneous determination of the position and the momentum of the particle and states that the uncertainty,  $\Delta x$ , involved in the measurement of the coordinate of the particle and the uncertainty  $\Delta p_x$  involved in the simultaneous measurement of its momentum are governed by the relationship

$$\Delta x \cdot \Delta p_x \geq h, \quad (36)$$

where  $h$  is the Planck constant.

An examination of a few idealized experiments will serve to show how the wave concept acts as a limitation on the particle concept, giving rise to the uncertainty principle. One such idealized experiment was given by Bohr. Suppose it is desired to determine the position of an electron, using some instrument such as a microscope of very high resolving power. It can be shown that the resolving power of a microscope is given by

$$\Delta x = \frac{\lambda}{2 \sin \alpha},$$

where  $\Delta x$  represents the distance between two points which can just be resolved by the microscope,  $\lambda$  is the wave length of the light used, and  $\alpha$  is the semivertical angle of the cone of light coming from the illuminated object.  $\Delta x$  represents the uncertainty



in the determination of the  $x$  coordinate of the position of the electron. To make  $\Delta x$  as small as possible, light of very short wave length must be used, either hard X rays or gamma rays. The minimum amount of light that can be used is a single quantum  $h\nu$ . When the electron scatters this quantum into the microscope, Figure 96, the electron will receive some momentum from the quantum (Compton effect). Since the scattered quantum can enter the microscope anywhere within the semivertical angle  $\alpha$ , its contribution to the  $x$  component of the momentum of the electron is unknown by an amount

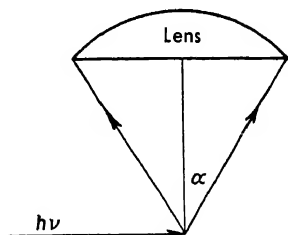


FIG. 96. — Schematic diagram of the gamma-ray microscope experiment.

$$\Delta p_x = 2p \sin \alpha = \frac{2h}{\lambda} \sin \alpha$$

where  $h/\lambda$  is the momentum of the quantum. The product of the uncertainties in the determination of the simultaneous values of the position and momentum of the electron is therefore

$$\Delta x \cdot \Delta p_x = \frac{\lambda}{2 \sin \alpha} \cdot \frac{2h}{\lambda} \sin \alpha = h.$$

Another illustration of the uncertainty principle is supplied by an experiment in which a beam of electrons passes through a narrow slit, and is then recorded on a photographic plate placed some distance away, Figure 97. Every electron which is registered on the photographic plate must have passed through the slit, and if its width is  $\Delta y$ , then the  $y$  coordinate of the electron is indeterminate by an amount  $\Delta y$ . Making this width smaller increases the accuracy in the knowledge of the  $y$  coordinate of the electron at the instant it passes through the slit. But with a very narrow slit a very definite diffraction pattern is observed on the photographic plate. The interpretation of this diffraction pattern is that the electron receives additional momentum parallel to the slit at the instant that it passes through the slit. If  $p$  is the momentum of the electron, the component in the  $y$  direction is  $p \sin \theta$ , where  $\theta$  is the angle of deviation. The electron may be anywhere within the diffraction pattern, so that if  $\alpha$  is the angular width of

the pattern, the uncertainty in the knowledge of the  $y$  component of the momentum of the electron is

$$\Delta p_y = 2p \sin \alpha.$$

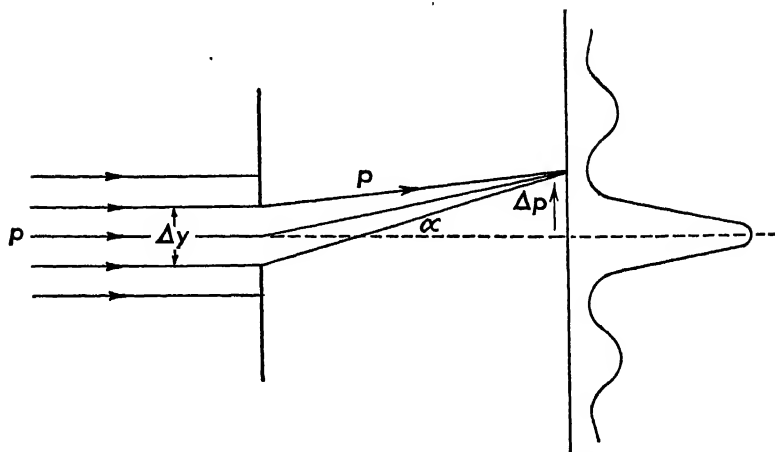


FIG. 97. — Diffraction of electrons by a slit. The intensity pattern obtained is shown on the right.

The angular width of the diffraction pattern is determined by the slit width  $\Delta y$  and is given by the equation

$$2\Delta y \sin \alpha = \lambda.$$

Hence the product of the uncertainties in the simultaneous determination of the  $y$  coordinate and  $y$  momentum of the electron in its passage through the slit is

$$\Delta y \cdot \Delta p_y = 2p \sin \alpha \cdot \frac{\lambda}{2 \sin \alpha} = p\lambda.$$

From de Broglie's hypothesis

$$p = \frac{h}{\lambda};$$

therefore

$$\Delta y \cdot \Delta p_y = h.$$

Another set of variables can be used to express Heisenberg's uncertainty principle. If  $\mathcal{E}$  is the energy of the system at time  $t$ , then it may be shown that

$$\Delta \mathcal{E} \cdot \Delta t \geq h, \quad (37)$$

where  $\Delta\mathcal{E}$  is the uncertainty in our knowledge of the value of the energy  $\mathcal{E}$  and  $\Delta t$  is the uncertainty in the knowledge of the time.

## 72. Probability Concept

The wave-particle parallelism must be extended to include an interpretation of the intensity of light and also the intensity of the electron beam. According to the wave theory of light, the intensity is determined by the square of the amplitude of the electric vector at the point under consideration. On the corpuscular theory the intensity of the beam of light must be determined by the number of photons per second which pass through a unit area perpendicular to their direction of motion, or

$$N \sim Y_0^2, \quad (38)$$

where  $Y_0$  is the amplitude of the electric vector and  $N$  is the number of photons per unit volume of the beam; also  $Nc$  is the number of photons passing through unit area in unit time. The intensity relationship  $N \sim Y_0^2$ , while adequate for intense beams, is no longer satisfactory when dealing with very weak beams for which  $N$  is a very small number ( $N \ll 1$ ). In this case it becomes difficult to determine the exact location of each particle in the continuous wave; that is, the expression  $N \sim Y_0^2$  involves an indeterminacy with respect to the position of these photons in space. An alternative approach to the problem is through a statistical interpretation. The square of the amplitude,  $Y_0^2$ , can be thought of as proportional to the *probability* of a photon crossing unit area perpendicular to the direction of motion in unit time at the point under consideration.

For example, if a beam of light passes through a narrow slit and is incident upon a photographic plate, a definite diffraction pattern will be obtained showing regions of great intensity alternating with regions of very small intensity. On the statistical interpretation, the probability of a photon striking the photographic plate is very great where the intensity is great and is very small where the intensity is small. In the case of a very weak beam of light, say, one in which a single photon passes through the slit every minute, it is impossible to predict just where any individual photon will strike the photographic plate. All that can be said is that the probability of the photon striking a certain portion of the plate is large just

where the wave theory predicts large intensity and the probability is small just where the wave theory predicts small intensity. If only a few photons strike the photographic plate, their arrangement will undoubtedly be haphazard. But if a sufficient time is allowed to elapse so that a large number of photons reach the photographic plate, the result will be the diffraction pattern predicted by the wave theory.

The above mode of description can be applied to the diffraction of an electron beam by a narrow slit. The wave associated with the electron is the de Broglie wave. There is a certain probability that an electron after passing through the slit will strike a given point on the photographic plate; this probability is proportional to the square of the amplitude of the associated de Broglie wave. While it is impossible to predict just where any one electron will strike the plate, yet after an interval of time, sufficient to allow a large number of electrons to strike the plate, a definite diffraction pattern will be observed, and the intensities at the different points will correspond to the amplitudes of the diffracted waves at those points.

The phenomena of transmission and reflection at a plane surface can be explained in a similar manner. If a system of waves is incident on a plane surface, part of it will be reflected and part transmitted, and their intensities will be proportional to the squares of the amplitudes of the reflected and transmitted waves respectively. According to the corpuscular theory, the particle associated with the incident wave has a certain probability of being reflected and a certain probability of being transmitted, these probabilities being proportional to the squares of the amplitudes of the corresponding waves.

From the discussion of the last two sections it can be asserted that while there is an indeterminacy in the description of phenomena from the corpuscular point of view, there is no lack of determinacy from the point of view of the wave theory. The wave functions necessary to describe these phenomena are continuous functions of the coordinates and the time. These wave functions are obtained from the solutions of the appropriate wave equations: in general, second-order partial differential equations involving the coordinates and the time. For the case of light, these wave functions are obtained from the solutions of the differential equa-

tions which form the basis of the electromagnetic theory of light. For the case of material particles, these wave functions are obtained from the solutions of a wave equation first formulated by Schrödinger and forming the basis of a new division of physics called *wave mechanics*.

### 73. Schrödinger's Equation for a Single Particle

A typical wave equation in Cartesian coordinates is

$$\frac{\partial^2 U}{\partial x^2} + \frac{\partial^2 U}{\partial y^2} + \frac{\partial^2 U}{\partial z^2} = \frac{1}{w^2} \frac{\partial^2 U}{\partial t^2}, \quad (39)$$

where  $U$  is the wave function which is propagated with the wave velocity  $w$ . For example, in the case of electromagnetic waves,  $U$  may represent any one of the components of the electric vector or of the magnetic vector which is propagated through space. Schrödinger's contribution was the incorporation of de Broglie's waves associated with material particles into the above equation.

For the case of a single particle of mass  $m$ , velocity  $v$ , and total energy  $\mathcal{E}$ , the following equations have been shown to apply

$$\mathcal{E} = h\nu, \quad (9)$$

$$p = \frac{h}{\lambda}, \quad (13)$$

$$w = \lambda v = \frac{\mathcal{E}}{p} = \frac{h\nu}{p}. \quad (26)$$

Since the kinetic energy of the particle is the difference between the total energy  $\mathcal{E}$  and the potential energy  $V$ , we can write

$$mv^2 = 2(\mathcal{E} - V),$$

assuming that  $v \ll c$  so that the relativity expressions need not be used.

Now

$$p = mv = \sqrt{2m(\mathcal{E} - V)}, \quad (16)$$

so that

$$w = \frac{h\nu}{\sqrt{2m(\mathcal{E} - V)}}. \quad (40)$$

In general, only those wave functions  $U$  which are harmonic

functions of the time are of physical significance. Such wave functions can be expressed as  $\sin 2\pi\nu t$  or  $\cos 2\pi\nu t$ , or combinations of sine and cosine functions represented by the exponential function  $e^{2\pi\nu i t}$ , where  $i = \sqrt{-1}$ . Suppose

$$U = u e^{2\pi\nu i t}$$

represents the wave function where  $u$  is a function of the coordinates only. Two successive differentiations of the function with respect to the time only yield

$$\begin{aligned} \frac{\partial^2 U}{\partial t^2} &= -4\pi^2\nu^2 u e^{2\pi\nu i t} \\ &= -4\pi^2\nu^2 U. \end{aligned} \quad (41)$$

Substitution of the values from equations (40) and (41) into the wave equation yields

$$\frac{\partial^2 U}{\partial x^2} + \frac{\partial^2 U}{\partial y^2} + \frac{\partial^2 U}{\partial z^2} = -\frac{8\pi^2 m}{h^2}(\mathcal{E} - V)U, \quad (42)$$

which is one form of Schrödinger's wave equation for a single particle. By canceling the exponential factor from each term of the wave equation, a similar equation is obtained for the amplitude  $u$ , which is

$$\frac{\partial^2 u}{\partial x^2} + \frac{\partial^2 u}{\partial y^2} + \frac{\partial^2 u}{\partial z^2} = -\frac{8\pi^2 m}{h^2}(\mathcal{E} - V)u. \quad (43)$$

It will be noticed that the time does not enter explicitly into this amplitude equation; in the wave mechanics of a particle, the function  $u$  is usually referred to as the *wave function*. The potential energy  $V$  is, in general, a function of the coordinates. The problem in wave mechanics is to put in the appropriate value for  $V$  and seek solutions of Schrödinger's equation. It is beyond the scope of this book to solve these partial differential equations, but the results of such solutions will be made use of wherever necessary in the discussion of atomic physics.

The interpretation of the wave function has already been indicated in the previous section in the discussion of the de Broglie waves associated with matter. Solutions of Schrödinger's equation will give  $u$  as a continuous function of the coordinates, and hence its value will be determined for every point in space. The

square of this wave function or amplitude,  $u^2$ , is proportional to the probability of finding the particle at any given point in space. Or if the product  $u^2 dv$  is formed, it can be considered as a measure of the probability of finding the particle in this volume element  $dv$ . Summing up these products over all space, and equating this sum to unity, or expressing it mathematically,

$$\int_{\text{space}} u^2 dv = 1, \quad (44)$$

is equivalent to saying that it is certain that the particle is somewhere in space. If the wave function  $u$  is chosen to satisfy the above integral equation, the function is said to be *normalized* and the product  $u^2 dv$  now measures the absolute value of the probability of finding the particle in the particular volume element  $dv$ . While the above discussion has been limited to a single particle, the effect produced by a large number of particles is simply the sum of the elementary effects produced by the individual particles. Thus, in wave mechanics, the problem of determining the motion of a single particle is reduced to that of determining the probability of finding the particle in any particular place at a given time.

## 74. Electron Optics

Nearly all the phenomena that are usually associated with light and X rays, and which form the subject of optics, can also be observed with electrons. Electrons can be reflected and refracted; interference and diffraction phenomena can be produced at will; electrons from a point source may be focused by passing them through properly shaped electric or magnetic fields; such fields play the role of lenses. A completely new branch of science, known as *electron optics*, has been developed within recent years, and investigations in this subject not only have led to a better understanding of physical phenomena but have also produced several important instruments which have wide applications. One of these is the *electron microscope*.

A microscope is used to provide an enlarged image of a small object as well as to show greater detail in its structure. The latter property is determined by the resolving power of the microscope. We have already seen that the limit of the resolving power of a microscope is determined by the wave length of the incident radi-

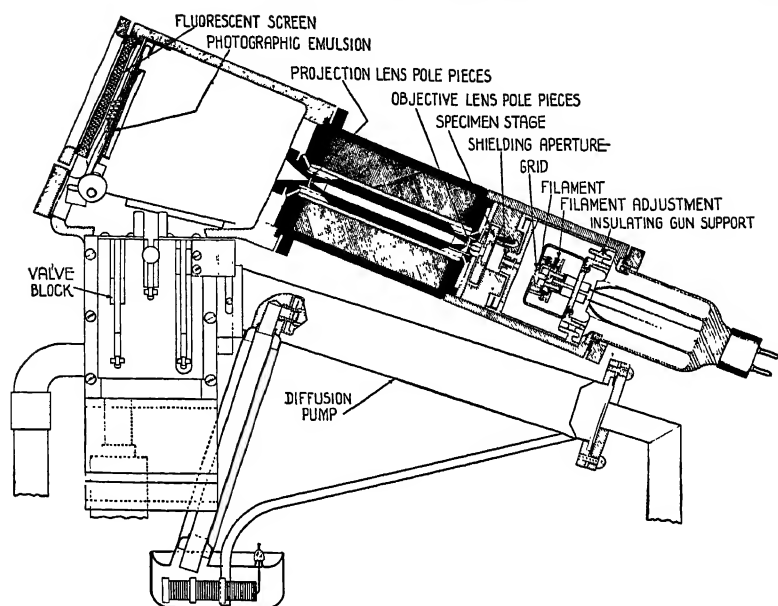


FIG. 98. — A simplified cross section of a small electron microscope unit.

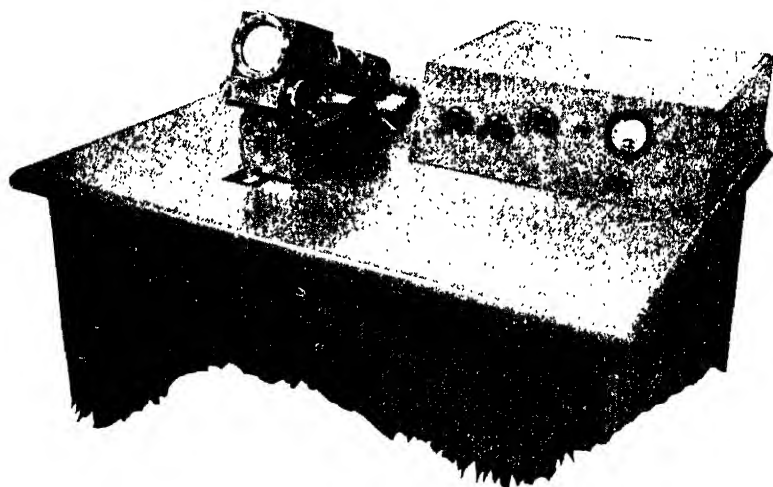


FIG. 99. — A photograph of the experimental model of the small electron microscope with the control panel. (Courtesy of RCA Laboratories.)

ation. In the case of optical microscopes, the limit of the resolving power of the optical microscope is of the order of magnitude of the wave length of visible light, which we may take as  $5000\text{\AA}$ .



But, since the wave lengths associated with electrons are determined by the relation

$$\lambda = \frac{h}{mv},$$

it is possible to get much smaller wave lengths by using appropriate accelerating voltages on the electrons and thus to produce

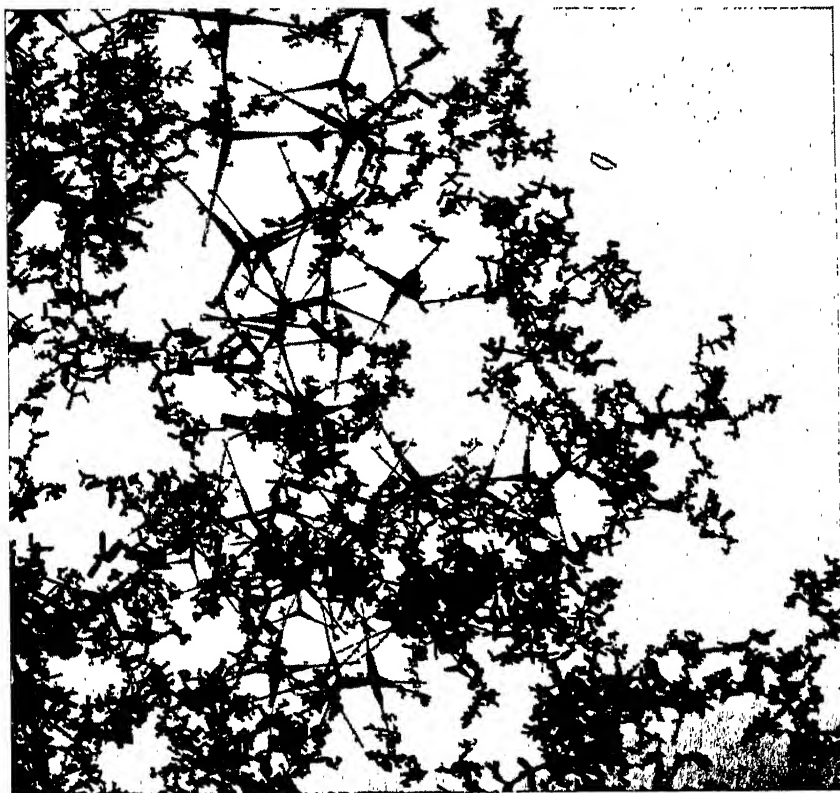


FIG. 100. — Photograph of some very fine zinc oxide crystals to show the resolving power and the magnification produced by the small electron microscope. Scale: 1 cm on plate represents 0.001 mm. (Courtesy of RCA Laboratories.)

microscopes with much greater resolving power. Electron microscopes have been produced with resolving powers of about  $20\text{\AA}$ , using accelerating voltages from 30 kv to 100 kv.

Figure 98 shows a simplified cross section of a compact, high-resolving-power electron microscope, and Figure 99 is a photograph of the experimental model with the control panel. This

microscope uses magnetic fields both for the objective lens and for the projection lens. Either an electromagnet or a permanent magnet may be used for these lenses. The specimen to be investigated has to be very thin so that electrons of about 30 kev energy can be transmitted through it without loss of energy. The instrument is designed so that the image can be focused on a fluorescent screen for visual examination, and is also arranged so that a photographic plate can be put in front of the screen to photograph the image. A diffusion pump is connected to the microscope to provide a vacuum of about  $5 \times 10^{-5}$  mm of mercury pressure. An idea of both the resolving power and the magnification of this microscope can be obtained from Figure 100, which is a photograph of some very fine zinc oxide crystals. This instrument can also be provided with an adapter so that it can be used as an electron diffraction camera. Other electron microscopes have been designed for the study of the surfaces of thick specimens by the reflection of electrons from the surface.

The development of the electron microscope has provided a powerful tool for the study of the structure of large molecules, the structure of bacteria, the photography of viruses and other very small objects. Further developments in this field will undoubtedly increase the resolving power to better values.

## REFERENCES

- BORN, M., *Atomic Physics*. New York: G. E. Stechert & Company, 1936, Chap. IV.
- HEISENBERG, W., *The Physical Principles of the Quantum Theory*. Chicago: University of Chicago Press, 1930, Chaps. I-IV.
- RICHTMYER, F. K., and E. H. KENNARD, *Introduction to Modern Physics*. New York: McGraw-Hill Book Company, Inc., 1942, Chap. VII.
- THOMSON, G. P., *Wave Mechanics of Free Electrons*. New York: McGraw-Hill Book Company, Inc., 1930, Chap. IV.

## PROBLEMS

1. Calculate the length of the wave associated with a particle of one gram mass moving with a velocity of 200 cm/sec. Discuss the probability of performing a successful diffraction experiment with a stream of such particles.

Ans.  $3.3 \times 10^{-29}$  cm.

2. Calculate the wave length associated with an alpha particle emitted by the nucleus of an atom of radon. Compare this wave length with the diameter of the nucleus.

*Ans.*  $6.13 \times 10^{-13}$  cm.

3. It can be shown that the rate at which a gas at absolute temperature  $T$  moves out of an orifice in an oven is the same as that of a gas moving out of the aperture with a uniform velocity equal to  $\frac{1}{4}\bar{c}$  where  $\bar{c}$  is the average velocity of the molecules. Further, the average kinetic energy of the molecules of a gas is given by

$$\frac{1}{2}MC^2 = \frac{3}{2}kT,$$

where

$$C^2 = \frac{3\pi}{8}\bar{c}^2.$$

$k$  is Boltzmann's constant and is equal to  $1.37 \times 10^{-16}$  ergs/molecule/deg.

(a) Derive an expression for the length of the waves associated with a stream of molecules of a gas at temperature  $T$ . (b) Calculate the wave length associated with a stream of helium molecules issuing from an oven at  $300^\circ$  abs. (c) Devise an experiment for showing the existence of these waves giving approximate dimensions of the essential parts of the apparatus.

$$\text{Ans. (a) } \lambda = h\sqrt{\frac{2\pi}{MkT}}.$$

$$\text{(b) } \lambda = 3.14\text{\AA}.$$

4. Electrons from a heated filament are accelerated by a difference of potential between the filament and the anode of 30 kv; a narrow stream of electrons coming through a hole in the anode is transmitted through a thin sheet of aluminum. (a) Assuming Bragg's law to hold, calculate the angle of deviation of the first-order diffraction pattern. (b) Determine the velocity of these waves in the aluminum foil.

$$\text{Ans. (a) } \phi = 2\theta = 55 \text{ min.}$$

$$\text{(b) } w = 9.04 \times 10^{10} \text{ cm/sec.}$$

5. A stream of electrons of 240 ev energy is incident upon the surface of platinum at an angle of  $30^\circ$  to the normal. The electron energy  $U$  in platinum is known to be about 12 ev. (a) Calculate the index of refraction of platinum for these electrons. (b) Determine the angle of refraction. (c) Determine the wave velocity of the electron waves in platinum. (d) Determine the velocity of the electrons in platinum.

$$\text{Ans. (a) } \mu = 1.025.$$

$$\text{(b) } 29^\circ.$$

$$\text{(c) } 9.5 \times 10^{11} \text{ cm/sec.}$$

$$\text{(d) } 9.48 \times 10^8 \text{ cm/sec.}$$



## Part II

# THE EXTRANUCLEAR STRUCTURE OF THE ATOM



# 5

## The Hydrogen Atom

### 75. Spectrum of Hydrogen

Hydrogen, the simplest of all the elements, has been investigated most extensively both experimentally and theoretically. The knowledge obtained from this study has acted as a guide to the study of the more complex elements. One of the greatest aids in determining the structure of the atoms of any one element has been the study of the radiation emitted and absorbed by the element. When the light from an element in the gas or vapor phase is analyzed with the aid of a spectroscope, it is found to consist of a series of very sharp lines of definite wave lengths characteristic of the element emitting the radiation. Most of the atomic spectra are very complex, and their analysis involves exceedingly careful and painstaking measurements of the wave lengths and their relative intensities. As a result of this work many of the spectral lines of each element were found to be related in a simple manner expressed by means of a simple equation suggested by Rydberg (1889) in which the reciprocal of the wave length, that is, the wave number, of a line is given as the difference between two numbers, or two terms. In this chapter we shall limit our considerations to the hydrogen atom.

As long ago as 1885, Balmer succeeded in obtaining a simple relationship among the wave numbers of the lines in the visible region of the hydrogen spectrum. Balmer's equation expressed in modern notation is

$$\frac{1}{\lambda} = \bar{\nu} = R_H \left( \frac{1}{2^2} - \frac{1}{n^2} \right), \quad (n = 3, 4, 5 \dots), \quad (1)$$

where  $\lambda$  is the wave length and  $\bar{\nu}$  is the wave number of the spectral line.  $R_H$  is a constant known as Rydberg's constant for hydrogen and  $n$  is an integer greater than 2. The empirical value of Rydberg's constant for hydrogen is

$$R_H = 109,677.76 \text{ cm}^{-1}.$$

By substituting for  $n$  in equation (1) the successive values 3, 4,

5, 6, . . . , we obtain the wave numbers of the lines in the Balmer series. Figure 101 is a photograph of the lines of the Balmer series. The relative positions of these lines on a wave number scale are shown in Figure 102. It is obvious from the equation that as  $n$

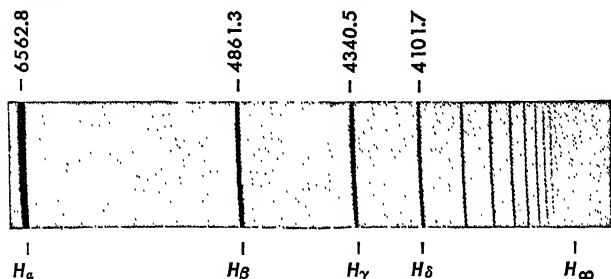


FIG. 101. — Photograph of the emission spectrum of hydrogen showing the Balmer series lines in the visible and near ultraviolet regions.  $H_\infty$  shows the theoretical position of the series limit. (Reprinted by permission from Hertzberg, *Atomic Spectra and Atomic Structure*, Prentice-Hall, Inc.)

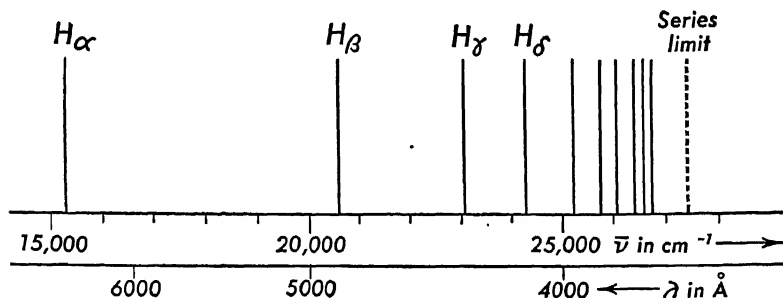


FIG. 102. — Graph of the positions of the Balmer series lines on wave number and wave length scales.

approaches infinity, the lines crowd together and approach a limit known as the *series limit*. The value of the limit of the Balmer series is  $R_H/2^2 = 27,419.44 \text{ cm}^{-1}$ .

Another way of expressing the Balmer formula is by writing the wave number of each line as the difference between two terms

$$\bar{\nu} = T_l - T, \quad (2)$$

where  $T_l = R_H/2^2$  is the value of the series limit, and  $T = R_H/n^2$  is the variable term. This mode of expressing the series relationship will be found very useful for more complex spectra.

## 76. Bohr's Theory of the Hydrogen Atom

The first quantitatively correct derivation of the Balmer formula on the basis of an atomic model was given by Bohr (1913),



in his theory of the hydrogen atom. This theory has played such an important role in the development of atomic physics that, even though it has been modified and extended by the later developments in quantum mechanics, it will be worth while to present the original simplified theory. Bohr adopted Rutherford's nuclear model of the atom; on this basis the hydrogen atom should consist of a singly charged positive nucleus and an electron outside the nucleus, since the atomic number is equal to unity. Assuming Coulomb's law of force and Newton's laws of motion to be applicable in the atomic domain, the path of the electron around the nucleus should be a conic section. As a first approximation assume that this conic section is a circle of radius  $r$  with the nucleus fixed at the center of the circle. If  $E$  is the charge on the nucleus and  $e$  the charge on the electron, then from Coulomb's law, the force of attraction between the nucleus and the electron is

$$F = \frac{Ee}{r^2} = -\frac{e^2}{r^2}, \quad (3)$$

since the atomic number  $Z = 1$  and  $E = -Ze = -e$ . From Newton's second law of motion

$$F = ma = -\frac{mv^2}{r}, \quad (4)$$

where  $m$  is the mass of the electron,  $a$  is its centripetal acceleration and  $v$  is its velocity. The minus sign indicates that the acceleration is directed toward the center of the circle. Equating (3) and (4), we get

$$\frac{e^2}{r^2} = \frac{mv^2}{r},$$

from which

$$mv^2 = \frac{e^2}{r}. \quad (5)$$

The potential at any point distant  $r$  from the charge  $E$  is  $E/r$  so that the potential energy of the electron is

$$\frac{Ee}{r} = -\frac{e^2}{r}. \quad (6)$$

The kinetic energy of the electron is  $\frac{1}{2}mv^2$ . Therefore the total

energy  $\mathcal{E}$ , which is the sum of the potential and kinetic energies, is

$$\mathcal{E} = \frac{1}{2}mv^2 - \frac{e^2}{r}, \quad (7)$$

which, upon the substitution of equation (5), becomes

$$\mathcal{E} = -\frac{e^2}{2r}. \quad (8)$$

Since in this discussion the nucleus has been considered stationary, equation (8) represents the total energy of the atom excluding the rest-mass energy of the two particles. It will be noticed that  $\mathcal{E} = 0$  when  $r = \infty$ ; that is, the zero level of energy is taken as that of the ionized atom. The minus sign shows that the energy of the atom is decreased as the electron comes closer to the nucleus. It is reasonable to assume that this decrease in energy is given out in the form of light.

On the basis of classical electrodynamics, the atom should radiate energy continuously at a rate proportional to the square of the acceleration of the electron. This would give rise to a continuous variation in the total energy  $\mathcal{E}$ , so that the radiation would consist of a continuous spectrum instead of the sharp line spectrum which is observed. To explain the observed sharp line spectrum of hydrogen, Bohr introduced two fundamental postulates. The first postulate is that of all the electron orbits, only those orbits are permissible for which the angular momentum of the electron is a whole multiple of  $h/2\pi$ , and that no energy is radiated while the electron remains in any one of these permissible orbits. Since the angular momentum of the electron in any orbit is  $mvr$ , only those orbits are permissible which satisfy Bohr's postulate, which may be stated as

$$mvr = \frac{nh}{2\pi}, \quad (9)$$

where  $n$  is an integer. These orbits are sometimes called *stationary* orbits.

The second postulate is that whenever radiant energy is emitted or absorbed by an atom, this energy is emitted or absorbed in whole quanta of amount  $h\nu$ , and that the energy of the atom is changed by this amount, thus

$$\mathcal{E}_i - \mathcal{E}_f = h\nu, \quad (10)$$

where  $\mathcal{E}_i$  represents the initial value of the energy of the :  
 $\mathcal{E}_f$  represents the final value of this energy,  $\nu$  is the frequency of  
 radiation emitted or absorbed by the atom, and  $h$  is the Planck  
 constant. If  $\mathcal{E}_i$  is greater than  $\mathcal{E}_f$ , energy is radiated, and if  $\mathcal{E}_i$  is  
 less than  $\mathcal{E}_f$ , energy is absorbed by the atom. Thus on Bohr's  
 theory, the atom radiates energy only when an electron jumps  
 from a stationary orbit of higher energy to one of lower energy.

The radii of these permissible orbits can be calculated by elimin-  
 ating  $\nu$  from equations (5) and (9), yielding

$$r = n^2 \frac{h^2}{4\pi^2 me^2}. \quad (11)$$

The smallest orbit will be that for which  $n = 1$ ; its radius  $r_1$  can  
 be determined by substituting the empirically determined values  
 of the constants  $h$ ,  $m$ , and  $e$ . This yields

$$r_1 = 0.529 \times 10^{-8} \text{ cm} = 0.529 \text{ \AA}.$$

It will be noticed that this numerical value is of the same order of  
 magnitude as that obtained on the basis of the kinetic theory of  
 gases.

The radius  $r_n$  of any other orbit of quantum number  $n$  is given  
 by

$$r_n = n^2 r_1,$$

so that radii of successive orbits increase as the square of  $n$ .

The energy  $\mathcal{E}_n$  of the atom when the electron is in the station-  
 ary orbit characterized by the quantum number  $n$  can now be  
 determined by eliminating  $r$  from equations (8) and (11), yielding

$$\mathcal{E}_n = - \frac{2\pi^2 me^4}{n^2 h^2}. \quad (12)$$

According to Bohr's second postulate, the frequency  $\nu$  of the  
 energy radiated when an electron goes from orbit  $n_i$  to orbit  $n_f$  is

$$\nu = \frac{\mathcal{E}_i - \mathcal{E}_f}{h}, \quad (13)$$

so that

$$\nu = \frac{2\pi^2 me^4}{h^3} \left( \frac{1}{n_f^2} - \frac{1}{n_i^2} \right). \quad (14)$$

Equation (14) has exactly the same mathematical form as Balm-

er's formula. To compare this equation with spectroscopic data, it will be more convenient to write it in terms of wave numbers where

$$\bar{\nu} = \frac{1}{\lambda} = \frac{\nu}{c} \quad (15)$$

yielding

$$\bar{\nu} = \frac{2\pi^2me^4}{ch^3} \left( \frac{1}{n_f^2} - \frac{1}{n_i^2} \right). \quad (16)$$

The identity of equation (16) with Balmer's formula can only be established by comparing the numerical value of  $R_H$  obtained spectroscopically with the numerical value of the factor

$$\frac{2\pi^2me^4}{ch^3},$$

using the values of  $m$ ,  $e$ ,  $c$ , and  $h$  determined by independent experiments. Putting in the values of these constants yields

$$\frac{2\pi^2me^4}{ch^3} = 109,740 \text{ cm}^{-1},$$

in excellent agreement with the value of  $R_H$  within the limits of error of the experiments. The numerical value of the above factor may be changed slightly by better determinations of  $e$  and  $h$ , but the impetus given to atomic physics by Bohr's original theory cannot be diminished.

In this simple model of the hydrogen atom the nucleus is at the center of the atom, while the electron may be in any one of the circular orbits characterized by the quantum numbers  $n = 1, 2, 3, 4, \dots$ . As long as the electron remains in its orbit no energy is radiated, but whenever an electron jumps from an outer orbit to an inner orbit, energy is radiated in the form of light. A line of the Balmer series corresponds to a jump of the electron from an initial orbit of quantum number  $n$  greater than 2 to the final orbit for which  $n = 2$  (see Figure 103). The red line or  $H_\alpha$  line of the Balmer series corresponds to a transition from orbit of quantum number  $n_i = 3$  to orbit of quantum number  $n_f = 2$ . Any one atom at any instant can emit only one photon of frequency  $\nu$ , but since there are always many atoms in any quantity of hydrogen which is examined spectroscopically, there are always other atoms

which emit photons of different frequencies so that the result is the series of lines actually observed. The relative number of atoms in which the electrons go from a given initial state to a given final

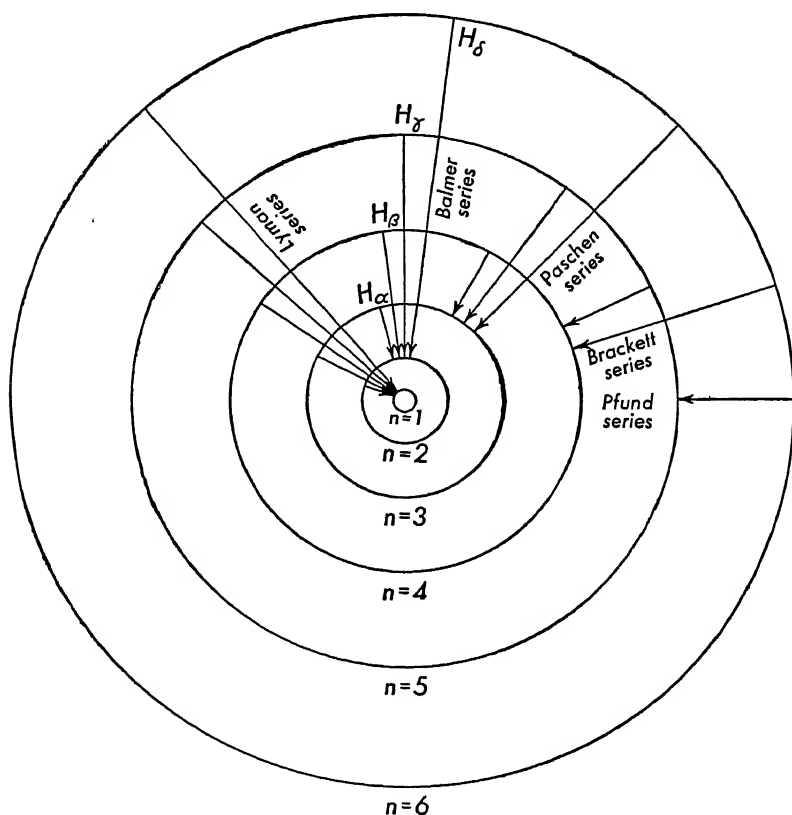


FIG. 103. — Quantum jumps giving rise to the different spectral series of hydrogen.

state determines the relative intensity of the particular spectral line corresponding to this electron transition.

In addition to the Balmer series, other groups or series of spectral lines of hydrogen have been discovered. The Lyman series lies entirely in the ultraviolet region; the wave numbers of the lines of the Lyman series are given by

$$\bar{\nu} = \frac{2\pi^2me^4}{ch^3} \left( \frac{1}{1^2} - \frac{1}{n_i^2} \right), \quad (n_i = 2, 3, 4, \dots),$$

that is, an electronic jump from any outer orbit to the innermost

orbit ( $n_f = 1$ ) gives rise to a line of the Lyman series. When the electron is in the lowest orbit,  $n = 1$ , the hydrogen atom is said to be in its *normal* state. When the electron is in any orbit for which

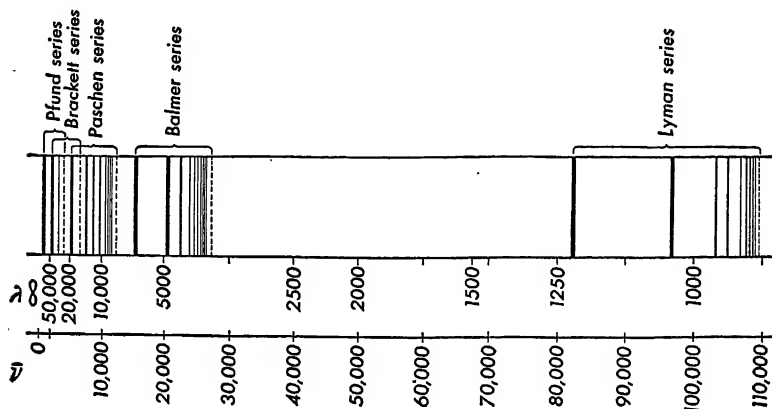


Fig. 104. — Relative positions of the lines of the different spectral series of hydrogen.

the quantum number  $n$  is greater than unity, the hydrogen atom is said to be in an *excited* state.

Three other series of lines are known for hydrogen; these series are all in the infrared region and are known as the Paschen series for which  $n_f = 3$ , the Brackett series for which  $n_f = 4$ , and the Pfund series for which  $n_f = 5$ . The relative positions of these spectral series are shown in Figure 104.

## 77. Motion of the Hydrogen Nucleus

The extraordinary success with which Bohr's simple hydrogen atom model not only explains quantitatively the Balmer series but also predicts the existence of the other spectral series encourages us to proceed with further refinements of the theory. The simplest method is to remove some of the restrictions imposed upon the original model. One such restriction was that the nucleus remained fixed at the center of the circular orbits. This can be true only if the nucleus has infinitely large mass. But if the mass of the nucleus is  $M$ , then both the nucleus and the electron will rotate about a common center of mass with a common angular velocity  $\omega$ . The new axis of rotation is on the line joining the nucleus and the electron, and divides this line in the inverse ratio of their masses.

If  $a$  is the distance of the electron from the axis of rotation and  $A$  the distance of the nucleus from the same axis, Figure 105, then

$$\frac{a}{A} = \frac{M}{m} \quad (17)$$

and

$$r = a + A, \quad (18)$$

from which

$$a = r \frac{M}{M + m} \quad (19)$$

and

$$A = r \frac{m}{M + m}. \quad (20)$$

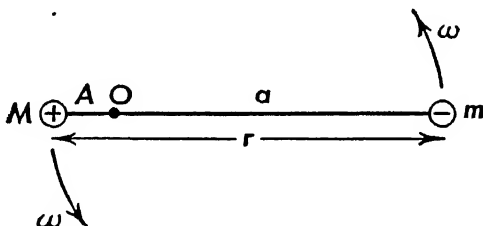


FIG. 105. -- Rotation of the nucleus and electron about a common axis through  $O$ .

Further if  $v$  is the linear velocity of the electron and  $V$  is the linear velocity of the nucleus, then

$$v = a\omega \quad (21)$$

and

$$V = A\omega. \quad (22)$$

The kinetic energy of the system is the sum of the kinetic energies of the electron and the nucleus, or

$$\begin{aligned} K.E. &= \frac{1}{2}MV^2 + \frac{1}{2}mv^2 \\ &= \frac{1}{2}MA^2\omega^2 + \frac{1}{2}ma^2\omega^2. \end{aligned} \quad (23)$$

Substituting the values for  $a$  and  $A$  from equations (19) and (20), we reduce the expression for the kinetic energy of the system to

$$\begin{aligned} K.E. &= \frac{1}{2} \frac{mM}{M+m} r^2 \omega^2 \\ &= \frac{1}{2} \mu r^2 \omega^2, \end{aligned} \quad (24)$$

where

$$\mu = \frac{mM}{M + m} = \frac{m}{1 + \frac{m}{M}}. \quad (25)$$

The expression for the kinetic energy of this system differs from that in which the nucleus was considered at rest in that the quantity  $\mu$  replaces the mass  $m$  of the electron. An examination of equation (25) shows that when  $M = \infty$ ,  $\mu$  is equal to  $m$ ;  $\mu$  is usually referred to as the *reduced* electronic mass. The introduction of the motion of the nucleus into the problem has the effect of replacing the electronic mass  $m$  by the reduced electronic mass  $\mu$  in equations for the energy of the system and hence also in the equation for the frequency of the emitted lines. If the calculations are carried through in detail, the expression for the wave numbers of the spectral lines becomes

$$\bar{\nu} = \frac{2\pi^2 me^4}{ch^3} \frac{1}{1 + \frac{m}{M}} \left( \frac{1}{n_j^2} - \frac{1}{n_i^2} \right) \quad (26)$$

or

$$\bar{\nu} = R \left( \frac{1}{n_j^2} - \frac{1}{n_i^2} \right), \quad (27)$$

where

$$R = \frac{2\pi^2 me^4}{ch^3} \cdot \frac{1}{1 + \frac{m}{M}} = R_\infty \frac{1}{1 + \frac{m}{M}} \quad (28)$$

and

$$R_\infty = \frac{2\pi^2 me^4}{ch^3}. \quad (29)$$

Equation (28) shows that the Rydberg constant is dependent upon the mass of the nucleus. The difference between equations (26) and (16) lies in the correction factor  $\frac{1}{1 + \frac{m}{M}}$ , which, though small,

is not outside the limits of accuracy of spectroscopic experiments. It will be more instructive to rewrite equation (26) to include the atomic number  $Z$  explicitly. Remembering that in equation (3)



the nuclear charge  $E$  was replaced by  $-Ze$ , the factor  $e^4$  should be  $(-Ze)^2e^2$  or  $Z^2e^4$ , so that equation (26) should read

$$\begin{aligned}\bar{\nu} &= Z^2 \cdot \frac{2\pi^2me^4}{ch^3} \cdot \frac{1}{1 + \frac{m}{M}} \left( \frac{1}{n_f^2} - \frac{1}{n_i^2} \right) \\ &= Z^2R \left( \frac{1}{n_f^2} - \frac{1}{n_i^2} \right).\end{aligned}\tag{30}$$

An examination of equation (30) leads to three very interesting conclusions. In the first place, spectral series similar to those of hydrogen should exist for ions which have a hydrogenlike structure, i.e., a nucleus of charge  $-Ze$  and a single external electron. For example, singly ionized helium, He, of nuclear charge  $-2e$  should give a series of spectral lines whose wave numbers are given by the equation

$$\bar{\nu} = 4R \left( \frac{1}{n_f^2} - \frac{1}{n_i^2} \right).$$

Except for the small change in the value of the Rydberg constant due to the difference in the nuclear masses, these wave numbers are four times as large as the wave numbers of the lines in the corresponding series of hydrogen. Such lines have actually been observed in the spectrum of helium. Other hydrogenlike ions whose spectra have been observed are doubly ionized lithium,  $Z = 3$ , and triply ionized beryllium,  $Z = 4$ . The following table shows the dependence of the Rydberg constant on the mass of the nucleus.

TABLE VIII

DEPENDENCE OF RYDBERG CONSTANT ON THE MASS OF THE NUCLEUS	
Hydrogenlike Ion	Rydberg Constant $R$ in $\text{cm}^{-1}$
II	109,677.76
He <sup>+</sup>	109,722.43
Li <sup>++</sup>	109,728.89
Be <sup>+++</sup>	109,730.79

A second interesting conclusion that follows from equation (30)

is that a knowledge of the Rydberg constant for hydrogen and ionized helium can be used to calculate the ratio of the mass of the proton to the mass of the electron. Using the subscripts H and He for the quantities characteristic of hydrogen and ionized helium, we get

$$\frac{R_H}{R_{He}} = \frac{1 + \frac{m}{M_{He}}}{1 + \frac{m}{M_H}}$$

By substituting the value

$$M_{He} = 3.9717M_H$$

obtained from mass spectroscopic data into the above equation as well as the values of  $R_H$  and  $R_{He}$ , we get

$$\frac{M_H}{m} = 1840,$$

in excellent agreement with values determined by other methods (see Chapter 2, § 21).

A third and extremely important conclusion is that even for the same value of  $Z$ , that is, for the same type of atom, there should be lines of slightly different wave numbers for nuclei of different masses. This has led directly to the discovery of the hydrogen isotope of mass number 2, now called *deuterium*. The history of the discovery of deuterium is very interesting. As a result of Aston's very precise measurements of the masses of many isotopes, the relative chemical atomic weights could be computed, taking into consideration the fact that oxygen consisted not only of the isotope of mass number 16 but also of small quantities of mass numbers 17 and 18. The relative chemical atomic weights of hydrogen and oxygen computed by Aston differed by about 2 parts in 10,000 from that determined by direct physical and chemical methods. Birge and Menzel (1931) suggested that this discrepancy could be explained by assuming the existence of two isotopes of hydrogen,  $H^1$  and  $H^2$ , in the ratio of 4500:1.

Urey, Murphy, and Brickwedde (1932) performed a series of experiments on the spectrum of hydrogen to find the isotope  $H^2$ . They used a 21-foot concave diffraction grating and photographed the lines of the Balmer series. The dispersion of the instrument

was  $1.3\text{\AA}$  per mm. They first used ordinary tank hydrogen in the discharge tube and obtained a faint trace of a line slightly displaced from the regular  $H_\beta$  line. On the assumption that this faint line was due to the presence of a small quantity of deuterium in the hydrogen, they decided to prepare samples of hydrogen containing larger concentrations of deuterium and thus increase the relative intensity of this line. To accomplish this, they took liquid hydrogen, allowed most of it to evaporate, and used the small part that remained. In the process of evaporation, the lighter constituent evaporates at a greater rate, leaving the residue with a greater concentration of the heavier constituent. Two different samples were used: (1) the part that remained after the liquid hydrogen evaporated at atmospheric pressure, (2) the part that remained after the liquid hydrogen evaporated at a pressure slightly higher than the triple point pressure. With these samples, the intensity of the displaced line was greatly enhanced, showing that they were now much richer in the isotope  $H^2$ . The results of their experiment on four lines of the Balmer series are given in Table IX.

TABLE IX

SEPARATION OF THE BALMER LINES DUE TO THE TWO ISOTOPES OF HYDROGEN				
Spectrum Lines	$H\alpha^1 - H\alpha^2$	$H\beta^1 - H\beta^2$	$H\gamma^1 - H\gamma^2$	$H\delta^1 - H\delta^2$
Calculated	$1.793\text{\AA}$	$1.326\text{\AA}$	$1.185\text{\AA}$	$1.119\text{\AA}$
Observed using ord. H		1.346	1.206	1.145
Observed using evap. H (1)		1.330	1.199	1.103
Observed using evap. H (2)	1.791	1.313	1.176	1.088

The discovery of deuterium led rapidly to methods for isolating it in comparatively large quantities, enabling scientists to use it in many different fields of investigation in chemistry and biology as well as in physics. In physics, deuterium and the ionized atom known as the *deuteron* have been of inestimable value in the study of atomic nuclei (see Chapter 8).

## 78. Elliptic Orbits for Hydrogen

Bohr's original theory, which dealt only with circular orbits, was extended by Sommerfeld to include elliptic orbits. To accomplish this, Sommerfeld generalized Bohr's first postulate for the determination of the permissible orbits to read

$$\oint p_i dq_i = n_i h, \quad (31)$$

where  $q_i$  is a coordinate which varies periodically,  $p_i$  is the corresponding value of the momentum, and  $n_i$  is an integer. The sym-

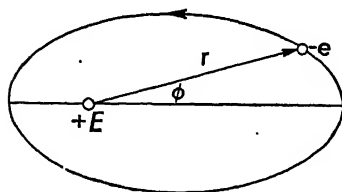


FIG. 106. — Elliptic orbit of the electron in the hydrogen atom.

bol  $\oint$  means that the integration is taken over a whole period of motion. In the case of circular orbits there is only one coordinate which varies periodically, namely the angle  $\phi$  which the radius vector makes with the  $x$  axis. In the case of elliptic motion, not only does the angle  $\phi$  vary, but the

length of the radius vector  $r$  also varies periodically (see Figure 106). The elliptic orbits will therefore be determined by the two quantum conditions

$$\oint p_\phi d\phi = n_\phi h \quad (32)$$

$$\oint p_r dr = n_r h, \quad (33)$$

where  $n_\phi$  is called the *angular* or *azimuthal* quantum number and  $n_r$  is called the *radial* quantum number. Let the origin of coordinates be taken at the nucleus which will be considered fixed, and let the mass of the electron be constant, that is, neglect the relativity variation of mass with velocity. The first integral can be evaluated very easily since the momentum  $p_\phi$  corresponding to the coordinate  $\phi$  is merely the angular momentum,  $p$ , of the electron in the elliptic orbit, and this, from Kepler's law, is a constant [see Appendix VII: equation (6)]. Integrating equation (32) over one period, from 0 to  $2\pi$ , yields

$$\int_0^{2\pi} p_\phi d\phi = n_\phi h$$

or

$$p_\phi = p = \frac{n_\phi h}{2\pi} = \frac{kh}{2\pi}; \quad (34)$$

that is, the angular momentum is always an integral multiple of  $h/2\pi$ ;  $n_\phi$  is now replaced by the letter  $k$  since the latter is more commonly used to denote the azimuthal quantum number.

The second integral, when evaluated (see Appendix IX), yields the equation

$$n_r h = \frac{2\pi p}{(1 - \epsilon^2)^{1/2}} - 2\pi p, \quad (35)$$

where  $\epsilon$  is the eccentricity of the ellipse. Substituting the value for  $p$  from equation (34) yields

$$n_r h = \frac{kh}{(1 - \epsilon^2)^{1/2}} - kh$$

or

$$n_r + k = \frac{k}{(1 - \epsilon^2)^{1/2}}.$$

If we set  
then

$$n = n_r + k, \quad (36)$$

$$1 - \epsilon^2 = \frac{k^2}{n^2}. \quad (37)$$

$n$  is called the principal quantum number. The total energy of the electron in the elliptic orbit depends only on the length of its semimajor axis (see Appendix IX) and is given by

$$\mathcal{E} = - \frac{Ze^2}{2a}. \quad (38)$$

The total energy can also be expressed in terms of the eccentricity (see Appendix IX), as follows:

$$\mathcal{E} = - \frac{mZ^2e^4(1 - \epsilon^2)}{2p^2}. \quad (39)$$

Substituting the values for  $\epsilon$  and  $p$  from equations (37) and (34) respectively, we get

$$\mathcal{E} = - \frac{2\pi^2 m e^4 Z^2}{n^2 h^2}, \quad (40)$$

which is identical with the expression for the energy of the electron in a circular orbit of quantum number  $n$ . The introduction of elliptic orbits does not result in the production of new energy terms; hence no new spectral lines are to be expected because of this *multiplicity* of orbits.

It is interesting to determine the possible electronic orbits for any given principal quantum number  $n$ . The length of the semimajor axis  $a$  is obtained from equations (38) and (40):

$$a = n^2 \frac{h^2}{4\pi^2 m e^2 Z} = n^2 \frac{a_0}{Z}; \quad (41)$$

while the semiminor axis is given by

$$b = a(1 - \epsilon^2)^{1/2}, \quad (42)$$

so that

$$b = nk \frac{a_0}{Z}, \quad (43)$$

where

$$a_0 = \frac{h^2}{4\pi^2 m e^2} = 0.529 \times 10^{-8} \text{ cm}$$

is the radius of the first Bohr orbit. These equations show that the length of the semimajor axis is determined solely by the principal quantum number  $n$ , while the length of the semiminor axis depends upon the azimuthal quantum number  $k$ . For the first orbit corresponding to the lowest energy level or the normal state of hydrogen, the principal quantum number  $n = 1$ . Since the sum of  $n_r$  and  $k$  must be unity, and each must be an integer, when  $n_r = 0$ ,  $k = 1$ , and when  $n_r = 1$ ,  $k = 0$ . On the basis of this theory of the structure of the atom, it was decided that  $k$  can never be zero since that would mean that the ellipse would be reduced to a straight line and that the electron would have to pass through the nucleus twice during every period. The smallest possible value for  $k$  is thus always unity. With  $n = k = 1$ , the first orbit is a circle identical with the first Bohr orbit. With  $n = 2$ ,  $k$  may have the values 1 or 2, so that there are two possible orbits for  $n = 2$ , a circle and an ellipse. Similarly there are three possible orbits for  $n = 3$ , a circle and two ellipses, Figure 107. For ionized helium,  $Z = 2$ , the orbits are similar but the radius of the first orbit is  $a_0/2$ . The orbits for the other hydrogenlike atoms can be constructed in the same manner.

It may at first sight appear strange that with the introduction of two quantizing conditions instead of one, no new energy levels and no new spectral lines are predicted. An examination of these

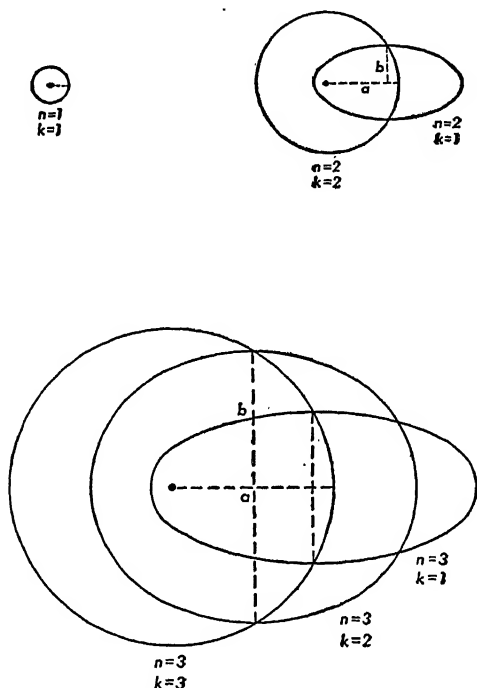


FIG. 107. — Possible electronic orbits for a given total quantum number  $n$ .

two conditions shows, however, that both of them have exactly the same periodicity; that is, as the angle  $\phi$  goes from 0 to  $2\pi$ , the radius vector  $r$  goes from its maximum value through the minimum value and back to its maximum value. A mathematical examination of multiply periodic systems shows that whenever the ratio of two of the periods of such a system is a rational number, the two quantum conditions degenerate into a single quantum condition. But if the ratio of the two periods is an irrational number, that is, if the two periods are incommensurable, then there will be two independent quantum conditions. In general, there will be as many independent quantum conditions of the form

$$\oint p_i dq_i = n_i h$$

as there are incommensurable periods in the motion. In such

cases the system is referred to as a nondegenerate system. One method for removing this degeneracy in the case of the elliptic motion of the electron in hydrogen, is to take into consideration the relativity change of mass as the velocity of the electron in its orbit changes. Sommerfeld has carried out this calculation and has shown that the path of an electron is a rosette, Figure 108, which may be considered as an ellipse whose major axis precesses

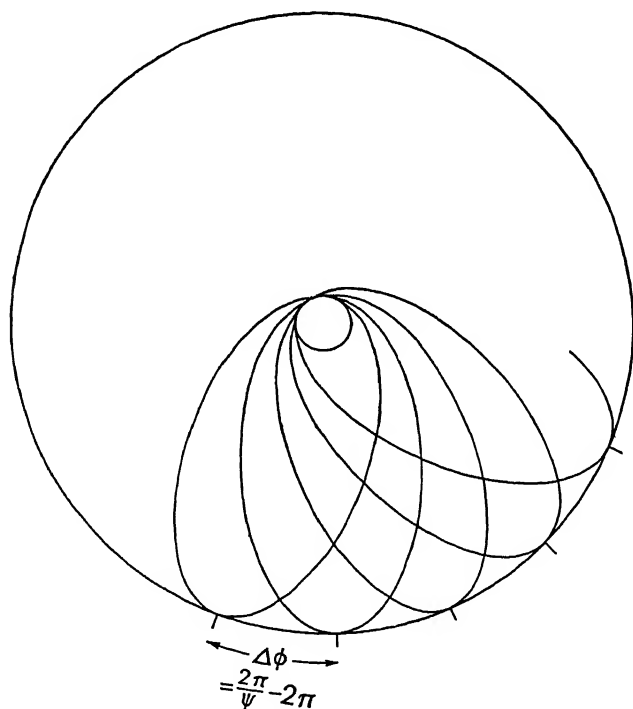


FIG. 108. — Rosette figure of electron path when the relativity correction is taken into consideration.

slowly in the plane of the ellipse about an axis through one of the foci. The equation of the path of the electron is

$$\frac{1}{r} = \frac{1 + \epsilon \cos \psi \phi}{a(1 - \epsilon^2)}$$

which differs from that of an ellipse in that the angle  $\phi$  is replaced by the angle  $\psi\phi$ , where  $\psi$  is a number less than unity and is given by

$$\psi^2 = 1 - \frac{Z^2 e^4}{c^2 p^2}.$$



When the angle  $\phi$  is increased by  $2\pi$ ,  $r$  does not return to its original value but reaches it only after the angle  $\psi\phi$  has been increased by  $2\pi$ , or when  $\phi$  has been increased by the angle  $2\pi/\psi$ . Hence the radius vector  $r$  returns to its original value only after the axis of the ellipse has precessed through an angle

$$\Delta\phi = \frac{2\pi}{\psi} - 2\pi.$$

The effect of the relativity correction on the expression for the total energy of the orbit is to introduce an additional term in equation (40). This additional term is

$$\Delta\mathcal{E} = -\frac{2\pi^2 me^4}{h^2} Z^4 \alpha^2 \left( \frac{n}{k} - \frac{3}{4} \right) \frac{1}{n^4},$$

where

$$\alpha = \frac{2\pi e^2}{ch} = 7.284 \times 10^{-3} \doteq \frac{1}{137}$$

is known as the Sommerfeld *fine structure* constant. This term shows that the energy does depend upon the azimuthal quantum number  $k$  which has the effect of splitting up the energy level into  $n$  terms very close together. The energy of the first orbit,  $n = 1$ , can have only one possible value since  $k = 1$ , or there is only one energy level for  $n = 1$ . For principal quantum number  $n = 2$ , the energy can have two possible values corresponding to the two values of  $k$ , 1 and 2; that is, there are two energy levels for  $n = 2$ . Similarly there are three possible energy values or energy levels for  $n = 3$ , and so on. For the first line of the Balmer series, corresponding to the change in the principal quantum numbers  $n_i = 3$  to  $n_f = 2$ , there are six possible transitions for the different values of  $k$ . This means that, with a spectroscope of very high resolving power, the  $H_\alpha$  line should appear to consist of six lines very close together. Actually the  $H_\alpha$  line has fewer components. To make experiment and theory agree, some of the transitions have to be ruled out by some *selection* principle. The selection principle chosen is that the azimuthal quantum number  $k$  can change only by  $+1$  or  $-1$  or, expressed in mathematical form,

$$\Delta k = \pm 1.$$

The application of this selection rule to the Balmer series shows that each line should consist of three components; similarly, each

line of the Paschen series should consist of five components, while the lines of the Lyman series should all be single lines. The fine structure of the Balmer lines and some of the lines of ionized helium have been carefully studied but the agreement with the theoretical predictions is not very good. Most of these discrepancies were later removed by the introduction of the hypothesis of electron spin (see Chapter 6). Further discussion of the fine structure of spectral lines will be postponed until the subject of electron spin has been considered.

## 79. Energy Level Diagram for Hydrogen

The results of the discussion of the spectrum of hydrogen can be presented in graphical form by means of an energy level diagram which makes use of the fact that the wave number of any spectral line is the difference between two terms which represent the energies of the initial and final states of the atom. The energy level diagram for hydrogen, neglecting fine structure, is shown in Figure 109. The energy levels are drawn as horizontal lines and the wave number scale, in  $\text{cm}^{-1}$ , is shown in the figure. The lowest energy level corresponds to the normal state of hydrogen. Transitions to this level from any higher level give rise to the Lyman series of lines. The origins of the other spectral lines are indicated in the figure. It will be noted that the energy levels crowd together as the principal quantum numbers get large, since each term is of the form

$$T = \frac{R}{n^2}.$$

From this it follows that the lines of a spectral series will converge toward the series limit.

Transitions from higher to lower energy levels can occur spontaneously. In order to get into one of these higher energy states, the atom must be *excited* by some external agency. Such excitation may take place because of the transfer of energy during collisions between atoms in a gas at high temperature. Atoms may also be raised from the normal to the excited states by impact with electrons having the right amount of kinetic energy. A simplified experimental arrangement for producing collisions between electrons and hydrogen atoms is shown in Figure 110. The tube contains hydrogen at low pressure. Electrons liberated from the hot

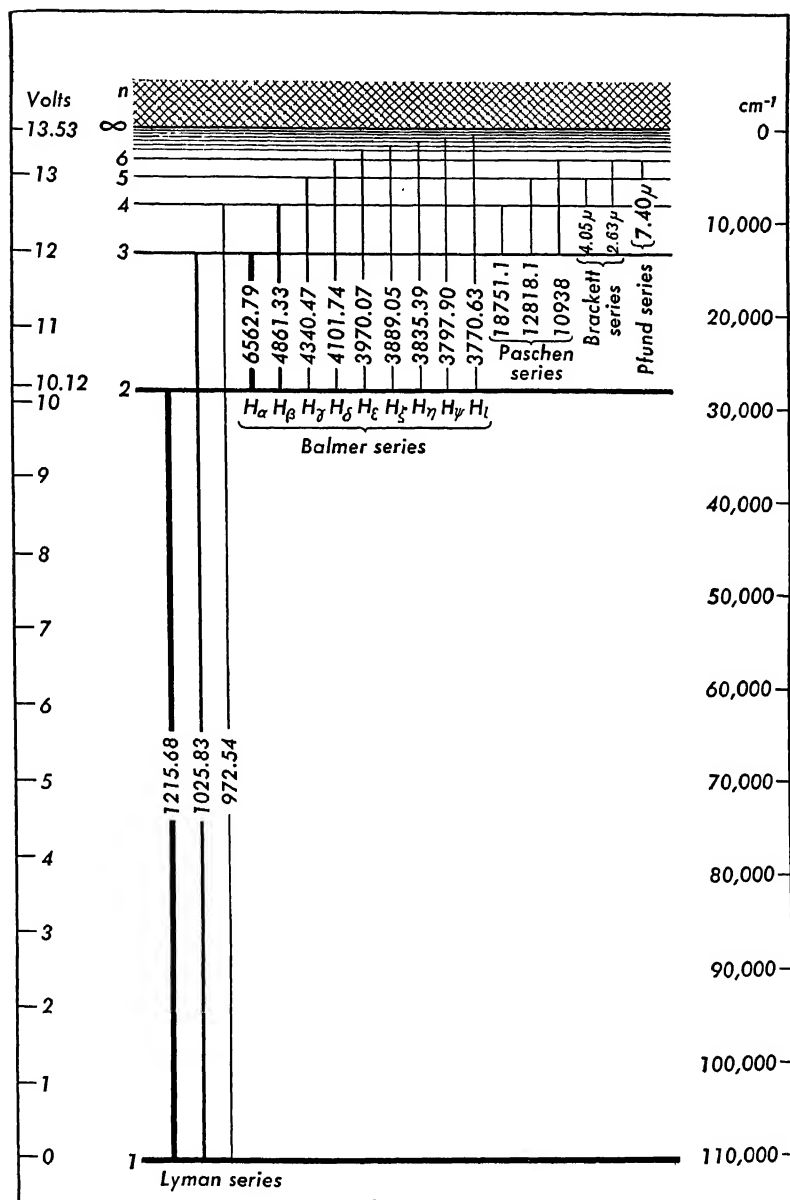


FIG. 109. — Energy level diagram for hydrogen. Wave lengths of the lines of the Lyman, Balmer, and Paschen series are given in Å.

filament  $F$  are accelerated toward the grid  $G$  by a difference of potential  $V$ . When they enter the region between the grid  $G$  and

the plate  $P$ , these electrons will have an amount of energy equal to  $Ve = \frac{1}{2}mv^2$ . If these electrons suffer no energy loss on collision, they will travel to the plate and be registered by the galvanometer.

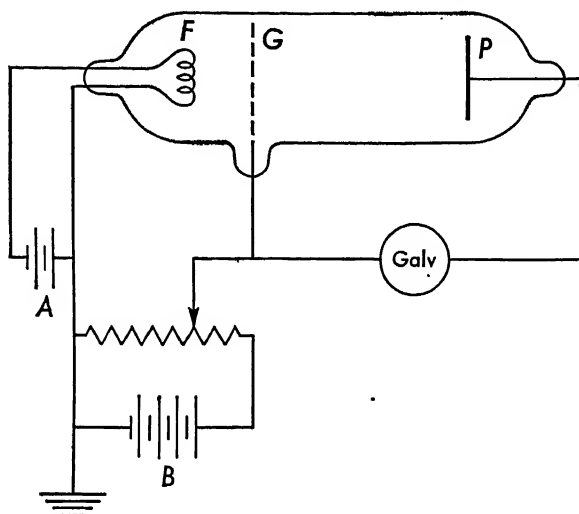


FIG. 110. — Method of determining the ionization potential of hydrogen.

As the voltage is increased, the current to the plate will be increased until the energy of the electrons is just the right amount to raise the hydrogen atom from the normal state to one of its excited states. When this value is reached there will be a drop in the current to the plate indicating that many electrons have given up their energy to hydrogen atoms to raise them to an excited state. As the voltage is increased still further, a point will be reached at which ionization of the gas will set in, resulting in a very large increase in the current through the tube. At this value of the voltage, known as the ionization potential, the electrons from the filament have just sufficient energy to ionize the hydrogen atom; that is, to remove the electron from the lowest orbit of hydrogen,  $n = 1$ , to  $n = \infty$ , i.e., outside the atom. The numerical value of this ionization potential can be computed from the values of the two energy levels  $\mathcal{E}_\infty$  and  $\mathcal{E}_1$ , and is

$$V = 13.53 \text{ volts.}$$

The value of the ionization potential determined empirically is 13.54 volts, in good agreement with the Bohr theory.

In the energy level diagram a shaded region of continuous energy values is shown extending beyond the last quantized orbit,  $n = \infty$ . This corresponds to the fact that the electrons which are knocked out of the hydrogen atom have kinetic energies representing the differences between the ionization energy and the energies of the incident electrons. The electrons outside the hydrogen orbits are not subject to quantum conditions since their motion is not periodic. The kinetic energies of these electrons may have any values whatever. When an electron in the neighborhood of a hydrogen ion falls into one of its orbits, the system will radiate energy. If the initial kinetic energy of the electron is zero, and it falls into orbit  $n = 2$ , the system will radiate an amount of energy corresponding to the limit of the Balmer series. If the initial kinetic energy of the electron is greater than zero, then when it falls into orbit  $n = 2$ , the system will radiate a greater amount of energy. The frequency of this radiation will be greater than the frequency of the series limit. Since the initial kinetic energy can have any value whatever, a *continuous* spectrum should appear at the end of the Balmer series beginning at the position of the series limit. The continuous spectrum at the end of the Balmer series has actually been observed.

Another important method of raising the hydrogen atom from the normal to one of its excited states is through the absorption of light. If the incident light contains one of the wave lengths of the Lyman series, say  $1025.8\text{\AA}$ , then those atoms which absorb this light will be raised from energy level  $n = 1$  to the higher energy level  $n = 3$ . The atoms in this higher state can return to the normal state by the emission of radiation either in a single step with the emission of the same wave length, or in two successive stages, from  $n = 3$  to  $n = 2$ , and then from  $n = 2$  to  $n = 1$ . In the latter case two lines will be emitted, the  $H_{\alpha}$  line of the Balmer series and the first line of the Lyman series,  $\lambda = 1215.7\text{\AA}$ . *Fluorescent radiation* is the name given to the light emitted by atoms which have been excited by the absorption of light.

The hydrogen atom may be ionized by the absorption of light of frequency greater than that of the Lyman series limit, i.e., of wave number greater than  $R_H$ . The kinetic energy of the electron knocked out of the hydrogen atom will then be the difference between the energy of the incident radiation and the energy of the

hydrogen atom in the normal state, or

$$\frac{1}{2}mv^2 = h\nu - h\nu_L.$$

But this is Einstein's photoelectric equation in which  $\nu_L$  is the frequency of the Lyman series limit, and  $\nu$  is the frequency of the incident radiation.

The energy level diagram of hydrogen can be used in the discussion of hydrogenlike atoms by merely changing the scale, since the energy terms differ only by the factor  $Z^2$ , neglecting relativity terms.

## 80. De Broglie's Hypothesis and the Quantization of Orbits

The older quantum theory sketched in the preceding sections, while very successful when applied to the hydrogen problem, could only be applied either in a semiempirical or in a qualitative manner to other problems in atomic physics. Schrödinger's wave mechanics, based upon de Broglie's hypothesis, has been much more successful in obtaining rigorous mathematical solutions for many of these problems. It is interesting to see how Bohr's quantization hypothesis comes out of this new theory and what the modern picture of the hydrogen atom is.

On de Broglie's hypothesis, the wave length associated with an electron is given by

$$\lambda = \frac{h}{mv}.$$

Instead of an electron moving in a stationary orbit, we must now think of a series of waves moving in this orbit. In order that the waves should not cancel one another by interference, they must move in such a manner as to produce a stationary or standing wave in the orbit. The necessary condition that must be fulfilled is that the length of path should be a whole multiple of the wave length. Or stated mathematically,

$$2\pi r = n\lambda$$

where  $n$  is a whole number and  $r$  is the radius of the orbit. Substituting the value for  $\lambda$ , we get

$$2\pi r = \frac{nh}{mv}$$

or

$$mvr = \frac{nh}{2\pi},$$

which is identical with Bohr's quantization hypothesis.

## 81. Application of Wave Mechanics to the Hydrogen Problem

In wave mechanics, Schrödinger's equation is used as the basic dynamical equation and in the case of the hydrogen problem, this equation and the appropriate restrictive conditions replace all of Bohr's postulates. In this problem an electron of charge  $e$  is at a distance  $r$  from a nucleus of charge  $E = -Ze$  so that the potential energy of the electron with respect to the nucleus is

$$V = -\frac{Ze^2}{r}.$$

With this value of the potential energy substituted in Schrödinger's equation (Chap. 4, § 73), it becomes more convenient to use spherical coordinates  $(r, \theta, \phi)$  instead of Cartesian coordinates  $(x, y, z)$ . There is a regular formal procedure for solving such second-order partial differential equations (see references at end of chapter). In the solution of this equation, wave functions  $u$  are sought subject to the restrictive conditions that they must be everywhere finite, single-valued, and continuous, with continuous first derivatives. It is found that solutions satisfying the above conditions exist for all positive values of the total energy  $\mathcal{E}$ , and for those negative values of the total energy which satisfy the condition that

$$\mathcal{E} = -\frac{2\pi^2 me^4 Z^2}{n^2 h^2}$$

where  $n$  is a positive integer. The above equation is identical with the expression for the energy of a stationary state characterized by the principal quantum number  $n$  in the Bohr theory. It must be remarked that no additional hypotheses or assumptions are introduced in the solution of Schrödinger's equation. The fact that certain quantities restricted to integral values appear as the result of solutions of partial differential equations is not new in mathematical physics. The solutions of the differential equations

governing the vibrations of strings and membranes, particularly those involving stationary modes of vibration, are solutions in which integers play a very important part. For example, a string fixed at both ends can have stationary modes of vibration set up in it only when the length of the string is an integral multiple of  $\lambda/2$ , where  $\lambda$  is the length of the wave traveling along the string. Thus, in the new wave mechanics, the quantum number  $n$  appears naturally as the result of the solution of a fundamental equation, although Bohr introduced it without any apparent reason, except that it did predict the correct values for the frequencies of the spectral lines of hydrogen.

The complete solution of Schrödinger's equation introduces not just the single integer  $n$ , but three integers usually denoted by the letters  $n$ ,  $l$ , and  $m$ . (The letter  $m$  is not to be confused with the mass of the electron.) While the quantum number  $n$  may have any integral value, the quantum numbers  $l$  and  $m$  are restricted in values by the conditions of the problem. The quantum number  $l$  may have the values

$$l = 0, 1, 2, \dots (n - 1).$$

By comparing these values with the values of the azimuthal quantum number  $k$  of the older theory, it is seen that  $l$  may be identified with  $k - 1$ . The quantum number  $m$  may take all integral values from  $-l$  through 0, to  $+l$ ; that is, it can have  $2l + 1$  values. For example, for  $l = 2$ ,  $m$  may have the values  $-2, -1, 0, +1, +2$ . The quantum number  $m$  is usually called the magnetic quantum number; it will be considered in greater detail in the next chapter.

The wave function  $u$  is, of course, dependent upon the values assigned to the quantum numbers  $n$ ,  $l$ , and  $m$ . The functions which satisfy Schrödinger's equation for the discrete energy states are usually called proper functions. While no immediate physical significance can be attached to these proper functions, it will be recalled that  $u^2 dv$  can be interpreted as the probability of finding the electron in the volume element  $dv$ . Of greater interest is the probability of finding the electron at a given distance  $r$  from the nucleus. If  $u^2$  is multiplied by the surface area of a sphere,  $4\pi r^2$ , then the term  $4\pi r^2 u^2 dr$  represents the probability of finding the electron within a spherical shell of radius  $r$  and thickness  $dr$ . In



Figure 111,  $r^2u^2$  is plotted against the distance  $r$  for quantum numbers  $n = 1, l = 0$ ;  $n = 2, l = 1$ ;  $n = 3, l = 2$ . These quantum numbers correspond to those representing the circular orbits in Bohr's

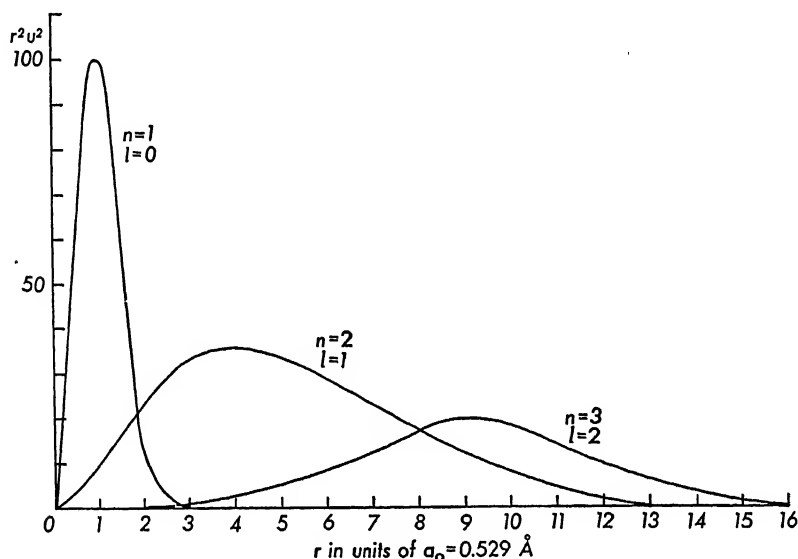


FIG. 111. — Curves showing the probability of finding the electron in the hydrogen atom within a spherical shell of radius  $r$  and thickness  $dr$  for some values of  $n$  and  $l$ .

theory. From the figure, it is seen that the probability of finding the electron at any distance from the nucleus has a maximum at the distance equal to the radius of the corresponding Bohr orbit.

The picture of the hydrogen atom from the standpoint of wave mechanics can be presented in another manner. The term  $eu^2dv$ , where  $e$  is the electronic charge, represents the probability of finding the electric charge in the volume element  $dv$ . This is sometimes called the density distribution of the electric charge in the atom or the *electronic cloud* around the nucleus. It must not be assumed that the electronic charge is smeared out over the atom, although calculations based on this assumption lead to correct results. The density at any point in the electronic cloud represents the probability of finding the electron in the particular volume element in the neighborhood of that point.

It may be argued that Bohr's simple picture of the hydrogen atom has been given up for a somewhat nebulous picture of the atom without gaining anything thereby. However, many things

which were inexplicable on Bohr's theory come naturally out of further refinements of wave mechanics. For example, Bohr had to postulate that an atom in a stationary state should not radiate, contrary to classical electrodynamics. In the wave mechanical theory of radiation, it is shown, in a manner analogous to the classical theory, that an atom in a stationary state will not radiate energy because the radiations from the different parts of the electronic cloud will cancel each other by interference. Further, it is shown that only those frequencies will occur in the spectrum of the atom which are formed by the differences in the frequencies of two atomic states. This leads directly to Bohr's frequency condition,

$$\nu = \frac{\mathcal{E}_i - \mathcal{E}_f}{h}.$$

Another important contribution is the calculation of the intensity of a spectral line. A surprising result of this calculation is the prediction that the most intense lines will be those for which the changes in the quantum numbers  $l$  and  $m$  obey the rules that

$$\Delta l = \pm 1$$

and

$$\Delta m = 0, \text{ or } \pm 1.$$

These selection rules apply not only to the hydrogen type of atom but to other atoms in which a single electron is responsible for the changes in the atomic energy states. There are no selection rules for the quantum number  $n$ .

## REFERENCES

- BORN, M., *Atomic Physics*. New York: G. E. Stechert & Company, 1936, Chap. V.
- HERZBERG, G., *Atomic Spectra and Atomic Structure*. New York: Prentice-Hall, Inc., 1937, Chap. I.
- RICHTMYER, F. K., and E. H. KENNARD, *Introduction to Atomic Physics*. New York: McGraw-Hill Book Company, Inc., 1942, Chap. VI.
- Solutions of Schrödinger's equation*
- BORN, M., *Atomic Physics*. New York: G. E. Stechert & Company, 1936, Appendix XVII.
- CONDON, E. U., and P. M. MORSE, *Quantum Mechanics*. New York: McGraw-Hill Book Company, Inc., 1929, Sections 16–20.

## PROBLEMS

1. Discuss the relationship between the frequency of rotation of the electron in the circular Bohr orbits and the frequency of the radiation emitted when the quantum number changes by unity. Show that for very large quantum numbers, the frequency of rotation of the electron and the frequency of the radiation emitted when the quantum number changes by unity approaches the value  $\nu = 2cR/n^3$ .

2. Derive an expression for the total energy of the hydrogen atom, taking into consideration the motion of the nucleus. Using this expression for the energy, derive equation (26) for the frequency of the emitted radiation.

3. Using the data from Table VIII, plot a curve showing the dependence of Rydberg's constant on the nuclear mass. Determine the value of  $R_\infty$  from this curve.

4. Assuming that an amount of hydrogen of mass number three sufficient for spectroscopic examination can be put into a tube containing ordinary hydrogen, determine the separation of the  $H_\alpha$  lines that should be observed.

$$\text{Ans. } \Delta\lambda = 2.38\text{\AA}.$$

5. (a) Draw an energy level diagram for the energy levels characterized by the principal quantum numbers  $n = 2$  and  $n = 3$ , taking the relativity corrections into consideration. Show the transitions permitted by the selection rule. (b) Draw a diagram showing the positions of these lines relative to the position of the line predicted without relativity correction.

# 6 Atomic Spectra and Electron Distribution

## 82. Introduction

The study of atomic spectra has yielded invaluable information concerning the arrangement and distribution of the electrons within the atom. Most of the principles and rules used in spectroscopy have been obtained empirically, but within the past few years, with the development of wave mechanics, many of them have been placed on a good theoretical foundation. One of the most important of these principles is Bohr's frequency condition, which states that the frequency of any line of the spectrum is proportional to the difference between the values of the energies of two states of the atom emitting the radiation; that is

$$\nu = \frac{\mathcal{E}_i - \mathcal{E}_f}{h}, \quad (1)$$

where  $\nu$  is the frequency of the emitted radiation,  $\mathcal{E}_i$  is the energy of the initial state of the atom,  $\mathcal{E}_f$  is the energy of the final state of the atom, and  $h$  is the Planck constant. Expressed in terms of the corresponding wave number  $\bar{\nu}$ , this equation becomes

$$\bar{\nu} = \frac{\mathcal{E}_i}{ch} - \frac{\mathcal{E}_f}{ch}, \quad (2)$$

where  $c$  is the velocity of light. Equation (2) shows that the wave number of any spectral line can be expressed as the difference between two terms:

$$\bar{\nu} = T_i - T_f, \quad (3)$$

where each term,  $T$ , expressed in wave numbers, represents an atomic energy state or energy level.

Atomic spectra can be grouped in two general classifications: (1) optical spectra and (2) X-ray spectra. For any given element, the wave numbers of the lines in the X-ray spectra are much greater than those in the optical spectra. From this it can be in-

ferred that the difference in energies between two states of an atom which emits an X-ray spectral line is very large and that the energy values of these atomic states are also very large. The wave numbers of the lines of the optical spectra are comparatively small. It will be shown not only that the difference between two atomic energy states is small, but that the energies of the atomic states giving rise to these optical lines are also small. In general, the optical spectrum of any given element is much more complex than the X-ray spectrum of the same element. In this chapter, a few typical optical and X-ray spectra will be considered, together with the relationship of these spectra to the extranuclear structure of the atom.

### 83. Optical Spectral Series

A great deal of work had been done in analyzing optical spectra in the century preceding the publication of Bohr's theory of hydrogen. The spectral lines of an element had been arranged in several *series*, and as aids in selecting lines belonging to the same series, various types of evidence were used such as (1) the physical appearance of the lines, whether "sharp" or "diffuse," (2) the methods used in producing the spectra, whether with the aid of an arc or a spark, and (3) the behavior of the lines when the emitting atoms were subjected to external electric and magnetic fields, e.g., the Zeeman effect.

Rydberg (1889) suggested that the optical series then known could be arranged in such a way that the wave number of any line in the series would be given by the difference between two terms as follows

$$\bar{\nu} = \bar{\nu}_{\infty} - \frac{RZ^2}{(n + \phi)^2}, \quad (4)$$

in which  $R$  is Rydberg's constant,  $n$  is an integer and  $\phi$  is a fraction less than unity which is practically constant for all lines of the series. The series approaches a limit for very large values of  $n$ ; the term  $\bar{\nu}_{\infty}$  is the wave number approached by the series in the limit as  $n$  approaches infinity.  $Z$  has the value unity for series due to neutral atoms, the value two for singly charged ions, three for doubly charged ions, and so on. The similarity between Rydberg's formula and Bohr's frequency condition is obvious. In

each case the wave number of a line of a spectral series is given as the difference between a fixed term and a variable term. The fixed term is the wave number of the series limit represented by either  $\bar{\nu}_\infty$  or  $T_i$ . The variable term assumes different values by assigning different integral values to  $n$ .

Of the several series of spectral lines from any one element, the most intense are the principal series, the sharp series, the diffuse series, and the fundamental or Bergmann series. In terms of Rydberg's formula, these series are represented by the following equations:

principal series

$$\bar{\nu} = P_\infty - \frac{R}{(n + P)^2} \quad (n = 2, 3, 4, \dots);$$

sharp series

$$\bar{\nu} = S_\infty - \frac{R}{(n + S)^2} \quad (n = 2, 3, 4, \dots);$$

diffuse series

$$\bar{\nu} = D_\infty - \frac{R}{(n + D)^2} \quad (n = 3, 4, 5, \dots); \quad (5)$$

fundamental series

$$\bar{\nu} = F_\infty - \frac{R}{(n + F)^2} \quad (n = 4, 5, 6, \dots).$$

The fixed term  $\bar{\nu}_\infty$  is replaced by  $P_\infty$ ,  $S_\infty$ ,  $D_\infty$ , or  $F_\infty$ , and the constant  $\phi$  in the variable term is replaced by  $P$ ,  $S$ ,  $D$ , or  $F$  in Rydberg's formula. The constants  $P$ ,  $S$ ,  $D$ , and  $F$  all have different values. It has been found empirically that the fixed terms have the following values:

$$P_\infty = \frac{R}{(1 + S)^2};$$

$$S_\infty = \frac{R}{(2 + P)^2};$$

$$D_\infty = \frac{R}{(2 + P)^2};$$

and

$$F_\infty = \frac{R}{(3 + D)^2}.$$

It will be noticed that the sharp and diffuse series both have the same series limit. A shorthand notation is frequently used in writing the equations for the different series. This is done by using the letters which appear in the denominator of the particular term to represent the term. Thus  $nP$  is written as an abbreviation of the term  $\frac{R}{(n+P)^2}$ ,  $nS$  for  $\frac{R}{(n+S)^2}$ ,  $nD$  for  $\frac{R}{(n+D)^2}$  and so on. In this notation, the lines of the different series are written as follows:

principal series

$$\bar{\nu} = 1S - nP \quad (n = 2, 3, 4, 5, \dots);$$

sharp series

$$\bar{\nu} = 2P - nS \quad (n = 2, 3, 4, 5, \dots);$$

diffuse series

$$\bar{\nu} = 2P - nD \quad (n = 3, 4, 5, 6, \dots); \quad (6)$$

fundamental series

$$\bar{\nu} = 3D - nF \quad (n = 4, 5, 6, 7, \dots).$$

From the analyses of their spectra, term values have been computed for many of the energy states of all the elements. While the wave number of any line can be expressed as the difference between two terms, the converse is not always true; that is, not all the differences that can be formed between the term values of an atom represent spectral lines. In order to account for the non-appearance of certain lines, selection rules are necessary. Such selection rules, originally formulated empirically, can be derived by means of wave mechanics. They are best stated in terms of possible changes in quantum numbers intimately related to the structure of the atom. The simplest formulation is in terms of an atom model, the so-called *vector model* of the atom. Many other points, such as the fine structure of some spectral lines, and the Zeeman effect, are best explained with the aid of this vector model.

## 84. Vector Model of the Atom: Orbital Angular Momentum

It will be recalled that in Bohr's theory of the hydrogen atom, the electron was assumed to be moving in a circular orbit with

angular velocity  $\omega$ . Angular velocity is a vector quantity and is represented by a vector along the axis of rotation, perpendicular to the plane of the orbit. Because of this angular velocity, the electron has a definite angular momentum,  $p_\phi$ , which, on Bohr's theory, was a whole multiple of  $h/2\pi$  represented by  $k \frac{h}{2\pi}$ , where  $k$  is the azimuthal quantum number. In the vector model of the atom, the quantum number  $k$  is replaced by the quantum number  $l$ , and the electron is assigned the orbital angular momentum

$$p_\phi = l \frac{h}{2\pi}. \quad (7)$$

Of course, angular momentum is also a vector quantity and is represented by a vector along the axis of rotation. If the unit of angular momentum is chosen as  $h/2\pi$ , then the angular momentum vector will be  $l$  units long. It will be convenient to use  $l$  to represent the orbital angular momentum. It must be remarked here, however, that wave mechanics shows that the magnitude of the angular momentum of an electron has the value

$$\sqrt{l(l+1)} \frac{h}{2\pi}. \quad (8)$$

While it will be more convenient in the discussion of the vector model of the atom to use the vector  $l$ , in any calculations that have to be made, its magnitude  $l$  will be replaced by the correct value  $\sqrt{l(l+1)}$ . It will be recalled that  $l$  can have the values 0, 1, 2,  $\dots$  ( $n-1$ ), where  $n$  is the principal quantum number.

In considering the more complex atoms, each electron outside the nucleus is assigned an orbital angular momentum as well as a principal quantum number  $n$ . The total orbital angular momentum of the atom, denoted by the letter  $L$ , is the vector sum of the orbital angular momenta of the individual electrons. However, this vector sum,  $L$ , is restricted by quantum conditions to integral values. For example, in the case of two electrons for which  $l = 2$  and  $l = 1$ , the sum  $L$  may have any one of the three values 3, 2, or 1. The method of adding these vectors is shown in Figure 112.

## 85. Electron Spin

In order to account for the fine structure of the lines in the spectral series of some of the elements and also to account for the



anomalous Zeeman effect, Uhlenbeck and Goudsmit (1925) introduced the hypothesis that the electron rotates or spins about an axis just like a top. The angular momentum of the electron due to its spin,  $p_s$ , is assigned the value

$$p_s = s \frac{h}{2\pi}, \quad (9)$$

where  $s$  has the value  $\frac{1}{2}$ . Vectorially this can be represented by  $\mathbf{s}$  of

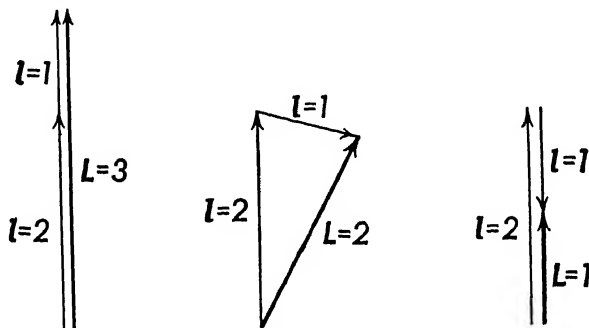


FIG. 112. — Method of addition of angular momentum vectors.

length  $\frac{1}{2}$  in units of  $h/2\pi$ . Again it must be noted that, according to wave mechanics, the magnitude of  $\mathbf{s}$  is  $\sqrt{s(s+1)}$  rather than  $s$ ; that is,  $\sqrt{3}/2$  rather than  $\frac{1}{2}$ . In the vector treatment of the atom,

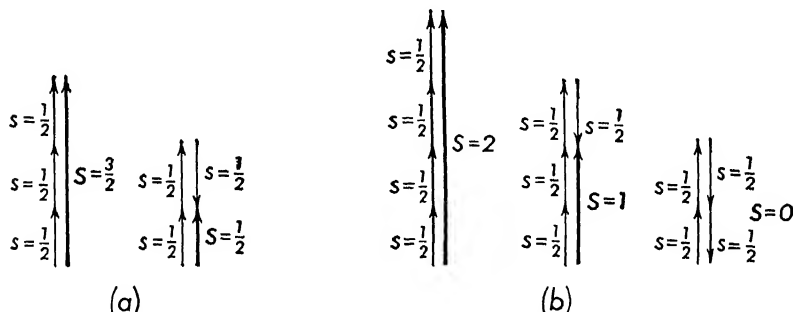


FIG. 113. — Addition of electron spin vectors (a) for three electrons, (b) for four electrons.

the *spin quantum number*  $s$  will be used, but in actual calculation its wave mechanics value will be substituted.

The vector sum,  $\mathbf{S}$ , of the angular momenta of several electrons is subject to the following restrictions: for an odd number of electrons,  $\mathbf{S}$  must be an odd multiple of  $\frac{1}{2}$ ; for an even number of elec-

trons,  $S$  must be an integer. This means that the vectors representing the spin must always be parallel or antiparallel, i.e., oppositely directed. This is shown in two typical cases in Figure 113, one for three electrons for which  $S$  can have the values  $\frac{1}{2}$  or  $\frac{3}{2}$ , the other for four electrons for which  $S$  can have the values 0, 1, or 2.

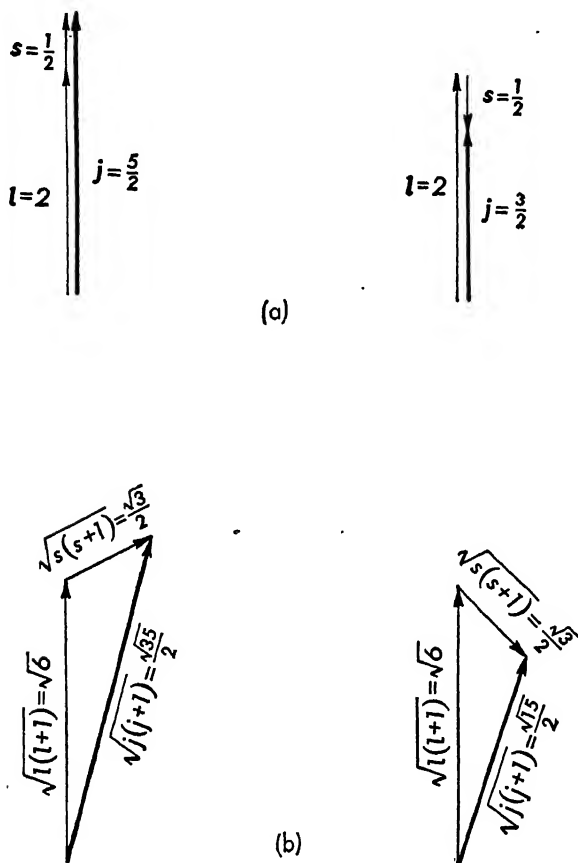


FIG. 114. — (a) Addition of the vectors  $l$  and  $s$  to form  $j$  according to the vector model. (b) Addition of the vectors  $l$  and  $s$  to form  $j$  according to wave mechanics.

## 86. Total Angular Momentum Vector

In many cases, for example in the alkali elements, the changes in the atomic configuration giving rise to the optical spectrum are produced by the motion of a single electron. The total angular

momentum of a single electron is the vector sum of the orbital and spin angular momenta of the single electron. The total angular momentum is given by  $j \frac{h}{2\pi}$  where  $j$  is the total angular momentum quantum number. The vector  $j$ , representing the total angular momentum, is defined by the equation

$$j = l + s, \quad (10)$$

with the restriction that the vector sum must always be an odd multiple of  $\frac{1}{2}$ . Since  $s$  is always equal to  $\frac{1}{2}$ ,  $j$  can have only two values for a given value of  $l$ , namely  $l + \frac{1}{2}$  and  $l - \frac{1}{2}$  except when  $l = 0$ , in which case  $j$  can have the value  $\frac{1}{2}$  only. Thus for  $l = 2$  and  $s = \frac{1}{2}$ , see Figure 114(a),  $j$  can have the values  $\frac{5}{2}$  and  $\frac{3}{2}$ .

Again it must be remarked that, from wave mechanical considerations, the magnitude of the vector  $j$  should be  $\sqrt{j(j+1)}$ . In the addition of vectors  $l$  and  $s$  to form the vector  $j$ , the magnitude of  $l$  is taken as  $\sqrt{l(l+1)}$ , and that of  $s$  is taken as  $\sqrt{s(s+1)}$ . The numerical values of  $l$ ,  $s$ , and  $j$  which are needed for determining the wave mechanical values of the corresponding vectors are the values obtained from the vector model of the atom. The angle between the vectors  $l$  and  $s$  in Figure 114(b) can be obtained from the figure with the aid of the cosine law, yielding

$$\cos(s, l) = \frac{j(j+1) - l(l+1) - s(s+1)}{2\sqrt{s(s+1)}\sqrt{l(l+1)}}. \quad (11)$$

If the changes in atomic states are produced by the action of two or more electrons, then the value of the total angular momentum of these electrons, denoted by  $J$ , will depend upon the interaction or the coupling between the orbital and the spin angular momenta. Experience has shown that the type of coupling which occurs most frequently is the Russell-Saunders or  $L$ - $S$  type of coupling. In this type of coupling all the orbital angular momentum vectors of the electrons combine to form a resultant  $L$ , and independently all their spin angular momentum vectors combine to form a resultant  $S$ . The total angular momentum of the atom is then given by the relation

$$J = L + S, \quad (12)$$

with the restriction that  $J$  must be an integer if  $S$  is an integer,

and  $J$  must be an odd multiple of  $\frac{1}{2}$  if  $S$  is an odd multiple of  $\frac{1}{2}$ . This type of coupling is illustrated in Figure 115 for  $L = 2, S = 1$ , and  $L = 2, S = \frac{3}{2}$ . It can be seen from the figure that the num-

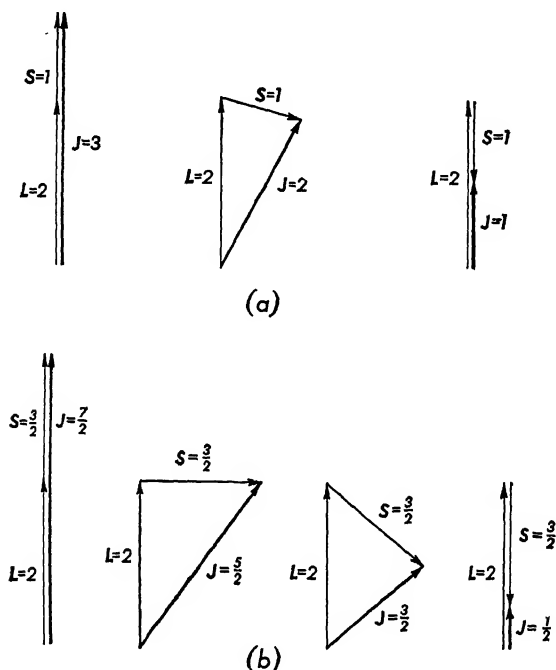


FIG. 115. — (a) Addition of the vectors  $L$  and  $S$  to yield integral values of  $J$ . (b) Addition of the vectors  $L$  and  $S$  to yield half-integral values of  $J$ .

ber of possible values of  $J$ , for  $L > S$ , is  $2S + 1$ . The reader can construct similar figures for other values of  $L$  and  $S$  and show that when  $L < S$ ,  $J$  can have  $2L + 1$  values. In particular, if  $L = 0$ ,  $J$  can have only one value, namely  $J = S$ .

## 87. Magnetic Moment of an Orbital Electron

An electron moving in a plane orbit of area  $A$  is equivalent to a current  $i$  given by

$$i = \frac{e}{cT} \quad (13)$$

where  $T$  is the period of the electron in its orbit,  $i$  the current in e.m. units,  $e$  the charge of the electron in e.s. units, and  $c$  the ratio of the e.m. to the e.s. unit of charge. A plane circuit carrying

current (see § 12) has a magnetic moment  $\mu$  given by

$$\mu = iA,$$

so that the magnetic moment of the orbital electron is

$$\mu = \frac{eA}{cT}. \quad (14)$$

To evaluate this magnetic moment, assume that the electron is moving in an elliptic orbit. With polar coordinates  $r$  and  $\phi$ , Figure 116, the area can be expressed as

$$A = \frac{1}{2} \int_0^{2\pi} r^2 d\phi.$$

Now the angular momentum of the electron  $p_\phi$  is constant and can be expressed as

$$p_\phi = mr^2 \frac{d\phi}{dt}.$$

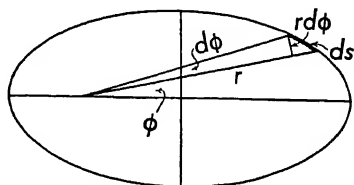


FIG. 116. — Elliptic orbit of an electron.

The elimination of  $r^2$  between the last two equations yields

$$A = \frac{1}{2} \int_0^T \frac{p_\phi}{m} dt = \frac{1}{2} \frac{p_\phi}{m} T. \quad (15)$$

The magnetic moment  $\mu$  is therefore

$$\mu = \frac{e}{2mc} p_\phi. \quad (16)$$

The angular momentum  $p_\phi$  can also be expressed in terms of the orbital quantum number  $l$  as

$$p_\phi = \frac{lh}{2\pi},$$

from which

$$\mu = l \frac{eh}{4\pi mc}. \quad (17)$$

The magnetic moment of the orbital electron is therefore an integral multiple of the quantity  $eh/4\pi mc$ . This quantity is known as the magnetic moment of a *Bohr magneton* and will be represented by the symbol  $M_B$ . Substitution of the numerical values for the constants yields

$$M_B = \frac{eh}{4\pi mc} = 9.27 \times 10^{-21} \text{ erg oersted}^{-1}.$$

Since the electronic charge is negative, the magnetic moment due to its orbital motion,

$$\mu = lM_B,$$

can be represented by a vector opposite to that of  $l$ .

### 88. Magnetic Moment Due to Spin

An electron spinning about its axis should also behave as a tiny magnet and possess a magnetic moment due to this spin. However, nothing is known about the shape of an electron or the manner in which its charge is distributed. Lacking this information, it is impossible to calculate its spin magnetic moment in a manner analogous to that used for the orbital motion. In order to obtain agreement with experimental results, it is necessary to assign to the spin magnetic moment the value

$$\mu_s = 2 \cdot \frac{e}{2mc} p_s, \quad (18)$$

where

$$p_s = s \frac{h}{2\pi};$$

so that

$$\mu_s = 2s \frac{eh}{4\pi mc}. \quad (19)$$

On the basis of the vector model of the atom,  $s$  is always  $\frac{1}{2}$ , so that the magnetic moment due to spin would have the value of one Bohr magneton. According to wave mechanics this value of  $s$  should be replaced by  $\sqrt{s(s+1)} = \sqrt{3}/2$ . In this case

$$\begin{aligned} \mu_s &= \sqrt{3} \frac{eh}{4\pi mc} \\ &= 1.62 \times 10^{-20} \text{ erg oersted}^{-1}. \end{aligned}$$

### 89. Magnetic Quantum Numbers

When the atoms of an element are placed in a very strong magnetic field of intensity  $H$ , the electrons, because of their magnetic moments, will experience torques tending to orient them. One of the effects of the introduction of this external magnetic field is that there now exists a definite direction in space to which the vector quantities may be referred. If the magnetic field is strong

enough to break down the coupling between the electrons so that each electron acts independently, then the spin and angular momentum vectors will take up definite positions in space with re-

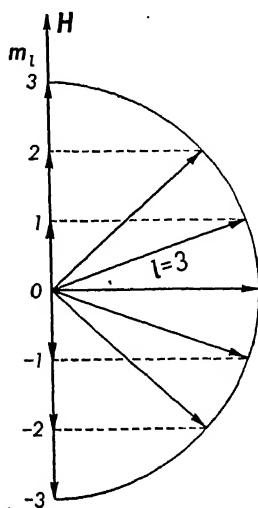


FIG. 117. — Projection of  $l$  in the direction of the magnetic field determines the magnetic orbital quantum number  $m_l$ .

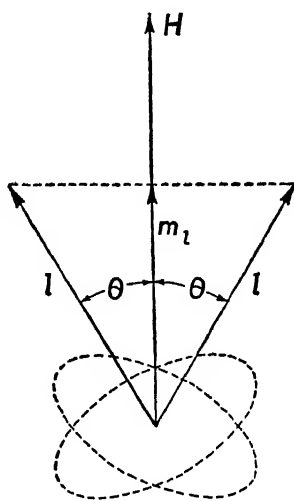


FIG. 118. — Precession of the angular momentum vector  $l$  about  $H$  as an axis.

spect to the magnetic field. These vectors, however, may be oriented only in certain definite directions with respect to the magnetic field. According to wave mechanics, the directions that the vector  $l$  may assume are such that its projection in the direction of the magnetic field must always have an integral value.

The projection of  $l$  on the magnetic field direction is denoted by  $m_l$ , and is called the *magnetic orbital quantum number*. The possible values of  $m_l$  are  $l, l-1, l-2, \dots, 0, \dots, -l$ , that is, there are  $2l+1$  possible values of  $m_l$ . This is illustrated in Figure 117 for  $l=3$ . The angle  $\theta$  between  $l$  and  $H$  is given by

$$\cos \theta = \frac{m_l}{l}. \quad (20)$$

The torque due to the magnetic field causes the angular momentum vector  $l$  to precess about the direction of the magnetic field as an axis, always maintaining the same inclination  $\theta$ , Figure 118. The additional energy  $\Delta \mathcal{E}$  due to the action of the mag-

netic field is given by

$$\Delta\mathcal{E} = \mu H \cos \theta. \quad (\text{Chap. 1, Eq. 17})$$

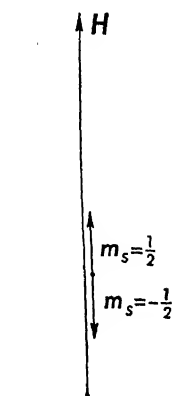
Substitution of the values of  $\mu$  and  $\cos \theta$  from equations (17) and (20) yields

$$\Delta\mathcal{E} = \frac{eh}{4\pi mc} H m_s. \quad (21)$$

This equation will be useful in the discussion of the Zeeman effect.

The vector  $s$  representing the spin angular momentum can assume only two possible positions with respect to the magnetic field: it may be parallel to it or antiparallel; that is, oppositely directed to it. Its projection along the direction of the magnetic field is denoted by  $m_s$ , which is called the magnetic

FIG. 119. — Projection of the spin vector  $s$  in the direction of the magnetic field showing the two possible values of  $m_s$ .



spin quantum number.  $m_s$  can have only two values,  $+\frac{1}{2}$  or  $-\frac{1}{2}$ , as illustrated in Figure 119.

There are similar restrictions on the positions that the total angular momentum vector  $j$  can assume in the presence of a magnetic field. Since we are dealing with only a single electron,  $j$  can have only odd half-integral values; the restriction on the positions of  $j$  is that  $m_j$ , the projection of  $j$  on the direction of the magnetic field, must have odd half-integral values. Figure 120(a) shows the possible values of  $m_j$  for  $j = \frac{3}{2}$ .

On the basis of wave mechanics,  $m_j$  remains a half-integer for the corresponding values of  $j$  even though the magnitude of  $j$  is  $\sqrt{j(j+1)}$ . The orientations of  $j$  with respect to the magnetic field are, however, slightly different as illustrated in Figure 120(b). It will be noted that there are  $2j + 1$  values for  $m_j$  in both methods of projection. The term *space quantization* is usually applied to the above restrictions imposed on the orientation of the vectors  $l$ ,  $s$ , and  $j$  in the presence of a magnetic field.

## 90. Pauli's Exclusion Principle

All these quantum numbers having been introduced, the problem now is to assign the appropriate set of quantum numbers to



each electron in the atom in order to specify the *state* of the electron. Wave mechanics does not offer any guiding principle for the assignment of these quantum numbers. However, Pauli (1925)

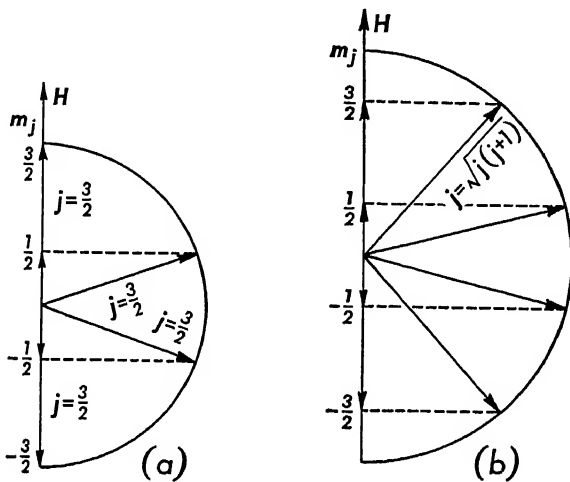


FIG. 120. — (a) Projection of  $\mathbf{j}$  in the direction of the magnetic field showing the possible values of  $m_j$  according to the vector model of the atom. (b) Projection of the vector  $\mathbf{j}$  to give the same values of  $m_j$  as in (a) according to wave mechanics.

introduced a principle, known as *Pauli's exclusion principle*, for the assignment of quantum numbers to the electrons in the atom. Pauli's exclusion principle states that no two electrons in an atom can exist in the same state. Now, the state of any one electron can be completely specified by a group of four quantum numbers, such as  $n, l, m_l, m_s$  or  $n, l, j, m_j$ . Hence Pauli's exclusion principle states that the group of values assigned to the four quantum numbers must be different for different electrons.

Electrons having the same value for the principal quantum number  $n$  form a definite *group*, or *shell*, or *energy level*. Electrons with the same  $n$  are further subdivided according to the value of the orbital angular momentum  $l$ . Differences in  $l$  values, for the same value of  $n$ , denote comparatively smaller energy differences than equal values of  $l$  and different values of  $n$ . Those electrons which possess the same value of  $l$  for a given  $n$  are said to be in the same subgroup, or subshell, or sublevel. The possible number of electrons in a subgroup depends upon the possible orientations of the vectors  $\mathbf{l}$  and  $\mathbf{s}$ ; that is, upon the possible values of  $m_l$  and  $m_s$ ,

or upon the possible values of  $j$  and  $m_j$ . Table X shows the maximum possible number of electrons in a given group for  $n = 1, 2$ , and 3.

TABLE X

POSSIBLE NUMBER OF ELECTRONS IN A GIVEN GROUP						
$n$	$l$	$m_l$	$m_s$	No. of Electrons in Subgroup	No. of Electrons in Completed Group	
1 1	0 0	0 0	$+\frac{1}{2}$ $-\frac{1}{2}$	2	2	
2 2	0 0	0 0	$+\frac{1}{2}$ $-\frac{1}{2}$	2	8	
2 2 2 2 2 2	1 1 1 1 1 1	-1 -1 0 0 1 1	$+\frac{1}{2}$ $-\frac{1}{2}$ $+\frac{1}{2}$ $-\frac{1}{2}$ $+\frac{1}{2}$ $-\frac{1}{2}$	6		
3 3	0 0	0 0	$+\frac{1}{2}$ $-\frac{1}{2}$	2		18
3 3 3 3 3 3	1 1 1 1 1 1	-1 -1 0 0 1 1	$+\frac{1}{2}$ $-\frac{1}{2}$ $+\frac{1}{2}$ $-\frac{1}{2}$ $+\frac{1}{2}$ $-\frac{1}{2}$	6		
3 3 3 3 3 3 3 3 3	2 2 2 2 2 2 2 2 2	-2 -2 -1 -1 0 0 1 1 2 2	$+\frac{1}{2}$ $-\frac{1}{2}$ $+\frac{1}{2}$ $-\frac{1}{2}$ $+\frac{1}{2}$ $-\frac{1}{2}$ $+\frac{1}{2}$ $-\frac{1}{2}$ $+\frac{1}{2}$ $-\frac{1}{2}$	10		

Several interesting facts can be obtained from a study of Table X. The maximum number of subgroups for a given value of  $n$  is  $n$ . The maximum possible number of electrons in a given

subgroup is  $2(2l + 1)$ . A subgroup is filled or completed when the sum of the vectors  $m_l$  is zero. Also the sum of the vectors  $m_s$  is zero for a completed subgroup. From wave mechanical considerations, it can be shown that for a closed shell  $S = 0$ ,  $L = 0$ , and  $J = 0$ ; that is, the contributions of the electrons in a closed shell to the total angular momentum of an atom are zero. Hence, in order to determine the angular momentum of an atom, only those electrons which are outside closed shells need be considered.

## 91. Distribution of Electrons in an Atom

In assigning electrons to the different groups and subgroups in an atom, we must have recourse not only to optical and X-ray spectra, but also to other phenomena such as the magnetic and chemical behavior of the element. The normal state of an atom is one in which all the electrons are in the lowest possible energy levels. In the atom of the simplest element, hydrogen,  $Z = 1$ , the normal state is characterized by the quantum numbers  $n = 1$ ,  $l = 0$ ;  $m_l$  is, of course, zero, and  $m_s$  may be either  $+\frac{1}{2}$  or  $-\frac{1}{2}$ . The atom of the next element, helium,  $Z = 2$ , has both its electrons in the shell  $n = 1$ ,  $l = 0$ .  $m_s$  is  $+\frac{1}{2}$  for one electron and  $-\frac{1}{2}$  for the second electron. This shell is now completed or closed. It will be recalled that helium is one of the inert gases; therefore it may be expected to have a very stable electron configuration. This should also be true of all the other inert gases.

In the atom of the next element, lithium,  $Z = 3$ , two electrons can be put in the shell  $n = 1$ ,  $l = 0$ , but the third electron must be put into a new shell  $n = 2$ ,  $l = 0$ . Lithium is one of the alkali elements and has a valence of unity. This means that a single electron, in shell  $n = 2$ , can be detached easily from the atom to form the lithium ion,  $\text{Li}^+$ . This is indicated by the fact that its ionization potential is only 5.37 volts, whereas for He it is 24.45 volts (see Table XI). Another interesting point is that the lithium ion,  $\text{Li}^+$ , has the same configuration as neutral helium. One may expect the atoms of the other alkali elements, sodium, potassium, rubidium, and caesium, to be built up in a similar manner, that is, a single valence electron starting a new shell outside a closed configuration typical of an inert gas. This is shown in Table XI, which gives the distribution of electrons in the atoms of the elements.

TABLE XI

DISTRIBUTION OF ELECTRONS IN THE ATOMS															
X-Ray Notation			K	L			M			N					
Values of $n, l$			1,0	2,0	2,1	3,0	3,1	3,2	4,0	4,1	4,2	4,3			
Spectral Notation			1s	2s	2p	3s	3p	3d	4s	4p	4d	4f			
Element	Atomic Number $Z$	First Ionization Potential in Volts										Lowest Spectral Term			
H	1	13.529	1										$2S_{1/2}$		
He	2	24.465	2										$1S_0$		
Li	3	5.37	2	1									$2S_{1/2}$		
Be	4	9.281	2	2									$1S_0$		
B	5	8.28	2	2	1								$2P_{1/2}$		
C	6	11.217	2	2	2								$3P_0$		
N	7	14.48	2	2	3								$4S_{3/2}$		
O	8	13.550	2	2	4								$3P_2$		
F	9	18.6	2	2	5								$2P_{3/2}$		
Ne	10	21.47	2	2	6								$1S_0$		
Na	11	5.12	Neon Configuration  10 Electron Core			1							$2S_{1/2}$		
Mg	12	7.61				2									$1S_0$
Al	13	5.96				2	1								$2P_{1/2}$
Si	14	8.12				2	2								$3P_0$
P	15	10.9				2	3								$4S_{3/2}$
S	16	10.3				2	4								$3P_2$
Cl	17	12.96				2	5								$2P_{3/2}$
A	18	15.69				2	6								
K	19	4.32	Argon Configuration  18 Electron Core						1				$2S_{1/2}$		
Ca	20	6.09							2				$1S_0$		
Sc	21	6.7							1	2			$2D_{3/2}$		
Ti	22	6.81							2	2			$3P_2$		
V	23	6.76							3	2			$4F_{3/2}$		
Cr	24	6.74							5	1			$7S_3$		
Mn	25	7.41							5	2			$6S_{5/2}$		
Fe	26	7.83							6	2			$5D_4$		
Co	27	8.5							7	2			$4F_{5/2}$		
Ni	28	7.603							8	2			$3F_4$		
Cu	29	7.63							10	1			$2S_{1/2}$		
Zn	30	9.36							10	2			$1S_0$		
Ga	31	5.97							10	2	1		$2P_{1/2}$		
Ge	32	8.09							10	2	2		$3P_0$		
As	33	10.							10	2	3		$4S_{3/2}$		
Se	34	9.5							10	2	4		$3P_2$		
Br	35	11.80							10	2	5		$2P_{3/2}$		
Kr	36	13.940							10	2	6		$1S_0$		

TABLE XI (Continued)

DISTRIBUTION OF ELECTRONS IN THE ATOMS																									
X-Ray Notation		K	L	M	N				O					P											
Values of $n, l$		1	2	3	4,0	4,1	4,2	4,3	5,0	5,1	5,2	5,3	5,4	6,0	6,1	6,2	6,3	6,4	6,5						
Spectral Notation		1s	s,p	s,p,d	4s	4p	4d	4f	5s	5p	5d	5f	5g	6s	6p	6d	6f	6g	6h						
Element	Atomic Number Z	First Ionization Potential in Volts																	Lowest Spectral Term						
Rb	37	4.159	Krypton Configuration  36 Electron Core						1											$^2S_{1/2}$					
Sr	38	5.667							2															$^1S_0$	
Y	39	6.5										1	2											$^2D_{3/2}$	
Zr	40	6.92										2	2											$^3F_2$	
Cb	41	—										4	1											$^6D$	
Mo	42	7.35										5	1												$^7S_3$
Mn	43	—										6	1												$^6D_{5/2}$
Ru	44	7.7										7	1												$^5F_5$
Rh	45	7.7										8	1												$^4F_{5/2}$
Pd	46	8.3										10													$^1S_0$
Ag	47	7.54	Palladium Configuration  46 Electron Core						1											$^2S_{1/2}$					
Cd	48	8.96							2															$^1S_0$	
In	49	5.76											1											$^2P_{1/2}$	
Sn	50	7.30											2											$^3P_0$	
Sb	51	8.5											2											$^4S_{3/2}$	
Te	52	8.96											3											$^3P_2$	
I	53	10.6											5											$^2P_{3/2}$	
Xe	54	12.078											6											$^1S_0$	
Cs	55	3.87	Xenon Configuration 54 Electron Core											1					$^2S_{1/2}$						
Ba	56	5.19																2					$^1S_0$		
La	57	5.6	Shells 1s to 4d contain 46 electrons						2	6	1			2					$^2D_{3/2}$						
Ce	58	6.54							1	2	6	1			2			2					$^3H_4$		
Pr	59								2	2	6	1			1			2					$^4K_{11/2}$		
Nd	60								3	2	6	1			1			2					$^6L_6$		
Il	61								4	2	6	1			1			2					$^6I_{9/2}$		
Sm	62								5	2	6	1			1			2					$^7F_0$		
Eu	63	5.64							6	2	6	1			1			2					$^8S_{7/2}$		
Gd	64	6.16							7	2	6	1			1			2					$^6D_2$		
Tb	65								8	2	6	1			1			2					$^8H_{17/2}$		
Dy	66								9	2	6	1			1			2					$^7K_{10}$		
Ho	67								10	2	6	1			1			2					$^6L_{10/2}$		
Er	68								11	2	6	1			1			2					$^6L_{10}$		
Tm	69								13	2	6	0			0			2					$^3F_{7/2}$		
Yb	70								14	2	6	0			0			2					$^1S_0$		
Lu	71								14	2	6	1			1			2					$^2D_{3/2}$		

TABLE XI (Concluded)

DISTRIBUTION OF ELECTRONS IN THE ATOMS																									
X-Ray Notation		K	L	M	N	O					P					Q									
Values of $n, l$		1	2	3	4	5,0	5,1	5,2	5,3	5,4	6,0	6,1	6,2	6,3	6,4	6,5	7,0	7,1							
Spectral · Notation						5s	5p	5d	5f	5g	6s	6p	6d	6f	6g	6h	7s	7p							
Element	Atomic Number $Z$	First Ionization Potential in Volts																Lowest Spectral Term							
Hf	72	7.94		Shells 1s to 5p contain 68 electrons					2		2							$^3F_2$							
Ta	73								3		2							$^4F_{3/2}$							
W	74								4		2							$^5D_0$							
Re	75								5		2							$^6S_{5/2}$							
Os	76								6		2							$^6D_4$							
Ir	77	8.9							7		2							$^4F_{3/2}$							
Pt	78								9		1							$^3D_3$							
Au	79								10		1							$^2S_{1/2}$							
Hg	80	10.38	10.69	Shells 1s to 5d contain 78 electrons						2								$^1S_0$							
Tl	81	6.07								2		1					$^2P_{1/2}$								
Pb	82	7.38								2		2					$^3P_0$								
Bi	83	8.0								2		3					$^4S_{3/2}$								
Po	84									2		4					$^3P_2$								
—	85									2		5					$^2P_{3/2}$								
Rn	86									2		6					$^1S_0$								
—	87			Radon Configuration 86 Electron Core														1	$^2S_{1/2}$						
Ra	88																								$^1S_0$
Ac	89																							1	$^2D_{3/2}$
Th	90																							2	$^3F_2$
Pa	91																							3	$^4F_{3/2}$
U	92											4						$^5D_0$							

It is convenient at this point to introduce the X-ray notation for the different groups. The group or shell for which  $n = 1$  is called the  $K$  shell,  $n = 2$  the  $L$  shell,  $n = 3$  the  $M$  shell, and so on. Beryllium, for example, with  $Z = 4$ , has two electrons in the completed  $K$  shell, and two additional electrons in the  $L$  shell, thus completing the first subgroup in this shell. Beryllium is one of the alkaline earth elements with a valence of 2. The atoms of the other elements of this group, magnesium, calcium, strontium, barium, and radium, should have similar structures, that is, two electrons outside an inert gas or closed shell configuration. This can be verified from Table XI.

Boron,  $Z = 5$ , has two electrons in the completed  $K$  shell and

three electrons in the  $L$  shell, two in the completed subgroup  $n = 2$ ,  $l = 0$ , and the third electron starting the new subgroup  $n = 2$ ,  $l = 1$ . The atoms of the other elements in this group, aluminum, gallium, indium, and thallium, similarly have three electrons outside a closed shell, two in a completed subgroup  $l = 0$ , and one in the next subgroup  $l = 1$ .

This process of atom building can be continued by the addition of an electron to the  $L$  shell subgroup  $l = 1$ , as the element of atomic number  $Z + 1$  is formed from element of atomic number  $Z$ . In each case the positive charge on the nucleus must be increased by one. The  $L$  shell will be completed with the element neon,  $Z = 10$ , with two electrons in the  $K$  shell and eight electrons in the  $L$  shell. Neon is one of the inert gases and has a very stable configuration. Fluorine,  $Z = 9$ , has two electrons in the  $K$  shell and seven electrons in the  $L$  shell. In chemical action it is found that fluorine has a valence of  $-1$ , indicating that it very easily forms an ion  $F^-$  by adding an electron to the  $L$  shell, forming a stable configuration similar to that of neon.

The next eight elements, from sodium,  $Z = 11$ , to argon,  $Z = 18$ , are formed by adding the additional electrons to the  $M$  shell for which  $n = 3$ . Sodium has an electron ( $n = 3$ ,  $l = 0$ ) outside a closed shell; magnesium has two electrons outside this closed shell, both in the subgroup  $l = 0$ , thus completing it. The next subgroup with  $l = 1$  is begun with aluminum,  $Z = 13$ , and completed with argon,  $Z = 18$ . It may be remarked here that the chemical properties of an element are determined mostly by the electrons in the outer shell of the atom.

Potassium,  $Z = 19$ , retains the argon configuration of the first eighteen electrons, but the nineteenth electron starts a new group,  $n = 4$ , belonging to the  $N$  shell. Calcium,  $Z = 20$ , has two electrons in the  $N$  shell  $n = 4$ ,  $l = 0$ . It might have been expected that these electrons would have been placed in the still incomplete  $M$  shell  $n = 3$ ,  $l = 2$ , but spectroscopic evidence is against this. However, the next group of atoms from scandium,  $Z = 21$ , to copper,  $Z = 29$ , have their additional electrons placed in the  $M$  shell  $n = 3$ ,  $l = 2$ , which is then completed. From gallium,  $Z = 31$ , to krypton,  $Z = 36$ , an inert gas, the additional electrons are added to the  $N$  shell  $n = 4$ ,  $l = 1$ . By examining Table XI, the reader will find the order in which electrons have been assigned

to the various groups and subgroups. It will be of interest to check this assignment with the chemical properties of the elements, remembering that these properties are controlled essentially by the outer electrons.

## 92. Spectral Notation

In the course of the development of spectroscopy, several types of notation have been used. The following is the modern notation. In describing the electron configuration small letters are used to represent the values of  $l$  as follows:

$$l = 0, 1, 2, 3, 4, 5, \dots$$

$$s, p, d, f, g, h, \dots$$

That is, if an electron is in a shell for which  $l = 0$ , it is called an  $s$  electron, for  $l = 1$ , a  $p$  electron, and so on. The value of the total quantum number  $n$  is written as a prefix to the letter representing its  $l$  value. The number of electrons having the same  $n$  and  $l$  values is indicated by an index written at the upper right of the letter representing their  $l$  value. Thus the eleven electrons of sodium in the normal state are designated as follows:

$$1s^2 2s^2 2p^6 3s;$$

that is, there are two  $1s$  electrons, two  $2s$  electrons, six  $2p$  electrons, and one  $3s$  electron. One must be careful not to confuse the symbol  $s$  written for  $l = 0$  with the same symbol used for the spin quantum number.

Capital letters are used to represent the total orbital angular momentum of an atom according to the following scheme:

$$L = 0, 1, 2, 3, 4, 5, \dots$$

$$S, P, D, F, G, H, \dots$$

The value of the total angular momentum of the atom,  $J$ , is written as a subscript at the lower right of the letter representing the particular  $L$  value of the atomic state. The number of possible values of  $J$  for a given value of  $L$  is written as a superscript at the upper left of the letter representing the  $L$  value. Thus  ${}^2P_{1/2}$ ,  ${}^2P_{3/2}$ , read "doublet  $P$  one half," etc., or  ${}^3P_2$ ,  ${}^3P_1$ ,  ${}^3P_0$ , read "triplet  $P$  two," . . . and so on. For example, in the case of the alkali atoms,  $J$  has two values for each of the  $P$ ,  $D$ ,  $F$  terms, but can have only



one value for the  $S$  term. But, by custom, to keep the notation symmetrical,  $S$  is allotted the superscript 2. As will be shown, this superscript is an indication of the multiplicity of the terms of the atomic configuration.

### 93. Spectrum of Sodium

The optical spectrum of sodium is typical of the spectra of all the alkali atoms. In its normal state, the sodium atom consists of a closed core of ten electrons and one additional electron in the  $3s$  state. Since the closed core contributes nothing to the angular momentum of the atom, only the states of this eleventh or optical electron need be considered in discussing the spectrum of neutral sodium.

The atoms of sodium can be raised from the normal state to higher energy states by bombarding them with electrons, or by

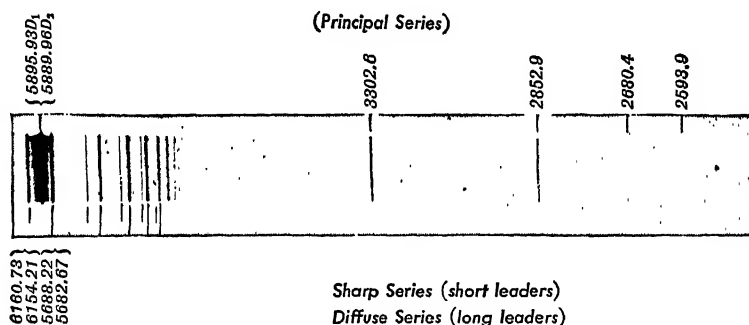


FIG. 121. — The emission spectrum of sodium showing lines of three series. The upper numbers are wave lengths of the lines of the principal series. The short leaders below the spectrum indicate the lines of the sharp series, while the long leaders indicate the lines of the diffuse series. (Reprinted by permission from Herzberg, *Atomic Spectra and Atomic Structure*, Prentice-Hall, Inc.)

subjecting them to high temperatures in a flame or in an electric arc, or by allowing them to absorb radiant energy from an external source. The atom in one of the higher energy states is said to be in an *excited* state. When the atom returns to a state of lower energy, radiation is emitted in the form of a photon of very definite frequency given by Bohr's frequency condition. The spectrum of sodium, see Figure 121, consists of several series of spectral lines, some of which were mentioned in § 83. When these spectral lines are examined with instruments of high resolving power, it is found that many of the lines consist of doublets, that

is, two lines very close together. Such lines are said to exhibit *fine structure*. For example, the well-known yellow line of sodium, frequently referred to as the sodium *D* line, consists of two lines close together of wave lengths  $5889.96\text{\AA}$  and  $5895.93\text{\AA}$ ; that is, they are separated by about  $6\text{\AA}$ . These lines form one of the doublets of the principal series. The other lines of the principal series are in the ultraviolet region. Lines of the principal series are due to transitions from a *P* state to the lowest *S* state. Since the smallest value of the principal quantum number for the optical electron of sodium is  $n = 3$ , the lowest state is designated as a  $3S$  state. Since  $l = 0$ , the value of  $j$  for this state is  $j = s = \frac{1}{2}$ . For the *P* state  $L = l = 1$ , and since  $J = L + \frac{1}{2}$  and  $L - \frac{1}{2}$ , the total angular momentum of the *P* state is  $\frac{1}{2}$  or  $\frac{3}{2}$ . Since there are two values of  $J$ , the *P* state is a doublet state and is designated as

$$^2P_{1/2}, ^2P_{3/2}.$$

Similarly for the *D* terms for which  $L = l = 2$ ,  $J = j = \frac{3}{2}$  or  $\frac{5}{2}$ , so that the *D* term is a doublet and is designated as

$$^2D_{3/2}, ^2D_{5/2},$$

and the *F* term  $L = l = 3$ ,  $J = j = \frac{5}{2}$  or  $\frac{7}{2}$ , is designated as

$$^2F_{5/2}, ^2F_{7/2}.$$

The *S* state is always a single state but since the other states of the atom are all doublets, the *S* state is also designated as

$$^2S_{1/2}.$$

The energy level diagram of sodium, Figure 122, shows the relative positions of these energy levels, drawn approximately to scale. The  $^2P_{3/2}$  level is actually slightly above the  $^2P_{1/2}$  level, but the separation is too small to be shown in the figure. For example, the separation of the  $^2P$  levels giving rise to the yellow lines of sodium is only  $17\text{ cm}^{-1}$ , whereas the term value is about  $25,000\text{ cm}^{-1}$ . Similarly the  $^2D$  and  $^2F$  levels are drawn as single levels. The principal quantum number  $n$  is written for each term in the figure. It will be noticed that the large wave numbers are associated with the low energy terms. This is due to the fact that the zero level of energy is taken as the energy of ionized atom; the energy values are all negative, but the minus signs have been



For this reason the higher voltages coincide with the higher energy levels, and the ionization potential, 5.12 volts, is placed at  $n = \infty$ .

The principal series of sodium is produced by transitions from the  ${}^2P$  states to the lowest state,  $3^2S_{1/2}$ . These lines are all doublets since they originate in the  ${}^2P_{1/2, 3/2}$  levels and end in the  ${}^2S_{1/2}$  level. The yellow lines of sodium are due to the transitions

$$\lambda = 5895.93 \text{ \AA}, 3^2S_{1/2} - 3^2P_{1/2} \quad (D_1 \text{ line})$$

$$\lambda = 5889.96 \text{ \AA}, 3^2S_{1/2} - 3^2P_{3/2} \quad (D_2 \text{ line}).$$

The wave number of any line of the principal series is given by

$$\nu = 3^2S_{1/2} - n^2P_{1/2}, \quad (n = 3, 4, 5, \dots)$$

or

$$\bar{\nu} = 3^2S_{1/2} - n^2P_{3/2} \quad (n = 3, 4, 5, \dots).$$

The lines of the sharp series are due to transitions from the higher  ${}^2S_{1/2}$  levels to the  $3^2P_{1/2, 3/2}$  levels, and their wave numbers are given by

$$\bar{\nu} = 3^2P_{1/2} - n^2S_{1/2} \quad (n = 4, 5, 6, \dots)$$

$$\bar{\nu} = 3^2P_{3/2} - n^2S_{1/2} \quad (n = 4, 5, 6, \dots).$$

Transitions from the  ${}^2D$  levels to the  $3^2P$  levels give rise to the diffuse series, and those from the  ${}^2F$  levels to the  $3^2D$  levels give rise to the fundamental series.

Transitions can take place between  $S$  and  $P$  states,  $P$  and  $D$  states,  $D$  and  $F$  states, but under normal conditions, no transitions can take place between  $S$  and  $D$  states, or  $S$  and  $F$  states, or  $P$  and  $F$  states. The transitions that can take place are given by the following selection rules for the vectors  $L$  and  $J$ :

$$\Delta L = \pm 1 \quad (22a)$$

$$\Delta J = \pm 1 \text{ or } 0. \quad (22b)$$

The selection rule for  $J$  prohibits transitions between some of the doublet levels even though they are not ruled out by the selection rule for  $L$ . For example, in the diffuse series, the transition  ${}^2P_{1/2} - {}^2D_{5/2}$  is forbidden, while the other three transitions are permitted.

The doublet character of the energy levels is typical not only of sodium and the other alkali elements, but also of the singly ionized alkaline earth elements such as  $\text{Be}^+$ ,  $\text{Mg}^+$ ,  $\text{Ca}^+$ , and so on.

A glance at Table XI will show that the singly ionized atoms of the alkaline earths have exactly the same electronic structure as the neutral alkali atoms, that is, a single electron outside a closed core typical of the configuration of the atoms of the inert elements. It should be emphasized that the doublet character of the energy levels is satisfactorily accounted for by the hypothesis that the electron possesses a spin.

## 94. Absorption of Energy

If white light is sent through sodium vapor and then examined with a reflection grating, it is found that those wave lengths which correspond to the lines of the principal series of sodium are missing. Such a spectrum is called an *absorption* spectrum. R. W. Wood and his collaborators performed a series of experiments on the absorption spectrum of sodium. In one such experiment the vapor was obtained by heating metallic sodium in a steel tube faced with quartz windows. It was necessary to use quartz windows in this experiment since most of the lines of the principal series of sodium are in the ultraviolet region. As many as sixty lines were observed in this absorption spectrum. That only lines of the princi-



FIG. 123. — Photograph of the absorption spectrum of sodium showing some of the lines in the ultraviolet region. The numbers are the wave lengths of the lines in Å. (Reprinted by permission from Herzberg, *Atomic Spectra and Atomic Structure*, Prentice-Hall, Inc.)

pal series appear in the absorption spectrum is due to the fact that most of the atoms in the tube are in the lowest state,  $3^2S_{1/2}$ . A photograph of the absorption spectrum of sodium is shown in Figure 123. In emission, the lines of the principal series correspond to transitions from the  $2^1P_{1/2, 3/2}$  levels to the ground state,  $3^2S_{1/2}$ ; in absorption, the transitions are from the lowest state,  $3^2S_{1/2}$  to the  $2^1P_{1/2, 3/2}$  levels.

An interesting experiment would be to send monochromatic light of wave length equal to that of the sodium *D* lines into a tube containing sodium vapor. R. W. Wood performed such an experiment, using the yellow light from an oxyhydrogen flame contain-

ing sodium. The yellow light was focused on the axis of an evacuated test tube containing sodium vapor. On looking down into the test tube it was found that the sodium vapor, near the wall of the tube where the incident beam entered, emitted yellow fluorescent radiation. Other investigations showed that the fluorescent radiation consisted only of the yellow lines of sodium. By

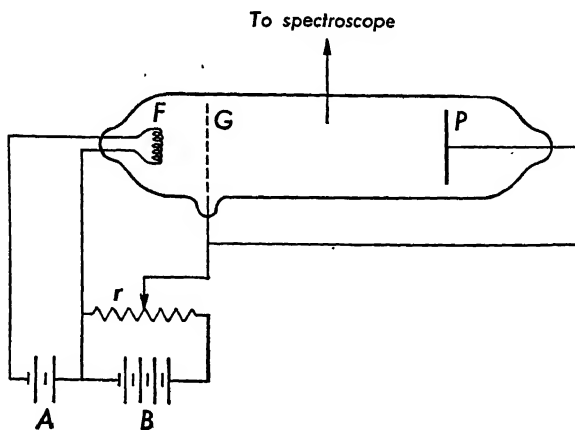


FIG. 124. — A diagram of the apparatus for determining the resonance and ionization potentials of sodium.

referring to the energy level diagram, it can be seen that the atoms in the normal state,  $3^2S_{1/2}$ , were raised to the next higher states,  $3^2P_{1/2, 3/2}$ , by the absorption of the yellow  $D$  lines. On returning to the normal state these atoms emitted radiation of the same wave length. This type of fluorescent radiation is called *resonance radiation*.

An entirely different method of raising the atoms from their normal to excited states is to utilize the kinetic energy of an electron beam. A simplified schematic diagram for accomplishing this is shown in Figure 124. The electrodes are in an evacuated tube containing a small amount of sodium vapor. Electrons from the heated filament  $F$  are accelerated by a difference of potential  $V$  to the grid  $G$ . The plate  $P$  is at the same potential as  $G$ , so that in the space between  $P$  and  $G$  the electrons are moving with a kinetic energy given by

$$\frac{1}{2}mv^2 = Ve.$$

Although electrons undoubtedly collide with some of the sodium

atoms, no radiation is observed when the voltage between  $F$  and  $G$  is below 2.1 volts. When this voltage is reached, the sodium vapor in the region between  $G$  and  $P$  is observed to emit yellow light. An examination of this light with a spectrograph shows that it consists of the sodium resonance lines only. The interpretation of this phenomenon is that an electron, on colliding with a sodium atom, loses an amount of energy, equivalent to 2.1 ev to the sodium atom, thereby raising it from the normal to the next higher state,  $3^2P_{1/2, 3/2}$ . On returning to its normal state, the sodium atom then emits the resonance radiation. This means that the energy of the incident electron must be at least equal to the quantum of energy corresponding to the sodium  $D$  lines. This can be checked by substituting the appropriate values in the formula

$$Ve = h\nu = \frac{hc}{\lambda},$$

and calculating  $\lambda$ . This yields  $\lambda = 5898\text{\AA}$ , in good agreement, within the limits of experimental error, with the wave lengths of the  $D$  lines of sodium. This potential, at which the resonance lines appear, is called the *resonance potential*.

When the voltage between the filament and grid in the above apparatus is increased to about 4 volts, the color of the light emitted by the sodium vapor changes, indicating that additional spectral lines are being emitted. At this voltage, the spectrogram shows the presence of the doublet  $3^2S_{1/2} - 4^2P_{1/2, 3/2}$  of wave lengths  $3302\text{\AA}$  and  $3303\text{\AA}$ , in addition to the  $D$  lines. Other lines appear at 4.4 and 4.6 volts. At 5.12 volts, ionization of the sodium vapor occurs as indicated by the very large increase in current from the filament to the plate, and at the same time, the spectrograph records the appearance of the entire optical spectrum of sodium.

The emission of the entire optical spectrum when the voltage reaches the value of the ionization potential, 5.12 volts, can readily be explained by the fact that the electrons from the filament which have an amount of energy equal to 5.12 electron volts are capable of ionizing the sodium atoms. In this process electrons are removed from the normal state,  $3s3^2S_{1/2}$ , of the sodium atoms. An electron returning to an ionized atom may enter any one of the

excited states and finally reach the normal state by a series of successive quantum jumps. Corresponding to each quantum jump there is an emission of radiation of appropriate frequency, giving rise to the lines observed in the optical spectrum. The intensity of a spectral line is determined by the number of atoms in which identical transitions take place simultaneously. The transitions giving rise to the intense spectral lines must have a greater probability of occurrence than those producing the weaker lines. The most probable transitions are those permitted by the selection rules. The probability that transitions will occur which are not permitted by the selection rules is vanishingly small under ordinary conditions.

## 95. Normal Zeeman Effect and the Vector Model

In our previous discussion of the Zeeman effect (Chapter 3), we found that the classical theory was adequate to explain the normal Zeeman effect but was totally inadequate to explain the anomalous Zeeman effect such as that exhibited by the sodium *D* lines. Let us now examine the treatment of the Zeeman effect on the basis of the vector model of the atom.

It was remarked earlier in this chapter that one of the reasons for the introduction of an electron spin was to explain the anomalous Zeeman effect. If the spin of the electron is left out of consideration, then the only angular momentum possessed by the electron is that due to its orbital motion of amount

$$l \frac{h}{2\pi}.$$

In the presence of a magnetic field of intensity  $H$ , the vector  $l$  precesses around the direction of the magnetic field as axis. The angular velocity of precession may be obtained by direct calculation or from a famous theorem due to Larmor, which states that the effect of a magnetic field on an electron moving in an orbit is to superimpose on the orbital motion a precessional motion of the entire orbit about the direction of the magnetic field with angular velocity  $\omega$  given by

$$\omega = \frac{e}{2mc} H, \quad (23)$$

in which  $e$  is in e.s. units. Figure 118 shows two positions of the



vector  $\mathbf{l}$  as it precesses about the magnetic field at constant inclination, and the corresponding positions of the electronic orbit. The additional energy of the electron due to this precessional motion was shown to be given by

$$\begin{aligned}\Delta\mathcal{E} &= \mu H \cos \theta \\ &= m_l \frac{eh}{4\pi mc} H,\end{aligned}\quad (21)$$

where  $m_l$  is the projection of  $\mathbf{l}$  on  $H$ . In terms of the Larmor precession, the expression for the additional energy can be written as

$$\Delta\mathcal{E} = m_l \omega \frac{h}{2\pi}. \quad (24)$$

Since  $m_l$  is restricted to the  $(2l + 1)$  integral values  $l, l - 1, \dots, 0, \dots, -l$ , the effect of the magnetic field is to split up each energy level into  $2l + 1$  components spaced an amount  $\frac{eh}{4\pi mc} H$  apart. This is illustrated in Figure 125 for two energy levels, one for which  $l = 2$ , the other,  $l = 1$ . If  $\mathcal{E}_0$  represents the energy of the level  $l = 1$  in the absence of a magnetic field, and  $\mathcal{E}_H$  represents the energy of this level in the presence of the magnetic field of intensity  $H$ , then

$$\mathcal{E}_H = \mathcal{E}_0 + \Delta\mathcal{E} = \mathcal{E}_0 + m_l' \frac{eh}{4\pi mc} H.$$

Similarly, if  $\mathcal{E}_0''$  and  $\mathcal{E}_H''$  represent the energies of the level  $l = 2$  without and with the magnetic field respectively, then

$$\mathcal{E}_H'' = \mathcal{E}_0'' + \Delta\mathcal{E}'' = \mathcal{E}_0'' + m_l'' \frac{eh}{4\pi mc} H.$$

The quantity of energy radiated in the presence of the magnetic field is given by

$$\begin{aligned}h\nu_H &= \mathcal{E}_H'' - \mathcal{E}_H' = \mathcal{E}_0'' - \mathcal{E}_0' + (m_l'' - m_l') \frac{eh}{4\pi mc} H \\ &= h\nu_0 + \Delta m_l \frac{eh}{4\pi mc} H,\end{aligned}\quad (25)$$

from which

$$\nu_H = \nu_0 + \Delta m_l \frac{eH}{4\pi mc}, \quad (26)$$

where  $\nu_H$  is the frequency of the radiation emitted with the mag-

netic field present, and  $\nu_0$  is the frequency of the radiation in the absence of the magnetic field. The restrictions imposed upon the changes in the magnetic quantum number  $m_l$  are given by the selection rule

$$\Delta m_l = 0, \text{ or } \pm 1. \quad (27)$$

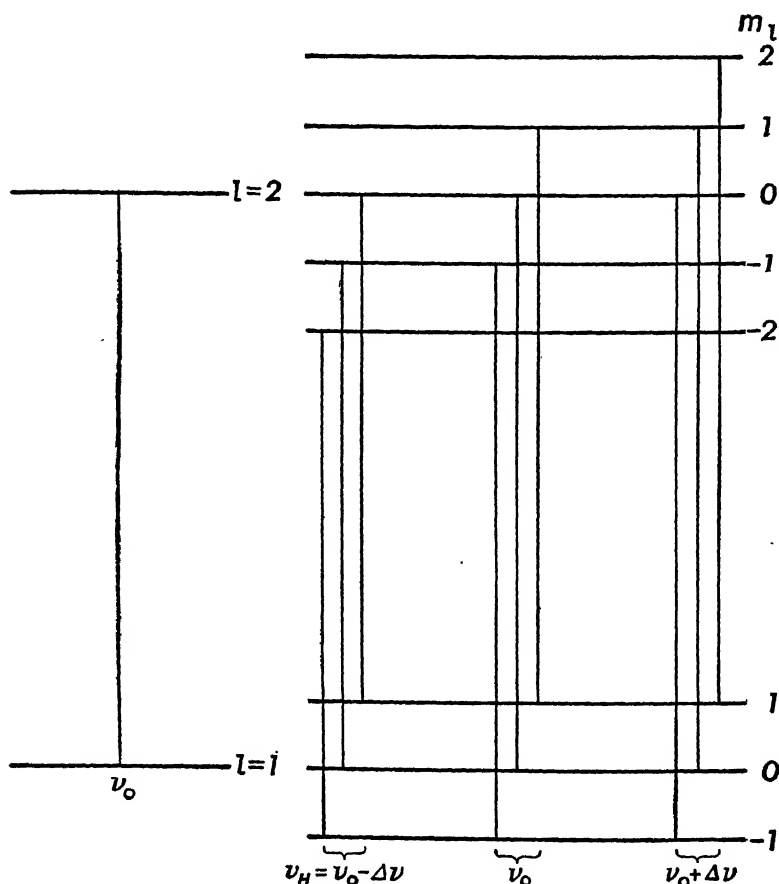


FIG. 125. — Splitting of energy levels in a magnetic field into  $2l + 1$  components. Section on the left represents the single transition in the absence of a magnetic field, while that at the right represents, for the same pair of terms, the splitting of the energy levels in a magnetic field and the possible transitions yielding the normal Zeeman effect.

Selection rule  $\Delta m_l = 0, \pm 1$ .

Application of this selection rule to equation (26) yields

$$\nu_H = \nu_0 \text{ for } \Delta m_l = 0 \quad (28a)$$

and

$$\nu_H = \nu_0 \pm \frac{eH}{4\pi mc} \text{ for } \Delta m_l = \pm 1 \quad (28b)$$

These frequencies are identical with those obtained on the classical theory for the normal Zeeman effect. Although there are nine possible transitions for the energy levels shown in Figure 125, these are grouped into only three different frequency components as indicated by equations (28a) and (28b). It is thus evident that the orbital angular momentum alone is not sufficient to account for the anomalous Zeeman effect although adequate for the normal Zeeman effect.

## 96. The Landé g-Factor

With the introduction of electron spin, the total angular momentum of the atom  $J$  becomes the vector sum of the orbital and spin angular momenta  $L$  and  $S$ , thus

$$J = L + S. \quad (12)$$

Because of the interaction between these two angular momenta, the vectors  $L$  and  $S$ , while maintaining their relative orientations, precess about their resultant  $J$ . The magnetic moment due to the orbital motion,  $\mu_L$ , is given by

$$\mu_L = L \frac{eh}{4\pi mc}. \quad (17)$$

Because of the negative charge,  $\mu_L$  is directed oppositely to  $L$ . The magnetic moment due to the spin of the electron is given by

$$\mu_S = 2S \frac{eh}{4\pi mc}. \quad (19)$$

Again  $\mu_S$  is directed oppositely to  $S$  because of the negative charge of the electron. The relationships between the magnetic moments and the angular momenta are shown in Figure 126. In the scale chosen,  $\mu_L$  is drawn twice the length of  $L$ ; hence  $\mu_S$  must be drawn four times the length of  $S$ . The resultant magnetic moment  $\mu$  is therefore not along  $J$ . Because the vectors  $L$  and  $S$  precess about  $J$ ,  $\mu_L$  and  $\mu_S$  must also precess about  $J$ . If each of these vectors is resolved into two components, one parallel to  $J$  and the other perpendicular to it, then the value of the perpendicular component

of each vector, averaged over a period of the motion, will be zero, since it is constantly changing direction. The effective magnetic

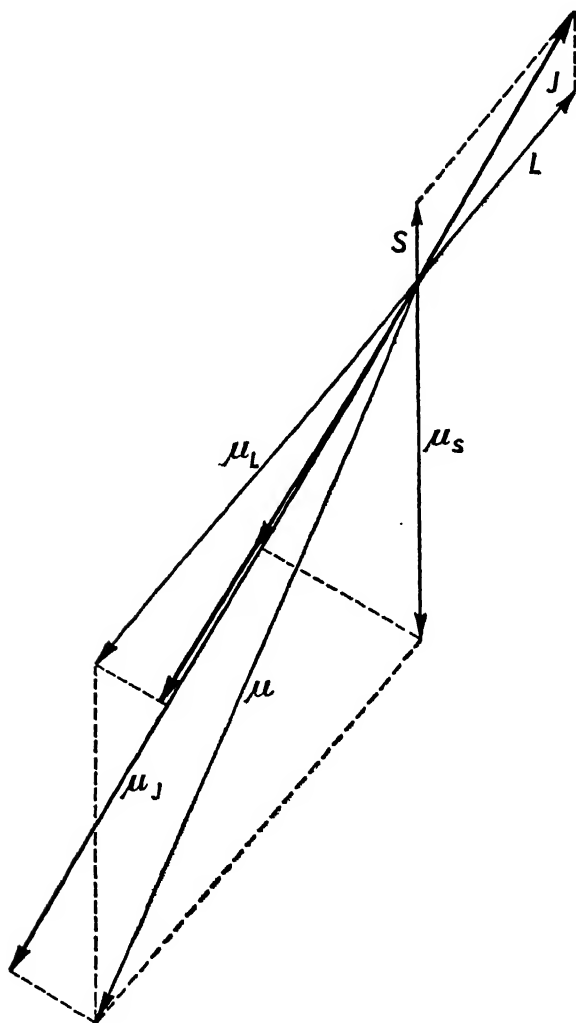


FIG. 126. — Diagram showing the relationship between the magnetic moment vectors and the angular momentum vectors.

moment of the atom will therefore be  $\mu_J$ , the sum of the components of  $\mu_L$  and  $\mu_S$  along  $J$ . This is given by

$$\mu_J = \mu_L \cos (L, J) + \mu_S \cos (S, J) \quad (29)$$

where  $\cos (L, J)$  represents the cosine of the angle between  $L$  and  $J$ ,

and similarly  $\cos(S, J)$  represents the cosine of the angle between  $S$  and  $J$ . By applying the cosine law to the triangle formed by  $L, S, J$  in a manner analogous to that used in deriving equation (11), we get

$$\cos(L, J) = \frac{L(L+1) + J(J+1) - S(S+1)}{2\sqrt{L(L+1)}\sqrt{J(J+1)}}$$

and

$$\cos(S, J) = \frac{S(S+1) + J(J+1) - L(L+1)}{2\sqrt{S(S+1)}\sqrt{J(J+1)}}$$

Substituting these values in equation (29) as well as the values of  $\mu_L$  and  $\mu_S$  from equations (17) and (19) respectively, we get

$$\mu_J = \frac{eh}{4\pi mc} \frac{3J(J+1) + S(S+1) - L(L+1)}{2\sqrt{J(J+1)}}$$

Multiplying numerator and denominator of the above equation by  $\sqrt{J(J+1)}$ , we get

$$\mu_J = \frac{eh}{4\pi mc} \sqrt{J(J+1)} \left( 1 + \frac{J(J+1) + S(S+1) - L(L+1)}{2J(J+1)} \right)$$

or

$$\mu_J = \frac{eh}{4\pi mc} g \sqrt{J(J+1)}, \quad (30)$$

where

$$g = 1 + \frac{J(J+1) + S(S+1) - L(L+1)}{2J(J+1)}. \quad (31)$$

$g$  is called the Landé  $g$ -factor. It determines the splitting of the energy levels in the presence of a weak external magnetic field and shows that this splitting is determined by the values of  $L, S$ , and  $J$ . For levels in which the total spin  $S$  is zero,  $\mu_J$  will be opposite in direction to  $L$ , and the energy levels will split up in a magnetic field in a manner identical with that shown for the normal Zeeman effect.

If the atom is placed in a magnetic field  $H$  which is relatively weak so that the coupling between  $L$  and  $S$  is not broken down, then their resultant  $J$  will precess about the direction of the magnetic field as an axis. The additional energy  $\Delta\mathcal{E}$  due to the action

of the magnetic field on this atomic magnet will be

$$\begin{aligned}\Delta\mathcal{E} &= \mu_J H \cos(J, H) \\ &= g \frac{eh}{4\pi mc} H \sqrt{J(J+1)} \cos(J, H).\end{aligned}\quad (32)$$

But  $\sqrt{J(J+1)} \cos(J, H)$  is the projection of the vector  $J$  on the direction of the magnetic field, and is given by the magnetic quantum number  $m_J$ , so that

$$\Delta\mathcal{E} = \frac{eh}{4\pi mc} H g m_J. \quad (33)$$

The quantity  $\frac{eh}{4\pi mc} H$

is called a *Lorentz unit*; it is a unit of energy used for expressing the splitting up of the energy levels in a magnetic field.

## 97. Anomalous Zeeman Effect

When the light from a sodium flame or arc, which has been placed in a magnetic field of about 30,000 oersteds, is examined with the aid of a spectroscope of high resolving power, it is found that each of the lines of the principal series exhibits the following anomalous Zeeman pattern: the longer wave-length component,  $3^2S_{1/2} - 2^2P_{1/2}$ , splits into four lines, while the shorter wave-length component splits into six lines. The splitting of the energy levels giving rise to these lines can be determined with the aid of equation (33). This will be done for the sodium  $D$  lines as typical of the lines of the principal series.

For the  $3^2S_{1/2}$  energy level,  $L = 0$ ,  $S = \frac{1}{2}$ ,  $J = \frac{1}{2}$ ; hence from equation (31)

$$g = 1 + \frac{\frac{1}{2} \cdot \frac{3}{2} + \frac{1}{2} \cdot \frac{3}{2}}{2 \cdot \frac{1}{2} \cdot \frac{3}{2}} = 2.$$

Since  $m_J$  can have the values  $\frac{1}{2}$  and  $-\frac{1}{2}$ ,  $gm_J$  can have the values  $+1$  and  $-1$ . Table XII gives the values for the quantum numbers necessary for the determination of the splitting factor  $gm_J$  for each of the energy levels of the sodium  $D$  lines.

Figure 127 shows the Zeeman components which appear when the light from the source is viewed perpendicular to the direction

TABLE XII

State	$L$	$S$	$J$	$g$	$m_J$	$gm_J$
$3^2S_{1/2}$	0	$\frac{1}{2}$	$\frac{1}{2}$	2	$\frac{1}{2}, -\frac{1}{2}$	1, -1
$3^2P_{1/2}$	1	$\frac{1}{2}$	$\frac{1}{2}$	$\frac{2}{3}$	$\frac{1}{2}, -\frac{1}{2}$	$\frac{1}{3}, -\frac{1}{3}$
$3^2P_{3/2}$	1	$\frac{1}{2}$	$\frac{3}{2}$	$\frac{4}{3}$	$\frac{3}{2}, \frac{1}{2}, -\frac{1}{2}, -\frac{3}{2}$	2, $\frac{2}{3}, -\frac{2}{3}, -2$

of the magnetic field. The lines designated by  $\sigma$  are polarized with the electric vector perpendicular to the direction of the magnetic field while the lines designated by  $\pi$  are polarized parallel to the

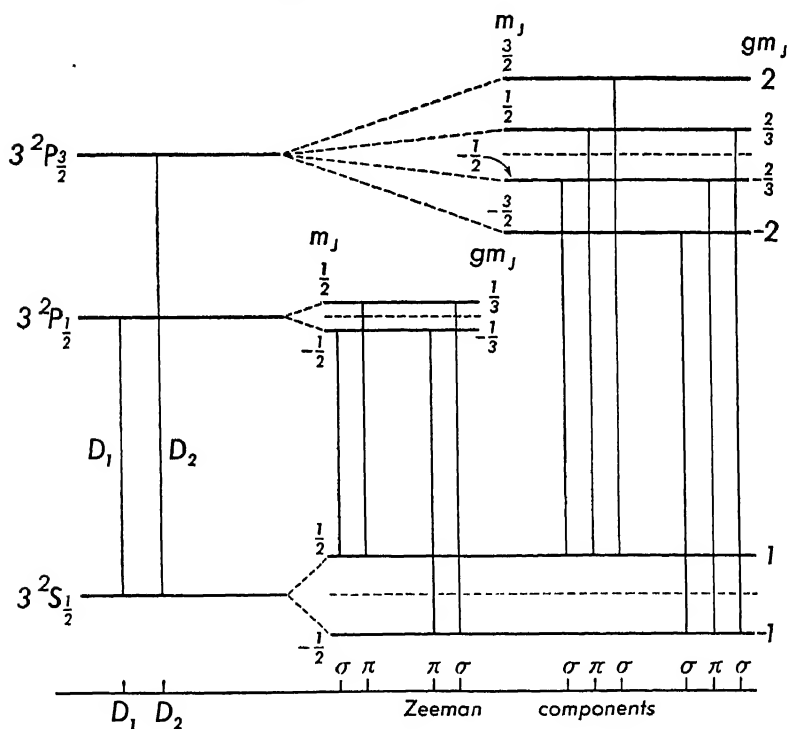


FIG. 127. - Diagram showing the splitting of the energy levels of the sodium  $D$  lines in a weak magnetic field and the transitions giving rise to the anomalous Zeeman pattern according to the selection rule  $\Delta m_J = 0, \pm 1$ .

magnetic field. The polarization of these lines can be predicted from wave mechanical considerations which lead to the result that transitions for which  $\Delta m_J = 0$  give rise to the  $\pi$  components, and the transitions for which  $\Delta m_J = \pm 1$  give rise to the  $\sigma$  components. When the light is viewed parallel to the magnetic field, only the

lines for which  $\Delta m_j = \pm 1$  appear, and these are now circularly polarized. The direction of circular polarization for  $\Delta m_j = +1$  is opposite to that for which  $\Delta m_j = -1$ . Thus the introduction of electron spin has led to complete agreement between the experimental results and the theory of the anomalous Zeeman effect.

## 98. The Stern-Gerlach Experiment and Electron Spin

A direct experimental demonstration of the existence of the magnetic moment of an electron, particularly that due to its spin, is given in an experiment first performed by Stern and Gerlach (1921), using neutral silver atoms. Similar experiments were performed later with other atoms such as hydrogen, lithium, sodium, potassium, copper, and gold. A glance at Table XI will show that the normal state of each of these atoms is a  $^2S_{1/2}$  state, for which  $L = 0$ ,  $J = S = \frac{1}{2}$ . That is, in the normal state of a silver atom, its entire magnetic moment is due to the spin of one electron. It has been shown that when such atoms are placed in a magnetic field of intensity  $H$ , they become oriented in such directions that  $m_j$ , the projection of  $J$  in the direction of the magnetic field, can have the two values  $+\frac{1}{2}$  and  $-\frac{1}{2}$  only. The additional energy of the atom due to its position in the magnetic field is given by

$$\Delta\mathcal{E} = \frac{eh}{4\pi mc} H \cdot g \cdot m_j. \quad (33)$$

If these small atomic magnets are placed in a uniform magnetic field, they will experience torques which will orient them with respect to the magnetic field. If the magnetic field is inhomogeneous, each atomic magnet will also experience a force which will accelerate it. The magnitude of this force on each magnet can be determined by differentiating equation (33) with respect to the space coordinate, say  $x$ , which yields

$$F = \frac{eh}{4\pi mc} \frac{\partial H}{\partial x} \cdot g \cdot m_j, \quad (34)$$

where  $\frac{\partial H}{\partial x}$  determines the inhomogeneity of the magnetic field.

In the Stern-Gerlach experiment, a narrow beam of silver atoms coming from an oven  $O$ , after passing through the defining slits  $S_1$  and  $S_2$ , was allowed to pass through an inhomogeneous



magnetic field and recorded on plate  $P$ , Figure 128. The entire apparatus was in an evacuated chamber. The inhomogeneous magnetic field was produced by an electromagnet with specially

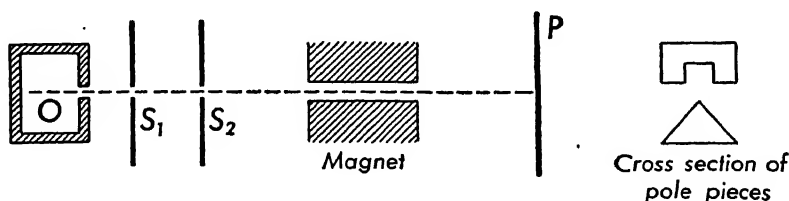


FIG. 128. — Arrangement of apparatus in the Stern-Gerlach experiment.

designed pole pieces. One pole piece was in the form of a knife-edge, while the other pole piece had a channel cut in it parallel to the knife-edge. Each silver atom could assume only one of two possible directions in the magnetic field, given by  $m_J = +\frac{1}{2}$  or  $-\frac{1}{2}$ . It has been shown that for the  $^2S_{1/2}$  state,  $g = 2$ , and  $gm_J = +1$  or  $-1$ , so that the force experienced by each atom due to the inhomogeneity of the field is

$$F = \pm \frac{eh}{4\pi mc} \cdot \frac{\partial H}{\partial x} = \pm M_B \frac{\partial H}{\partial x}, \quad (35)$$

where

$$M_B = \frac{eh}{4\pi mc} = 0.927 \times 10^{-20} \text{ c.m. units.}$$

In terms of the vector model, those atoms with electron spins directed parallel to the magnetic field will experience a force in one direction, while those with oppositely directed spins will experience a force in the opposite direction. According to this, the beam of atoms should split into two beams in its passage through the inhomogeneous magnetic field. This splitting of the beam into two parts of approximately equal intensity was actually observed in these experiments. Figure 129 shows the type of pattern observed in these experiments. From the amount of the separation of the two beams and the degree of inhomogeneity of the magnetic field, it was shown that the component of the magnetic moment of the atom in the direction of the field was equal to one Bohr magneton,  $M_B$ .

The results of the Stern-Gerlach experiment, together with the

explanation of the multiplicity of atomic energy levels and the anomalous Zeeman effect, strongly support the hypothesis of the existence of an electron spin.

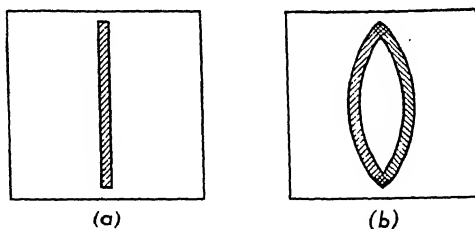


FIG. 129. — Type of pattern on photographic plate made by a beam of silver atoms (a) without magnetic field on, (b) with magnetic field on.

## 99. Spectra of Two-Electron Atoms

Atoms of the alkaline earth elements, beryllium, magnesium, calcium, strontium, barium, and radium, have two electrons outside a closed configuration typical of the inert elements. The total angular momentum of any one of these atoms is merely the sum of the angular momenta of the two electrons outside the closed core. When the atom is in the normal state, both electrons have the same principal quantum number  $n$  and are in the completed subgroup for which  $l = 0$ . The application of Pauli's principle leads to the conclusion that the two electrons must have their spins in opposite directions, so that the total spin quantum number  $S = s_1 + s_2 = \frac{1}{2} - \frac{1}{2} = 0$ . The total angular momentum  $J = L + S = 0$ , so that the normal state is a singlet state and is designated by the symbol  $^1S_0$ .

The excited states of a two-electron system can arise from a variety of configurations of the two electrons consistent with the Pauli exclusion principle. The  $P$  states, for example, are due to those combinations of the angular momenta  $l_1$  and  $l_2$  whose vector sum  $L = l_1 + l_2$  is unity. For the  $D$  states  $L = l_1 + l_2 = 2$ , and so on. The spin vector  $S$  can have only two values  $S = \frac{1}{2} + \frac{1}{2} = 1$  or  $S = \frac{1}{2} - \frac{1}{2} = 0$ . If  $S = 0$ , then  $J = L$ , and the state is a singlet state such as  $^1P_1$  for  $L = 1$ ,  $^1D_2$  for  $L = 2$ , and so on. If  $S = 1$ , then  $J$  can have the three values  $L + 1$ ,  $L$ ,  $L - 1$ , yielding a triplet state such as  $^3P_2$ ,  $^3P_1$ ,  $^3P_0$ , for  $L = 1$ ;  $^3D_3$ ,  $^3D_2$ ,  $^3D_1$  for  $L = 2$ , and so on. A two-electron system therefore has two distinct sets of energy levels, the singlet set arising from configura-

tions in which the electron spins are in opposite directions,  $S = 0$ , and the triplet set arising from configurations in which the electron spins are in the same direction,  $S = 1$ . In this latter set must be included those states for which  $L = 0$  and  $S = 1$ , even though  $J$  has only the single value unity. These states are designated as  ${}^3S_1$  states, and are customarily called triplet states.

The energy level diagram of calcium showing some of the singlet and triplet states is given in Figure 130. These energy levels are for those configurations in which one electron always remains in the  $4s$  state ( $n_1 = 4$ ,  $l_1 = 0$ ), while the second electron changes its state. Other energy levels, in which neither electron is in the  $4s$  level, are known to exist, but they will not be considered here. Some of the transitions giving rise to spectral lines are indicated in the figure. It is found that, as a general rule, singlet terms combine with other singlet terms and triplet terms combine with other triplet terms. Intercombination lines due to transitions between triplet and singlet states have been found, but are few in number and are usually less intense than the nonintercombination lines. Several intercombination lines are shown in the figure.

When the changes in the atomic states are produced by jumps of a single electron, only those spectral lines will be observed which are permitted by the selection rule  $\Delta l = \pm 1$ . In such cases, the selection rule for  $L$  is also  $\Delta L = \pm 1$ . The selection rule for  $J$  is  $\Delta J = 0$  or  $\pm 1$ , with the exception that the transition from  $J = 0$  to  $J = 0$  is forbidden. Transitions between singlet states produce spectral series consisting of singlet lines. Transitions between triplet states produce spectral series consisting of lines which exhibit fine structure when examined with instruments of high resolving power. The lines of the principal series, due to the transitions  $5{}^1S_1 - n{}^3P_{2,1,0}$ , never have more than three components. Similarly the lines of the sharp series, due to the transitions  $4{}^3P_{2,1,0} - n{}^3S_1$ , may have three components. The lines of the diffuse series,  $4{}^3P_{2,1,0} - n{}^3D_{3,2,1}$  and of the fundamental series,  $3{}^3D_{3,2,1} - n{}^3F_{4,3,2}$ , may have as many as six components.

If a calcium atom should find itself in a  $4{}^3P_2$  state or a  $4{}^3P_0$  state, then, according to the selection rules, it will not be able to return to the normal state with the emission of radiation. Such states are called *metastable* states. The atom may go from the

metastable state to the normal state if it gives up the appropriate amount of energy to another atom during a collision process. Or the atom may absorb radiation which will raise it from the met-

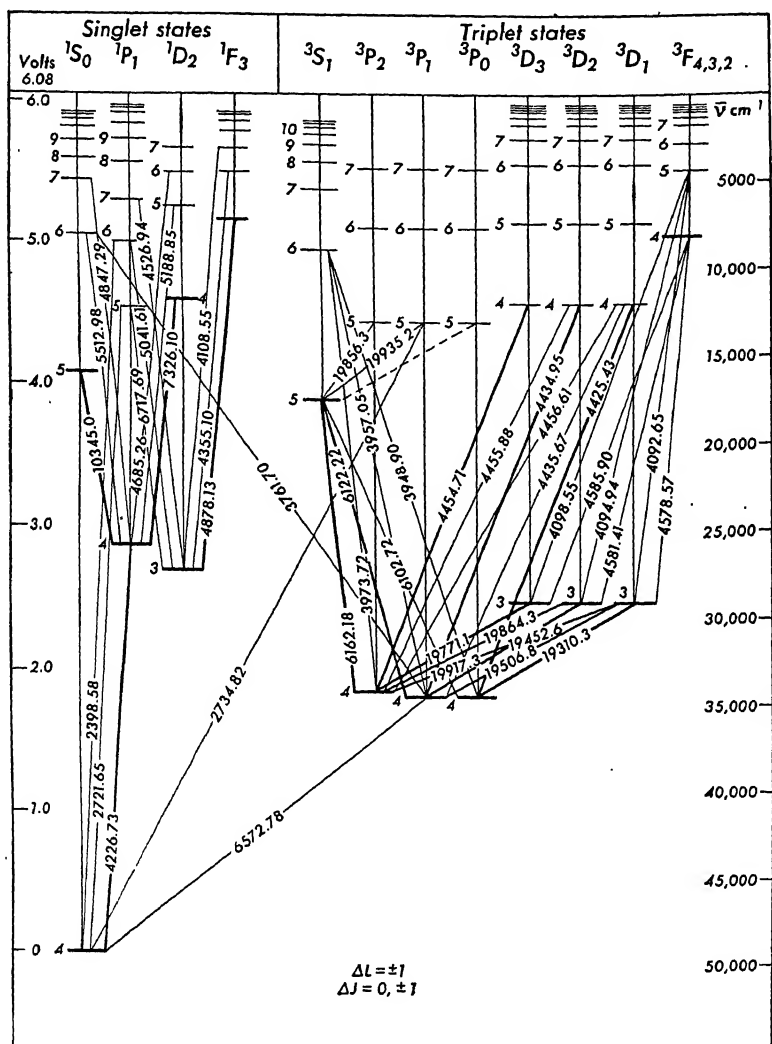


FIG. 130. — Energy level diagram of calcium. Wave lengths of the lines are in Å.

astable state to a higher energy state, from which, selection rules permitting, it may return to the normal state with the emission of radiation.

It is interesting to note that the lines of the singlet series exhibit the normal Zeeman effect, while the lines of the triplet series exhibit the anomalous Zeeman effect. This is in agreement with deductions from the Landé  $g$ -formula. For the singlet series,  $S = 0$ ,  $J = L$ , and therefore  $g = 1$ , so that the splitting up of the energy levels will be in whole multiples of the Lorentz unit, and the permitted transitions will produce the normal Zeeman pattern.

In addition to the alkaline earth elements, there are other elements such as zinc, cadmium, and mercury, which possess singlet and triplet sets of atomic energy levels as determined from spectroscopic analysis. Examination of Table XI shows that these atoms contain two electrons outside closed configurations. Helium, which possesses only two electrons, must also be included in the above group. An interesting point about helium is that no intercombination lines due to transitions between its triplet and singlet states have ever been found. Because of this fact, it was at one time supposed that there were two different kinds of helium, parhelium, possessing singlet states, and orthohelium, possessing triplet states. The difference between the two sets of states is, of course, due to the two possible orientations of the electron spin axes.

## 100. Nuclear Spin and Nuclear Particles

Many of the lines of the spectral series, when examined with spectroscopes of very high resolving power, are found to consist of several lines very close together. Such lines are said to exhibit *hyperfine* structure. Two distinct types of hyperfine structure have been observed. One type, in which the lines of a spectral series all have the same number of components, has been explained as due to the presence of two or more isotopes of the element. The discovery of the hydrogen isotope of mass number 2, discussed in § 77, depended upon the finding of an additional component in the lines of the Balmer series displaced slightly from the Balmer lines coming from hydrogen atoms of mass number 1. The relative intensities of the components of a line are directly related to the relative abundance of the isotopes. Such isotopic hyperfine structure has been observed in the spectral lines of many elements.

The second type of hyperfine structure cannot be explained as due to the presence of isotopes because it has been found in the

spectral lines of elements, such as bismuth, which are believed to consist of single isotopes only. In these cases, the number of components is different for different spectral lines, and their relative displacements are such that they cannot be explained on the basis of the existence of other isotopes. The explanation of this type of hyperfine structure of spectral lines, suggested by Pauli, is that the nucleus of the atom also spins about an axis, and possesses a nuclear angular momentum due to spin of amount

$$I \frac{h}{2\pi},$$

where  $I$  is the nuclear spin quantum number.

The total angular momentum of the atom will now be the vector sum of the nuclear angular momentum and the total electronic angular momentum, and is denoted by  $F \frac{h}{2\pi}$  where

$$F = I + J. \quad (36)$$

$F$ , the vector sum of  $I$  and  $J$ , is called the hyperfine quantum number and is restricted to integral or odd half-integral values. It is beyond the scope of this book to give an extended discussion of the analysis of hyperfine structure. Some of the results of this analysis, however, are of interest, since they have been used in predicting the types of particles that probably exist in the nucleus. For this reason, some of the values of the *nuclear* spin quantum number  $I$  are listed in Table XIII.

An examination of Table XIII shows that the spin quantum number  $I$  is zero for isotopes of even atomic number and even mass number; that is, the spectral lines from these isotopes exhibit no hyperfine structure. The isotopes whose spectral lines exhibit hyperfine structure can be classified into three groups: (1) for isotopes of even atomic number and odd mass number,  $I$  is an odd half-integer; (2) for isotopes of odd atomic number and odd mass number,  $I$  is also an odd half-integer, and (3) for isotopes of odd atomic number and even mass number,  $I$  is an integer.

The argument which follows is based on the assumption that the spin angular momentum of the nucleus is the vector sum of the spin angular momenta of the particles within the nucleus and

that these spins are aligned with their axes either parallel or antiparallel. That is, we are carrying over into the nucleus the same type of hypothesis which was found to work for the electrons outside the nucleus. Before the discovery of the neutron, the nucleus

TABLE XIII

THE NUCLEAR SPIN QUANTUM NUMBERS OF SOME ELEMENTS			
Atomic Number $Z$	Element	Isotopic Mass Number $A$	Nuclear Spin Quantum Number $I$
1	H	1	$\frac{1}{2}$
1	H	2	1
2	He	4	0
3	Li	6	1
3	Li	7	$\frac{3}{2}$
7	N	14	1
8	O	16	0
9	F	19	$\frac{1}{2}$
15	P	31	$\frac{1}{2}$
17	Cl	35	$\frac{3}{2}$
80	Hg	199	$\frac{1}{2}$
80	Hg	201	$\frac{3}{2}$
80	Hg	198, 200 } 202, 204 }	0
82	Pb	207	$\frac{1}{2}$
82	Pb	204, 206, 208	0
83	Bi	209	$\frac{9}{2}$

was assumed to consist of  $A$  protons and  $A-Z$  electrons; the resultant nuclear charge was therefore equivalent to  $Z$  protons. The total number of particles in the nucleus was thus  $2A-Z$ . Since  $2A$  is always an even number, every element of odd atomic number would possess an odd number of particles, and its spin quantum number  $I$  should be an odd half-integer. This is not always found to be so experimentally. For example, nitrogen,  ${}^7\text{N}^{14}$ , has a spin quantum number  $I = 1$ . Similarly, the lithium isotope,  ${}^6\text{Li}$ , has a spin quantum number  $I = 1$ . Consider the odd isotopes of mercury of mass numbers 199 and 201. Since  $Z = 80$ ,

$2A-Z$  is an even number for each of these isotopes, but  $I$  is found to be an odd half-integer in each case. After the discovery of the neutron, Heisenberg suggested that the nucleus should consist of protons and neutrons only, and that each particle should have a spin angular momentum of  $\frac{1}{2} \frac{h}{2\pi}$ . On this basis the number of protons in the nucleus is equal to the atomic number  $Z$ , and the number of neutrons in the nucleus is  $A-Z$ . The total number of particles in the nucleus is equal to the mass number  $A$ . The isotopes of any one element therefore differ only in the number of neutrons in the nucleus. The discrepancies in the values of the spin quantum numbers mentioned above now disappear. On Heisenberg's hypothesis,  $I$  should be an integer for isotopes of even atomic mass number, and should be an odd half-integer for isotopes of odd atomic mass number. These predictions are in agreement with experimental results.

### 101. Characteristic X-Ray Spectra

Moseley (1913) made a systematic investigation of the characteristic X-ray spectra of the elements. The elements investigated were used as targets in X-ray tubes and the radiation from each target was analyzed with the aid of a single crystal spectrometer. A potassium ferrocyanide crystal was mounted on the spectrometer table and the spectrum was recorded on a photographic plate. The spectrometer and the photographic plate were placed in an evacuated chamber to avoid absorption of the long

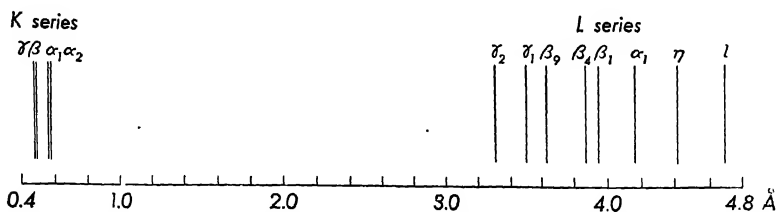


FIG. 131. — Relative positions of the  $K$  and  $L$  X-ray series spectral lines of silver.

wave-length X rays in the air. The spectral lines observed were grouped into two series, a short wave-length group known as the  $K$  series, and a comparatively long wave-length group known as the  $L$  series. The wide separation of these two series of lines is illustrated in Figure 131 for the case of silver in which the  $K$  series



wave lengths extend from  $0.485\text{\AA}$  to  $0.563\text{\AA}$ , while the  $L$  series lines are in the wave-length range  $3.3\text{\AA}$  to  $4.7\text{\AA}$ . Other investigators have found two other series of lines of still longer wave

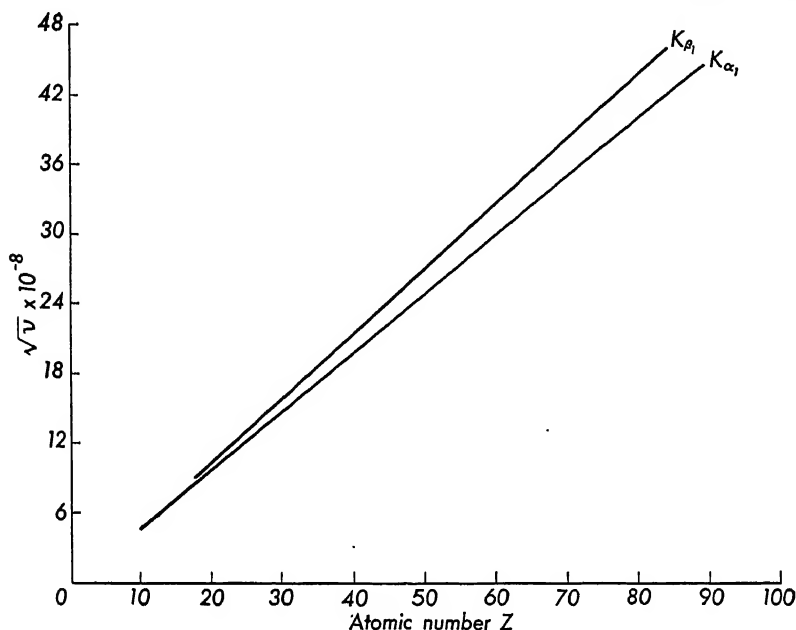


FIG. 132. — Moseley diagram in which the square root of the frequency is plotted against the atomic number of the emitting element for two lines of the  $K$  series.

lengths in the heavier elements,  $Z > 66$ , classified as  $M$  series and  $N$  series.

Moseley found that the character of a given series was practically the same for all the elements studied, and that the frequency of a particular line of a series varied in a regular manner from element to element in the periodic table. By plotting the square root of the frequency of one of the lines, say the  $K_{\alpha}$  line (the most intense line of the  $K$  series), against the atomic number of the element emitting this line, Moseley obtained a straight line. Figure 132 shows such a graph, now known as a Moseley diagram. The  $K_{\alpha}$  line is actually a doublet; in Moseley's work this doublet was not resolved but appeared as a single line. The equation of any one of the lines on a Moseley diagram, to a good approximation, is given by

$$\nu = C(Z - a)^2 \quad (37)$$

where  $C$  and  $\alpha$  are constants. For the  $K_\alpha$  line,  $C$  was found to be equal to  $\frac{3}{4}R$ , where  $R$  is the Rydberg constant, and  $\alpha$  was found to be practically 1. The equation for the frequency of the  $K_\alpha$  line of any element can therefore be written as

$$\nu_{K_\alpha} = \frac{3}{4}R(Z - 1)^2. \quad (38)$$

It must be remembered that Moseley did this work more than a quarter of a century ago. Some of the elements now known were then unknown. The atomic number of an element merely represented its position in the arrangement of the elements according to their atomic weights. In order to obtain a straight line for the curve,  $\sqrt{\nu}$  against  $Z$ , Moseley had to rearrange the orders of nickel and cobalt, assigning the lower atomic number to the element of higher atomic weight. Furthermore a gap had to be left at  $Z = 43$ , showing the existence of an element, masurium, then unknown.

Moseley's work followed closely upon the introduction of Rutherford's nuclear theory of the atom and Bohr's theory of hydrogen. The relationship between Bohr's theory and Moseley's work can best be shown by rewriting equation (38) for the frequency of the  $K_\alpha$  line to read

$$\nu_{K_\alpha} = R(Z - 1)^2 \left( \frac{1}{1^2} - \frac{1}{2^2} \right). \quad (39)$$

The interpretation of this equation on the Bohr theory is that the  $K_\alpha$  line is emitted when an electron goes from the orbit of principal quantum number  $n = 2$  to the orbit of principal quantum number  $n = 1$ . The appearance of the factor  $(Z - 1)$  rather than  $Z$  in equation (39) can be explained by assuming that the electron which goes from orbit  $n = 2$  to  $n = 1$  is "screened" from the total nuclear charge  $Z$  by the negative charge of a single electron. This explanation can best be understood by considering the manner in which X rays are produced. The element in the target consists of neutral atoms in which the first shell,  $n = 1$ , contains two electrons, and, according to Pauli's principle, no more electrons can get into this  $K$  shell. The only time an electron can go from the  $L$  shell,  $n = 2$ , to the  $K$  shell is when one of the electrons is missing from the  $K$  shell. The obvious inference is that, during the operation of the X-ray tube, a cathode ray knocks out an electron from the  $K$  shell of an atom. Since most of the other shells have

their full quota of electrons, this  $K$  electron will have to go either to one of the unoccupied outer levels or completely outside the atom, depending upon the amount of energy transferred to the atom by the incident cathode ray. As a result of this process, the  $K$  shell will now have only one electron in it. If an electron from the  $L$  shell should go into the  $K$  shell, it will do so with the emission of a quantum of radiation whose frequency is that of the  $K_{\alpha}$  line. The electron which goes from the  $L$  shell to the  $K$  shell moves in an electric field which is essentially that of the positive nuclear charge and the negative charge of the single electron still remaining in the  $K$  shell. This electric field is therefore equivalent to that of a positive charge of magnitude  $(Z - 1)e$ . The effect of the outer electrons on this electric field can be shown to be very small.

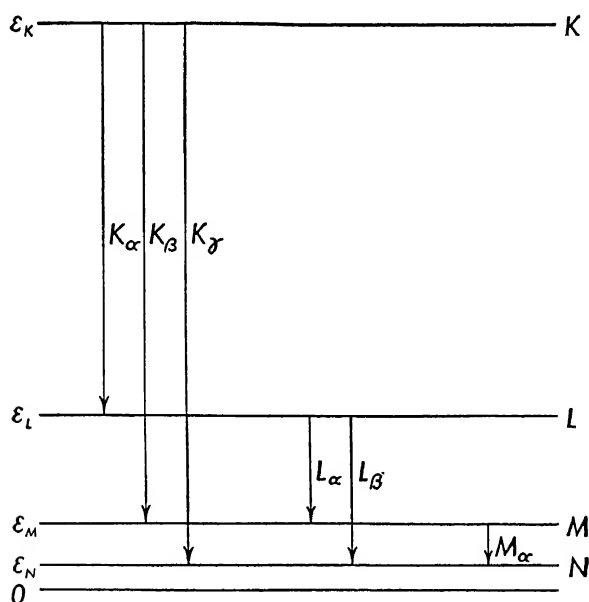


FIG. 133. — Simplified X-ray energy level diagram.

## 102. X-Ray Energy Level Diagram

A simplified energy level diagram can be used to show the changes in atomic configuration which give rise to the  $K$  and  $L$  series of X-ray spectral lines. In this diagram, Figure 133, the zero energy level is taken as that of the normal state of the neutral

atom. This differs from the optical case in which the zero level of energy is that of the ionized atom. Let us assume that the cathode ray which is incident on an atom has sufficient energy to remove one electron from the  $K$  shell to the outside of the atom. If  $\mathcal{E}_K$  represents the work done in removing this  $K$  electron, then the energy of the system can be represented at a level  $\mathcal{E}_K$  above the zero level. This atom is now ionized with one electron missing from the  $K$  shell.

Let us consider the same neutral atom once more and suppose that the impinging cathode ray has not sufficient energy to remove an electron from the  $K$  shell, but does have sufficient energy to remove one from the  $L$  shell to the outside. Then, if the atom is ionized by the removal of one electron from the  $L$  shell, the energy of the system will be  $\mathcal{E}_L$ , and can be represented by a line at the proper height above the zero level. Similarly  $\mathcal{E}_M$  represents the work done in ionizing a neutral atom by removing an electron from the  $M$  shell, and  $\mathcal{E}_N$  represents the work done in removing an electron from the  $N$  shell of a neutral atom.

Suppose that the atom is now in the energy state  $\mathcal{E}_K$ , that is, one electron is missing from the  $K$  shell. If an electron goes from the  $L$  shell to the  $K$  shell, the atom will then be in the energy state represented by  $\mathcal{E}_L$ ; that is, one electron will now be missing from the  $L$  shell. The frequency of the spectral line radiated when an electron goes from the  $L$  to the  $K$  shell, or when the energy state of the atom is changed from  $\mathcal{E}_K$  to  $\mathcal{E}_L$ , is given by Bohr's frequency condition:

$$\nu_{K_\alpha} = \frac{\mathcal{E}_K - \mathcal{E}_L}{h}. \quad (40)$$

There is also a definite probability that an electron might go from the  $M$  shell directly to the  $K$  shell, leaving the atom in the energy state  $\mathcal{E}_M$ . The line emitted in this transition is the  $K_\beta$  line; its frequency is given by

$$\nu_{K_\beta} = \frac{\mathcal{E}_K - \mathcal{E}_M}{h}. \quad (41)$$

Or an electron may go from the  $N$  shell directly to the  $K$  shell with the emission of the  $K_\gamma$  spectral line of frequency

$$\nu_{K_\gamma} = \frac{\mathcal{E}_K - \mathcal{E}_N}{h}. \quad (42)$$

Similar analyses can be used for the transitions producing the  $L$  and  $M$  series of spectral lines. For example, if the atom is in the energy state  $\mathcal{E}_L$ , an electron may go from the  $M$  shell to the  $L$  shell with the emission of the  $L_\alpha$  line of frequency

$$\nu_{L_\alpha} = \frac{\mathcal{E}_L - \mathcal{E}_M}{h}. \quad (43)$$

When the voltage across the X-ray tube is sufficiently high, a very large number of atoms in the target of the tube will be raised to the energy state  $\mathcal{E}_K$ , others to the energy state  $\mathcal{E}_L$ , and so on, by the action of the cathode rays incident upon the target. The  $K$  series of spectral lines will be emitted by those atoms in which the electrons go directly from the  $L$ ,  $M$ , or  $N$  shells to the  $K$  shell; the  $L$  series of spectral lines will be emitted by those atoms in which the electrons go directly from the  $M$  or  $N$  shells to the  $L$  shell. The intensity of a spectral line will be proportional to the number of atoms in which the appropriate transitions take place. The  $K_\alpha$  line, for example, is the most intense line of the  $K$  series, while the  $K_\gamma$  line is the faintest one. In most of the atoms in the energy state  $\mathcal{E}_K$ , therefore, electrons go from the  $L$  shells to the  $K$  shells. Stated in a different manner, the probability that an electron will go from the  $L$  shell to the  $K$  shell is much greater than the probability that an electron will go from the  $M$  shell directly to the  $K$  shell. The probability that an electron will go from the  $N$  shell to the  $K$  shell is very small.

With the precision and resolving power available in modern X-ray spectroscopy, many of the lines have been resolved into two or more components. The  $K_\alpha$  line, for example, has been resolved into two components  $K_{\alpha 1}$  and  $K_{\alpha 2}$  for all elements of atomic number greater than 15. The  $K_\beta$  line has been resolved into two components for most of the elements of atomic number greater than 36. The  $K_\gamma$  line has not yet been resolved. The fine structure observed in X-ray spectral lines must obviously be due to the multiplicity of some of the energy levels. One might determine this multiplicity from an analysis of the emission spectra. It will be more instructive, however, to show how this multiplicity of the energy levels can be determined by more direct experiments in which electrons from the inner shells of atoms are removed from them by the action of X rays from an external source. This is an

extension of the photoelectric effect to the region of X-ray wave lengths. There are two general experimental methods for investigating this phenomenon. One is to study the absorption spectra of the X rays, the other is to determine the energies of the electrons ejected from the atoms.

### 103. X-Ray Absorption Spectra

A method for studying the X-ray absorption spectrum of an element is illustrated in Figure 134. The continuous spectrum from some suitable target *T* is used in this experiment. A narrow

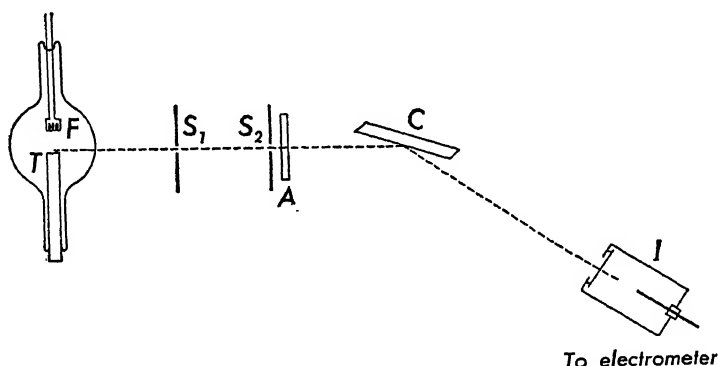


FIG. 134. — Diagram showing arrangement of apparatus for measuring the absorption of X rays.

beam of X rays coming through the slits *S*<sub>1</sub> and *S*<sub>2</sub> is incident upon the absorbing material *A* containing the element under investigation. The transmitted beam is then analyzed by the crystal *C* of the X-ray spectrometer, and the intensity of each wave length  $\lambda$  is measured by the ionization it produces in the ionization chamber *I*. A photographic plate may be used in place of the ionization chamber; the intensity will then be determined by the blackening on the photographic plate.

Each particular setting of the crystal corresponds to a definite wave length given by Bragg's law  $n\lambda = 2d \sin \theta$ . The usual procedure is to measure the intensity, *I*<sub>0</sub>, of a given wave length with the absorbing material removed from the path of the X rays, then to insert the absorbing material in the path of the X rays and measure the new intensity *I* for the same wave length. This procedure is repeated over a wide range of wave lengths. For each

particular wave length,

$$I = I_0 e^{-\mu x}, \quad (\text{Chap. 3, Eq. 40})$$

where  $\mu$  is the absorption coefficient for the wave length used, and  $x$  is the thickness of the absorbing material.

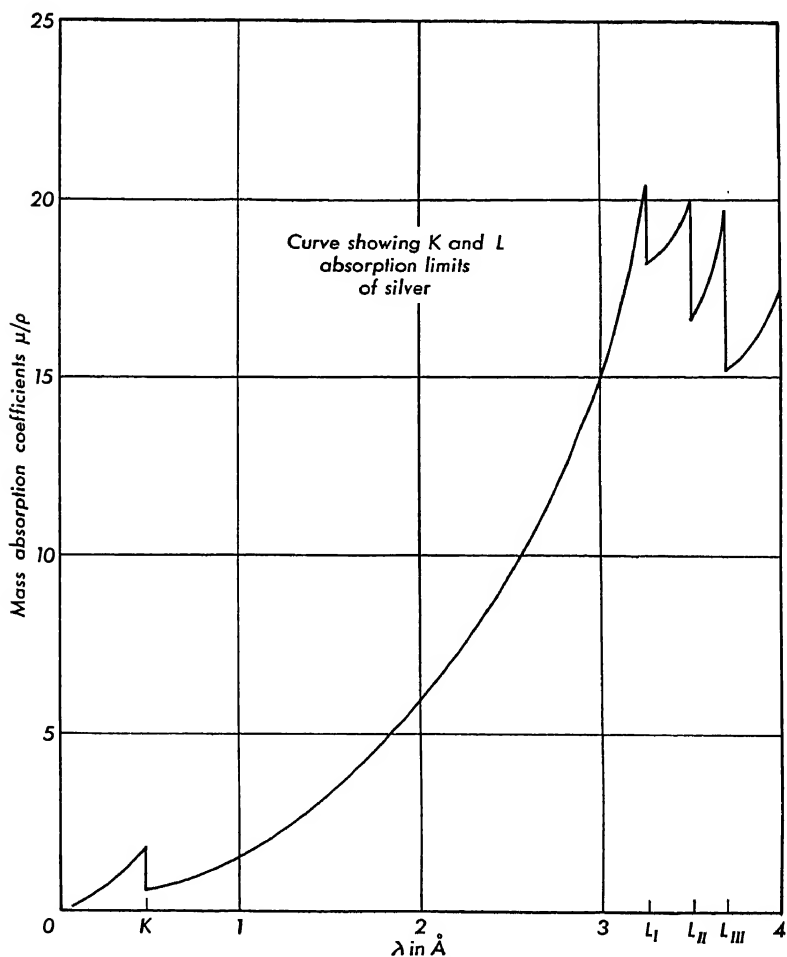


FIG. 135. — Curve showing the K and L X-ray absorption limits of silver.

The results of a typical experiment, using a thin foil of silver as the absorbing material, are shown in Figure 135 where the mass absorption coefficient  $\mu/\rho$  (see § 59), is plotted against the wave length  $\lambda$ . It is found that the mass absorption coefficient increases with the wave length, approximately as  $\lambda^3$ , until a particular wave

length  $\lambda_K$ , at the position  $K$ , is reached, at which wave length  $\mu/\rho$  drops suddenly to a lower value. In the wave-length region between  $K$  and  $L_I$ , the mass absorption coefficient again increases as  $\lambda^3$ ; at  $L_I$  it drops in value. There are three such breaks in the curve close together marked  $L_I$ ,  $L_{II}$ , and  $L_{III}$ . The wave length at which the first break occurs is called the wave length of the  $K$  absorption limit. The other breaks occur at the  $L_I$ ,  $L_{II}$ , and  $L_{III}$  absorption limits.

In the case of silver, the wave length of the  $K$  absorption limit is  $\lambda_K = 0.4845 \text{ \AA}$ . This is slightly less than the shortest wave length which occurs in the  $K$  series lines, the  $K_\gamma$  line, for which  $\lambda = 0.4860 \text{ \AA}$  (see Table XIV). In the production of the lines of the  $K$  series, it was found that an amount of energy,  $\mathcal{E}_K$ , had first to be supplied to the atom to remove an electron from the  $K$  shell, after which an electron from some outer shell, in going into the  $K$  shell, would emit a quantum of radiation. The energy of this quantum is, of course, always less than  $\mathcal{E}_K$ , as shown by equations (40), (41), and (42). When the element forms the target of an X-ray tube, this energy,  $\mathcal{E}_K$ , comes from the kinetic energy of the incident cathode rays or electrons. When the element, however, is used as an absorber of X rays, this energy must come from the incident X rays. If the energy of an incident quantum or photon,  $h\nu$ , is greater than  $\mathcal{E}_K$ , the photon will be able to knock an electron out of the  $K$  shell, thus raising the atom to the energy state  $\mathcal{E}_K$ . The smallest value of the energy of a photon which will be able to remove an electron from the  $K$  shell is

$$h\nu_K = \mathcal{E}_K = \frac{hc}{\lambda_K} \quad (44)$$

where  $\lambda_K$  and  $\nu_K$  represent the wave length and frequency, respectively, of the  $K$  absorption limit. If the energy of the incident photon,  $h\nu$ , is less than  $\mathcal{E}_K$ , then the photon will not be able to remove an electron from the  $K$  shell, but it may have enough energy to be able to remove an electron from one of the higher levels,  $L$ ,  $M$ , or  $N$ .

The fact that there are three absorption limits  $L_I$ ,  $L_{II}$ , and  $L_{III}$  very close together and in the range of wave lengths of the  $L$  series, indicates that the  $L$  shell probably consists of three energy levels. The wave length of the  $L_I$  absorption limit is smaller than that of



TABLE XIV

WAVE LENGTHS OF THE K SERIES LINES AND THE K ABSORPTION LIMIT FOR SOME ELEMENTS (Wave Lengths in Å.)						
Ele- ment	$K_{\alpha_2}$	$K_{\alpha_1}$	$K_{\beta_3}$	$K_{\beta_1}$	$K_{\gamma}$	K Abs. Limit
29 Cu	1.5412	1.5374	—	1.3894	1.3782	1.3774
42 Mo	0.7121	0.7078	0.6315	0.6310	0.6197	0.6185
46 Pd	0.5886	0.5843	0.5201	0.5095	0.5092	0.5080
47 Ag	0.5627	0.5583	0.4967	0.4960	0.4860	0.4845
74 W	0.2134	0.2086	0.1848	0.1840	0.1791	0.1782
78 Pt	0.1900	0.1822	—	0.1637	0.1589	0.1577
79 Au	0.1848	0.1780	—	0.1590	0.1543	0.1532
82 Pb	0.1700	0.1652	—	0.1461	0.1413	0.1405
92 U	0.1310	0.1264	—	0.1119	0.1084	0.1066

any line of the  $L$  series. The energy of each one of the states  $L_I$ ,  $L_{II}$ , and  $L_{III}$  can be obtained from the graph with the aid of equations of the type of equation (44); thus

$$\mathcal{E}_{L_I} = \frac{hc}{\lambda_{L_I}}. \quad (45)$$

It is difficult to obtain the wave lengths of the  $M$  absorption limits by this method because of the absorption of these long wave-length X rays by the element under investigation. It will be recalled that the absorption coefficient varies as the cube of the wave length. In the case of silver, the wave length of the  $M$  limit is about 10 times that of the  $L$  limit so that the absorption would be approximately 1000 times as great. However, the wave lengths of the  $M$  absorption limits have been determined in this manner for some of the heavier elements. In each case, five absorption limits were found in the  $M$  region, indicating that the  $M$  shell consists of five energy levels close together.

#### 104. X-Ray Critical Voltages

The correctness of the above interpretation of the absorption limits can be demonstrated in a fairly direct manner by using the element under investigation as the target in an X-ray tube and

controlling carefully the voltage across the tube. The maximum kinetic energy which the electrons incident upon the target possess is  $Ve$  where  $V$  is the voltage across the tube. The energy required to remove an electron from the  $K$  shell of an atom can be expressed as

$$\mathcal{E}_K = h\nu_K = \frac{hc}{\lambda_K} = V_K e. \quad (46)$$

$V_K$  is called the critical voltage, and is the minimum voltage which, when applied between the anode and cathode of the X-ray tube, will give the impinging electron enough energy to remove electrons from the  $K$  shells. If the voltage across the tube is less than  $V_K$ , the atoms in the target cannot be raised to the energy state  $\mathcal{E}_K$ ; hence the lines of the  $K$  series will not appear in the spectrum. When the voltage across the tube is increased until the value  $V_K$  is reached, then all the lines of the  $K$  series appear simultaneously. This indicates that many of the atoms were raised to the energy state  $\mathcal{E}_K$ , making possible transitions to lower energy states with the radiation of quanta corresponding to the lines of the  $K$  series.

The critical voltage for the production of the  $K$  lines of silver, for example, can be determined from equation (46) by substituting for  $\lambda_K$  its value  $0.4845\text{\AA}$ , and the accepted values for  $e$ ,  $h$ , and  $c$ , yielding  $V_K = 25.5$  kilovolts. When the voltage across a silver target X-ray tube is, say, 20 kilovolts, the spectrum is found to consist of the  $L$  series lines superimposed on the continuous radiation. When the voltage across the tube is increased, the intensities of these two spectra are increased, but no new lines appear until the voltage across the tube reaches the value 25.5 kilovolts, when all the lines of the  $K$  series appear simultaneously. Further increase in voltage produces an increase in the intensities of the characteristic spectra relative to the continuous spectrum.

### 105. Magnetic Spectrum Analysis

The X-ray energy levels of an atom can be determined in an independent way by utilizing the photoelectric effect with X rays of known wave length. If an X-ray quantum of energy  $h\nu$  ejects an electron from an inner shell of the atom, thereby raising the atom to a higher energy state, then the kinetic energy of the

ejected electron will be given by

$$\frac{1}{2}mv^2 = h\nu - \mathcal{E}_{K,L} \dots, \quad (47)$$

where  $\mathcal{E}_{K,L} \dots$  represents the appropriate final energy state of the atom. By measuring the energy of the ejected electron, it is possible to determine the particular energy level from which it was ejected.

H. R. Robinson developed the magnetic spectrograph for de-

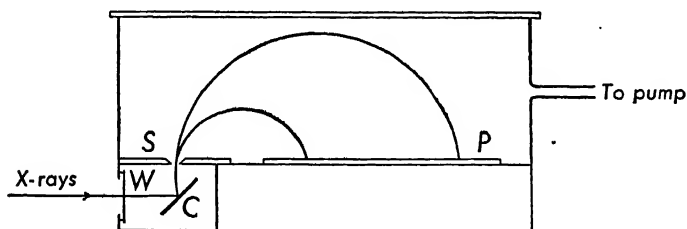


FIG. 136. — Robinson's magnetic spectrograph.

termining the velocities of the ejected electrons. A diagram of the apparatus is shown in Figure 136. The element to be investigated, usually in the form of a very thin foil, is placed upon a holder at  $C$ . A narrow beam of monochromatic X rays, usually the intense  $K\alpha$  line from a known target material, enters through the thin window  $W$  in the evacuated box  $B$  and strikes the element on  $C$ . The entire apparatus is in a uniform magnetic field of intensity  $H$  perpendicular to the plane of the figure. The electrons which are ejected from the element at  $C$  move in circular paths under the influence of the magnetic field. Only those electrons which pass through the slit  $S$  will be able to strike the photographic plate  $P$ . Because of the geometry of the apparatus, all electrons with the same velocity will be focused at the same distance from the source  $C$ . The radius of the electronic path is half the distance from  $C$  to the point on the photographic plate which has been blackened by the electrons.

The velocities of the electrons ejected from  $C$  can be found with the aid of the well-known equation

$$Hev = \frac{mv^2}{r}$$

or

$$v = Hr \cdot \frac{e}{m},$$

where  $r$  is the radius of the path of an electron. In any one experiment, the electron ejected from the innermost shell will have the smallest velocity and its path will have the smallest radius  $r$ . Electrons ejected from the outer shells of the atom, such as the  $M$  and  $N$  shells, will have greater energy and be focused farther out on the photographic plate. From the positions of the lines on the photographic plate, the energies of the ejected electrons can be computed. By substituting the value of the electronic energy in equation (47), the energy required to remove the electron from its particular shell can be determined.

The values of the energy levels of a large number of elements were determined in this way by Robinson. His measurements are in agreement with results obtained from X-ray absorption spectra. In addition, he determined the energy values of the  $M$  levels of many elements as well as some of the  $N$  levels.

## 106. X-Ray Terms and Selection Rules

The X-ray term structure or energy level diagram can be built up from analyses of the emission and absorption spectra of the elements, and from the determination of the energy levels by the magnetic spectrum analysis of the energies of electrons ejected from these levels. The complete energy level diagram of uranium,  $Z = 92$ , is shown in Figure 137, with the X-ray notation for these levels and some of the transitions giving rise to the X-ray spectral lines. It must be remembered that each X-ray energy level represents a state of an atom which has one electron missing from a closed shell. Pauli pointed out that in a configuration in which an electron is missing from a completed subgroup, the spectral term is the same as if that one electron alone occupied the subgroup. Normally there are two  $1s$  electrons in the  $K$  shell; if one electron is removed, the energy state of the atom will be that of a  $1s$  electron, namely,  $^2S_{1/2}$ , just as in the case of an alkali atom. The  $L$  shell consists of two subgroups, one for which  $l = 0$  and the other  $l = 1$ . There are normally two electrons in the subgroup  $n = 2, l = 0$ ; if one  $2s$  electron is removed, the energy state of the atom will be that of a single electron for which  $n = 2, l = 0$ , namely, a  $2s\ ^2S_{1/2}$  configuration. This is the energy level  $L_I$ . There are normally six  $2p$  electrons in the completed subgroup  $n = 2, l = 1$ . If one  $2p$  electron is removed, the energy state of

the atom will be a  $P$  state; this state will be a doublet state corresponding to the two possible values of  $j$ , that is,  $j = \frac{1}{2}$ , or  $j = \frac{3}{2}$ . The two energy states  $L_{II}$  and  $L_{III}$  therefore correspond to the

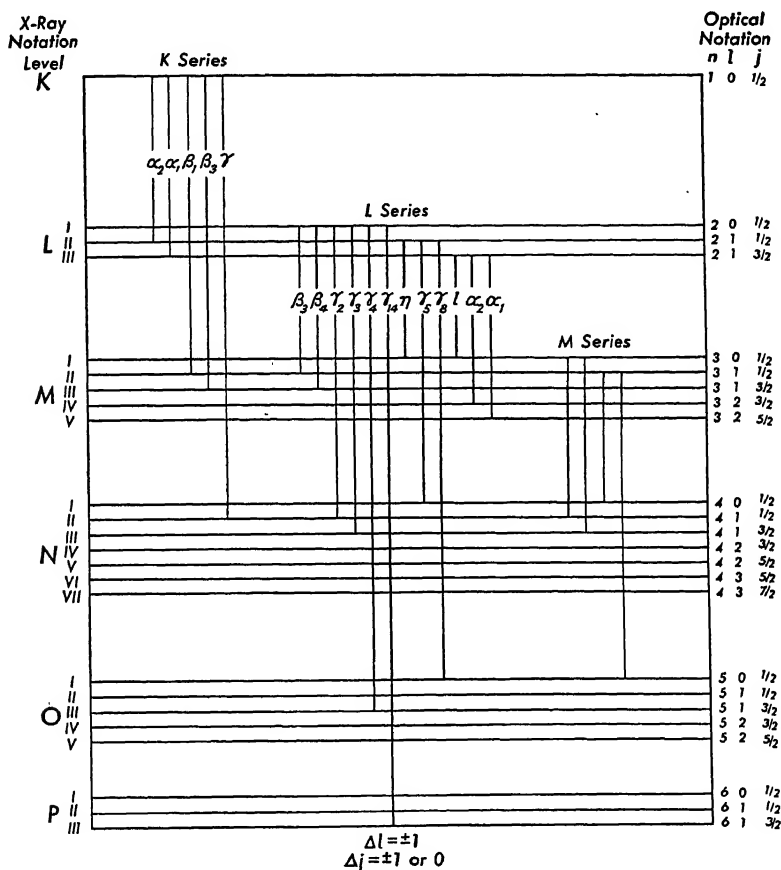


FIG. 137. - X-ray energy level diagram for a heavy element such as uranium showing some of the transitions giving rise to spectral lines. (Not drawn to scale.)

doublet terms  $^2P_{1/2}$  and  $^2P_{3/2}$  respectively, again similar to the terms of the alkali atoms. This procedure can be carried out for each of the subgroups. For example, the removal of an electron from a subgroup for which  $l = 2$  gives rise to the  $^2D_{3/2}$  and  $^2D_{5/2}$  terms. The optical notations and the  $(n, l, j)$  values for each energy level are shown in the figure. One difference between X-ray energy levels and alkali terms should be noted: the higher X-ray energy states are designated by the smaller quantum numbers.

The selection rules for the permitted transitions are the same as those for the alkali atoms, namely,

$$\Delta L = \pm 1.$$

$$\Delta J = 0 \text{ or } \pm 1.$$

While no restrictions are placed on changes in the principal quantum number  $n$ , transitions for which  $\Delta n = 0$  are very rare, and the lines produced by such transitions are of very small intensity. The above selection rules account for the transitions giving rise to the more intense lines of the X-ray spectral series. Some fainter lines, forbidden by the above selection rules, have also been observed, as well as some lines which cannot be accounted for by any transitions between states represented in the energy level diagram. A discussion of these lines is beyond the scope of this book.

## REFERENCES

### *Optical spectra*

- BACHER, R. F., and S. GOUDSMIT, *Atomic Energy States*. New York: McGraw-Hill Book Company, Inc., 1932.
- BORN, M., *Atomic Physics*. New York: G. E. Stechert & Company, 1936, Chap. VI.
- HERZBERG, G., *Atomic Spectra and Atomic Structure*. New York: Prentice-Hall, Inc., 1937, Chaps. I, II.
- RICHTMYER, F. K., and E. H. KENNARD, *Introduction to Modern Physics*. New York: McGraw-Hill Book Company, Inc., 1942, Chap. VIII.
- WHITE, H. E., *Introduction to Atomic Spectra*. New York: McGraw-Hill Book Company, Inc., 1934.
- WOOD, R. W., *Physical Optics*. New York: The Macmillan Company, 1934, Chaps. V, XVII, XXI.

### *X-ray spectra*

- COMPTON, A. H., and S. K. ALLISON, *X-Rays in Theory and Experiment*. New York: D. Van Nostrand Company, Inc., 1935, Chaps. I, VII, VIII.
- RICHTMYER, F. K., and E. H. KENNARD, *Introduction to Modern Physics*. New York: McGraw-Hill Book Company, Inc., 1942, Chap. X.
- SIEGBAHN, M., *The Spectroscopy of X-Rays*. New York: Oxford University Press, 1925, Chaps. IV-VI, VIII.

## PROBLEMS

1. Using vector diagrams, determine the different values for the total orbital angular momentum of a two-electron system for which  $l_1 = 3$  and  $l_2 = 2$ .

*Ans.*  $L = 5, 4, 3, 2, 1$ .

2. Using vector diagrams, determine the possible values of the total angular momentum of an  $f$  electron (a) according to the vector model, (b) according to wave mechanics. (c) Determine the angle between the vectors  $\mathbf{s}$  and  $\mathbf{l}$  in part (b).

*Ans.* (a)  $j = \frac{7}{2}, \frac{5}{2}$ .

(b)  $j = \frac{\sqrt{63}}{2}, \frac{\sqrt{35}}{2}$ .

(c)  $60^\circ, 131^\circ 49'$ .

3. Using vector diagrams, determine the possible values of the total angular momentum of an electron system for which (a)  $L = 2, S = 3$ , (b)  $L = 3, S = 2$ .

4. Using vector diagrams, determine the possible values of the total angular momentum of an electron system for which (a)  $L = 3, S = \frac{5}{2}$ , (b)  $L = 2, S = \frac{3}{2}$ .

5. Determine the electron configuration of (a) barium in the normal state, and (b) mercury in the normal state.

6. Determine the angular velocity of the precessional motion of an electron orbit when a source of light is placed in a magnetic field of 30,000 oersteds. Compare this precessional velocity of the orbit with the change in the angular velocity of the electron on the basis of the classical Lorentz theory.

*Ans.*  $2.64 \times 10^{11} \text{ sec}^{-1}$ .

7. Determine the maximum change in the energy of a  $p$  electron due to the precessional motion of its orbit in a magnetic field of 30,000 oersteds.

*Ans.*  $2.76 \times 10^{-16} \text{ ergs}$ .

8. Draw a diagram showing the relative separations of the sodium  $D$  lines and their Zeeman components produced by a magnetic field of 30,000 oersteds. Use a wave number scale.

9. (a) Using the wave lengths given in the energy level diagram of calcium, determine the values of the two lowest resonance potentials. (b) If electrons of 2.8 ev energy are used to excite the calcium atoms, which spectral lines will be emitted by calcium?

10. Two resonance potentials have been observed with mercury vapor, 4.86 and 6.67 volts. The ionization potential of mercury is 10.38 volts. Compute (a) the wave lengths of the mercury resonance radiation, (b) the wave number of the lowest state of mercury. Check your results by reference to standard tables or energy level diagrams.

11. After studying the X-ray spectrum of platinum, determine the minimum voltage that must be used across the X-ray tube to ensure the appearance of the  $K$  series lines.

*Ans.* 79 kv.

12. Using the data in Table XIV, calculate the energies in electron volts, of the  $L_{II}$  and  $L_{III}$  energy levels for the elements listed in the table. Plot the square roots of these energies against atomic number and discuss any regularities observed in these curves. How do these curves compare with the Moseley diagram?

13. The mass absorption coefficient of X rays of wave length  $\lambda = 0.7\text{\AA}$  is 5 per gram per  $\text{cm}^2$  for aluminum, and 50 per gram per  $\text{cm}^2$  for copper. The density of aluminum is 2.7 grams per  $\text{cm}^3$  and that of copper is 8.93 grams per  $\text{cm}^3$ . What thickness, in cm, of each of these substances is needed to reduce the intensity of the X-ray beam passing through it to one-half its initial value?

*Ans.* Al—0.051 cm.

Cu—0.0016 cm.

14. In an experiment with the magnetic spectrograph, the  $K_{\alpha 1}$  line from a silver target X-ray tube is incident upon a thin copper foil inside the spectrograph. If the intensity of the magnetic field is 100 oersteds, calculate the radius of the smallest electron path that will be observed. What is the origin of these electrons?

*Ans.* 3.88 cm.

15. The wave lengths of the lines obtained on a spectrogram were measured and classified into three series as follows:

Principal Series	Sharp Series	Diffuse Series
6707.85 $\text{\AA}$	8126.5 $\text{\AA}$	6103.5 $\text{\AA}$
3232.6	4971.9	4603.0
2741.3	4273.3	4132.3
2562.5	3985.8	3915.0
2475.3	3838.2	3794.7

From the above data the series limit, expressed in wave numbers, was determined as 43,486  $\text{cm}^{-1}$  for the principal series, and 28,582  $\text{cm}^{-1}$  for the sharp and diffuse series.



- (a) Convert the wave lengths given above to wave numbers.
- (b) Construct an energy level diagram using a wave number scale.
- (c) Determine the ionization potential of this element and then place a voltage scale on the energy level diagram.
- (d) Identify the element.
- (e) Determine the first resonance potential of this element.
- (f) Determine the principal quantum numbers for each energy level.



# Part III

## THE NUCLEUS



# 7

## Natural Radioactivity

### 107. Résumé of Some Known Properties of Nuclei

Many of the important properties of atomic nuclei, as well as the experimental evidence for these properties, were discussed in previous chapters. It was shown that the total number of particles in a nucleus is equal to the mass number  $A$  of the particular isotope of the element, and that these particles were of two kinds, protons and neutrons, each of approximately unit mass. It was further shown that the number of protons in the nucleus is equal to the atomic number,  $Z$ , of the element, and that the number of neutrons in the nucleus is  $A - Z$ .

From the results of the experiments on the scattering of alpha particles, it was concluded that the nucleus occupies only a very small fraction of the volume of an atom and that nuclear radii do not exceed  $10^{-12}$  cm. It was further shown that the nucleus possesses angular momentum due to spin and also possesses a magnetic moment.

In this and the following chapters we shall discuss many nuclear processes and transformations which not only are interesting in themselves but also provide additional information concerning the nucleus. Among these processes and transformations are (1) the natural radioactivity of some of the heavier elements, (2) the disintegration of nuclei by bombardment with particles and radiation, (3) artificial radioactivity induced by the bombardment of nuclei with particles and radiation, and (4) nuclear fission.

### 108. Natural Radioactive Transformations

An element which is naturally radioactive is found to emit either alpha particles or beta particles. Sometimes gamma rays accompany the emission of these particles. When the nucleus of an atom emits an alpha particle, the atom is transformed into a new atom, since its atomic mass is decreased by four units and its atomic number is decreased by two units. For example, radium, with  $A = 226$  and  $Z = 88$ , is known to emit alpha particles;

hence the product of this transformation, known as radon, will have  $A = 222$  and  $Z = 86$ . That we are dealing with nuclear transformations is confirmed by the fact that radium, which is a solid, is in the same chemical group as barium, while radon is one of the inert gases. In this particular case it is easy to separate the product from its parent substance. When a beta particle is emitted by a nucleus of atomic number  $Z$ , the atomic number of the new atom formed becomes  $Z + 1$ , but the mass number remains unaltered since the mass of a beta particle is negligible in comparison with that of a nucleus.

The rate at which a particular radioactive material disintegrates is a constant independent of all physical and chemical conditions. Given a large number of atoms of any one radioactive element, the number,  $dN$ , that will disintegrate in a small time interval,  $dt$ , is found to be proportional to the number of atoms,  $N$ , present at the time  $t$ ; that is

$$-dN = \lambda N dt, \quad (1)$$

where  $\lambda$  is a constant for the particular radioactive element. Integrating this equation, we get

$$N = N_0 e^{-\lambda t}, \quad (2)$$

where  $N_0$  represents the number of atoms present at the time  $t = 0$ . Equation (2) shows that the number of atoms of a given radioactive substance decreases exponentially with time providing no new atoms are introduced. Half of the material will have disintegrated at the end of a certain time interval  $T$ , which can be determined by setting  $N = N_0/2$  and  $t = T$  in equation (2), yielding

$$\lambda T = \log_e 2,$$

so that

$$T = \frac{0.693}{\lambda}. \quad (3)$$

$T$  is called the *half-life period* of the element. It can be seen that at the end of a time interval equal to  $2T$ , one quarter of the original material will still be in existence. The number of atoms still in existence at any time  $t$  is shown in Figure 138. It is impossible to tell just when one particular atom will disintegrate because radio-

active disintegrations follow the laws of chance or probability. At the end of a certain time  $t$ ,  $N$  of the original atoms will still be in existence. In the next interval of time  $dt$ ,  $dN$  of these atoms will have disintegrated. The *average lifetime*,  $T_a$ , of a single atom may

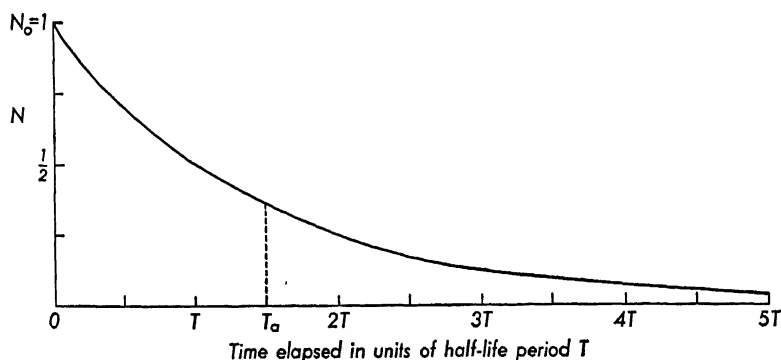


FIG. 138. — Exponential decay of a radioactive element with time.

be computed by multiplying  $dN$ , the number of atoms disintegrating, by the time,  $t$ , during which they existed, summing these products over all the atoms and then dividing by the total number of atoms at the start,  $N_0$ . Thus

$$T_a = \frac{\int_0^{N_0} t dN}{N_0}.$$

Now, from equation (2),

$$dN = -N_0 \lambda e^{-\lambda t} dt;$$

substitution of this value for  $dN$  in the above equation yields

$$T_a = - \int_0^0 t \lambda e^{-\lambda t} dt = + \int_0^\infty t \lambda e^{-\lambda t} dt = \frac{1}{\lambda}. \quad (4)$$

The reciprocal of the disintegration constant  $\lambda$  is thus the average lifetime of a radioactive atom. If the half-life period is known from experimental data, then the average lifetime,  $1/\lambda$ , can be computed from equation (3).

The half-life periods, and hence the average lifetimes, vary considerably among the naturally radioactive elements. Radium, for example, has a half-life period of 1590 years while that of radon is 3.82 days. Thorium C' has the shortest half-life,  $3 \times 10^{-7}$  seconds, while thorium has one of the longest,  $1.39 \times 10^{10}$  years.

## 109. Radioactive Series

Practically all of the naturally radioactive elements lie in the range of atomic numbers from  $Z = 81$  to  $Z = 92$ . These elements have been grouped into three series, the uranium-radium

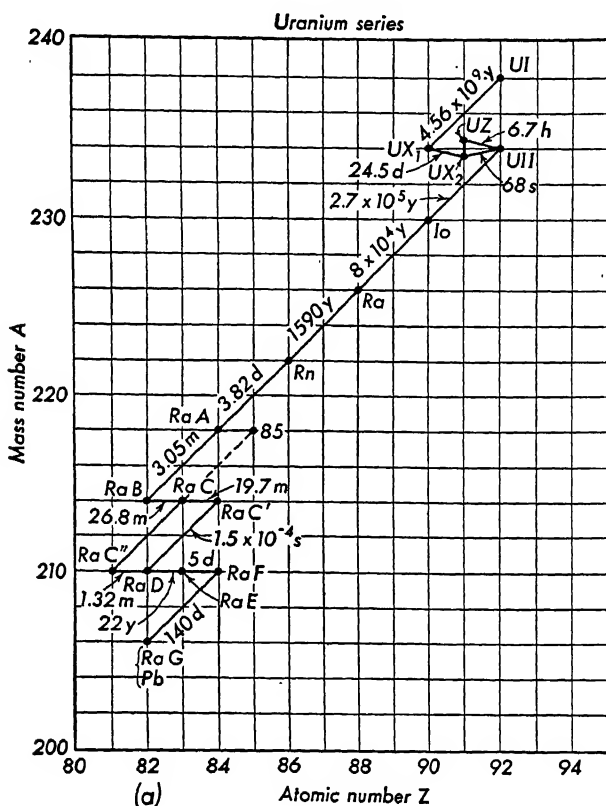


FIG. 139 (a). — The naturally radioactive uranium series.

series, the thorium series, and the actinium series. Any one of the radioactive elements can be traced back through a series of transformations to the parent element of the series. The uranium series, shown in Figure 139(a), starts with uranium I ( $A = 238$ ,  $Z = 92$ ), and goes through a series of transformations which involve the emission of alpha and beta particles forming such substances as radium, radon, radium A . . . down to radium G ( $A = 206$ ,  $Z = 82$ ), which is isotopic with lead and is not radioactive. In the figure, the mass number  $A$  is plotted against the atomic



number  $Z$ . An emission of an alpha particle is indicated by a displacement to the left by two units; an emission of a beta particle by a displacement to the right of one unit.

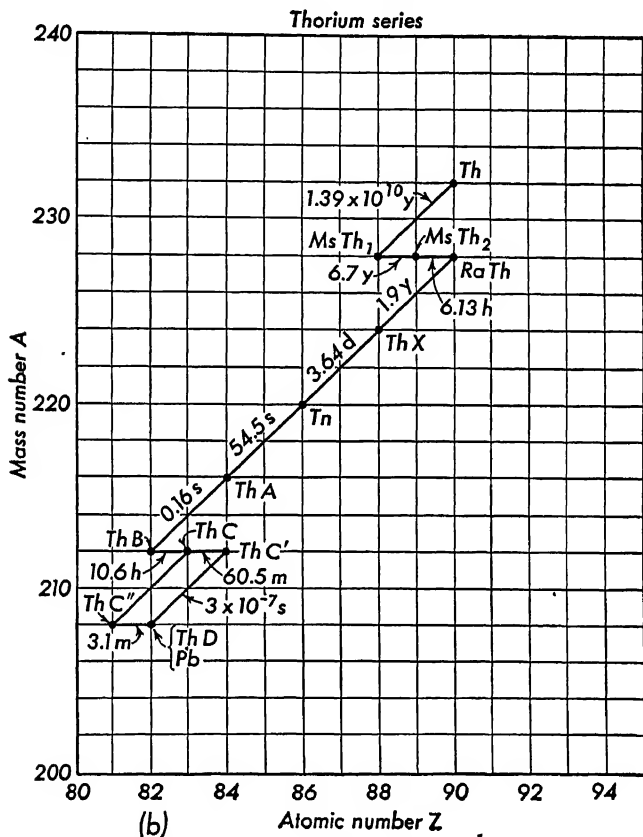


FIG. 139 (b). — The naturally radioactive thorium series.

An interesting branching takes place at radium C. Of all the RaC atoms disintegrating, 99.96% do so with the emission of a beta particle forming RaC', which then disintegrates with the emission of an alpha particle forming RaD. In the second branch, 0.04% of the RaC atoms disintegrate with the emission of an alpha particle forming RaC'', and when the latter disintegrates, it does so with the emission of a beta particle forming RaD. Nuclei which are identical in mass number and in atomic number but which have different radioactive properties were designated by Soddy (1917) as *nuclear isomers*. Thus RaC nuclei are isomeric.

UZ and UX<sub>2</sub> were shown to be a pair of nuclear isomers by Hahn (1921), and Feather and Bretsher later showed that this pair of nuclear isomers are *genetically related*; that is, one type of atom is

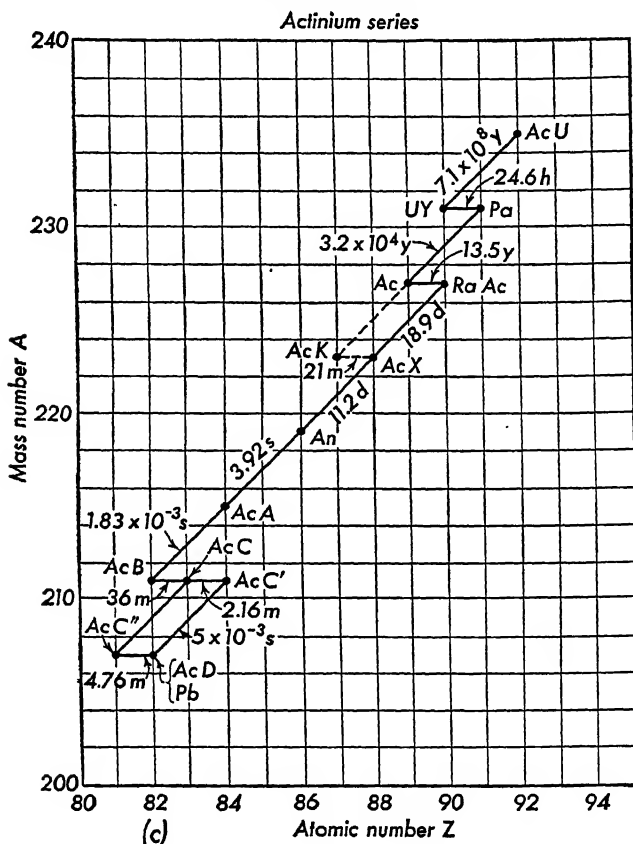


Fig. 139 (c). — The naturally radioactive actinium series.

formed from the other. The subject of nuclear isomers will be considered in greater detail in § 126.

The thorium series, Figure 139(b), starts with thorium ( $A = 232$ ,  $Z = 90$ ), goes through a series of transformations in many respects similar to the uranium series, and ends with thorium D ( $A = 208$ ,  $Z = 82$ ), which is also isotopic with lead. The actinium series, Figure 139(c), was at one time believed to be an independent series, but its origin has recently been traced to an isotope of uranium, known as actino-uranium. This isotope, of mass number 235, has actually been found in samples of uranium. The end

product of the actinium series is actinium D ( $A = 207$ ,  $Z = 82$ ), which is another isotope of lead.

Only four elements whose atomic numbers are less than 81 are known to be naturally radioactive. Table XV lists the particular isotope of each of these elements which is radioactive, the particle emitted, and the half-life period.

TABLE XV

Atomic No.	Element	Mass No.	Emitted Particle	Half-Life Period
19	Potassium	40	beta	$1.42 \times 10^8$ yr
37	Rubidium	87	beta	$6.3 \times 10^{10}$ yr
62	Samarium	148	alpha	$1.4 \times 10^{11}$ yr
71	Lutecium	176	beta	$7 \times 10^{10}$ yr

## 110. Range of Alpha Particles

There are several methods for investigating the alpha particles which are emitted by radioactive nuclei. Their velocities may be measured by the magnetic spectrograph method described in § 34. Another method frequently used for investigating the alpha particles is the determination of the range of the particle in a gas such as hydrogen, nitrogen, or air, using a Wilson cloud chamber. This apparatus consists essentially of a cylinder  $C$  containing a gas saturated with water vapor, and a piston  $P$  which may be lowered very rapidly to produce a sudden expansion of the gas in chamber  $C$ , Figure 140. As a result of this expansion, the gas is cooled and

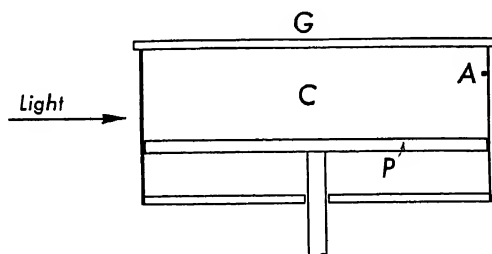


FIG. 140. — Schematic diagram of a Wilson cloud chamber.

becomes supersaturated with water vapor. If there are any ions present in the gas, the water vapor will condense on these ions, forming small droplets. These droplets may be viewed or photo-

graphed through the glass plate  $G$  covering the top of the cylinder; illumination is usually supplied through a window in the wall of the chamber. If a source of alpha particles is placed inside the

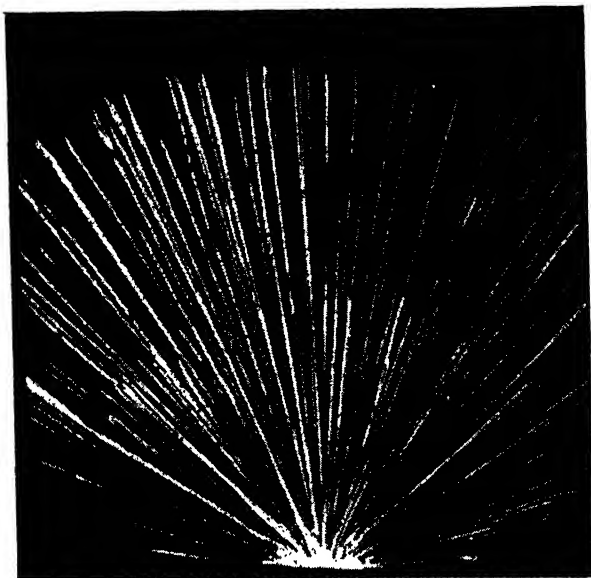


FIG. 141. — Tracks of alpha particles from thorium ( $C + C'$ ) in a Wilson cloud chamber showing two distinct ranges. (From Rutherford, Chadwick, and Ellis, *Radiations from Radioactive Substances*. By permission of The Macmillan Company, publishers.)

chamber at  $A$ , then, in their passage through the gas in the chamber, the alpha particles will ionize the gas molecules along their paths. During each expansion of the gas, water droplets form on the ions, showing the path of each individual alpha particle. Typical alpha-ray tracks are shown in Figure 141. These tracks are in general straight lines almost up to the end of the range. Occasionally a track is bent sharply or else it branches off into two tracks. These are usually ascribed to collisions with nuclei; they will be discussed in detail later, § 115.

Another method for determining the range of alpha particles in a gas is to measure the ionization produced in a gas at different distances from the source of the alpha particles. A typical arrangement for this type of measurement is shown in Figure 142. The source of alpha particles,  $A$ , is placed in a recess in a block of lead, providing a fairly well-collimated beam of alpha rays. The

ionization chamber consists of a wire grid  $G$  and a plate  $P$  connected to an electrometer for measuring the ionization produced in the narrow region between  $P$  and  $G$ . The distance between the alpha-particle source and the ionization chamber is usually varied by moving the source. Typical curves showing the ionization produced at different distances from the source are shown in Figure 143. It will be noticed that for the greater part of the range, the ionization current in the first part of the range is practically constant, then increases and reaches its maximum value just before the end of the range. The peak near the end of the range is due to an increase in the efficiency of ionization by slow alpha particles.

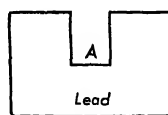
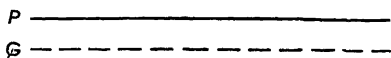


FIG. 142. — Schematic diagram of apparatus for measuring the range of alpha particles.

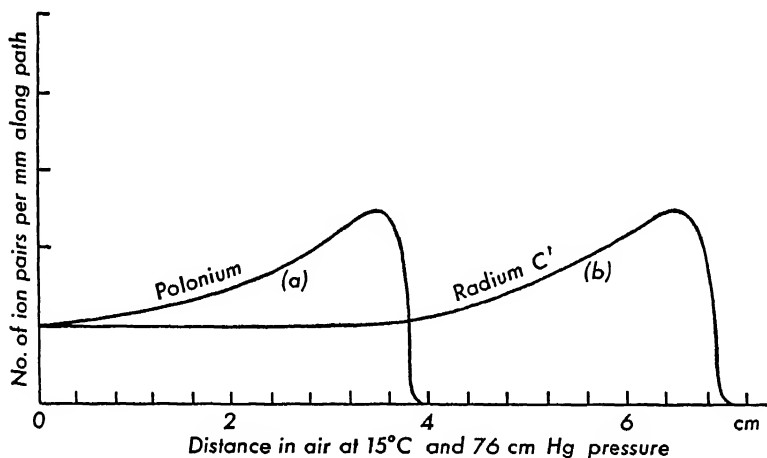


FIG. 143. — Graphs showing the ionization along the path of an alpha particle from (a) polonium, (b) radium  $C'$ .

It has been found that, in most cases, the alpha particles from a given element have a very definite range. This range  $R$  is usually expressed in centimeters of air at  $15^{\circ}\text{C}$  and at a pressure of 76 cm of mercury. The ranges of the alpha particles from some

of the elements are given in Table XVI together with their energies as determined by Halloway and Livingston. The alpha particles from some of the elements, such as thorium C', fall into several

TABLE XVI

RANGE AND ENERGY OF ALPHA PARTICLES		
Element	Mean Range in cm in Air at 15°C	Energy in Mev
Polonium	3.842	5.298
Radon	4.051	5.486
Radium A	4.657	5.998
Thoron	5.004	6.2818
Thorium A	5.638	6.774
Radium C'	6.907	7.680
Radium C'	7.792	8.277
Radium C'	9.04	9.066
Radium C'	11.51	10.505
Thorium C'	8.570	8.776
Thorium C'	9.724	9.488
Thorium C'	11.580	10.538

groups of ranges corresponding to their velocity spectrum. The relationship between the range of an alpha particle and its velocity cannot be expressed by any one simple formula, but those of medium range are found to follow Geiger's empirical formula

$$R = av^3, \quad (5)$$

where  $a$  is a constant numerically equal to  $9.6 \times 10^{-28}$  when  $R$  is expressed in cm and  $v$  in cm per sec.

An important relationship exists between the range of an alpha particle and the average lifetime of the emitter, known as the Geiger-Nuttall law, which is usually written in the form

$$\log R = A \log \lambda + B, \quad (6)$$

where  $A$  is a constant which has practically the same value for each of the three radioactive series and  $B$  is a constant which has

a different value for each series. This relationship is plotted for each series in Figure 144; the range  $R$  is expressed in cm and the

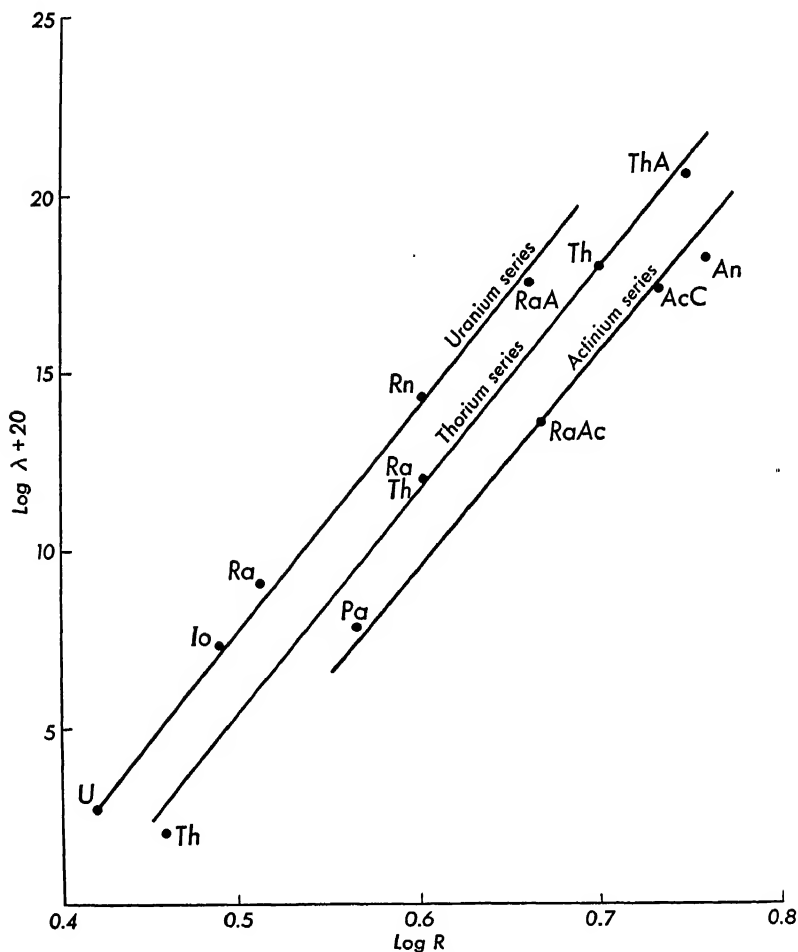


FIG. 144. — The Geiger-Nuttall law.

disintegration constant  $\lambda$  is expressed in  $\text{sec}^{-1}$ . This equation has been used to estimate the half-life periods of some of the products of disintegration which could not be easily determined by direct measurements.

### 111. Beta-Ray Spectra

The most commonly used method for determining the energies of the beta particles emitted by radioactive elements is the meas-

urement of the radii of curvature of their paths in a magnetic field of known intensity  $H$ . Various experimental arrangements have been used in making these measurements. One arrangement is practically identical with that used by Robinson, Figure 136, for

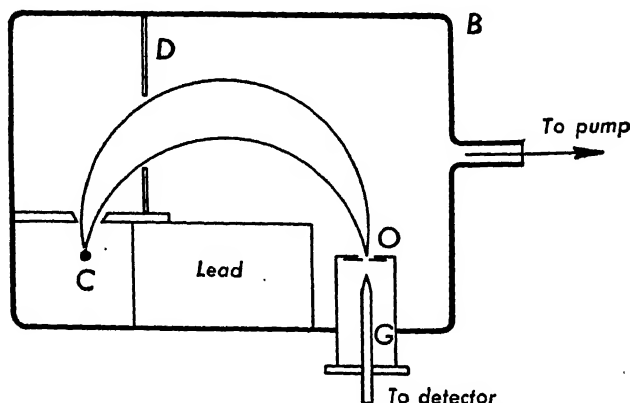


FIG. 145. — Robinson's magnetic spectrograph using a Geiger counter for detecting beta particles.

the determination of the velocities of the electrons ejected by X rays from an element placed at  $C$ . In the magnetic spectrum analysis of beta rays,  $C$  is replaced either by a fine wire on which the radioactive substance has been placed, or else by a small thin-walled glass tube containing the radioactive substance. The beta rays are recorded on a photographic plate and their velocity distribution determined.

Another method for detecting the beta rays is shown in Figure 145 in which the photographic plate is replaced by a Geiger counter  $G$  and the beta rays from the source at  $C$  are bent around by the magnetic field and focused upon the aperture  $O$ . In this type of experiment the number of beta particles entering the aperture  $O$  is counted at a given value of the magnetic field of intensity  $H$ . The intensity of the magnetic field is then changed to a new value and the number of beta particles entering the aperture  $O$  is again determined. In this manner the velocity distribution of the beta particles is determined. The radius of curvature of the path of a beta particle in a magnetic field can also be determined by photographing the track of the beta particle in a Wilson cloud chamber, Figure 146.



The results of these measurements show that there are apparently two distinct types of beta-ray spectra, one a sharp line spectrum, and the other a continuous spectrum. It has definitely been



FIG. 146. — Cloud chamber photograph of beta-ray tracks in a magnetic field of 1,000 oersteds. The beta rays come from the disintegration of  $B^{12}$ ; their energies range from about 6 to 12 Mev. The heavy track across the diameter of the chamber is that of a proton of about 9 Mev energy. (Photograph taken by H. R. Crane.)

shown, however, that the sharp line spectra are due to electrons which have been ejected from the  $K$ ,  $L$ ,  $M$ , and  $N$  shells of the atom by the action of gamma rays from the nucleus of the same atom or neighboring atoms; this is similar to the photoelectric effect with X rays and presents a very convenient means for determining the energies of the gamma rays (§ 113). The continuous beta-ray spectrum is that produced by the electrons which have been ejected from the nuclei of radioactive atoms. The

curve in Figure 147 shows the continuous beta-ray spectrum of radium E. The number of particles having a given energy is plotted as ordinate, and the energy of these particles, expressed in

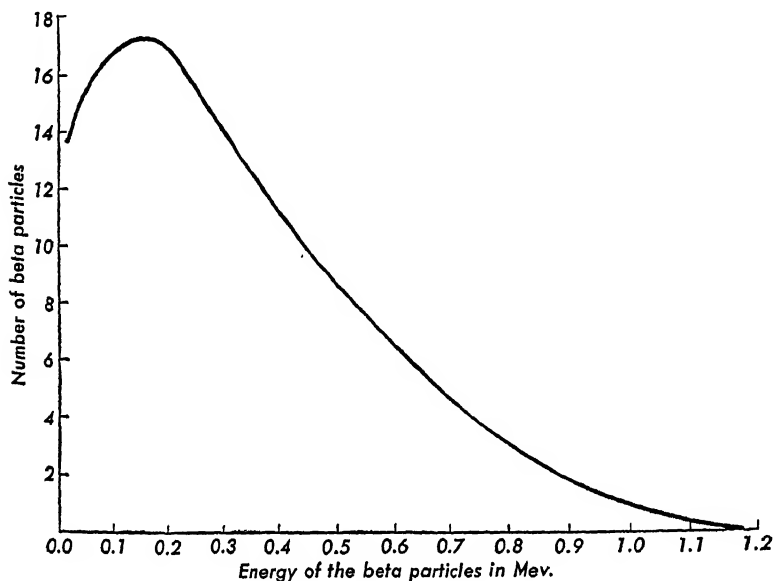


FIG. 147. — Distribution of energy among the beta particles of radium E.

million electron volts, as abscissa. It will be noted that the curve has a definite upper limit for the energy of the disintegration electrons and also passes through a maximum toward the low energy part of the spectrum. The high end-point energy represents the energy which is released in this radioactive disintegration. Table XVII gives some of the high energy end-points of the continuous spectra of some of the beta-ray emitters.

The beta-ray spectrum of an element differs remarkably from most of the other spectra characteristic of the same element in that these characteristic spectra, optical, X-ray, alpha-ray, and gamma-ray, are line spectra, while the beta-ray spectrum is a continuous one. It was found possible to interpret the optical and X-ray line spectra in terms of the changes in atomic energy states due to changes in the extranuclear electronic configurations. It seems reasonable to try to extend this interpretation to the line spectra of the particles emitted by radioactive nuclei. It will be difficult, however, to fit a continuous spectrum, such as that ex-

hibited by the beta rays, into such a scheme. Additional difficulties present themselves when one attempts to account for the origin of both the alpha and beta rays in a nucleus built out of

TABLE XVII

HIGH ENERGY END-POINTS OF SOME BETA-RAY SPECTRA	
Element	End-Point Energy in Mev
Th B	0.36
Ra B	0.65
Ra E	1.17
Th C	2.20
Ra C	3.15

neutrons and protons only. Any adequate nuclear theory must, of course, be able to account for these observations. We shall return to a discussion of these points after a consideration of additional nuclear phenomena (§ 128).

## 112. Gamma-Ray Spectra

In many cases, gamma rays are found to accompany the emission of alpha particles and beta particles. It has been shown that the gamma rays are of the same nature as X rays, and that the wave lengths of some of the longer gamma rays have been measured by means of a single crystal spectrometer (§ 55). The gamma rays have been found to consist of sharp lines of definite wave lengths. These wave lengths are, in general, very short, and cannot be measured with great accuracy by the crystal spectrometer because the angle of reflection from the crystal is so small that it becomes difficult to separate the reflected beam from the direct beam. Two other well-known effects have been used successfully in studying the gamma rays; one is the photoelectric effect, and the second is the Compton effect.

Just as X rays were shown to be emitted as the result of changes in atomic energy states, so the emission of gamma rays can be ascribed to changes in nuclear energy states. A plausible hypothesis is that the transformation of an atom with the emission

of either an alpha or a beta particle may leave the product nucleus in an excited state, and that the gamma rays are emitted when the product nucleus goes to lower excited states or to the normal state. There is considerable experimental evidence which shows that gamma rays come from the product nucleus; most of this evidence is derived from analyses of the sharp line beta-ray spectra.

### 113. Gamma Rays from Beta-Particle Emitters

It was noted previously that the sharp line beta-ray spectra were produced by a type of photoelectric effect in which some of the gamma rays from the nucleus ejected electrons from the *K*, *L*, *M*, or *N* shells of the atom. The fact that these electrons are ejected from their shells with very definite energies indicates that the gamma rays themselves must have sharply defined energies, and thus should show sharp line gamma-ray spectra. Those gamma-ray spectra which have been studied with the crystal spectrometer have been found to consist of several lines of definite wave length, in agreement with the above conclusions.

Whenever a gamma-ray photon of frequency  $\nu$  and energy  $h\nu$  ejects an electron from one of the atomic shells, say the *K* shell, it must supply an amount of energy  $\mathcal{E}_K$  to remove this electron, thus leaving the extranuclear part of the atom in an excited state. The kinetic energy of the electron will be given by

$$\frac{1}{2}mv^2 = h\nu - \mathcal{E}_K.$$

If the velocity of the electron is very large, then, of course, the relativity expression for the kinetic energy must be used. Similar equations will hold for electrons ejected from the *L*, *M*, and *N* shells. By measuring the energies of the ejected electrons with the magnetic spectrograph, and using the values of the atomic energy levels from X-ray data, it is possible to compute the energy and hence the frequency of the gamma rays emitted by a nucleus. This will be illustrated for the case of the gamma rays emitted during the beta-ray transformation of radium D ( $Z = 82$ ) to radium E ( $Z = 83$ ).

The magnetic spectrum analysis of the beta-ray spectrum of RaD shows five sharp lines superposed on the continuous spectrum. The measured values of the energies of these lines are listed in Table XVIII. The gamma-ray spectrum emitted as a result of

the transformation RaD to RaE, as determined by the crystal method, is exceedingly simple; it consists of a single line of wave length  $\lambda = 0.261\text{\AA}$ . This corresponds to an energy  $h\nu = 0.472 \times 10^5 \text{ ev}$  for the gamma-ray photon. On the assumption that the gamma rays come from the product nucleus, RaE, the electrons ejected by these gamma rays must come from the outer shells of this type of atom. Since RaE is isotopic with bismuth,  $Z = 83$ ,

TABLE XVIII

DETERMINATION OF GAMMA-RAY ENERGY FROM SHARP LINE BETA-RAY SPECTRUM FOR TRANSFORMATION RaD $\xrightarrow{\beta}$ RaE (Energies in Electron Volts)						
Line No.	Kinetic Energy of Ejected Electron	Origin of Ejected Electron	Energy of Excited State of Atom	Energy of Electron + Energy of Excited State	Energy of Gamma Ray Photon from Crystal Measurement	Wave Length of Gamma Ray in $\text{\AA}$
1	$0.309 \times 10^5$	$L_I$	$0.163 \times 10^5$	$0.472 \times 10^5$	$0.472 \times 10^5$	0.261
2	0.315	$L_{II}$	0.157	0.472		
3	0.338	$L_{III}$	0.134	0.472		
4	0.433	$M_I$	0.040	0.473		
5	0.461	$N_I$	0.010	0.471		

the excited energy states of the atom can easily be determined from tables of X-ray absorption limits. It is then possible to locate the probable origin of the electrons giving rise to the sharp line beta-ray spectrum. The origin of these electrons is shown in Table XVIII, as well as the energy of each shell as obtained from X-ray data for the element bismuth. The sum of the kinetic energy of the ejected electron and the energy required to remove the electron from the atom should equal the energy of the gamma ray. The results are in very good agreement with the spectroscopic measurement of the energy of the gamma-ray line.

It will be noticed that no electrons are ejected from the  $K$  shell of RaE by the gamma rays. From X-ray data, it is known that the  $K$  absorption limit of RaE ( $Z = 83$ ) is  $\lambda = 0.137\text{\AA}$ , corresponding to an energy of  $0.90 \times 10^5$  electron volts. This is much greater than the energy of the gamma-ray photon; hence it will not be able to eject any electron from the  $K$  shell of radium E.

Similar analyses have been made of the sharp line beta-ray spectra of most of the other beta-ray emitters, leading to determinations of the energies and wave lengths of the gamma-ray spectra of these elements. Wherever possible, these wave lengths have been checked by independent measurements with the crystal spectrometer.

The *internal conversion* of the gamma-ray energy into kinetic energy of electrons, by means of the photoelectric effect, leaves the atoms in excited states. In returning to the normal state, these atoms should emit characteristic X rays corresponding to the changes in the atomic energy states. These X rays have been observed and measured in many cases, and afford additional checks on the assignment of the origins of the ejected electrons.

#### 114. Gamma Rays Accompanying Alpha-Particle Emission

Some radioactive nuclei which emit alpha particles also emit gamma rays of definite frequencies. Careful measurements of the gamma-ray energies and the alpha-particle energies have led to the conclusion that the gamma rays are emitted by the product nucleus which has been left in an excited state after the emission of an alpha particle. As a simple example, consider the alpha-particle transformation of radium into radon. The gamma-ray spectrum accompanying this transformation has been found to consist of a single line of wave length  $\lambda = 0.0652\text{\AA}$ , and of energy  $1.89 \times 10^5$  ev. Now, the ranges in air of the alpha particles emitted during this disintegration have been found to be 3.26 cm and 3.08 cm, with energies of  $48.79 \times 10^5$  ev and  $46.95 \times 10^5$  ev, respectively. The difference between these two energies is  $1.84 \times 10^5$  ev, practically the same as the energy of the gamma-ray photon. This fact can be explained by assuming that when a normal radium nucleus emits an alpha particle of 3.26 cm range, the product nucleus, radon, is in its normal state, but when a radium nucleus emits an alpha particle of 3.08 cm range, the product nucleus is left in an excited state and then returns to the normal state by the emission of a gamma-ray photon. The energy of this gamma-ray photon should therefore be equal to the difference in energies observed in the alpha-particle spectrum of radium.

Similar correlations between alpha-particle energies and the energies of the gamma-ray photons have been established in sev-

eral other cases. These correlations have naturally led to attempts to construct nuclear energy level diagrams similar to those made for the extranuclear portion of the atom. In most cases the

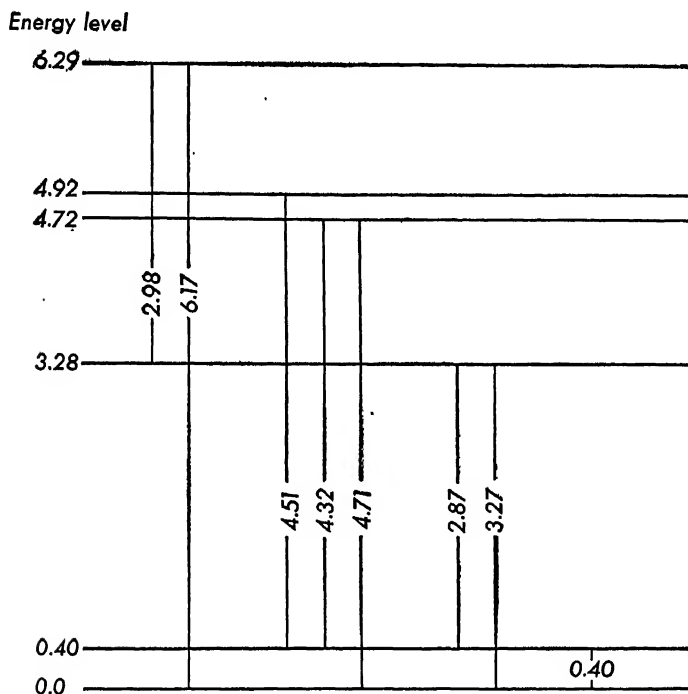


FIG. 148. — Nuclear energy level diagram of  $\text{ThC}''$  showing transitions giving rise to the gamma-ray spectrum and the observed energies of the gamma-ray lines. All energies in  $10^6$  ev.

data necessary for constructing such diagrams are as yet insufficient. In a few cases, nuclear energy level diagrams have been constructed and one of the best-known examples is that of the nucleus of thorium C'' shown in Figure 148. The guiding principle has been to account for all of the observed gamma-ray lines with the minimum number of energy levels. These energy levels represent the possible excited states of the thorium C'' nucleus as a result of the disintegration of thorium C with the emission of an alpha particle. It is possible to account for six of the gamma-ray lines by differences between the energies of the alpha particles emitted during this disintegration.

## REFERENCES

- FEATHER, N., *Nuclear Physics*. London: Cambridge University Press, 1936, Chaps. I, IV, V.
- RASETTI, F., *Elements of Nuclear Physics*. New York: Prentice-Hall, Inc., 1936, Chaps. I-IV.
- RUTHERFORD, E., J. CHADWICK, and C. B. ELLIS, *Radiations from Radioactive Substances*. London: Cambridge University Press, 1930, Chaps. I, X-XII.

## PROBLEMS

1. (a) Determine the constants  $A$  and  $B$  of the Geiger-Nuttall law. (b) How do these constants depend upon the particular radioactive series? (c) Using the data from Figure 139, calculate the range of the alpha particles from AcU.

Ans. (c) 3.13 cm.

2. From the data in Table XVI plot a curve of energy against range of the alpha particles.

3. From the data in Table XVI plot a curve of the range of the alpha particles against the cube of their velocities and compare this curve with Geiger's law.

4. Radium disintegrates with a comparatively long half-life,  $T = 1590$  yr, into radon, which in turn disintegrates with a comparatively short half-life,  $T = 3.8$  da. In such cases the rate at which radium disintegrates can be considered practically constant, and if the radium is kept in a closed container, the amount of the product radon builds up to a steady value; that is, just as much radon is formed during a short time interval as the amount which disintegrates during the same time interval. The product is then said to be in *secular equilibrium* with the parent substance.

- (a) Show that the rate at which radon accumulates in the presence of radium is given by

$$\frac{dN}{dt} = \lambda_1 N_1 - \lambda_2 N$$

where  $N$  is the amount of radon present at any instant,  $N_1$  is the original amount of radium, and  $\lambda_2$  and  $\lambda_1$  are their respective disintegration constants.

- (b) If the amount of radium is assumed to remain constant, show that the amount of radon present after a time  $t$  is given by

$$N = \frac{\lambda_1}{\lambda_2} N_1 (1 - e^{-\lambda_2 t}).$$



(c) Show that after a sufficient lapse of time for secular equilibrium to be established, the amount of radon present is

$$N_2 = \frac{\lambda_1}{\lambda_2} N_1.$$

5. (a) From Problem 4, plot a curve with  $N/N_2$  as ordinates and the time (in units of  $T$ ) as abscissae.

(b) Suppose that after a long time  $t$ , the amount of radon  $N_2$  is pumped off; if we start measuring the amount of radon present from this instant then  $N = N_2 e^{-\lambda_2 t}$ . Plot this equation with  $N/N_2$  as ordinates on the same axes as part (a).

(c) Sum the ordinates of the two curves and discuss the results.

## 8

## Disintegration of Nuclei

## 115. Disintegration of Nitrogen by Alpha-Particle Bombardment

The artificial transmutation of one element into another, the dream of alchemists for centuries, was first definitely accomplished by Rutherford in 1919 in a very simple type of experiment. A diagram of the apparatus used by Rutherford is shown in Figure 149. The chamber *C* was filled with a gas such as nitrogen, and alpha particles from a radioactive source at *A* were absorbed in the gas. A sheet of silver foil, *F*, itself thick enough to absorb the alpha particles, was placed over an opening in the side of the

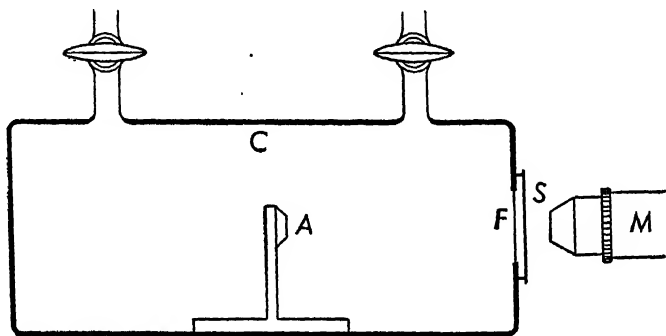


FIG. 149. — Diagram of the apparatus used by Rutherford in the first successful experiment on artificial disintegration of nuclei.

chamber. A zinc sulphide screen, *S*, was placed outside this opening and a microscope, *M*, was used for observing any scintillations occurring on the screen *S*. Scintillations were observed when the chamber was filled with nitrogen, but when the nitrogen was replaced by oxygen or carbon dioxide, no scintillations were observed on the screen *S*. Rutherford concluded that the scintillations were produced by high energy particles which were ejected from nitrogen nuclei as a result of the bombardment of these nuclei by the alpha particles. Magnetic deflection experiments indicated that these particles were hydrogen nuclei, or protons. Later experiments by Rutherford and Chadwick showed that these ejected protons had ranges up to 40 cm in air. Other light elements in the

range from boron to potassium were also disintegrated by bombardment with alpha particles. Since then alpha particles, used as projectiles, have been successful in causing the disintegration of many elements.

The disintegration of nuclei has also been studied with the aid

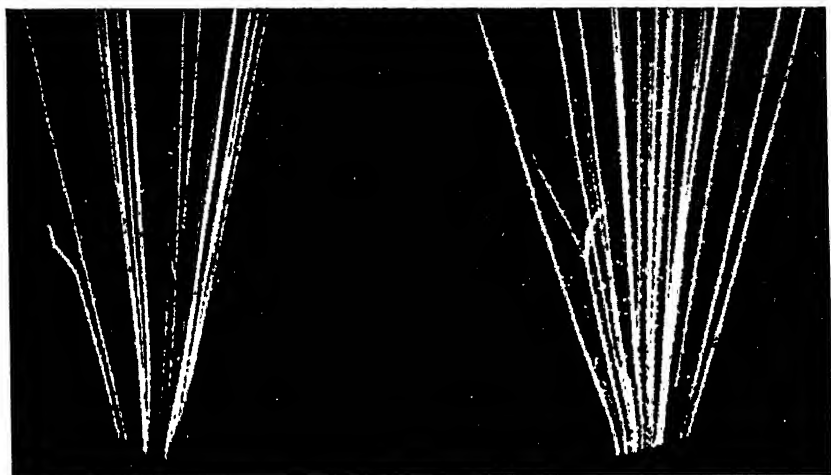
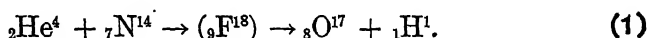


FIG. 150. — A pair of stereoscopic photographs of alpha-particle tracks showing a collision with a nitrogen nucleus resulting in the ejection of a proton. (From Rutherford, Chadwick, and Ellis, *Radiations from Radioactive Substances*. By permission of The Macmillan Company, publishers.)

of the Wilson cloud chamber. One of the first of these investigations was that of Blackett, who photographed the tracks of alpha particles in a Wilson cloud chamber containing about 90 per cent nitrogen and 10 per cent oxygen. The majority of the tracks photographed were straight tracks typical of alpha-particle tracks. Many of the tracks were observed to be forked tracks, indicating that an elastic collision had taken place between an alpha particle and a nitrogen nucleus. It is an easy matter to distinguish between the track made by an alpha particle and that made by a nitrogen nucleus. The heavier particle produces more ion pairs per centimeter of path and thus forms a thicker track. Of about 500,000 tracks photographed, eight tracks were of an unusual type. Each of these tracks was a forked track containing two branches, Figure 150, one a very thick track typical of a heavy particle, the other a very thin track typical of a light particle such as a proton.

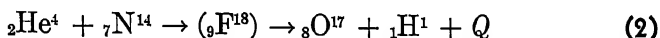
In order to be able to measure accurately the lengths of the tracks and the angles which the forked components make with the original direction of the alpha particle, it is necessary to photograph them from two different positions so as to be able to determine the plane in which the tracks are formed. A common method is to use two cameras at right angles to one another, thus obtaining a pair of stereoscopic photographs from which the correct space relationships of the several tracks can be determined. Measurements on the type of tracks illustrated in Figure 150 showed that the momentum of the system was conserved but that the sum of the kinetic energies of the particles after impact was less than the kinetic energy of the alpha particle before impact. On the basis of a theory of the nucleus advanced by Bohr (1936), the disintegration of nitrogen by bombardment with alpha particles may be thought of as consisting of two separate parts. The first is the capture of the alpha particle by the nitrogen nucleus resulting in the formation of a new *compound nucleus*, and the second is the immediate breaking up of the compound nucleus into two particles one of which is a proton. These two processes can be represented by means of a *nuclear reaction* equation analogous to one representing a chemical reaction. The nuclear reaction equation for this process is



The alpha particle, since it is a helium nucleus, is represented by the symbol  ${}_2\text{He}^4$ . In order to satisfy the principle of the conservation of charge, the atomic number of the compound nucleus must be the sum of the atomic numbers of the helium and nitrogen nuclei. The compound nucleus formed in this case is fluorine,  $Z = 9$ . The symbol representing the compound nucleus will always be enclosed in parentheses. Since this unstable fluorine disintegrates with the emission of a proton, the remaining part, or product nucleus, must be oxygen,  $Z = 8$ .

The guiding principle in determining which isotope of an element is formed during a nuclear reaction is that the mass number of the compound nucleus must equal the sum of the mass numbers of the initial particles, and also the sum of the mass numbers of the final particles. This is not the same as the principle of the conservation of mass, since the mass numbers differ slightly from the

actual values of the atomic masses. The principle of conservation of mass is no longer a separate and independent principle, but is part of the more general principle of the conservation of energy, since, as has previously been noted, a mass  $m$  is equivalent to an amount of energy  $mc^2$ , where  $c$  is the speed of light. Equation (1) can be rewritten to satisfy the general principle of the conservation of energy as follows



where  $Q$ , expressed in a.m.u., represents the energy evolved or absorbed during the nuclear reaction. If  $Q$  is positive, energy has been evolved, and if  $Q$  is negative, energy has been absorbed.  $Q$  is called the *nuclear reaction energy* or the *disintegration energy*, and is equal to the difference in the masses of the initial and final particles. If the sum of the masses of the final particles exceeds that of the initial particles,  $Q$  must be negative; the energy absorbed in such a nuclear reaction must have been obtained from the kinetic energies of the particles. If  $\mathcal{E}_1$  is the kinetic energy of the alpha particle just before capture,  $\mathcal{E}_2$  the kinetic energy of the proton, and  $\mathcal{E}_3$  the kinetic energy of the product nucleus, then

$$Q = \mathcal{E}_2 + \mathcal{E}_3 - \mathcal{E}_1. \quad (3)$$

Of course, in those cases in which  $Q$  is positive, the sum of the kinetic energies of the final particles will be greater than the kinetic energy of the incident alpha particle. In practically all cases the kinetic energy of the nucleus which captures the alpha particle is comparatively small and may be neglected in this type of calculation.

In the above reaction, equation (2), the best value of  $Q$  obtained from measurements of the kinetic energies of the particles, is

$$Q = -1.26 \text{ Mev.}$$

The value of  $Q$  can be compared with the difference in the masses of the initial and final particles, using the values of the atomic masses given in Appendix IV.

<i>Initial particles</i>	<i>Final particles</i>
$\text{He}^4 = 4.00386$	$\text{H}^1 = 1.00813$
$\text{N}^{14} = 14.00753$	$\text{O}^{17} = 17.00450$
<u>18.01139</u>	<u>18.01263</u>

The masses of the final particles exceed those of the initial particles by the amount

$$\Delta m = 0.00124 \text{ a.m.u.}$$

Remembering that 1 a.m.u. = 931.8 Mev, the calculated value of  $Q$  becomes

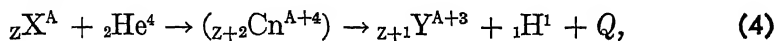
$$Q = - 0.00124 \times 931.8 \text{ Mev} = - 1.16 \text{ Mev.}$$

These two results agree very well within the limits of error of the experiment.

The results of this calculation show that the masses determined by means of the mass spectrograph check very well with those calculated from nuclear reaction data. If, in any one nuclear reaction, three of the four masses are known, a measurement of the reaction energy is sufficient to yield the mass of the fourth atom.

## 116. Capture of an Alpha Particle and the Ejection of a Proton

The disintegration of the nitrogen nucleus by alpha particles is historically the first of a series of nuclear reactions in which an alpha particle is captured by a nucleus forming a compound nucleus which immediately disintegrates into a new nucleus by the ejection of a proton. Such reactions are known as the  $\alpha$ - $p$  type of reaction, in which the first letter,  $\alpha$ , designates the nature of the bombarding particle, and the second letter,  $p$ , designates the nature of the ejected particle. The  $\alpha$ - $p$  type of reaction has been observed with most of the lighter elements up to nickel. This type of artificial disintegration may be represented by the nuclear reaction equation



where Cn represents the compound nucleus formed as a result of the capture of an alpha particle by the atom X of mass number  $A$  and atomic number  $Z$ ; the ejection of a proton from this compound nucleus results in the formation of a new atom Y of mass number  $A + 3$ , and atomic number  $Z + 1$ . In the majority of these cases, the reaction energy, or the disintegration energy,  $Q$ , has been found to be negative. A few of these  $\alpha$ - $p$  reactions are listed on page 303.

${}_5\text{B}^{10} + {}_2\text{He}^4 \rightarrow ({}_7\text{N}^{14}) \rightarrow {}_6\text{C}^{13} + {}_1\text{H}^1$	$Q = + 4.4 \text{ Mev}$
${}_9\text{F}^{19} + {}_2\text{He}^4 \rightarrow ({}_{11}\text{Na}^{23}) \rightarrow {}_{10}\text{Ne}^{22} + {}_1\text{H}^1$	$Q = + 1.58 \text{ Mev}$
${}_{13}\text{Al}^{27} + {}_2\text{He}^4 \rightarrow ({}_{15}\text{P}^{31}) \rightarrow {}_{14}\text{Si}^{30} + {}_1\text{H}^1$	$Q = + 2.26 \text{ Mev}$
${}_{14}\text{Si}^{28} + {}_2\text{He}^4 \rightarrow ({}_{16}\text{S}^{32}) \rightarrow {}_{15}\text{P}^{31} + {}_1\text{H}^1$	$Q = - 2.23 \text{ Mev}$
${}_{16}\text{S}^{32} + {}_2\text{He}^4 \rightarrow ({}_{18}\text{A}^{36}) \rightarrow {}_{17}\text{Cl}^{35} + {}_1\text{H}^1$	$Q = - 2.10 \text{ Mev}$
${}_{19}\text{K}^{39} + {}_2\text{He}^4 \rightarrow ({}_{21}\text{Sc}^{43}) \rightarrow {}_{20}\text{Ca}^{42} + {}_1\text{H}^1$	$Q = - 0.89 \text{ Mev}$
${}_{21}\text{Sc}^{45} + {}_2\text{He}^4 \rightarrow ({}_{23}\text{V}^{49}) \rightarrow {}_{22}\text{Ti}^{48} + {}_1\text{H}^1$	$Q = - 0.3 \text{ Mev}$

In most of these artificial disintegration experiments it is desirable to have the bombarded element in the form of a solid, so that when a stream of alpha particles is directed against this solid target, a larger fraction of them will be absorbed in a very small volume. The effectiveness of the alpha particles in producing this type of disintegration is dependent upon the energies of the alpha particles and upon the nuclear charge. A measure of this effectiveness, sometimes called the *yield*, is the ratio of the number of protons produced to the number of alpha particles completely stopped in the target. The yield for the  $\alpha$ - $p$  type of reaction ranges in values from  $10^{-7}$  to  $10^{-5}$  for alpha particles of 3-8 Mev incident upon elements of small atomic number.

One of the  $\alpha$ - $p$  reactions which has been studied very carefully is that in which aluminum formed the target for the alpha particles. The energies of the protons emitted in this reaction have been studied for different values of the energy of the incident alpha particles. One method of presenting these results is shown in the curve in Figure 151. This curve is known as a distribution-in-range curve. It is obtained by plotting the number of protons penetrating a certain thickness of air, or its equivalent, as ordinate against the corresponding value of the absorber thickness. It will be noticed that the protons produced in this particular experiment form two homogeneous groups, one of about 28 cm range, and the second of about 58 cm range. Other homogeneous groups of protons have been observed, using alpha particles of different energies. The longest range group of protons observed in this reaction is about 66 cm.

The fact that protons are ejected with definite ranges, or definite energies, indicates that the product nucleus, in this case silicon, possesses several energy levels. The product nucleus is left in the ground state by the ejection of the proton of longest range,

and it is left in one of its excited states by the ejection of a proton of smaller range. One might then expect gamma rays to be emitted during this reaction by those nuclei which go from the excited states to the normal or ground state, and the energies of these

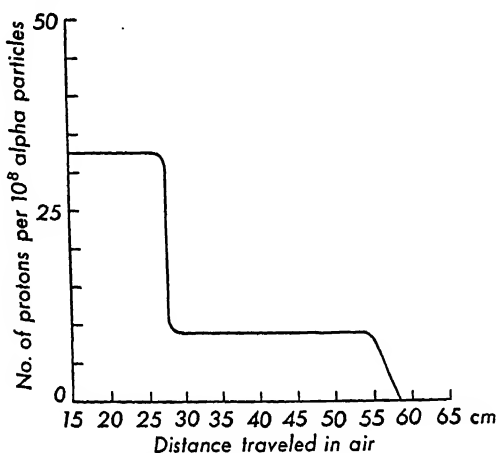


FIG. 151. — Distribution-in-range curve of protons.

gamma rays should be equal to the differences in the energies of the various proton groups. Gamma rays have actually been observed in the above reaction and in several of the other  $\alpha$ - $p$  reactions, although the data at present are not very extensive.

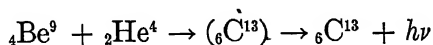
The value of the reaction energy,  $Q$ , listed with each of the  $\alpha$ - $p$  type of reaction, is the largest reaction energy, and corresponds to the emission of protons of maximum range. In each case, therefore, the product nucleus is left in its normal state. Reactions in which  $Q$  has been measured accurately have been used for the determination of the masses of the product nuclei. The values of the atomic masses obtained in this way can be used as independent checks on the measurements made with the mass spectrograph. In some cases where such data are not available, the nuclear reaction equations form the only reliable methods for determining the masses of the isotopes formed in the reaction.

## 117. Discovery of the Neutron

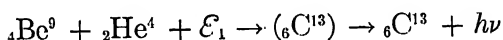
The capture of an alpha particle by a nucleus does not always result in the emission of a proton by the compound nucleus formed as a result of this capture. In one particular reaction studied, that



resulting from the bombardment of beryllium by alpha particles, a very penetrating type of radiation was found to be emitted by the newly formed compound nucleus. It was at first assumed that this radiation was of the nature of gamma rays, resulting from the nuclear reaction



where  $h\nu$  is the energy of the gamma-ray photon. The measurements of Bothe and Becker (1930) of the absorption of these rays in lead showed that each photon should possess an energy of about 7 Mev. The Curie-Joliot (1932) showed that these rays had the very interesting property of being able to knock out protons from paraffin and other substances containing hydrogen. The protons knocked out of paraffin by these rays had a range in air of about 40 cm, or an energy of about 5 Mev. Assuming that these protons were produced as the result of elastic collisions with the gamma-ray photons, calculations showed that each photon must have possessed an amount of energy of about 55 Mev. These results were entirely inconsistent with the results from the experiments on the absorption of these rays in lead. Furthermore, the amount of energy available for gamma radiation, when computed for the above reaction from the known masses of the particles, is much less than 55 Mev. If an alpha particle of 5 Mev energy is captured by a beryllium nucleus, the energy available for the emission of a gamma ray from the carbon nucleus can be obtained as follows:



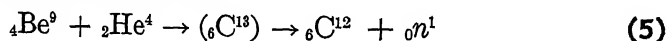
$$9.01496 + 4.00389 + .00536 = 13.00756 + h\nu$$

or

$$h\nu = 0.01665 \text{ a.m.u.} = 15.5 \text{ Mev};$$

that is, the maximum amount of energy available for the gamma-ray photon is 15.5 Mev. Chadwick (1932) performed a series of experiments on the recoil of nuclei which were struck by the rays coming from beryllium bombarded by alpha particles, and showed that if these rays were assumed to be gamma rays then the results of the experiments led to values for the energies of these rays which depended upon the nature of the recoil nucleus. For example, the protons ejected from paraffin had energies of 5.7 Mev which led to

a value of 55 Mev for the energy of the gamma ray; nitrogen recoil nuclei had energies of about 1.2 Mev, indicating that the photon which struck this nucleus must have had an energy of about 90 Mev. In general, if the recoil atoms are to be attributed to collisions with photons, then the amount of energy that has to be assigned to the photon will increase with the increase in mass of the recoil atom. This is contrary to the principles of conservation of energy and momentum during collisions. However, Chadwick showed that all these difficulties disappear completely if we adopt the hypothesis that the radiation coming from the beryllium bombarded with alpha particles does not consist of photons, but consists of particles of mass very nearly equal to that of the proton but having no charge. These particles are called *neutrons* and are formed as a result of the reaction



where  ${}_0n^1$  is the symbol representing the neutron, showing that it has zero charge and mass number unity.

One arrangement used by Chadwick for demonstrating the existence and properties of neutrons is shown in Figure 152. The source of alpha particles is a disk *D* on which polonium has been deposited. This disk and the beryllium target are placed in an

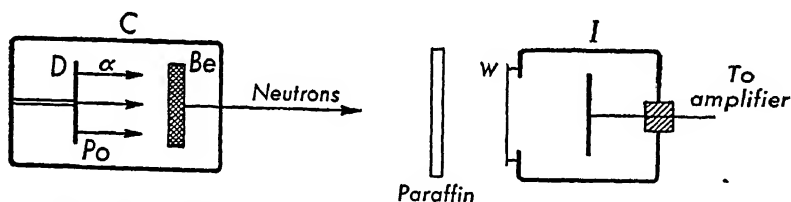


FIG. 152. — Arrangement of apparatus for the detection of neutrons.

evacuated chamber *C*. The neutrons coming from the beryllium pass through the thin wall of this chamber and enter the ionization chamber *I* through the thin window *w*. This ionization chamber is connected to an amplifier and then to a recording device such as an oscillograph, a loud-speaker, or an electrical counter.

Since the neutrons possess no electric charge, they produce no ionization directly in their passage through the chamber. But some neutrons which strike the walls of the ionization chamber cause the ejection of nuclei which then produce ions in the chamber, and are thus recorded on the film of the oscillograph or on the

electrical counter; if a loud-speaker is used, a "click" is heard for every nucleus which produces intense ionization. The results of these experiments show that when the neutrons from beryllium go directly into the ionization chamber, a few counts per minute are recorded. If thin sheets of lead are placed in front of the ionization chamber, the number of counts produced is not reduced appreciably. If, however, a thin slab of paraffin is placed in front of the window  $w$ , then the number of counts per minute increases markedly. This increase is due to the fact that the neutrons, in collisions with the nuclei of the hydrogen atoms contained in paraffin, give up a considerable fraction of their energy to those nuclei or protons, and those protons which enter the ionization chamber are then recorded. If the paraffin is removed and the neutrons are allowed to enter the chamber directly, the number of counts falls immediately to its former low value. This is just the opposite of what would happen if radiation of the nature of gamma rays were used; that is, the introduction of any absorbing material in the path of the gamma radiation produces a decrease in the intensity of the transmitted radiation. The radiation from beryllium therefore cannot be of the nature of gamma rays.

When neutrons pass through matter, they lose energy as a result of collisions with other nuclei and so give rise to the recoil atoms. If the mass of the neutron is approximately unity, then in collision with hydrogen nuclei the ejected protons will have velocities of all values up to a maximum which is the same as the velocity of the neutrons. The mass,  $M$ , of the neutron can be calculated, to a first approximation, from the measured values of the maximum velocities of the hydrogen and nitrogen recoil atoms. It can be shown, on the basis of mechanics, that the maximum velocity of the recoil nucleus is given by

$$v = \frac{2M}{M + M_r} V \quad (6)$$

where  $V$  is the velocity of the incident neutron,  $v$  the velocity of the recoil atom, and  $M_r$  the mass of the recoil atom. If two experiments are performed, one in which the maximum velocity of the recoil protons is measured, and the other in which the maximum velocity of the recoil nitrogen atoms is determined, then

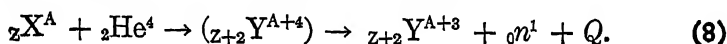
$$\frac{v_H}{v_N} = \frac{M + M_N}{M + M_H} \quad (7)$$

In Chadwick's experiment the measured value of the maximum velocity of the recoil proton,  $v_H$ , was  $3.3 \times 10^9$  cm/sec, and of the recoil nitrogen atoms,  $v_N = 4.7 \times 10^8$  cm/sec. The assumption that the mass of nitrogen is 14 times that of hydrogen yields  $M = 1.15$  as the approximate mass of the neutron. More accurate measurements yield for the mass of the neutron,  $M = 1.00893$  (§ 124).

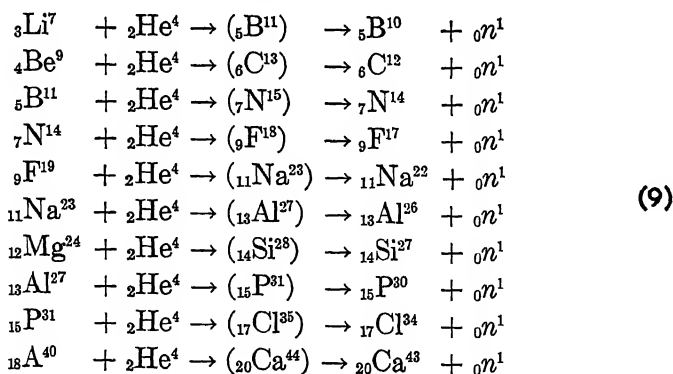
Because of their lack of charge, neutrons should be able to penetrate atomic nuclei very easily, and a study of these nuclear reactions should yield valuable information concerning nuclear properties and nuclear structure (§ 125).

### 118. Capture of an Alpha Particle and the Emission of a Neutron

The bombardment of beryllium by alpha particles with the subsequent emission of neutrons is one of many nuclear reactions of the type designated as  $\alpha$ - $n$  type and is given by the formula



Several of these reactions are listed below.



The above list, of course, does not exhaust all possible  $\alpha$ - $n$  reactions. In many cases, in addition to the emission of neutrons, the product nucleus is left in excited states as is evidenced by the fact that gamma rays have been observed in some of these reactions. For example, in the beryllium reaction, gamma rays have been observed consisting of three definite components with energies of 2.7, 4.2, and 6.6 Mev.

The energies of the neutrons emitted in the  $\alpha$ - $n$  type of reaction can be investigated in several different ways. One method is to measure the ranges of the protons which are ejected from paraffin by the action of the neutrons. Another method is to irradiate the gas in an expansion chamber with the neutrons and to measure the ranges of the nuclei which are set in motion as a result of collisions with the neutrons. From such experiments it has been found that the neutrons from an  $\alpha$ - $n$  reaction possess very high energies; in many cases the energies of the neutrons have been found to consist of several sharp energy groups. For example, the neutrons from beryllium have energies of 13.7, 12.0, 7.6, 6.2, and 4.6 Mev, and probably several groups in the range from 0.5 to 1.5 Mev.

### 119. Discovery of the Positron

Shortly after the discovery of the neutron, another new particle, the *positron*, was discovered by C. D. Anderson (1932) in his experiments on the particles produced by the action of the very penetrating rays known as *cosmic rays*, which come to the earth

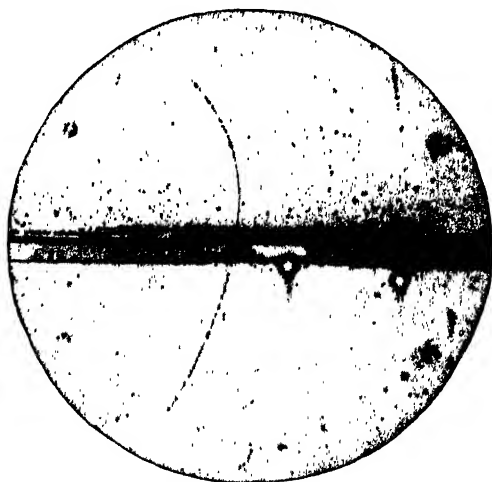


FIG. 153. — Cloud chamber photograph of the path of a positron in a magnetic field. The positron originated at the bottom of the chamber and passed through a sheet of lead 6 mm thick. The magnetic field is directed into the paper. (Photograph by Carl D. Anderson.)

from all directions in space. Anderson was taking Wilson cloud chamber photographs of the tracks of the particles in a strong mag-

netic field. A few tracks were found to be curved, showing that they were formed by charged particles passing through the gas in the cloud chamber. From the appearance of these tracks, they were judged to be due to particles of electronic mass and electronic charge, but from the direction of the curvature of these tracks it



FIG. 154. — A pair of stereoscopic photographs of the tracks of a group of charged particles produced in a cloud chamber by the action of cosmic rays. The picture on the left is the direct image; the one on the right is a reflected image. The magnetic field of 7,900 oersteds is directed into the paper. In the picture on the left the three tracks on the left are electron tracks, and the three on the right are positron tracks. The energies of these particles, from left to right, are 3.5, 55, 190, 78, 70, and 90 Mev. (Photograph by Carl D. Anderson.)

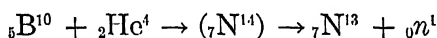
was evident that the particles producing them must have been positively charged. Anderson called these particles *positrons*. One of the first photographs to establish definitely the existence of a positron is shown in Figure 153. The particle originated at the bottom of the chamber, passed through a lead plate 6 mm thick, and then continued with a smaller amount of energy. From the curvatures of these two parts of the track in the magnetic field of known strength, in this case directed into the plane of the figure, and from the amount of ionization along the paths, it was concluded that the positron had an energy of 63 Mev before entering the lead and emerged from it with 23 Mev energy. Figure 154 shows a pair of stereoscopic pictures of the tracks of a group of charged particles produced at the top of the cloud chamber by the action of cosmic rays. Three of the tracks are produced by electrons and three by positrons.

About a year after the discovery of the positron by Anderson,

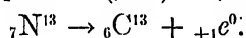
sources of positrons became plentiful and easily obtainable as a result of the discovery by the Curie-Joliot of the phenomenon of artificial or induced radioactivity.

## 120. Discovery of Artificial or Induced Radioactivity

One of the most important discoveries in nuclear physics came from experiments on the bombardment of light nuclei by alpha particles. In the course of such experiments using boron and aluminum as targets, M. and Mme Curie-Joliot (1934) observed that the bombarded substances continued to emit radiations even after the source of alpha particles had been removed. Ionization measurements and magnetic deflection experiments showed that the radiations consisted of positrons. Further, the intensity of the radiation was found to decrease exponentially with time, just as in the case of the naturally radioactive elements. The half-life period,  $T$ , of the positron disintegration was measured in each case. The explanation of this phenomenon given by the Curie-Joliot was that the product nucleus formed in the  $\alpha$ - $n$  reaction in each case was an unstable isotope, which then disintegrated with the emission of a positron. The nuclear reactions for these elements are

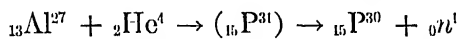


then

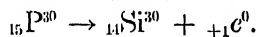


$$T = 11 \text{ min.}$$

(10)



then



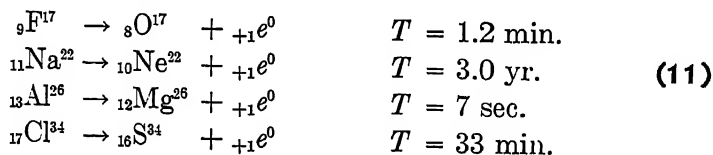
$$T = 2.5 \text{ min.}$$

The symbol  ${}_+1\text{e}^0$  is used to represent the positron since its charge is equal to that of a proton and its mass number is zero. A glance at the table of known stable isotopes (Appendix V) reveals that the product nuclei formed in the  $\alpha$ - $n$  reactions listed above are not among the known stable isotopes, but that the nuclei formed after the emission of the positron are known stable isotopes.

Of course, the best method for the identification of an element is a chemical analysis. Because of the minute amount of material which is made radioactive by alpha-particle bombardment, it is necessary to use a somewhat indirect chemical test to identify the

radioactive isotope. The general method used is to dissolve the irradiated substance and then to add to this solution small quantities of neighboring elements in the ordinary inactive form. The various elements are then separated by chemical methods, generally the precipitation of an insoluble salt, and sometimes the formation of a gaseous compound. These materials are put in different tubes and each one is tested for radioactivity. The chemical identification of the radioelement is then easily made. The Curie-Joliot's made chemical tests on each of the materials investigated and in each case they were able to identify the radioactive isotope. For example, in the boron reaction, they made a target of boron nitride, BN, irradiated it with alpha particles for several minutes, and then heated it with caustic soda. One of the products of this chemical reaction was gaseous ammonia,  $\text{NH}_3$ . The fact that this ammonia was the only one of the chemical substances which was radioactive indicated that the nitrogen,  ${}^{13}_{7}\text{N}$ , was the radioelement produced in this experiment. Its half-life period was found to be the same as that produced in other boron targets, while no radioactivity was observed when ordinary nitrogen was used as a target.

Several of the other product nuclei formed in the  $\alpha$ - $n$  reactions listed in § 118 have also been found to be unstable and to disintegrate with the emission of positrons. These are given below, together with the measured half-life periods:



## 121. Artificially Produced Projectiles for Nuclear Experiments

At the same time that experiments on the disintegration of nuclei by alpha particles were being performed, physicists began designing apparatus for producing high voltages so as to secure high energy particles for nuclear bombardments. Until such high voltage sources became available, work in nuclear physics was confined almost entirely to those laboratories which possessed part of the small quantity of the naturally radioactive substances available in convenient form. With the development of high voltage apparatus, many physicists in other laboratories were enabled to



enter the field of nuclear physics and to make many important contributions to this branch of atomic physics.

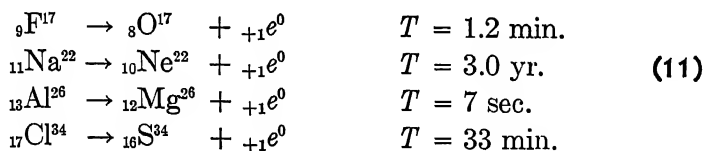
One of the most common sources of high voltage is the alternating current transformer. Since direct current is usually desired in these experiments, the alternating current is rectified by means of two-element thermionic tubes, commonly called kenotrons. Voltages up to one million volts have been obtained with such arrangements. This high voltage is used to accelerate positive ions which have been produced in an auxiliary tube by the ionization of the gas in the tube. Some sources of positive ions are adaptations of the type of positive-ray tubes used in measurements of  $E/M$ ; other sources of positive ions are low voltage arcs maintained in a tube containing a gas. The most common types of positive ions used in nuclear experiments are protons, deuterons, and helium nuclei.

Another source of high voltage which has been used to accelerate charged particles for nuclear experiments is the electrostatic generator which has been developed by Van de Graaff. This device consists essentially of a continuous belt made of some insulating material such as silk, linen, or paper, which passes over two pulleys. One pulley is at ground potential and is driven by an electric motor; the other pulley is mounted inside a hollow metallic cylinder or sphere of large radius of curvature. The hollow body is insulated from the rest of the apparatus. In the operation of this generator, an electric charge obtained from a comparatively low voltage source is placed on the portion of the belt which is moving upward from the lower pulley. This charge is carried up by the belt into the hollow sphere where the charge is removed to the sphere by means of a fine metallic brush.

In this generator a continuous stream of charges is transferred by the belt from a low voltage source to the insulated metallic sphere. The potential of a sphere depends directly upon the quantity of electricity which resides on its surface. The conditions limiting the amount of charge which may be put on a sphere are the nearness of other objects, such as the walls and ceiling of the laboratory, and the breakdown of the air near the sphere due to the intense electric field around it. Electrostatic generators have been operated successfully with the spheres raised to potentials as high as 2.5 million volts above ground potential. In some

radioactive isotope. The general method used is to dissolve the irradiated substance and then to add to this solution small quantities of neighboring elements in the ordinary inactive form. The various elements are then separated by chemical methods, generally the precipitation of an insoluble salt, and sometimes the formation of a gaseous compound. These materials are put in different tubes and each one is tested for radioactivity. The chemical identification of the radioelement is then easily made. The Curie-Joliot's made chemical tests on each of the materials investigated and in each case they were able to identify the radioactive isotope. For example, in the boron reaction, they made a target of boron nitride, BN, irradiated it with alpha particles for several minutes, and then heated it with caustic soda. One of the products of this chemical reaction was gaseous ammonia,  $\text{NH}_3$ . The fact that this ammonia was the only one of the chemical substances which was radioactive indicated that the nitrogen,  ${}^{13}\text{N}$ , was the radioelement produced in this experiment. Its half-life period was found to be the same as that produced in other boron targets, while no radioactivity was observed when ordinary nitrogen was used as a target.

Several of the other product nuclei formed in the  $\alpha$ -n reactions listed in § 118 have also been found to be unstable and to disintegrate with the emission of positrons. These are given below, together with the measured half-life periods:



## 121. Artificially Produced Projectiles for Nuclear Experiments

At the same time that experiments on the disintegration of nuclei by alpha particles were being performed, physicists began designing apparatus for producing high voltages so as to secure high energy particles for nuclear bombardments. Until such high voltage sources became available, work in nuclear physics was confined almost entirely to those laboratories which possessed part of the small quantity of the naturally radioactive substances available in convenient form. With the development of high voltage apparatus, many physicists in other laboratories were enabled to

enter the field of nuclear physics and to make many important contributions to this branch of atomic physics.

One of the most common sources of high voltage is the alternating current transformer. Since direct current is usually desired in these experiments, the alternating current is rectified by means of two-element thermionic tubes, commonly called kenotrons. Voltages up to one million volts have been obtained with such arrangements. This high voltage is used to accelerate positive ions which have been produced in an auxiliary tube by the ionization of the gas in the tube. Some sources of positive ions are adaptations of the type of positive-ray tubes used in measurements of  $E/M$ ; other sources of positive ions are low voltage arcs maintained in a tube containing a gas. The most common types of positive ions used in nuclear experiments are protons, deuterons, and helium nuclei.

Another source of high voltage which has been used to accelerate charged particles for nuclear experiments is the electrostatic generator which has been developed by Van de Graaff. This device consists essentially of a continuous belt made of some insulating material such as silk, linen, or paper, which passes over two pulleys. One pulley is at ground potential and is driven by an electric motor; the other pulley is mounted inside a hollow metallic cylinder or sphere of large radius of curvature. The hollow body is insulated from the rest of the apparatus. In the operation of this generator, an electric charge obtained from a comparatively low voltage source is placed on the portion of the belt which is moving upward from the lower pulley. This charge is carried up by the belt into the hollow sphere where the charge is removed to the sphere by means of a fine metallic brush.

In this generator a continuous stream of charges is transferred by the belt from a low voltage source to the insulated metallic sphere. The potential of a sphere depends directly upon the quantity of electricity which resides on its surface. The conditions limiting the amount of charge which may be put on a sphere are the nearness of other objects, such as the walls and ceiling of the laboratory, and the breakdown of the air near the sphere due to the intense electric field around it. Electrostatic generators have been operated successfully with the spheres raised to potentials as high as 2.5 million volts above ground potential. In some

generators the voltage of the belt charging device was as low as 10 kilovolts.

In recent designs, the electrostatic generator has been built completely inside of a steel container in which the air is main-

tained at a high pressure, sometimes as high as 150 pounds per square inch. At high pressures the air can withstand stronger electric fields before breakdown occurs. Also, since the air is contained in a steel tube it may be dried and cleaned, thus making for steadier operating conditions.

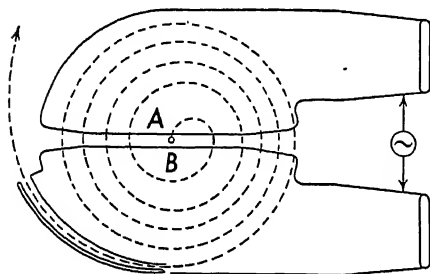


FIG. 155. — Schematic diagram showing the path of a charged particle in a cyclotron. Magnetic field is perpendicular to the paper.

Another device for producing high energy particles which has come into fairly common use is the *cyclotron* developed by Lawrence and Livingston. It consists essentially of a short hollow cylinder divided into two sections, A and B, Figure 155. Each section is usually referred to as a “dee” because of its resemblance to the letter D. These dees are placed between the poles of a very large electromagnet. Some of the cyclotrons at present in use have magnets whose pole pieces are from 30 to 60 inches in diameter; the diameters of the dees are approximately the same as those of the pole pieces. The dees are placed in another metal cylinder, as shown in Figure 156, and the whole assembly is placed between the poles of the electromagnet so that the magnetic field is perpendicular to the base of the cylinder and parallel to its axis.

There are two methods in general use for producing ions inside the dees. One method is to introduce a gas such as hydrogen into the system at a low pressure. A filament situated in the center of the chamber just outside the dees is heated, and a small difference of potential is applied between the filament and the metal box to give the electrons from the filament sufficient energy to ionize some of the hydrogen atoms. This produces a vertical column of positive ions, some of which travel into the space between the dees. Another method is to produce the ions in a separate small source with a narrow opening into the space between the dees; this

is usually referred to as a capillary ion source. The pressure of the gas in the ion source can be adjusted for optimum conditions while the rest of the system is maintained at as low a pressure as possible. This avoids electrical discharges inside the dees and also

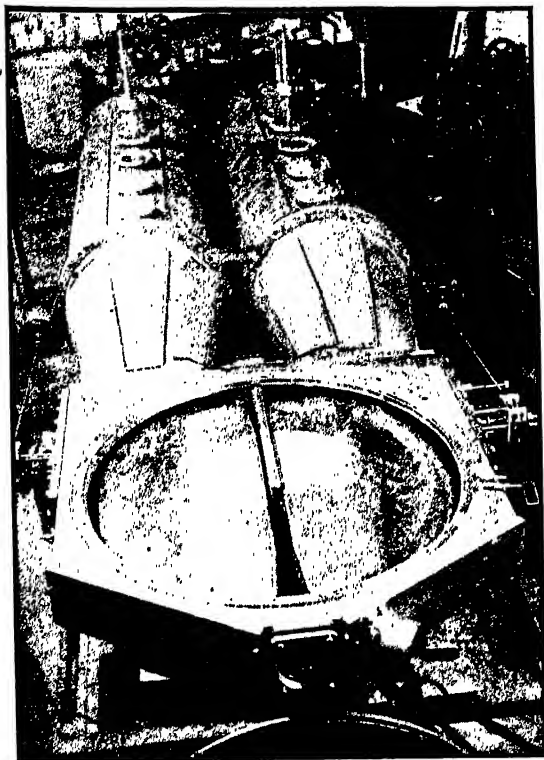


FIG. 156. - Shop assembly photograph of the M.I.T. cyclotron chamber, showing the construction of the chamber and dees. (From the *Journal of Applied Physics*, Jan., 1944. Courtesy of the Radioactivity Center at the Massachusetts Institute of Technology.)

makes it possible to use narrower dees and a smaller air gap between the poles of the magnet.

The two dees, *A* and *B*, are connected to the terminals of a high frequency alternating current circuit so that the charge on each half changes a few million times per second. When *A* is positive, the protons are accelerated toward *B*. The magnetic field causes each proton inside *B* to travel in a circle of radius *r* given by

$$H e v = \frac{M v^2}{r}.$$

After it has traversed half a circle, the proton comes to the edge of  $B$ . If, in the meantime, the potential difference between  $A$  and  $B$  has changed direction so that  $B$  is now positive and  $A$  negative, the proton will receive an additional acceleration and go from  $B$  to  $A$ , traveling in a circular path of larger radius inside  $A$ . After traversing a half circle in  $A$ , it will reach the edge of  $A$  and receive an additional acceleration from  $A$  to  $B$  because, in the meantime, the potential difference between  $A$  and  $B$  will have changed sign. The proton will continue traveling in semicircles of increasing radii each time it goes from  $A$  to  $B$  and from  $B$  to  $A$ . This is due to the fact that the time required by the proton to travel half a circumference is independent of the radius of the circle. This can be shown very simply since the time,  $t$ , required to travel the distance  $\pi r$ , when the particle is moving with velocity  $v$ , is

$$t = \frac{\pi r}{v};$$

but

$$v = \frac{HEr}{M},$$

so that

$$t = \frac{\pi M}{HE}. \quad (12)$$

For any given value of  $M/E$ , the time required to traverse half a circumference is determined by the magnetic field intensity. By adjusting the magnetic field intensity  $H$ , the time can be made the same as that required to change the potentials of  $A$  and  $B$ .

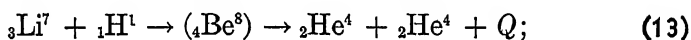
After the protons have traversed many semicircular paths and approach the circumference of the cylinder,  $A$ , an auxiliary electric field is used to deflect them from the circular path and make them come out through a thin window. The substance to be bombarded by the protons is placed near the window, and the investigation of the results of this bombardment can then be performed in a suitable manner.

Instead of ordinary hydrogen, heavy hydrogen or deuterium can be introduced into the chamber of the cyclotron, so that deuterons become available as bombarding particles; or if helium is used in this chamber, we have an artificial source of alpha particles.

The voltage between the sections *A* and *B* may have any value from about 10,000 to 200,000 volts. The particle as it emerges from the cyclotron may have an energy of several million electron volts due to the successive accelerations it experiences in going from one section to the other. The cyclotron is thus a comparatively low-voltage source of high energy particles.

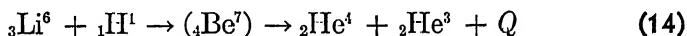
## 122. Disintegrations by Protons

The first successful disintegration experiments utilizing protons as bombarding particles were performed by Cockcroft and Walton (1932). The protons were produced in a hydrogen discharge tube operated at voltages up to 500,000 volts. When the protons were used to bombard a lithium target, alpha particles were observed on a fluorescent screen. This experiment was later repeated by Dee and Walton, using a Wilson cloud chamber for detecting the alpha particles. This nuclear reaction is given by the equation

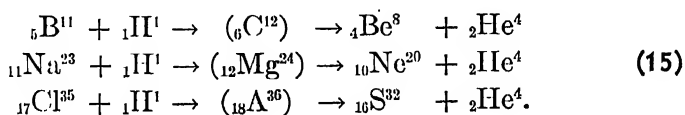


that is, the compound nucleus formed as a result of the capture of the proton by the lithium nucleus breaks up into two alpha particles which travel in almost opposite directions. Each alpha particle has a range of 8.31 cm in air corresponding to an energy of about 8.63 Mev. The reaction energy *Q* is found to be 17.28 Mev, and checks very well with the value obtained from the difference in the masses of the initial and final particles.

There are many other interesting disintegrations produced by bombardment with protons. The nuclear reaction which occurs with the lithium target containing only the isotope of mass number 6 is given by the equation

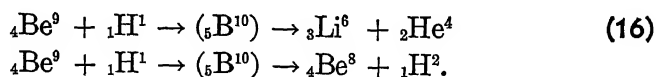


in which two helium atoms, one of mass number 4, and the other of mass number 3, are produced with ranges of 0.8 cm and 1.2 cm respectively. The measured value of *Q* is 3.94 Mev. Some of the other reactions observed are given below:



The boron reaction listed above has been studied very extensively and it has been found that in the majority of cases the beryllium nucleus is left in an excited state and then disintegrates with the emission of two alpha particles.

Not all reactions in which the proton is the bombarding particle are of the above type,  $p-\alpha$ , in which an alpha particle is one of the final products. In the case of beryllium two different reactions have been observed, one in which an alpha particle is emitted and another in which a deuteron is emitted. These reactions are given by the equations



Gamma rays have also been observed as the result of the bombardment of an element by protons. In some of these cases the gamma-ray photons possess such high energies that the only possible explanation seems to be that the proton is simply captured by the nucleus, and that the compound nucleus thus formed is in an excited state. This nucleus then returns to its normal state with the emission of a gamma-ray photon of definite energy. One such example is the reaction



The gamma-ray photon was found to have an amount of energy  $h\nu$  equivalent to 17 Mev.

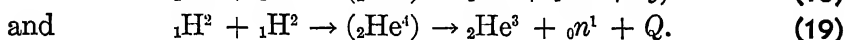
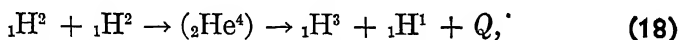
### 123. Disintegrations by Deuterons

A great many nuclear reactions have been observed with high energy deuterons as the bombarding particles. In most of these experiments, the high energy deuterons were produced in a cyclotron. These energies have usually been of the order of several Mev. The reactions involving deuterons may be classified according to the type of particle or particles emitted by the compound nucleus which is formed as a result of the capture of the deuteron. Alpha particles, protons, and neutrons have been produced in these processes. In some cases the product nucleus, formed as a result of the emission of one of these particles, is radioactive and disintegrates with the emission of a positron or an electron. Gamma rays have been observed in some of the reactions which



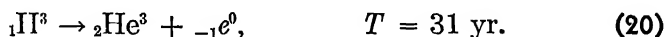
involve the emission of a particle. In a few cases the compound nucleus has been observed to break up into three particles. Only a few typical examples of each of these reactions resulting from the capture of a deuteron will be considered in this section.

One of the simplest and most important of these reactions is the one in which the high energy deuterons are used to bombard a target containing deuterium. Deuterium targets have been made by freezing heavy water (deuterium oxide) onto a surface kept cold by means of liquid air. Other deuterium targets have been made out of compounds such as ammonium sulphate, in which the ordinary hydrogen was replaced by deuterium. Two different nuclear reactions have been observed as a result of the bombardment of deuterium by deuterons:



The first of these reactions has been studied with the aid of a Wilson cloud chamber, which enabled the particles to be identified as isotopes of hydrogen of mass numbers 1 and 3. The ranges of these particles in air have been found to be 14.7 cm and 1.6 cm, respectively, yielding a value for  $Q = 3.98$  Mev. With the value of  $Q$ , and the known masses of  $\text{H}^1$  and  $\text{H}^2$ , the mass of  $\text{H}^3$  can be determined very accurately. This is at present the most accurate method for determining the mass of  $\text{H}^3$ , and the value given in Appendix IV has been calculated in this way.

Hydrogen of mass number  $A = 3$  is not found as one of the constituents of ordinary hydrogen. The reason for this is that this isotope of hydrogen is unstable. O'Neal and Goldhaber showed that it disintegrates with the emission of a beta particle as follows:



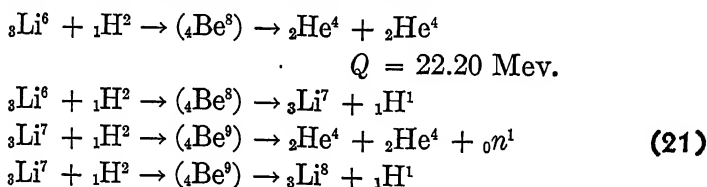
The beta rays emitted by this radioactive isotope of hydrogen have a maximum kinetic energy of only 15 kev.

Radioactivity is now a phenomenon which is no longer unique but extends throughout the entire range of the periodic table, from the lightest to the heaviest element.

The energy of the neutrons formed in the bombardment of deuterium by deuterons has been investigated by observing the

recoil tracks of the atoms of the gas in a cloud chamber. It was observed that the neutrons were practically homogeneous in energy. Recent measurements show that the energy of the neutrons emitted at right angles to the direction of motion of the deuterons is 2.38 Mev plus one quarter of the deuteron energy. This reaction forms a very convenient source of neutrons of known energy. Furthermore, neutrons have been observed for comparatively low values of incident deuteron energies, that is, of the order of 6 kev. Of course, the neutron yield increases rapidly with the deuteron energy. The value of the reaction energy has been found to be  $Q = 3.18$  Mev, and with this value of  $Q$  the mass of  $\text{He}^3$  can be determined.

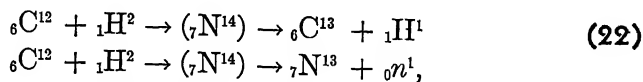
Some of the nuclear reactions produced by the capture of a deuteron by lithium which have been observed are as follows:



followed by  ${}_3\text{Li}^8 \rightarrow {}_4\text{Be}^8 + {}_{-1}e^0$ .  $T = 0.88$  sec.

The isotope of mass number 8 is radioactive and disintegrates with the emission of a beta particle, that is, an electron  ${}_{-1}e^0$ . The beta rays liberated in the disintegration of  $\text{Li}^8$  have a continuous energy distribution up to a maximum, just as in the case of the beta-ray spectra of the naturally radioactive elements. The upper limit, or end-point of the beta-ray spectrum of lithium is about 12 Mev. There is strong experimental evidence to show that the disintegration energy,  $Q$ , in the case of beta-ray emitters, is equal to the maximum energy observed in the beta-ray spectrum.

In the case of carbon bombarded by deuterons, two reactions have been observed:

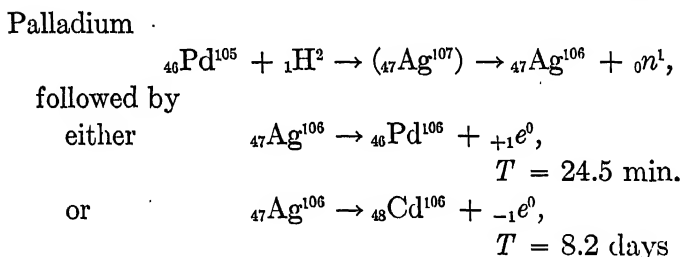
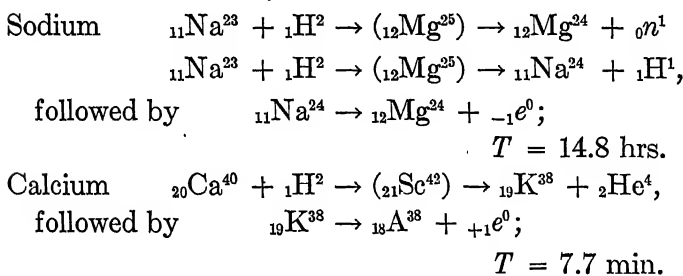


followed by  ${}_7\text{N}^{13} \rightarrow {}_6\text{C}^{13} + {}_{+1}e^0$ .

The half-life period of the radionitrogen formed in this reaction is identical with that observed in the reaction produced by the capture of an alpha particle by boron. The positron spectrum shows

a continuous range of energies. The maximum value of the positron energy in this case is 1.20 Mev.

The following are some of the reactions which have been observed for some of the heavier elements:



This is an unusual case in which the radioactive element, silver, disintegrates with the emission of either a positron or an electron. Silver,  $A = 106$ , is thus isomeric. Other examples of isomers have been reported (see § 126).

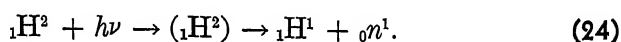
In each of the above examples, chemical tests were made to identify the product nuclei. In studying the radioactive elements several different nuclear reactions were used to produce the same radioactive nucleus. For example, the radioactive silver isotope was produced not only by the reaction given above but also by bombarding rhodium with alpha particles of 12 Mev energy:



The same radioactive isotope of silver was also produced by bombarding cadmium ( $A = 106$ ) with neutrons, and by bombarding the stable isotope of silver ( $A = 107$ ) with neutrons. In each of these four reactions the same two periods were obtained for the positron and electron emissions, respectively, from the radioactive isotope of silver ( $A = 106$ ).

## 124. Disintegration of Nuclei by Photons

Atomic nuclei have been disintegrated by being bombarded with high energy photons. In most cases this process of *photo-disintegration* results in the emission of neutrons by the nuclei which have been raised to excited states by the absorption of these photons. In the early experiments, high energy gamma-ray photons were used, but with the development of the betatron, X-ray photons of sufficiently high energy have become available for these experiments. Of very great interest is the disintegration of the deuteron, the lightest of the complex nuclei, by the action of the gamma rays. This nuclear reaction is



According to our present view of the structure of the nucleus, the deuteron consists of a proton and a neutron held together by some force of attraction. A measurement of the minimum amount of energy necessary to disrupt the deuteron would also give the binding energy of the proton and neutron in the nucleus. Chadwick and Goldhaber, who discovered the above reaction, used gamma rays from  $\text{ThC}''$ , and measured the energy of the protons liberated by the amount of ionization they produced. The energy of the gamma-ray photon is known to be 2.62 Mev. If the energies of the neutron and proton released in this reaction are subtracted from this, the result should be the binding energy of these particles. Since the neutron and proton have nearly equal masses, when the deuteron disintegrates, the two particles will have approximately equal energies. Hence the energies of the two particles can be obtained by merely doubling the measured value of the proton energy, yielding 0.45 Mev for the total kinetic energy of the final particles. The binding energy is thus 2.17 Mev. This disintegration has also been observed with gamma rays from  $\text{RaC}$  of energy 2.198 Mev.

Since the masses of the proton and deuteron are known very accurately from measurements with the mass spectrograph, the photodisintegration of the deuteron affords the most accurate means of determining the mass of the neutron. The value so determined is 1.00893.

To produce the photodisintegration of the heavier nuclei, the

energy of the incident photon must exceed the binding energy of the particle to be ejected. In many cases in which photodisintegration results in the emission of a neutron, the product nucleus is radioactive; the reaction can then be studied by observing this

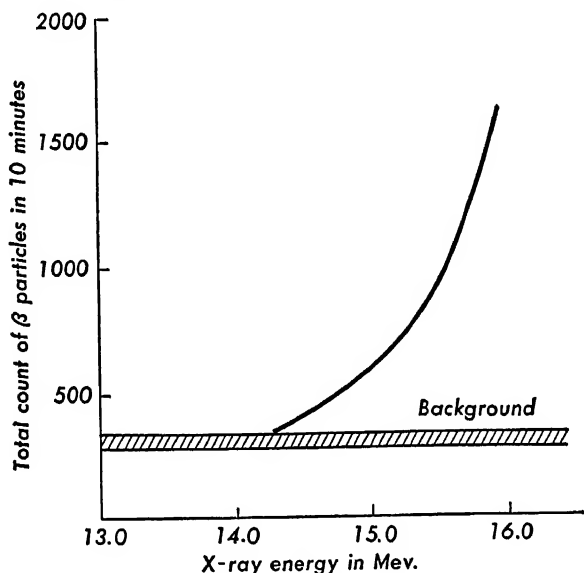


FIG. 157. — Excitation curve for the photodisintegration of  $\text{Fe}^{53}$  showing the threshold at 14.2 Mev.

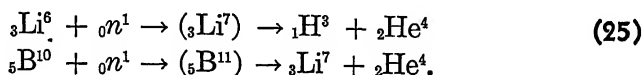
radioactivity and determining its half-life period. The particular isotope involved in this photodisintegration can then more readily be identified. Baldwin and Koeh have recently performed such experiments using the high energy X-ray photons emitted from the betatron. By varying the energy of the X-ray photons used in irradiating the samples of material, they were able to determine the minimum amount of energy, that is, the *threshold* for the photodisintegration of several different nuclei in the range of atomic numbers  $Z = 6$  to  $Z = 47$ . In each case the production of the photonuclear effect was measured by the intensity of the beta rays emitted by the irradiated sample. Figure 157 shows a typical curve obtained by irradiating flat plates of iron, 10 cm  $\times$  8 cm  $\times$  1 cm, with X rays for ten minutes, and then placing the iron plate near a counter sensitive to beta rays. From the curve, the threshold of iron,  $A = 53$ , is found to be 14.2 Mev. Other values of the threshold for photodisintegration are given in Table XIX.

TABLE XIX

THRESHOLD VALUES OF THE ENERGY REQUIRED FOR PHOTODISINTEGRATION			
Isotope			Threshold in Mev.
<i>Z</i>	<i>El</i>	<i>A</i>	
1	H	2	2.17
4	Be	9	1.63
6	C	11	18.7-19.4
7	N	13	11.1
8	O	15	16.3
26	Fe	53	14.2
29	Cu	62	10.9
30	Zn	63	11.6
34	Se	79 or 81	9.8
42	Mo	91 or 93	13.5
47	Ag	106	9.5
47	Ag	108	9.3

## 125. Disintegration by Neutrons

Neutrons, because they possess no electric charge, have proved to be very effective in penetrating the positively charged nuclei, thereby producing nuclear transformations. Not only are high energy neutrons capable of penetrating the nucleus, but comparatively *slow* neutrons have also been found to be extremely effective. A great deal of work has been done with slow neutrons and the information so obtained is the basis of the nuclear model proposed by Bohr. The simplest method of obtaining slow neutrons is to allow the fast neutrons from some source, such as the alpha-particle-beryllium reaction, to pass through some hydrogen-containing substance such as paraffin or water. A neutron gives up a large fraction of its energy in a collision with a hydrogen nucleus, and after many collisions it will come to thermal equilibrium with the material; that is, its average energy will be equal to the energy of thermal agitation, which is equivalent to  $\frac{1}{40}$  electron volt at room temperature. In one type of reaction,  $n$ - $\alpha$ , the capture of a slow neutron results in the emission of an alpha particle. Two such cases which have been studied extensively are



The second reaction is being used widely as a sensitive detector of neutrons. The ionization chamber is lined with boron, usually in the form of a compound. The capture of a neutron by boron

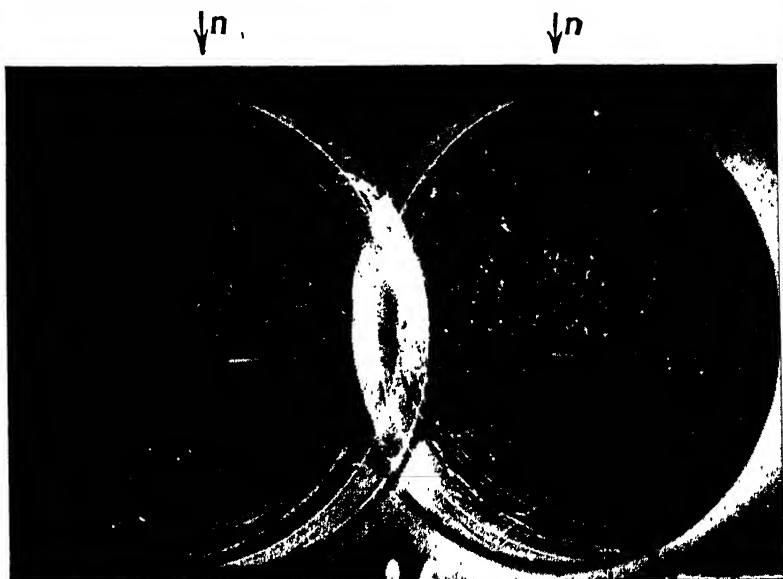
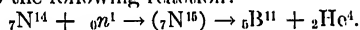


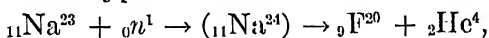
FIG. 158. — Stereoscopic photograph showing three disintegrations produced by neutrons according to the following reaction:



The arrow indicates the direction of the incident neutron. The cloud chamber contained nitrogen at a pressure of about 0.2 atmos. (From a photograph supplied to the author by Dr. Martin D. Kamen.)

causes the liberation of an alpha particle which is easily detected by the ionization it produces in the chamber. (See Figure 158.)

When fast neutrons are captured by heavier nuclei resulting in the emission of an alpha particle, the product nucleus is usually radioactive. Some typical reactions are

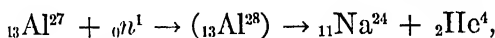


followed by

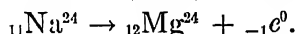


$$T = 12 \text{ sec.}$$

(26)



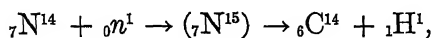
followed by



$$T = 14.8 \text{ hr.}$$

The capture of a neutron may sometimes result in the emission of a proton by the compound nucleus. This process has been ob-

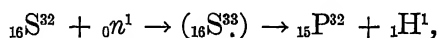
served with slow neutrons in the case of nitrogen in the reaction



followed by  ${}_6\text{C}^{14} \rightarrow {}_7\text{N}^{14} + {}_{-1}e^0$ . (27)

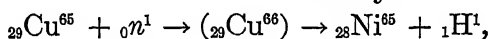
$$T = 5300 \text{ yr.}$$

The other  $n$ - $p$  reactions have all been performed with fast neutrons, and in every case the product nucleus has been found to be radioactive with the emission of electrons. Some typical reactions are



followed by  ${}_{15}\text{P}^{32} \rightarrow {}_{16}\text{S}^{32} + {}_{-1}e^0$ .

$$T = 14.3 \text{ days.} \quad (28)$$



followed by  ${}_{28}\text{Ni}^{65} \rightarrow {}_{29}\text{Cu}^{65} + {}_{-1}e^0$ .

$$T = 160 \text{ min.}$$

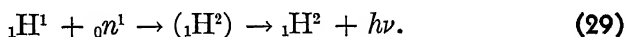
The above  $n$ - $p$  type of reaction has several interesting consequences. It will be noticed that the bombarded nucleus and the final stable nucleus are identical, while the incident neutron has been transformed, apparently, into a proton and an electron. If the mass of the intermediate radioactive nucleus, for example,  $\text{P}^{32}$ , is equal to the mass of the initial nucleus,  $\text{S}^{32}$ , then the energy available for the radioactive disintegration must come from the mass difference between a neutron and a hydrogen atom plus the initial energy of the neutrons. If slow neutrons are used as bombarding particles, the energy available is equivalent to 0.0008 a.m.u or 0.75 Mev. Now the end-point energy of the beta-ray spectrum is equal to the disintegration energy, and if this end-point energy is less than 0.75 Mev, then slow neutrons will be effective in producing the above reaction. But if the end-point energy exceeds 0.75 Mev, the additional energy must come from the kinetic energy of the incident neutrons, and hence only fast neutrons can then be effective in producing this reaction. For example, the end-point energy of the beta-ray spectrum from  $\text{P}^{32}$  is 1.69 Mev; hence only fast neutrons bombarding  $\text{S}^{32}$  will be effective in producing this reaction. This reaction can then also be used to differentiate between slow and fast neutrons.

Another interesting conclusion is that if the mass of the nucleus formed in an  $n$ - $p$  reaction exceeds the mass of the bombarded nu-



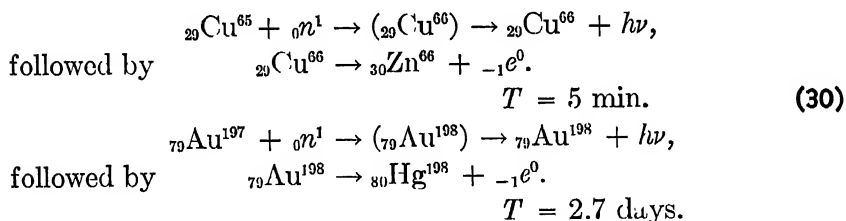
cleus by more than 0.0008 a.m.u., then only fast neutrons will be effective in producing this reaction.

Sometimes the capture of a neutron is not accompanied by the emission of a particle, but by the emission of a gamma-ray photon. In this case the compound nucleus is evidently raised to one of its excited states as the result of this capture, and then returns to its normal state with the emission of a gamma-ray photon. Such gamma rays have been observed coming from the paraffin used to slow down neutrons. The ultimate capture of some of the slow neutrons by the hydrogen nuclei in the paraffin yields the reaction

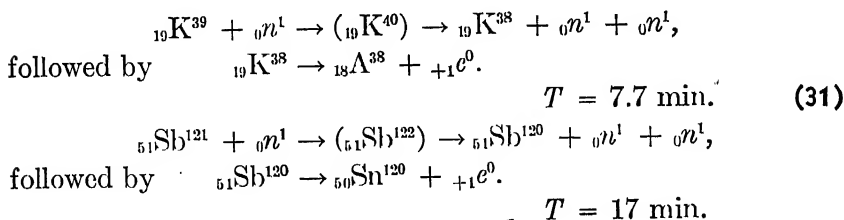


This process is just the reverse of the photodisintegration of the deuteron discussed in the previous section.

The process  $n\text{-}\gamma$  has been observed with a great many elements, particularly the heavier ones. In most cases, the isotopes formed by the capture of a neutron have been found to be radioactive. A few typical cases are



There are many cases in which the capture of a fast neutron has resulted in the emission of two neutrons by the compound nucleus. In most cases the product nucleus is unstable. A few such cases follow:

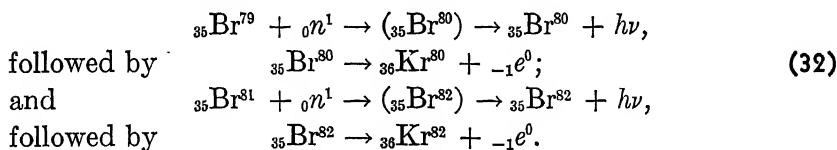


The ability to produce a radioactive isotope of almost any element has made a new tool available to the chemist, biologist, and

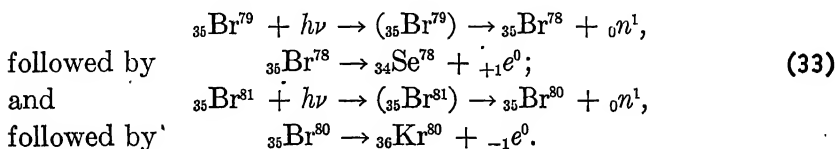
physiologist for the detailed study of various processes. By introducing the radioactive isotope along with the nonradioactive isotopes of an element, the progress of this element can be traced in the process under investigation by means of the beta rays emitted by the radioactive isotope. In many cases a choice of several different half-life periods is available to suit the needs of the particular experiment. A great deal of work has already been done with the radioactive isotopes of carbon, sodium, iron, phosphorus, and iodine used as *tracers* in various processes.

## 126. Nuclear Isomers

Nuclear isomers, which, as we have seen, occur rarely among the naturally radioactive elements, have been found in abundance among the artificially produced radioactive elements. One of the first pairs of nuclear isomers which were produced is that occurring in bromine. When a sample containing bromine is bombarded by slow neutrons, radioactive elements are formed which disintegrate with the emission of electrons with three different half-life periods, 18 min, 4.2 hr, and 36 hr. Chemical tests show that the radioactive elements are isotopes of bromine. But there are only two stable isotopes of bromine of mass numbers 79 and 81, and only the following two reactions can take place:



Now when bromine is bombarded with gamma rays, the following reactions have been observed:



Again three periods have been observed, 6.3 min, 18 min, and 4.2 hr. Two of these periods are common to both sets of reactions and must therefore be assigned to the isotope which is common to both sets of reactions, namely, bromine of mass number 80. Thus

bromine of mass number 80 consists of isomeric nuclei which are radioactive, emitting electrons of two different periods.

The fact that radioactive nuclei of the same isotope can disintegrate in two different ways with two different periods can be explained in terms of the different possible modes by which a nucleus can go from a less stable form to a more stable form. Nuclei, as we have seen, have different energy levels, with each one having an angular momentum associated with it due to the spin of the nuclear particles. A radioactive nucleus such as  $\text{Br}^{80}$  may be formed in an excited state; the angular momentum of this state may differ considerably from that of the ground state. In such a case, the probability of a nucleus going from the excited state to the ground state is small but finite. Just as in optical

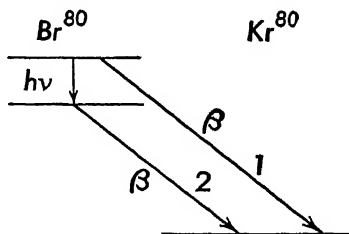


FIG. 159. — Isomeric nuclei of bromine. (1) A bromine nucleus may disintegrate directly from the metastable state, or (2) a bromine nucleus may go first to the ground state and then emit a beta particle.

spectra, we call such an excited state a *metastable state* and the nucleus may remain in this state for an appreciable time. As shown in Figure 159, the nucleus may emit a beta particle directly from this excited state and form  $\text{Kr}^{80}$ , or it may first go to the ground state of  $\text{Br}^{80}$  by the emission of a gamma ray and then emit a beta particle with a different half-life from the ground state. The above explanation of nuclear isomerism has been amply verified experimentally. Because of the large difference between the periods of the two isomers it was possible to make a complete separation of the two nuclear isomers of bromine and show that the excited or metastable state decays with the 4.4 hour half-life, while the ground state of bromine decays with the 18 minute half-life.

The chemical separation of the nuclear isomers depends upon the utilization of the gamma ray emission process for breaking the chemical bond which holds bromine in some suitable compound. For example, the gamma ray may be internally converted; that is, it may knock electrons out of the extranuclear part of an atom in the compound and the energy of this electron may be sufficient to break a chemical bond. Or if the gamma ray has a high energy, its emission will be accompanied by the recoil of the nucleus,

which may be sufficient to eject the atom from the compound. The new product can then be separated by suitable chemical means.

Nuclei of isotopes which are formed in an excited state, and which can disintegrate either directly from this metastable state or first go to a state of lower energy and then disintegrate with the emission of a particle of different energy and different half-life period, are said to be nuclear isomers which are *genetically related*, since one form grows out of the other. Among the naturally radioactive nuclei we mentioned that  $UX_2$  and  $UZ$  have been found to be genetically related *nuclear isomers*;  $UX_2$  is the metastable form from which  $UZ$  is derived. While these two nuclear isomers have different names, it is no longer the practice to give them different names.

Nuclear isomers are not limited to the emission of electrons during radioactive disintegration. Scandium, for example, has isomeric nuclei of mass number  $A = 44$  which disintegrate with the emission of positrons. The metastable state has a half-life period  $T = 2.44$  days; it may go to the ground state by the emission of a gamma ray of 0.28 Mev and then decay from the ground state with a half-life of  $T = 3.92$  hours. The maximum energy of the positrons emitted during the latter disintegration is 1.33 Mev.

Some of the known genetically related nuclear isomers are listed in Table XX.

TABLE XX

GENETICALLY RELATED NUCLEAR ISOMERS			
Radioactive Isotope	Emitted Particle	Half-Life Period of Ground State	Half-Life Period of Metastable State
21 Sc <sup>44</sup>	Positron	3.92 hr	2.44 da
27 Co <sup>60</sup>	Electron	5.3 yr	10.7 min
30 Zn <sup>69</sup>	Electron	57 min	13.8 hr
35 Br <sup>80</sup>	Electron	18 min	4.4 hr
45 Rh <sup>104</sup>	Electron	44 sec	4.2 min
52 Te <sup>127</sup>	Electron	9.3 hr	90 da
52 Te <sup>129</sup>	Electron	72 min	32 da
91 UZ : UX <sub>2</sub>	Electron	6.7 hr	1.14 min

In nuclear isomers which are not genetically related, the upper state and the ground state can undergo independent radioactive disintegrations to neighboring elements. For example, silver of

mass number  $A = 106$  has two isomeric forms; one disintegrates with the emission of a positron of half-life period  $T = 24.5$  minutes and the other disintegrates by  $K$ -electron capture with a half-life period  $T = 8.2$  days. Similarly manganese, of mass number  $A = 52$ , has two isomeric forms: one disintegrates with the emission of a positron of half-life period  $T = 21$  minutes, and the other disintegrates either with the emission of a positron or by  $K$ -electron capture with a half-life period  $T = 6.5$  days. (See § 130.)

## 127. Nuclear Processes and Model of the Nucleus

The empirical data on nuclear physics accumulated in the past few years have altered profoundly our concept of the structure of the nucleus. In the light of the above data, Bohr has proposed a model in which the nucleus is likened to a drop of liquid. In this model, the particles in the nucleus, protons and neutrons, behave very much like particles of a liquid, always remaining a constant distance apart and sharing among them the total energy of the nucleus. The process of nuclear disintegration is compared to the evaporation of particles from a liquid surface, while the process of nuclear capture is compared to the condensation of the vapor.

The concept of energy levels, which was built up for the extranuclear structure, may be carried over into the nuclear structure with some slight modifications. In the extranuclear structure different energy states of the atom corresponded to different electron configurations, but in the case of the liquid drop model of the nucleus, its energy states cannot be described in terms of definite configurations for each of the nuclear particles. A definite nuclear energy state may be due to any one of a large number of configurations of its particles. Because of the strong interactions among the particles, there is a certain probability that a single particle, such as a proton or a neutron, may at one time possess a sufficiently large amount of energy to be able to escape from the nucleus. This is analogous to the process of evaporation of a liquid.

The fact that there are about three hundred stable isotopes of the various elements indicates that the nucleus is essentially a very stable unit, and also that a group of  $Z$  positive charges can exist together with  $A - Z$  neutrons in a very small region of space, which

may be thought of as a sphere of radius not much larger than  $10^{-12}$  cm. Yet Rutherford's alpha-particle scattering experiments definitely showed that there is a force of repulsion between positive charges as given by Coulomb's law, down to distances of about  $3 \times 10^{-12}$  cm for such heavy nuclei as gold. It is obvious that inside the nucleus Coulomb's law cannot hold and must be replaced by some other law of force which will result in an attraction between the charged particles when inside the nucleus. While the exact nature and form of this law of force are not known at present, one may picture the potential energy of a charged particle at different distances from the center of the nucleus in the following way: for the region in which Coulomb's law holds, the potential at any point is given by  $Ze/r$ , where  $r$  is the distance from the center of the nucleus. The potential energy of a charge  $e$  in the neighborhood outside the nucleus is therefore  $Ze^2/r$ . Inside the nucleus, the potential energy must decrease rapidly because of the forces of attraction between the particles. To a first approximation, the part of the potential energy inside the nucleus may be considered as constant and equal to some value  $U_0$ , which may be either positive or negative. Figure 160 shows the assumed form of the potential energy curve as a function of the distance from the nucleus. The Coulomb potential energy curve is joined to the straight line  $U_0$  by means of a steep curve. The height of the curve  $H$  is usually referred to as the height of the *potential barrier*.

A charged particle, such as a proton, deuteron, or alpha particle, which is projected toward the nucleus with kinetic energy  $\mathcal{E}_1$  will experience a force of repulsion as it approaches the nucleus. According to classical physics, the kinetic energy of this particle will be decreased to zero at some point  $r_1$ , and it will then move away from the nucleus with the same energy  $\mathcal{E}_1$ . But from experiments on nuclear disintegrations it is known that a fraction of such particles can penetrate the potential wall and get inside the nucleus, that is, are "captured" by the nucleus. There must, therefore, be a definite probability that a positively charged particle, whose energy is less than the height of the potential barrier, can penetrate the potential wall. This probability can be calculated on the basis of wave mechanics. Once the particle is inside the nucleus, its energy is quickly distributed among all the particles of the newly formed compound nucleus. In the case of the cap-

ture of an alpha particle, once the particle is inside the nucleus, it may no longer be considered as an independent entity, but as two protons and two neutrons among all the other protons and neutrons.

The manner in which the probability of penetration of the po-

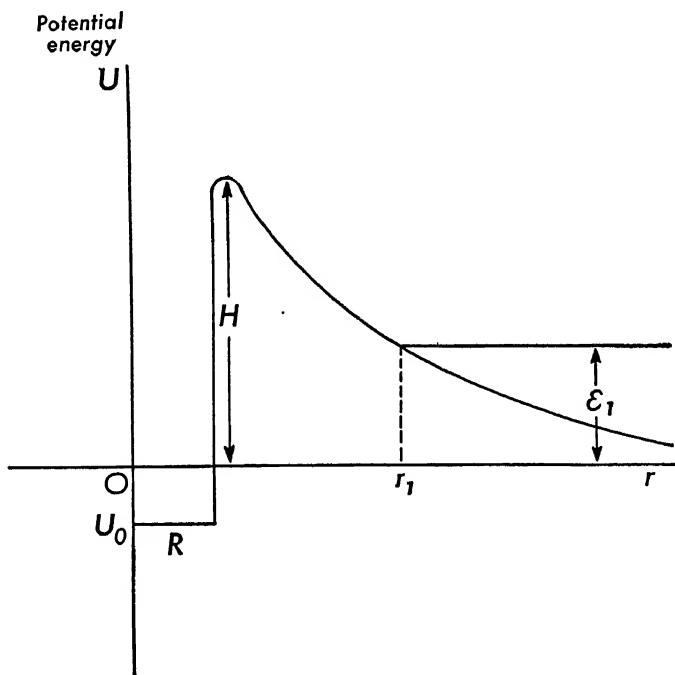


FIG. 160. — Assumed form of the potential energy curve in the neighborhood of a nucleus.  $R$  is the radius of the nucleus.

tential wall varies with the energy of the incident particle can be determined in those cases in which the capture of the particle results in the emission of some other particle. The yield — that is, the ratio of the number of emitted particles to the number of incident particles — will then be proportional to the probability of penetration. It has been found that while the yield, in general, increases with the increasing energy of the incident particle, there are many instances in which the yield is very great for a small range of energy values, and decreases for particle energies both greater and smaller than this particular value of the energy. For example, when a thin film of magnesium is bombarded with alpha particles, the yield curve of protons exhibits the form shown in

Figure 161. The values of the alpha-particle energy for the maxima on the yield curve are called *resonance energies*. Of course, there is no potential wall for neutrons, since they possess no charge

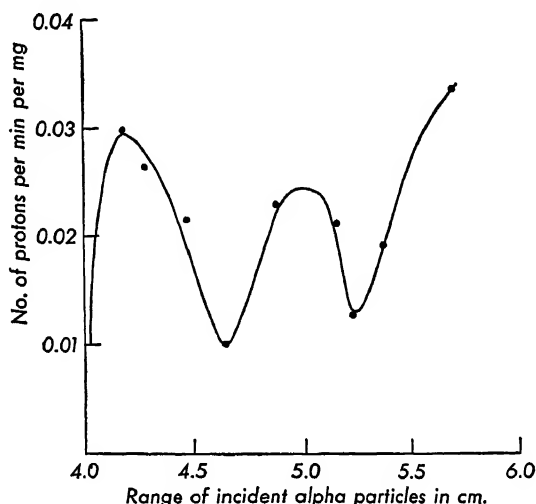


FIG. 161. — Yield curve of protons liberated when magnesium is bombarded by alpha particles. The positions of the maxima show the resonance values of the energies.

and hence even very slow neutrons with energies less than one electron volt can penetrate the nucleus.

With the compound nucleus in a high energy state, either through the capture of a particle or through excitation by radiation, there is a definite probability that one of the many energy exchanges in the nucleus will result in giving a single particle sufficient energy to leave the nucleus. In most cases the outgoing particle will carry with it only a small amount of the energy of the excited state of the nucleus, thus leaving the residual or product nucleus in an excited state. This product nucleus will then return to a lower energy state either with the emission of a gamma-ray photon or with the emission of another particle so that the disintegration process will result in three final particles.

To explain the emission of alpha particles from a nucleus containing only protons and neutrons requires the addition of another step in the process, namely, that at the instant of emission two protons and two neutrons should form an alpha particle. The probability of the emission of an alpha particle is therefore the



product of two probabilities: (1) the probability that an alpha particle will be formed by the combination of two protons and two neutrons, and (2) the probability that an alpha particle will be able to penetrate the potential wall even though its energy is less than that corresponding to the height of the potential barrier. Wave mechanical calculations have led to a relationship between the average lifetime of an alpha-particle emitter and the energy of the alpha particle which is very similar to the Geiger-Nuttall law arrived at empirically, lending great support to this theory of alpha-particle disintegration.

## 128. Emission of Positrons and Electrons

Induced radioactivity with the emission of either positrons or electrons is a process differing greatly from the disintegration of compound nuclei with the emission of heavy particles. The radioactive nucleus, for example, has a much longer lifetime than the compound nucleus which disintegrates with the emission of one or more heavy particles. It will be recalled that the beta rays from the naturally radioactive elements have a continuous distribution of energies, from very low energy values to a maximum value known as the end-point energy. Measurements of the energies of the electrons and positrons emitted by artificially radioactive elements show that they also form a continuous range of values up to a definite maximum. Pauli (1931) has suggested that the end-point energy of the beta-ray spectrum represents the actual disintegration energy. To account for the continuous distribution of energy and the conservation of energy in nuclear processes, Pauli suggested that two particles are emitted by the nucleus in a beta-ray disintegration, and that the total energy of these two particles is a constant which is equal to the end-point energy observed in the beta-ray spectrum. One of the particles is the electron itself and the other particle is supposed to be a neutral particle of negligible rest mass; this particle is called a *neutrino*. There is another reason for the introduction of the neutrino into beta-particle disintegrations: the conservation of angular momentum principle must also be satisfied in nuclear processes. Now the electron is known to possess a spin angular momentum of  $\frac{1}{2} \frac{h}{2\pi}$ . To conserve angular momentum, the neutrino must be given a spin angular

momentum of  $\frac{1}{2} \frac{h}{2\pi}$  in a direction opposite to that of the electron spin. An exactly similar hypothesis is introduced for the positron emitters.

The remaining problem is to determine the origin of the electron and neutrino. The present view, stated in an elementary way, is that the neutron breaks up into a proton which remains in the nucleus, and an electron and a neutrino which are ejected from the nucleus. This is analogous to the emission of a light quantum when an atom goes from one energy state to another. There are no photons in the atom, but when an atom goes from a state characterized by one set of quantum numbers to another state, a photon is emitted. One may imagine the neutron to represent one quantum state of a heavy particle and the proton to represent another quantum state of the same heavy nuclear particle. When this heavy particle goes from the neutron quantum state to the proton quantum state, it does so with the emission of a pair of particles, an electron and a neutrino. In an analogous manner, a positron and a neutrino are emitted when a proton is transformed into a neutron.

Several attempts have recently been made to substantiate the above hypothesis by getting some direct experimental evidence of the existence of the neutrino. Most of these results have been negative. This is not surprising in view of the fact that a neutrino has very small mass and no charge. However, in some cloud chamber experiments by Crane and Halpern (1938) on the disintegration of chlorine,  $\text{Cl}^{38}$ , which emits electrons, they found that the measured value of the momentum of the electron was not always equal to the measured value of the momentum of the product nucleus formed in the process of disintegration. Assuming that the principle of the conservation of momentum holds in nuclear processes, then, if an electron only is emitted during this disintegration, the momentum of the electron should be equal and opposite to the momentum of product nucleus. In the above experiment it was found that the product nucleus, which was formed as the result of the emission of a low velocity electron, had a greater momentum than the electron. The momentum of a product nucleus accompanying the emission of a high velocity electron was found to be about equal to that of the electron. Crane and Hal-

pern interpreted these results to mean that a neutrino is emitted simultaneously with the electron. On the neutrino hypothesis, a high energy electron is accompanied by a low energy neutrino and a low energy electron is accompanied by a high energy neutrino; since the sum of the two energies must equal the end-point energy of the beta-ray spectrum. Hence, when an electron of high velocity is emitted, the total momentum of the two light particles is practically equal to that of the electron, and this in turn should be the same as the momentum of the product nucleus. But when a low velocity electron is emitted, the momentum of the neutrino must make up the difference between the momentum of the product nucleus and that of the electron.

It must be noted that there is no visible evidence of the path of the neutrino in these cloud chamber experiments; further experiments will be necessary before its existence can be definitely established, but undoubtedly many such experiments will be performed in the near future.

## 129. Nuclear Magnetic Moments

We have previously shown that a nucleus has an angular momentum due to its spin. (See § 100.) In addition, the nucleus also possesses a magnetic moment. Accurate data on the magnetic moments of atomic nuclei should provide additional information on the nature of the nuclear forces and should also help in selecting an appropriate nuclear model. Within the past few years a new and very precise method for the determination of nuclear magnetic moments has been developed by Rabi and his co-workers. This method is a direct outgrowth of the Stern-Gerlach type of experiment for the determination of the magnetic moment of the electron due to its spin. It is known as the *magnetic resonance method* because it depends essentially upon resonance between the precession frequency of the nuclear magnet about a constant magnetic field direction and the frequency of an impressed high frequency magnetic field.

Just as the magnetic moment of an electron is expressed in terms of a Bohr magneton, so the nuclear magnetic moment is expressed in terms of a *nuclear magneton*  $M_n$  defined by the equation

$$M_n = \frac{eh}{4\pi Mc} \quad (34)$$

in which  $M$  is the mass of the proton. The nuclear magneton is thus only about  $1/1840$  of a Bohr magneton. If  $I$  is the nuclear spin quantum number, the angular momentum of the nucleus due to its spin is  $I\hbar/2\pi$ . Just as we had to introduce the Landé  $g$ -factor to relate the magnetic moment of the electrons of an atom to their total angular momentum (see § 96), so we have to introduce a nuclear  $g$ -factor to relate the magnetic moment  $\mu$  of a nucleus to its spin angular momentum. This relationship can be written as

$$\mu = gIM_n = gI \frac{e\hbar}{4\pi Mc} \quad (35)$$

in which  $g$  is the nuclear  $g$ -factor. It can be seen that the nuclear  $g$ -factor is the ratio of the nuclear magnetic moment, expressed in units of nuclear magnetons, to the spin angular momentum, expressed in units of  $\hbar/2\pi$ .

When a nucleus of magnetic moment  $\mu$  is in a constant magnetic field of intensity  $H$ , it will precess about the direction of the magnetic field with a frequency  $\nu$  given by Larmor's theorem

$$\nu = \frac{\mu H}{I\hbar}. \quad (36)$$

The magnetic moment  $\mu$  of a nucleus can thus be found by determining the Larmor frequency  $\nu$  which the nucleus of spin quantum number  $I$  acquires in a known constant magnetic field  $H$ . Instead of working with nuclei alone, Rabi and his co-workers used beams of molecules whose total electronic angular momentum is zero. Figure 162 shows the paths of typical molecules in the different magnetic fields used in the magnetic resonance experiment for measuring nuclear magnetic moments, and Figure 163 is a schematic diagram of the apparatus. A narrow stream of molecules issues from the source at  $O$ . A very small fraction of these molecules will pass through the collimating slit  $S$  and reach the detector at  $D$ . In the absence of any inhomogeneous magnetic deflecting fields, the molecules traverse straight-line paths  $OSD$  and form the so-called *direct* beam.

The magnets  $A$  and  $B$  are specially designed to produce inhomogeneous magnetic fields. The magnetic fields are in the same direction but their gradients,  $\frac{dH}{dz}$ , are in opposite directions as

shown in Figure 162. A molecule with magnetic moment  $\mu$  will be deflected in the direction of the gradient if  $\mu_z$ , the projection of  $\mu$  in the direction of the field, is positive, and will be deflected in the opposite direction if  $\mu_z$  is negative. Molecules which left

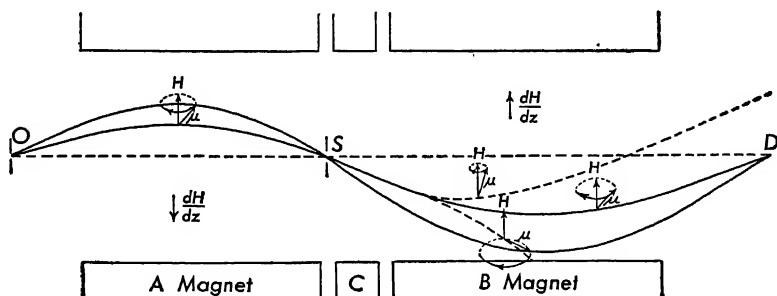


FIG. 162. — Paths of molecules in the molecular beam resonance experiment. The two solid curves indicate the paths of two molecules which have different magnetic moments and velocities and whose moments are not changed during passage through the apparatus. This is indicated by the small gyroscopes drawn on one of the paths, in which the projection of the magnetic moment along the field remains fixed. The two dotted curves in the region of the *B* magnet indicate the paths of two molecules, the projection of whose nuclear magnetic moments along the field has been changed in the region of the *C* magnet. This is indicated by means of the two gyroscopes drawn on the dotted curves, for one of which the projection of the magnetic moment along the field has been increased, and for the other of which the projection has been decreased.

the source along the line *OSD* will be deflected to one side. Other molecules which leave *O* at some angle to the line *OSD* will follow paths indicated by the solid lines and reach the detector *D*. The force experienced by any such molecule in the inhomogeneous field due to the *A* magnet is

$$F = \mu_z \left( \frac{\partial H}{\partial z} \right)_A; \quad (37)$$

a similar expression holds for the force due to the *B* magnet. The actual deflection produced by each magnetic field can be established from a knowledge of the velocity of the molecule, which is determined by the temperature of the source, and from the geometry of the apparatus. If no change occurs in  $\mu_z$  as the molecule goes from the *A* field to the *B* field, the deflections in these fields will be in opposite directions. It is a simple matter to adjust the two magnetic field gradients to make these deflections equal

in magnitude and thus bring the molecules to the detector, that is, to "refocus" the beam. When the two magnetic fields are properly adjusted, the number of molecules reaching the detector *B* in any given time interval is about the same whether the magnets are on or off.

Magnet *C* produces a homogeneous magnetic field of intensity *H*. In the same region there is a high frequency alternating magnetic field (not shown in Figure 162) produced by sending current

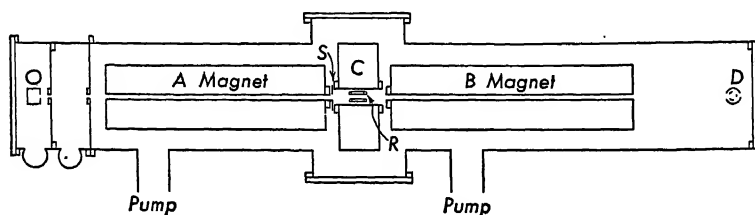


FIG. 163. — Schematic diagram of the apparatus used in the molecular beam experiment.

in opposite directions through two parallel wires *R* placed between the pole faces of the magnet *C*, see Figure 163. The oscillating magnetic field  $H_1$  is at right angles to the homogeneous magnetic field *H* produced by the *C* magnet. When a molecule of magnetic moment  $\mu$  enters this region, it will precess about *H* with the Larmor frequency  $\nu$ . The interaction with the oscillating magnetic field  $H_1$  will produce a torque which may either increase or decrease the angle between  $\mu$  and *H*; in general, if the frequency *f* of the alternating magnetic field is different from the Larmor frequency of precession  $\nu$ , the net effect produced will be small, since the torque produced by the alternating magnetic field will rapidly get out of phase with the precessional motion. But when  $f = \nu$ , the increase or decrease produced in the angle between  $\mu$  and *H* will be cumulative and this change in angle will become quite large. The molecule will then follow one of the dotted paths when it gets into the region of the *B* magnet and will not enter the detector at *D*. In some of the experiments, the frequency of the alternating magnetic field is kept at a constant value, and the intensity of the magnetic field *H* produced by the *C* magnet is varied. Figure 164 is a typical curve which shows the beam intensity plotted as a function of the magnetic field strength *H* while the frequency of the alternating field is kept constant. It will be ob-

served that resonance occurs for a definite value of  $H$ ; the resonance value is the minimum value of the curve. The resonance curve of the  $\text{Li}^7$  nucleus shown in Figure 164 was obtained with a beam of  $\text{LiCl}$  molecules. In other experiments with the  $\text{Li}^7$  nucleus, molecular beams of  $\text{LiF}$  and  $\text{Li}_2$  were used.

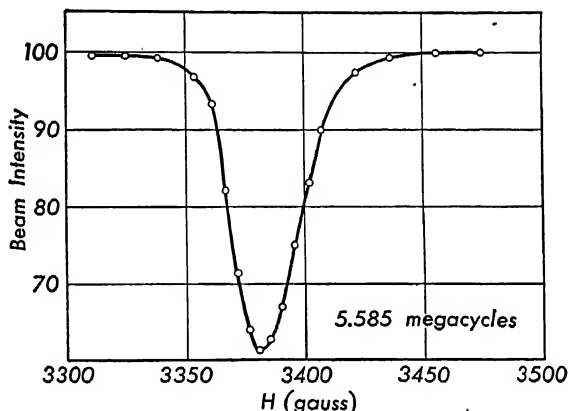


FIG. 164. — Resonance curve of the  $\text{Li}^7$  nucleus observed in  $\text{LiCl}$ .

Solving equations (35) and (36) for  $g$  and substituting the resonance frequency  $f$  for the Larmor frequency  $\nu$ , we get

$$g = \frac{4\pi M c}{e} \frac{f}{H} \quad (38)$$

Since the values of the constants  $M$ ,  $e$ , and  $c$ , are accurately known, the substitution of the measured values of the resonance frequency  $f$  and the intensity of the homogeneous magnetic field  $H$  in equation (38) will yield the  $g$ -factor for the particular nucleus under investigation. If its nuclear spin quantum number  $I$  is known, then

$$\mu = gI \quad (39)$$

will give the magnetic moment of the nucleus in nuclear magnetons, while substitution of the values of  $g$  and  $I$  in equation (35) will give the nuclear magnetic moment in e.m. units. For example, in the case of the  $\text{Li}^7$  nucleus,  $I = 3/2$  and the measured value of  $g$  is 2.1688; hence its nuclear magnetic moment is 3.2532 nuclear magnetons.

Of very great importance in nuclear physics are the magnetic moments of the proton, deuteron, and neutron. Millman and

Kusch made a precise measurement of the magnetic moment of the proton, while Kellogg, Rabi, Ramsey, and Zacharias made a precise determination of the ratio of the magnetic moments of the proton and deuteron. From these measurements the magnetic moment of the proton was found to be 2.7896 nuclear magnetons and that of the deuteron was found to be 0.8565 nuclear magneton. If we assume that a deuteron consists of a proton and a neutron and that the magnetic moment of the deuteron is the sum of the magnetic moments of the proton and the neutron, then the magnetic moment of the neutron is  $\mu_n = -1.933$  nuclear magnetons. Alvarez and Block made an independent determination of magnetic moment of the neutron by sending a beam of slow neutrons through a modified type of molecular beam magnetic resonance apparatus. Using the value  $I = 1/2$  for the spin of the neutron, they obtained  $\mu_n = -1.935$  nuclear magnetons for the magnetic moment of free neutrons.

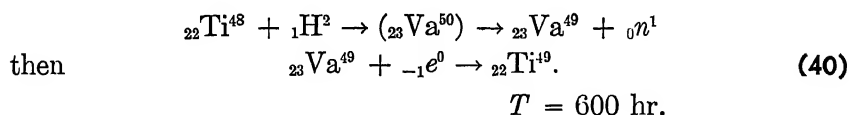
### 130. Nuclear K-Electron Capture

In nuclear reactions, the extranuclear electrons are generally ignored except in a few special cases. For example, we saw that the sharp line beta-ray spectrum was due to the internal conversion of the gamma-ray energy and provided a method for measuring the energy of the gamma-ray photons. The external electrons do play a part in some of the nuclear reactions which might take place by positron emission, particularly if such a reaction involves a comparatively small release of energy. Instead of the nucleus emitting a positron in its radioactive decay, it may capture an electron from the extranuclear part of the atom, usually one of the  $K$  electrons, to form the same product nucleus. The capture of the  $K$  electron by the nucleus will leave the product atom in an excited state with one electron missing from the  $K$  shell; it will then return to the normal state by the emission of  $X$  rays characteristic of the product atom. As a matter of fact, this type of nuclear reaction is detected by means of the  $X$  rays emitted during this process.

Probably the most clear-cut example of  $K$ -electron capture is the radioactive disintegration of vanadium,  ${}_{23}\text{V}^{49}$ , into titanium,  ${}_{22}\text{Ti}^{49}$ , with the capture of a  $K$  electron by the vanadium nucleus to form a titanium atom in the  $K$  state. This reaction was in-



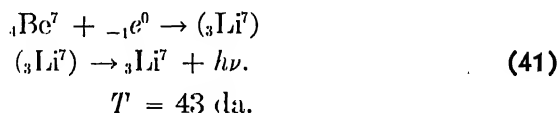
vestigated carefully by Walke, Williams, and Evans, who found that vanadium decays only by *K*-electron capture with a half-life  $T = 600$  hours. The radioactive vanadium was formed by bombarding titanium with deuterons, the following reactions taking place:



The active product was separated chemically from the titanium and found to be vanadium, but no radiations of any kind other than Ti  $K\alpha$  radiation were found to be emitted by the vanadium precipitate. The only conclusion, therefore, is that the excited vanadium nucleus captured one of its *K* electrons to form titanium with one electron missing from its *K* shell with the subsequent emission of X rays characteristic of titanium. Furthermore, the intensity of these X rays diminishes exponentially with the time, so that at the end of 600 hours, the intensity has dropped to half its original value.

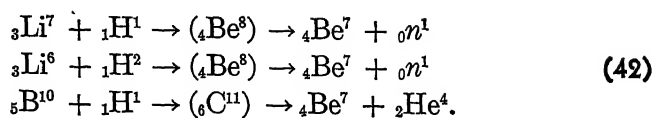
The fact that no radiation other than X rays is emitted in the radioactive disintegration of vanadium by *K*-electron capture to titanium indicates that the product titanium nucleus is in the ground state or state of lowest energy. Since the capture of an electron by the nucleus results in the change of a proton into a neutron, this must be accompanied by the emission of a neutrino in order to conserve the angular momentum of the nucleus.

In many cases of radioactive disintegration by *K*-electron capture, gamma rays accompany this process; in other cases the disintegration can take place either by positron emission or by *K*-electron capture, so that both processes are observed in the same radioactive sample. For example, the isotope of beryllium of mass number  $A = 7$ , which disintegrates by *K*-electron capture, also emits gamma rays of 0.485 Mev. The reaction is



This radioactive beryllium isotope can be produced by any of

the following reactions:



On the other hand, the vanadium isotope of mass number  $A = 48$  can disintegrate either by positron emission or by  $K$ -electron capture with a half-life of 16 days. Walke, Williams, and Evans have found that in about three tenths of the cases the disintegration is by electron capture and the remainder by positron emission. Gamma rays are also emitted during this disintegration.

### 131. Production of Pairs of Charged Particles

In cloud chamber experiments on the passage of high energy gamma rays through a heavy element such as lead, pairs of oppositely charged particles were observed to originate from a common point. From the densities of the tracks it was evident that these particles had exactly the same mass as that of an electron. The velocities and hence the kinetic energies of these particles could be determined from the measurements of the radii of curvature of their paths in a magnetic field. The results of these measurements support the view that a positron and an electron are formed as the result of the interaction of a gamma-ray photon with a heavy nucleus. From calculations on the number produced, it is believed that this pair formation occurs in the intense electric field outside the nucleus rather than inside it.

If a gamma-ray photon of energy  $h\nu$  is transformed into a pair of particles, each of rest mass  $m_0$ , then, according to the principle of conservation of energy,

$$h\nu = 2m_0c^2 + \mathcal{E}_1 + \mathcal{E}_2, \tag{43}$$

where  $m_0c^2$  is the rest-mass energy of each particle and  $\mathcal{E}_1$  and  $\mathcal{E}_2$  are the kinetic energies of the particles at the instant of production. Now,  $m_0c^2$  is equivalent to  $5.11 \times 10^5$  ev energy; hence only gamma-ray photons whose energies are greater than 1.02 Mev can form a pair of charged particles.

Experiments on the production of pairs of charged particles have been performed successfully with the gamma-ray photons from  $\text{ThC}''$  ( $h\nu = 2.62$  Mev). In this case the total kinetic energy

of the positron and electron formed by each photon should be 1.6 Mev. Cloud chamber measurements of the energies of these particles are in good agreement with this calculated value. Figure 165 is a cloud chamber photograph, taken by Crane, showing

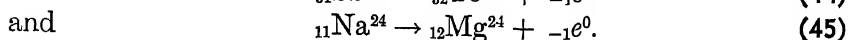
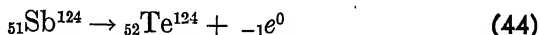


FIG. 165. — Cloud chamber photograph of the paths of a pair of oppositely charged particles, an electron and a positron, formed from the disintegration of a 5.7 Mev gamma ray photon in its passage through a sheet of lead 0.002 inch thick. Magnetic field of 1,680 oersteds is directed into the paper. (Photograph by H. R. Crane.)

the paths of a pair of oppositely charged particles, a positron and an electron, which were produced by a gamma-ray photon which entered the lead foil 0.002 inch thick. The gamma-ray photon came from a target of fluorine which had been bombarded by protons. The known energy of the photon is 5.7 Mev. From measurements of the radii of curvature of the paths of the particles in the known magnetic field, Crane computed the sum of energies of these two particles to be 4.7 Mev. This checks very well with equation (43) when the rest-mass energy of the two particles, 1.02 Mev, is added to the sum of their kinetic energies.

The production of pairs of particles represents a new method

for measuring the energy of the gamma rays. Kruger and Ogle have recently used this method for studying the energies of the gamma-ray photons emitted during the following two radioactive transformations:



The gamma-ray photons produced in each of these transforma-

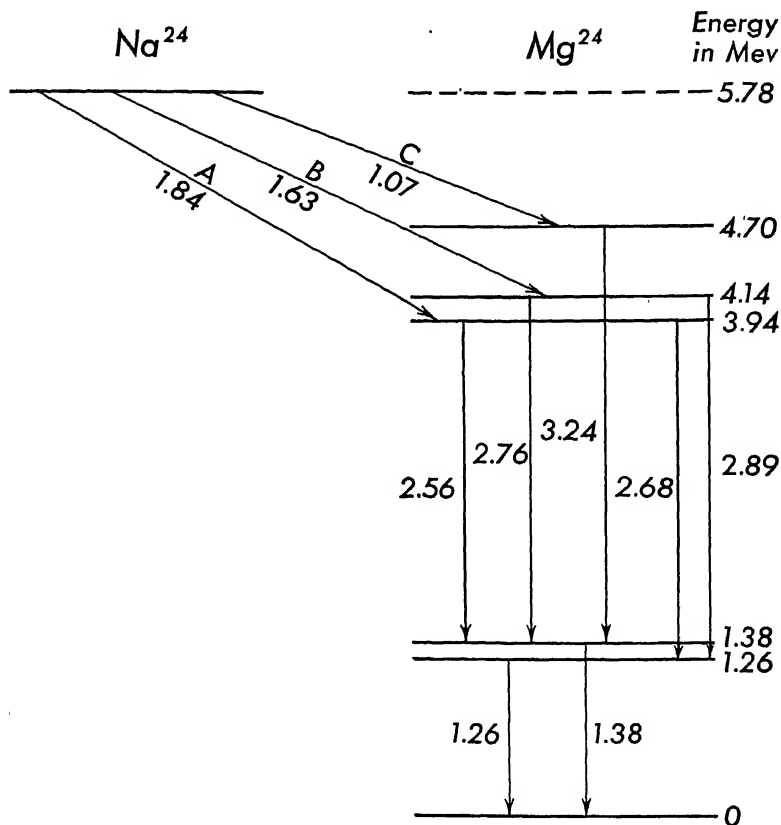


FIG. 166. — Energy level diagram of the nucleus  $\text{Mg}^{24}$  formed in the beta-ray disintegration of  $\text{Na}^{24}$ . The energies are in Mev.

tions were collimated by means of a long slit in a lead block and allowed to pass through a cloud chamber perpendicular to the magnetic field. Stereoscopic photographs were made after each expansion and pairs of particles located. Only those pairs which satisfied certain stringent conditions were used in making meas-

urements. Some of these conditions were that both tracks should start at the same point; that they should lie in the same plane, and that there should be no obvious scattering in that portion of the track in which the radius of curvature was measured.

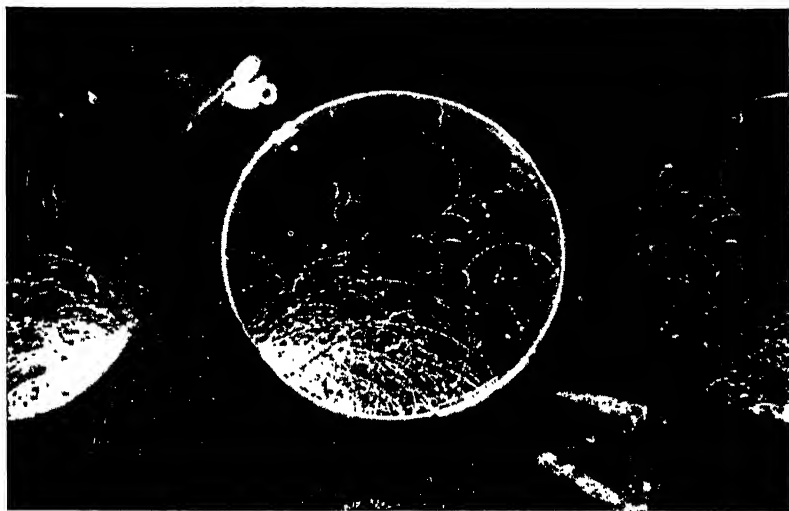


FIG. 167. — Cloud chamber photograph of a triplet; the triplet consists of the paths of a positron and two electrons. The triplet was produced by the conversion of a gamma ray into a positron and an electron in the field of another electron. The magnetic field is directed into the paper. (From a photograph by P. Gerald Kruger and W. E. Ogle.)

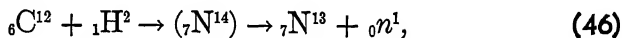
By the above method, Kruger and Ogle found that the gamma-ray photons from the transition  $\text{Sb}^{124} \rightarrow \text{Te}^{124}$  all have the same energy, 1.70 Mev, while the gamma-ray photons from the transition  $\text{Na}^{24} \rightarrow \text{Mg}^{24}$  have five distinct values: 2.56, 2.68, 2.76, 2.89, and 3.24 Mev. By correlating the gamma-ray spectrum found by this method with the beta-ray energies previously found by others, they suggest the nuclear energy level diagram for  $\text{Mg}^{24}$  shown in Figure 166.

An interesting side light of this investigation is the discovery of triplet paths in the cloud chamber photographs as shown in Figure 167. These triplets consist of the paths of a positron and two electrons, and are accounted for by the production of a pair of particles by the splitting up of a gamma ray when it is in the field of an electron. This electron suffers a recoil when the gamma ray is transformed into an electron and a positron. Measurements

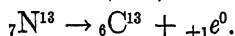
show that both the momentum of the system and the energy of the system are conserved in this process.

### 132. Annihilation of Charged Particles

The transformation of a photon into a positron and an electron is sometimes referred to as the *materialization of energy*. The reverse process, in which a positron and an electron combine and their energy is transformed into the energy of gamma rays, is usually referred to as the *annihilation of matter*. This process has been observed by Thibaud, Crane, and Lauritsen, and others. A convenient source of positrons is a block of carbon which has been bombarded with deuterons producing radioactive nitrogen according to the reaction



followed by



In one experiment, some recently activated carbon was placed at the bottom of an ionization chamber and the ionization measured. To distinguish between the ionization produced by the positrons and that produced by the gamma rays, a second ionization chamber was placed directly below the first one. The walls and window of the ionization chamber were sufficiently thick to prevent any of the charged particles from entering the chamber, so that only the ionization produced by the gamma rays was recorded. It was found that the ionization produced by the gamma rays decreased exponentially with time in exactly the same way as that due to the positrons; that is, the half-life period was the same whether determined from the rate of emission of positrons or from the intensity of the gamma rays associated with this process. It seems reasonable to assume that the gamma rays have their origin in the annihilations of the positrons by electrons. To check this assumption, a freshly activated piece of carbon was placed, with the activated side upward, directly above one of the ionization chambers. It may be assumed that as many positrons are emitted upward as downward. Those that are emitted downward are absorbed in the rest of the carbon and give rise to gamma rays which are measured by the ionization produced in the chamber. The upward-moving positrons escape into the air. However, when a thin sheet of aluminum is placed on top of the carbon, the

upward-moving positrons will be absorbed in the aluminum, and give rise to gamma rays. The amount of ionization produced with the aluminum on the carbon was found to be about twice as great as that produced without the aluminum, indicating that the positrons were annihilated in the aluminum, giving rise to gamma-ray photons.

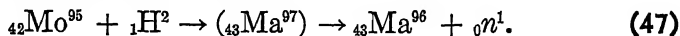
Measurements of the intensity of the ionization produced by the gamma rays showed that the number of photons produced was twice the number of positrons absorbed. The energy of these gamma-ray photons has been measured and found to be about 0.5 Mev. This is approximately the same as the rest-mass energy of the positron and of the electron; hence positrons and electrons are most likely to combine when their speeds are small. Since the combined mass of the electron and positron is equivalent to about 1 Mev, the result of their annihilation must be the production of two gamma-ray photons each of 0.5 Mev energy, but traveling in opposite directions in order to conserve momentum. The fact that two photons traveling in opposite directions are produced by the annihilation of a positron and an electron was demonstrated by using two Geiger-Müller counters, one on each side of an activated carbon block. The counters were arranged so that they would record only *coincidences*, that is, photons entering the two counters simultaneously. The number of coincidences observed, and their decrease with time, checked very well with the known rate of emission of positrons by the carbon block.

It should be noted that, in the annihilation of matter, two oppositely charged particles combine to produce two equal photons, while in the materialization of energy, a single photon breaks up into two oppositely charged particles.

### 133. Production of New Elements

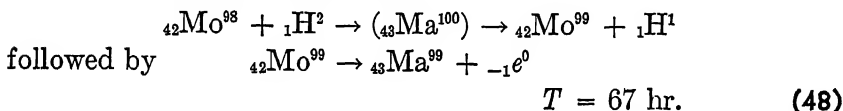
Until recently there were three places vacant in the periodic table of elements for elements of atomic number less than 92, one at  $Z = 43$ , another at  $Z = 85$ , and the third at  $Z = 87$ . With the number of different types of bombarding particles made available by the physicist and the variety of nuclear reactions known, it should be possible to produce these missing elements by bombarding nuclei of neighboring atoms of the periodic table with suitable particles. One of the first produced in this manner was

element  $Z = 43$ , now known as *masurium*; it was produced by Perrier and Segrè (1937) by bombarding molybdenum,  $Z = 42$ , with high energy deuterons accompanied by the emission of a neutron. Seaborg and Segrè showed that the masurium isotope formed in this reaction has a mass number  $A = 96$ , so that the reaction may be written as follows:

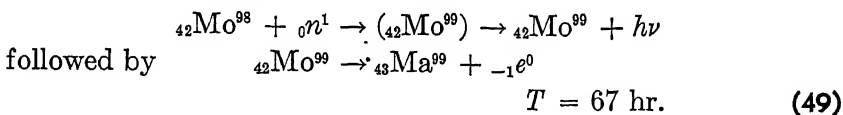


This isotope of masurium has also been produced in a  $(p-n)$  reaction with molybdenum and in an  $(\alpha-n)$  reaction with columbium,  $Z = 41$ . This isotope is radioactive, emitting positrons of half-life period  $T = 2.7$  hours.

In the bombardment of molybdenum with deuterons, a radioactive isotope of molybdenum was produced which disintegrated with the emission of an electron with a half-life period  $T = 67$  hours. The nuclear reactions are

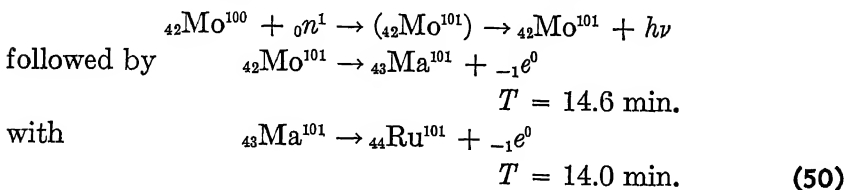


Seaborg and Segrè also produced the same radioactive isotope by bombarding molybdenum with neutrons with the reaction



This isotope of masurium is in a metastable state and decays to the ground state with the emission of a gamma ray with a half-life period  $T = 6.6$  hours.

Another isotope of masurium of mass number  $A = 101$  has been produced by the beta-particle disintegration of a radioactive isotope of molybdenum with the following nuclear reactions:

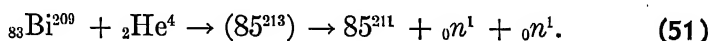


Longer-lived masurium isotopes have also been produced, and this has made possible the study of some of its chemical properties;

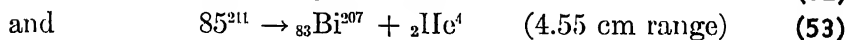


the assignment of mass numbers to these isotopes is not yet certain. Some isotopes decay by electron emission, others by *K*-electron capture. Some of the latter have half-life periods of 62 days and 90 days. Masurium is a chemical homologue of rhenium; that is, they both appear in the same column in the periodic table. It can be separated readily from molybdenum by chemical means, but because of the small amount of masurium formed, only a few of its chemical properties have actually been determined.

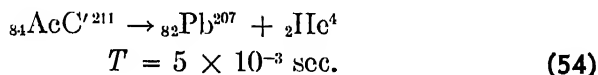
The element of atomic number  $Z = 85$  has been produced by Corson, MacKenzie, and Segrè by bombarding bismuth with 32 Mev alpha particles. They found six different activities as a result of this bombardment, but all had exactly the same half-life period,  $T = 7.5$  hours. These activities were (1) an alpha-particle group of 6.55 cm range, (2) another alpha-particle group of 4.52 cm range, (3) a gamma ray with an energy of 0.5 Mev, (4) an X ray or gamma ray of about 80 Kev, (5) a low energy X ray, and (6) a few low energy electrons. Their analysis of this experiment is as follows: since bismuth has only one stable isotope, the first reaction is



Element 85 then disintegrates in one of two ways, either by *K*-electron capture to actinium C', or by alpha-particle emission to bismuth, according to the following reactions:



Actinium C' disintegrates immediately,  $T = 5 \times 10^{-3}$  seconds, with the emission of an alpha particle of 6.55 cm range; this is very close to the known range of the alpha particles of the actinium C' formed in the actinium radioactive series. This reaction is



If the actinium C' is formed by *K*-electron capture, this must be followed by the emission of *K*-series X rays. The X rays were measured by absorption methods and found to be identical with those of polonium,  $Z = 84$ , an isotope of AcC'. The X-ray photons were also counted with the same thin-walled Geiger counter that was used for counting the alpha particles, and taking into

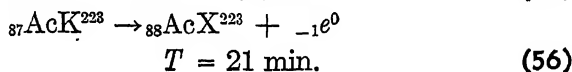
account the difference in the counting efficiencies for the two types of radiation, it was estimated that there were equal numbers of alpha particles and X-ray photons emitted. This is to be expected if element 85 decays by *K*-electron capture to  $\text{AcC}'$ ; the *K*-electron capture is followed by the emission of an X-ray photon and the  $\text{AcC}'$  immediately disintegrates with the emission of an alpha particle.

Element 85 is a chemical homologue of iodine although it is found to have some of the properties of a metal. Its resemblance to iodine was shown in a series of experiments by Hamilton and Soley, who found that it is concentrated in the thyroids of normal and thyrotoxic guinea pigs in a manner similar to that of iodine.

Element 87, now called actinium K, has been found as one of the products in the natural radioactive disintegration of actinium. About 1 per cent of the actinium nuclei disintegrate with the emission of alpha particles forming  $\text{AcK}$ ,



followed by



$$T = 21 \text{ min.} \quad (56)$$

The branching of actinium is shown in the actinium series of Figure 139(c).

### 134. The Meson

The existence of a new type of particle has been postulated as a result of the observations of the energies and penetrating power of cosmic rays. This new particle is called a *meson* and has either a positive or negative charge equivalent to that of an electron, but its mass is approximately 200 times that of an electron.

It has been found that cosmic rays at sea level consist of two groups of particles, one a *soft* component which is absorbed in about 10 cm of lead, the other a *hard* component which can penetrate more than a meter of lead. The soft group of particles has been definitely identified as consisting of electrons, positrons, and their accompanying gamma radiations. The argument that the penetrating radiation consists of mesons, rather than electrons or protons, is based upon measurements of the curvature of their tracks in a magnetic field, the density of ionization along their tracks as observed in Wilson cloud chamber photographs, and

upon their ranges. For example, some tracks, whose curvature indicated an energy of about 500 Mev on the assumption that they were due to electrons, had an ionization per centimeter of path too great for electrons. On the other hand, if these tracks were assumed to be due to protons, then their energy, calculated from the curvature of their paths, was much too small to account for their great range. If the charge of the penetrating particle is assumed to be equivalent to that of an electron, then from the known laws relating the mass of a particle, its range, the density of the ionization along its track, and the energy, the mass of the particle can be calculated. Such calculations lead to values for its mass from about 100 to 300 times the mass of an electron.

It is interesting to note that the existence of a charged particle of mass intermediate between the mass of an electron and that of a proton was first postulated by Yukawa (1935) in attempting to account for the interaction between the heavy particles in nuclei. It is probable that the mesons are produced in the upper atmosphere by the action of the primary cosmic rays, and, as suggested by Euler and Heisenberg (1938), these mesons probably disintegrate in a manner similar to that of radioactive substances with a calculated half-life period of about  $2 \times 10^{-6}$  sec.

In a series of experiments recently performed by M. Schein, G. S. Klaiber, A. J. Hartzler, and D. C. Baldwin, the X rays produced by the 100 Mev betatron were allowed to enter a cloud chamber placed in a magnetic field, and stereoscopic photographs were taken to study the nuclear processes produced by the action of these high energy photons. Some new processes were observed which showed the ejection of several particles from a nucleus, but of particular interest here are processes which indicated the emission of mesons from nuclei of various substances such as glass, lead, and so forth. The mesons were identified by a study of the tracks they produced in the cloud chamber. The ionization along each track was compared with that produced by electrons and protons; measurements were made of the curvature of these tracks and the range of the particles and, in some cases, of the change in direction of the track as the particle passed through a foil of brass 0.25 mm thick. The results of these measurements indicate that the particles producing these tracks are mesons.

The betatron was operated at different energies in the above series of experiments. Meson tracks were found in the cloud chamber only when the betatron was operated at energies higher than 60 Mev. An interesting result of these investigations is that while most of the mesons had masses about 200 times the mass of an electron, some mesons produced by lower energy photons had masses of the order of 60 times the electronic mass. Furthermore, both positive and negative mesons were found in about equal numbers.

The actual mechanism of the production of mesons is not yet known. It is possible that mesons are produced by the breaking up of a nuclear particle under the action of high energy photons, or they may exist as nuclear particles and be ejected from the nucleus by the action of the photons. Further study in this direction will undoubtedly give us more information on the structure of the nucleus and nuclear processes.

## REFERENCES

- BETHE, H. A., and M. S. LIVINGSTON, "Nuclear Dynamics, Experimental," *Reviews of Modern Physics*, IX (1937), 245.
- FEATHER, N., *Nuclear Physics*. London: Cambridge University Press, 1936, Chaps. VII-XI.
- POLLARD, E., and W. L. DAVIDSON, JR., *Applied Nuclear Physics*. New York: John Wiley and Sons, Inc., 1942.
- RASETTI, F., *Elements of Nuclear Physics*. New York: Prentice-Hall, Inc., 1936, Chap. VI.
- RUTHERFORD, E., J. CHADWICK, and C. B. ELLIS, *Radiations from Radioactive Substances*. London: Cambridge University Press, 1930, Chaps. X-XII.
- SEABORG, G. T., "Table of Isotopes," *Reviews of Modern Physics*, XVI (1944), 1.

## PROBLEMS

1. A particle of mass  $M$  moving initially with velocity  $V$  makes an elastic collision with a particle of mass  $m$  initially at rest. Using the principles of the conservation of energy and momentum, show that if the particle of mass  $m$  is given a velocity  $v$  in the same direction as  $V$ , then

$$v = \frac{2M}{M + m} V.$$

2. A particle of mass  $M_1$ , kinetic energy  $E_1$ , velocity  $V_1$  and momentum  $P_1$  is captured by a nucleus ( $M_0, E_0, V_0, P_0$ ) at rest. A light particle ( $M_2, E_2, V_2, P_2$ ) is ejected and the heavy particle ( $M_3, E_3, V_3, P_3$ ) recoils. Using the principles of conservation of energy and momentum, show that when the light particle is emitted at an angle of  $90^\circ$  with the path of the incident particle, the energy of the light particle is

$$E_2 = \frac{M_3}{M_2 + M_3} \left( Q - \frac{M_1 - M_3}{M_3} E_1 \right)$$

where  $Q$  is the difference in mass between the initial particles and the final particles.

3. A beam of 0.4 Mev deuterons is directed against a deuterium target. Calculate the energy of the neutrons emitted at  $90^\circ$  with respect to the incident beam, assuming that the mass of  $\text{He}^3$  is 3.01711.

*Ans.* 2.48 Mev.

4. When  ${}_{11}\text{B}^{11}$  is bombarded with 200 kev protons, alpha particles of 4.41 cm range in air are emitted at right angles to the path of the incident beam. Using the result of problem 2, determine the mass of the residual  ${}_{4}\text{Be}^8$  nucleus.

*Ans.* 8.00794.

5. List all the elementary particles known in physics and give the following data for each particle: (a) mass, (b) charge, (c) spin, (d) wave length, (e) source.

6. When chlorine,  $A = 37$ , is bombarded with neutrons, gamma rays are emitted and the resultant nucleus is radioactive, emitting beta particles. A target containing chlorine was bombarded with neutrons for a short time, after which counts were taken of the number of beta particles emitted in successive ten-minute intervals. These counts, after correction for background readings, were as follows: 344, 267, 235, 189, 160, 145, 112, 97, 81, 65, 55, 50, 39, 37, 27, 25, 20, 14, 14, 11, 9.

(a) Write the equation for each reaction. (b) Plot a curve of the logarithm of the activity (no. of counts per ten minutes), against the time in minutes. (c) From the slope of the above curve determine the half-life period of the beta-ray emitter.

*Ans.* (c) 39 min.

7. (a) Show that the energy of an ion of mass  $M$  and charge  $E$  which is circulating within the dees of a cyclotron along a path having a radius of curvature  $R$  is such as to correspond to a total acceleration through

an equivalent voltage  $V$  given by

$$V = \frac{1}{2} H^2 R^2 \frac{E}{M}$$

in which  $V$ ,  $H$ , and  $E$  are in e.m. units.

(b) Show that the energy of this particle, in Mev, is given by

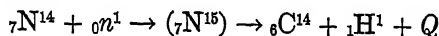
$$\mathcal{E} = 3.12 \times 10^5 H^2 R^2 \frac{E^2}{M}$$

with  $E$  and  $H$  in e.m. units.

(c) Calculate the energy of a proton which is moving in a circle of 60 cm radius in a magnetic field of 10,000 oersteds.

*Ans.* 17.2 Mev.

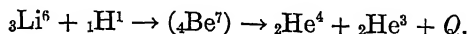
8. In the reaction



$Q$  is 0.55 Mev. Assuming all the other atomic masses known, calculate the mass of  ${}^6\text{C}^{14}$ .

9. Show that the radius of curvature  $R$  of the path of a particle inside the dees of a cyclotron is proportional to the  $\sqrt{n}$  where  $n$  is the number of times the particle has been accelerated across the space between the dees.

10. When lithium is bombarded with protons, the following reaction occurs



The measured value of the reaction energy  $Q = 3.945$  Mev. Calculate the mass of  $\text{He}^3$  from this reaction.

*Ans.* 3.01696.

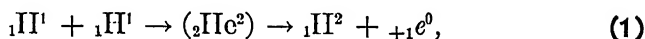
11. In the molecular beam magnetic resonance method, a resonance minimum is obtained for  $\text{F}^{19}$  nucleus with a beam of  $\text{NaF}$  at a frequency of  $5.634 \times 10^6$  cycles per second in a homogeneous magnetic field of 1408 gauss. Calculate its nuclear magnetic moment in nuclear magnetons.

*Ans.* 2.622.

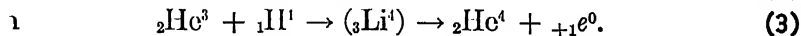
# Nuclear Energy

## A Source of Stellar Energy

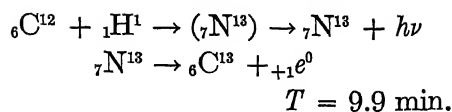
Ever since the discovery of the transmutation of elements, it has been thought that the conversion of mass into other forms of energy, which occurs during such transmutation, would provide a possible explanation of the origin of a great part of the energy radiated by the stars, but it was not until sufficient evidence had been accumulated in the laboratory concerning the probabilities of various types of reactions and their energy releases that it became possible to develop a fairly quantitative explanation. Astrophysical evidence shows that the most abundant type of nucleus present in the stars classified in the *main sequence* is the proton. Bethe (39) developed the theory for the production of stellar energy in which protons, by suitable nuclear reactions, are transmuted to helium nuclei, thereby releasing energy which is transformed into radiation. One sequence of reactions which takes place in the cooler stars and provides most of the luminosity of the so-called red dwarfs, and approximately one half the luminosity of the sun, starts with the reaction between a proton and a proton to form a deuteron, that is,



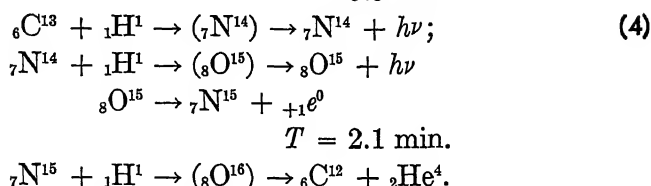
is followed by two additional proton reactions to form an alpha particle,



Another type of reaction in which protons are converted into helium nuclei, but this time with the aid of carbon and nitrogen *catalysts*, is used to account for most of the energy of stars in the *main sequence* which are more massive than the sun. This type of reactions is



and



It will be noted that this chain of reactions can start with either nitrogen or carbon, since each one is reproduced in the reaction, except that in about one case in  $10^5$ , the last reaction will lead to the formation of  ${}_8\text{O}^{16}$  and the emission of a gamma ray. Since the positrons will combine readily with electrons resulting in the formation of gamma rays, the net result is the combination of four protons and two electrons to form an alpha particle with the consequent release of energy. The mass difference released as energy in this chain of reactions is thus simply the difference between the masses of four hydrogen atoms and one helium atom or 0.0286 a.m.u. which is equivalent to about  $43 \times 10^{-6}$  erg or 26.7 Mev. If our present theory of beta decay is correct, a small amount of this energy will be carried away by the neutrinos which are emitted during the radioactive parts of the cycle. Bethe estimates this to be about  $3 \times 10^{-6}$  erg, leaving about  $40 \times 10^{-6}$  erg for each alpha particle formed or  $10 \times 10^{-6}$  erg for each proton consumed. In the particular case of the sun, it has been estimated that a gram of its mass contains about  $2 \times 10^{23}$  protons; hence if all the protons were consumed the energy released would be  $2 \times 10^{18}$  ergs. If the sun were to continue to radiate at its present rate, it would take about 30 billion years to exhaust its supply of protons.

### 136. Discovery of Nuclear Fission

By 1934 a reasonable amount of data had been accumulated on the disintegration of nuclei which were bombarded by neutrons to lead Fermi and his co-workers to try to produce elements of atomic number greater than 92 by bombarding uranium with neutrons. In their early experiments they found four beta-ray activities with different half-life periods as a result of bombarding uranium with neutrons. Now uranium is a naturally radioactive



substance which disintegrates with a long half-life period by the emission of alpha particles; hence these beta-ray activities indicated that some new process was taking place. This new process was interpreted as the formation of one or more *transuranic* elements, that is, elements of atomic number greater than 92. Some chemical tests were therefore tried to verify this hypothesis. Element 93, for example, is a chemical homologue of manganese; that is, it occurs in the same column of the periodic table. In one chemical experiment, a manganese salt was added to a solution of a uranium salt which had been bombarded with neutrons and then precipitated out as manganese dioxide. Two of the beta-ray activities came down with the precipitate. Other chemical tests were tried which ruled out the possibility that these beta-ray activities could be due to any of the elements in the range of atomic numbers 86 to 92 inclusive. It was therefore concluded that element 93 had been produced. A chemist, Noddack, criticized this conclusion on the basis that many elements are precipitated with  $\text{MnO}_2$  and suggested the possibility that the bombarded nuclei were split into nuclei of elements of lower atomic number. This suggestion was apparently ignored, and other workers, particularly I. Curie and her co-workers, and Hahn, Strassmann, and Meitner, entered this field in search of the transuranic elements. Uranium, thorium, and protoactinium were bombarded with neutrons and many different beta-ray activities discovered. These were carefully checked by both physical and chemical methods to determine the nature of the emitters, and until early in 1939 they were generally ascribed to radioactive substances of atomic number greater than 92. Several new radioactive series were suggested to account for these activities; each one started with uranium and by a series of beta-particle disintegrations led to elements of atomic numbers as high as 96 and 97. It must be pointed out that chemical analysis in this region of the periodic table is extremely difficult and it becomes even more difficult because of the very small samples of newly formed radioactive material available.

In 1939 Hahn and Strassmann found, after a series of very careful chemical experiments, that one of the radioactive elements formed by the bombardment of uranium with neutrons was an isotope of the element barium,  $Z = 56$ . Another of the radioactive elements thus formed was the rare-earth element lantha-

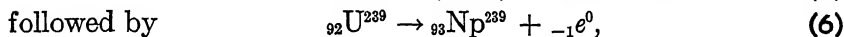
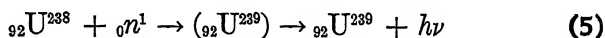
num,  $Z = 57$ . It is obvious that the lanthanum is formed by the beta decay of the barium. Hahn and Strassmann therefore suggested that the beta-ray activities previously ascribed to transuranic elements are probably produced by radioactive isotopes of elements of lower atomic number. The process that is started by bombarding uranium with neutrons is one in which the new uranium nucleus becomes unstable and splits up into two nuclei of medium atomic masses; if one nucleus formed is barium,  $Z = 56$ , the other nucleus must be krypton,  $Z = 36$ . This type of disintegration process in which a heavy nucleus splits up into two nuclei of nearly comparable masses is called *nuclear fission*.

As soon as the discovery of nuclear fission was announced early in 1939, physicists in laboratories throughout the world where neutron sources were available immediately repeated and confirmed these experiments. Within the next two years the results were extended to include the nuclear fission of thorium and protoactinium, the measurement of the energies of the bombarding neutrons necessary to produce fission in the particular isotope of the heavy element, the amount of energy released in nuclear fission, and analyses of the products of nuclear fission together with their genetic relationships.

### 137. Transuranic Elements

It was not until 1940 that the existence of transuranic elements was definitely established. At present four transuranic elements are known; these are the elements of atomic numbers 93, 94, 95, and 96.

McMillan and Abelson discovered the first transuranic element, that of atomic number 93, now known as *neptunium*. This is produced by the resonance capture of comparatively low energy neutrons by uranium,  $A = 238$ ; the new uranium isotope,  $A = 239$ , formed by this process disintegrates by beta-ray emission with a half life of 23 minutes resulting in the formation of neptunium. The following are the nuclear reactions:



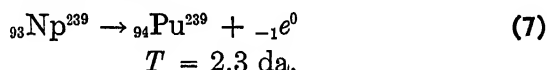
$$T = 23 \text{ min.}$$

The resonance energy of the neutrons in the above reaction is

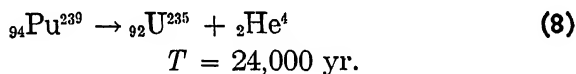
38 ev. This resonance capture of neutrons is sometimes referred to as radiative capture since the compound nucleus of uranium 239 emits a gamma-ray photon in going to the normal state.

McMillan and Abelson performed chemical experiments with the minute quantities, so-called *tracer* amounts, of the element formed in the above process and showed that its oxidation states differed from those of uranium. This was the first time that the existence of a new element was established by chemical experiments on a tracer scale of investigation.

The neptunium formed in the above reaction is also radioactive, emitting a beta particle to form a new transuranic element of atomic number 94, now known as *plutonium*. The following is the nuclear reaction for this process:

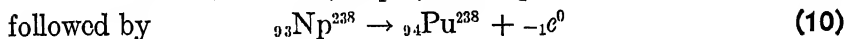
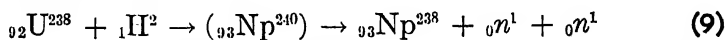


This isotope of plutonium is radioactive with a long half-life period and emits an alpha particle according to the following reaction:



It is this isotope of plutonium which has played such an important part in the atomic bomb project because it is fissionable with both slow neutrons and fast neutrons.

A different isotope of plutonium was discovered shortly after the discovery of neptunium. This transuranic element was discovered by Seaborg, McMillan, Wahl, and Kennedy late in 1940. They bombarded uranium with deuterons and showed that the following reactions occurred:



$$T = 2.0 \text{ da}$$

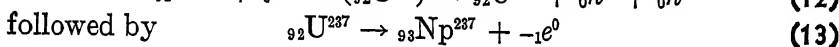
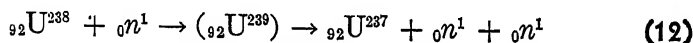


$$T = 50 \text{ yr.}$$

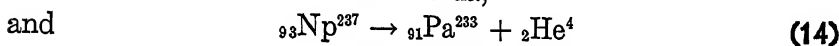
The chemical properties of plutonium determined with the minute amounts available from the above reactions formed the basis for setting up the so-called *chain-reacting* units at Clinton,

Tenn., and Hanford, Wash., for the production of plutonium on a large scale for use in the atomic bomb. Once the chemical properties of plutonium were known it seemed reasonable to hunt for these elements in nature. Pitchblende ore, one of the sources of uranium was examined by Seaborg and Perlman; they made a chemical separation of neptunium and plutonium and were able to show the presence of a small quantity of alpha-activity in the transuranium fraction which they attributed to plutonium,  $A = 239$ . The amount of plutonium in the pitchblende corresponds to about 1 part in  $10^{14}$ , an amount which could not possibly be found had the chemical properties not been known. It probably is being formed continuously as a result of the radiative capture of neutrons by some of the uranium present in the ore.

Another isotope of neptunium,  $A = 237$ , was discovered by Wahl and Seaborg in 1942. This is produced in the following reactions:



$$T = 7 \text{ da,}$$



$$T = 2.25 \times 10^6 \text{ yr.}$$

The fact that this isotope is comparatively stable makes it particularly suitable for the chemical investigations of the properties of neptunium.

Two new elements of atomic numbers 95 and 96 were produced in 1945 by bombarding uranium,  $A = 238$ , and plutonium,  $A = 239$ , respectively, with 40 Mev helium ions produced in the 60-inch Berkley cyclotron. The work with the cyclotron was done by J. G. Hamilton and his co-workers, while the identification of the new elements 95 and 96 and the study of the chemical properties by the tracer technique were carried out by Seaborg, James, Morgan, and Ghiorso.

As a result of the intensive analysis of the chemical properties of the heavier elements, Seaborg suggests that the elements of atomic numbers greater than 88 probably form another transition group analogous to the rare earth group of atomic numbers 58 to 71. In this latter group, see Table XI, each succeeding element is formed by the addition of an electron to the  $4f$  shell until

this shell is completed with 14 electrons. Seaborg suggests that in this new transition group electrons are added to the  $5f$  shell, the first  $5f$  electron probably appearing in thorium and the seventh  $5f$  electron in element 96.

### 138. Energy Released in Nuclear Fission

An idea of the amount of energy that can be released in nuclear fission may be obtained by considering the difference between the

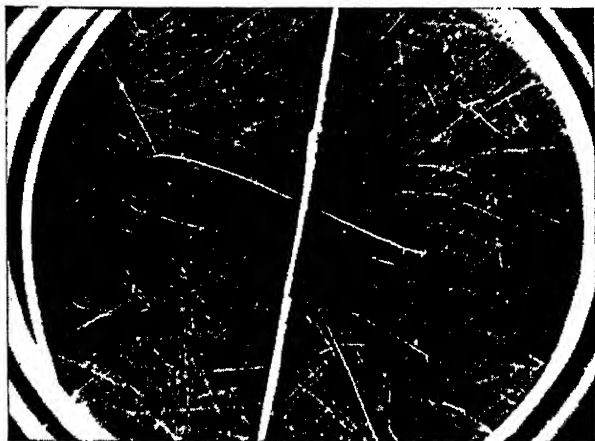


FIG. 168. — Cloud chamber photograph of the tracks produced by two fission particles; these particles are the product of the fission of uranium which has captured a neutron. The uranium is on the foil shown in the center of the chamber. (From a photograph by J. K. Bøggild, K. J. Brøstrom, and T. Lauritsen.)

mass of the initial nucleus and the masses of the nuclei produced by its fission. For example, suppose that the isotope of uranium,  $Z = 92$ ,  $A = 239$ , which is formed by the capture of a neutron, breaks up into barium,  $Z = 56$ , and krypton,  $Z = 36$ . From the packing fraction curve of Figure 29, we find that the difference in the packing fractions of uranium and nuclei of the type of barium and krypton is about  $9 \times 10^{-4}$ . The packing fraction is the mass defect per particle, and since there are 239 particles in the excited uranium nucleus, the total mass defect is

$$\Delta m = 239 \times 9 \times 10^{-4} \text{ a.m.u.} = 0.216 \text{ a.m.u.}$$

Using the conversion factor of  $932 \text{ Mev} = 1 \text{ a.m.u.}$ , the amount of energy released during this fission process will be approximately 200 Mev. This energy will be divided between the two particles;

the exact division can be determined by applying to this process the principle of conservation of momentum as well as the principle of conservation of energy. If we assume that the heaviest isotopes of barium and krypton are formed, then one will have an energy of about 125 Mev and the other about 75 Mev. If two particles of equal mass are formed in this fission process, they will travel in opposite directions with equal energies of about 100 Mev each. The fission process is therefore capable of yielding tremendous amounts of energy. Figure 168 is a cloud chamber photograph of the pairs of particles produced by the fission of uranium. Measurements of the energies of such particles show two ranges of energy, one of about 100 Mev and the other of about 72 Mev, in agreement with the above approximate calculations.

Uranium fission can be produced by both slow and fast neutrons. On the basis of Bohr's theory of nuclear processes, nuclear fission takes place in two steps: (1) the formation of the compound nucleus in which the energy is temporarily stored among the different degrees of freedom of the nuclear particles in a manner similar to that of thermal agitation of a liquid, and (2) the transformation of a sufficient portion of this energy into potential energy of deformation of the compound nucleus which will lead to its fission. The possibility of the occurrence of fission by bombarding a nucleus with neutrons depends, therefore, on the difference between the critical energy  $\mathcal{E}_c$  of such an unstable deformation of the nucleus, and the energy used to excite the nucleus; the latter is determined by the binding energy,  $W_n$ , of the added neutron. Bohr and Wheeler have made estimates of these values for some of the heavy elements; these are listed in Table XXI.

TABLE XXI

Bombarded Nucleus	Compound Nucleus	Critical Energy $\mathcal{E}_c$ in Mev	Binding Energy $W_n$ in Mev	$\mathcal{E}_c - W_n$ in Mev
92 U 234	92 U 235	5.0	5.4	- 0.4
92 U 235	92 U 236	5.3	6.4	- 1.1
92 U 238	92 U 239	5.9	5.2	0.7
91 Pa 231	91 Pa 232	5.5	5.4	0.1
90 Th 232	90 Th 233	6.9	5.2	1.7
90 Io 230	90 Io 231	6.5	5.3	1.2

From Table XXI it can be seen that the uranium isotope of

mass number  $A = 235$  should be responsible for the fission produced by slow neutrons. This was confirmed experimentally by Nier, Booth, Dunning, and Grosse. They first separated small quantities of the uranium isotopes,  $A = 235$  and  $A = 238$ , by means of the mass spectrometer, and then bombarded each of these isotopes with slow neutrons. They observed practically no fission with uranium,  $A = 238$ , but did get a fairly large number of fissions with  $A = 235$ . Furthermore, the rate of fission per microgram of uranium 235 observed in this experiment was in good agreement with the number obtained under the same experimental conditions from unseparated samples of uranium containing the normal percentage of uranium 235.

### 139. Some Products of Nuclear Fission

Many different atomic nuclei have been produced by the fission of uranium and thorium as a result of bombarding them with neutrons. Most of these fission products have been identified by chemical tests; others, by means of the X rays emitted by the excited atoms produced during fission. In many cases the particular isotopes produced have been identified by comparing their half-life periods with those produced by other types of nuclear reactions. The fact that so many different fission products have been produced indicates that the excited uranium or thorium nucleus can split up in many different ways. As shown in Tables XXII and XXIII, all of the presently known fission products are elements in the middle of the periodic table with atomic numbers ranging from  $Z = 34$  to  $Z = 58$ .

We have already noted that there is a large excess of neutrons in uranium over that of the stable isotopes of elements that are produced by nuclear fission. The fission products are therefore unstable and will disintegrate either by the ejection of their excess neutrons, or else by the radioactive emission of beta particles. Both processes have been detected. Many of these beta-ray processes have been followed from the initial fission product to a final stable nucleus. For example, one of the products of the fission of uranium is an isotope of antimony of mass number  $A = 133$ . Now antimony has only two stable isotopes, one of mass number 121, the other of mass number 123. The fission product is therefore unstable because it has at least ten neutrons too many; this isotope

TABLE XXII

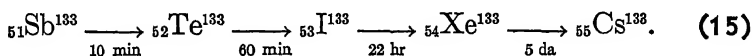
FISSION PRODUCTS PRODUCED BY BOMBARDING URANIUM WITH NEUTRONS							
Isotope Produced			Half-Life Period	Isotope Produced			Half-Life Period
Z	El	A		Z	El	A	
35	Br	83	140 min	50	Sn	> 125	20 min
		84	30 min				80 hr
		85	3.0 min				70 min
		87	50 sec				11 da
36	Kr	88	3 hr	51	Sb	127	80 hr
		89	2.5 min			129	4.2 hr
		> 90	< 0.5 min			> 131	< 10 min
38	Sr	90	5 yr				5 min
40	Zr	93	63 da			133	< 10 min
		95	17 hr	52	Te	129	32 da
42	Mo	99	67 hr			131	30 hr
		101	14.6 min				25 min
		> 101	12 min			135	1 min
		—	60 da	53	I	137	30 sec
44	Ru	105	4 hr	54	Xe	138	17 min
		—	45 da			139	< 0.5 min
		—	4 min			140	< 0.5 min
46	Pd	111	26 min	56	Ba	> 140	6 min
		112	17 hr				18 min
47	Ag	112	3.2 hr				< 1 min
48	Cd	115	2.5 da	58	Ce		15 min
		117	3.75 hr				4-5 hr
	(Cd)		48.7 min				40 hr
49	(In)	115	4.1 hr				
	In	117	117 min				

TABLE XXIII

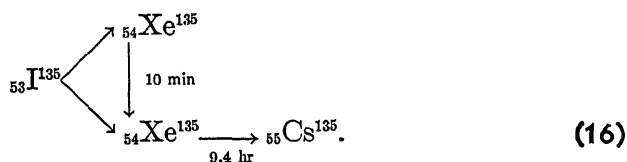
FISSION PRODUCTS PRODUCED BY BOMBARDING THORIUM WITH NEUTRONS							
Isotope Produced			Half-Life Period	Isotope Produced			Half-Life Period
Z	El	A		Z	El	A	
34	Se		several hr	51	Sb	133	< 10 min
			several da	52	Te	> 131	43 min
35	Br	83	140 min	53	I	> 131	77 hr
		84	30 min	54	Xe	139	54 min
36	Kr	88	3 hr			140	< 0.5 min
		> 90	< 0.5 min			> 140	< 0.5 min
42	Mo	99	67 hr	56	Ba	> 140	6 min
44	Ru	105	4 hr				18 min
46	Pd	111	26 min	57	La	> 140	3.5 hr
		112	17 hr				



disintegrates with the emission of a beta particle with a half-life period of 10 minutes. The tellurium isotope thus formed is also unstable and disintegrates with the emission of a beta particle; this chain of reactions is continued until a stable isotope is reached. Wu and Segrè have checked this series of beta disintegrations and give the following chain of reactions:

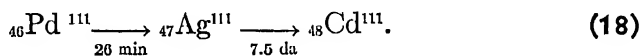
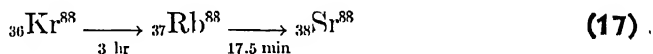


In the same series of experiments, they investigated the relationship between an iodine activity with a half-life period of 6.6 hours, and two xenon activities, with half-life periods of 10 minutes and 9.4 hours, and have concluded that two isomeric forms of xenon are formed by the beta decay of the iodine of mass number  $A = 135$  according to the following scheme:



The upper isomeric form of xenon emits a gamma ray of 0.5 Mev with a half-life period of 10 minutes going to the lower isomeric state of xenon which then disintegrates by the emission of a beta particle with a half-life period of 9.4 hours.

A few of the other beta-ray chains which start with one of the fission products are



The assignment of the mass number to the particular isotope produced during the fission process is aided by the production of the same beta-ray activity by other methods. For example, the isotope  ${}_{46}\text{Pd}^{111}$  can be produced in a  $d-p$  reaction with palladium and in an  $n-\gamma$  reaction with palladium. The silver isotope of mass number  $A = 111$  can be produced in three different ways: in a  $d-n$  reaction with palladium; in an  $\alpha-p$  reaction with palladium; in an  $n-p$  reaction with cadmium.

## 140. Photofission of Nuclei

Almost any method which will make a nucleus sufficiently unstable can be used to produce the fission of uranium and thorium. One method is to bombard these nuclei with high energy photons. Haxby, Shoupp, Stephens, and Wells (1941) were the first to produce such fission with gamma rays. Gamma-ray photons of 6.3 Mev energy, obtained by bombarding fluorite,  $\text{CaF}_2$ , with high energy protons, were used to irradiate a 12 cm<sup>2</sup> piece of uranium metal placed on the high voltage plate of an ionization chamber. The fission products were measured by the pulses of ionization they produced in this chamber. Recently Baldwin and Koch (1945) used the high energy X-ray photons produced by the betatron to induce the fission of uranium. Uranium oxide coated on a cylinder was irradiated with X-ray photons of energies from 8 Mev to 16 Mev. The fission fragments were collected on a paper cylinder held over this sample. The beta decay of the fission fragments was then examined with a counter. Fission products were observed for all values of the X-ray energies used in irradiating the uranium down to about 8 Mev. They estimate that the threshold for the photofission of uranium is less than 7 Mev.

Baldwin and Koch also tried to produce photofission in lead but were unsuccessful, even with X-ray photons of 16 Mev energy.

## 141. Neutrons Released in Fission

We have mentioned that one method by which an isotope having an excess of neutrons should be able to reach a stable form is by ejecting these neutrons from its nuclei. The early workers in the field of nuclear fission immediately recognized the possibility of a chain of reactions being started in which these secondary neutrons would produce further nuclear fissions and the process would continue until all of the uranium would be used up; this would result in the release of tremendous amounts of energy and, in fact, would open up a new source of energy.

One of the first problems to be solved is the determination of the number of neutrons released for each fission process produced. Szilard and Zinn (1939) performed an experiment to determine the number of fast neutrons emitted in the fission of uranium by slow neutrons. The arrangement of the apparatus used by them is

shown in Figure 169. The neutrons were emitted as a result of the photodisintegration of beryllium by the action of the gamma rays from radium. A helium-filled ionization chamber connected to a linear amplifier was used as a detector of fast neutrons. The neu-

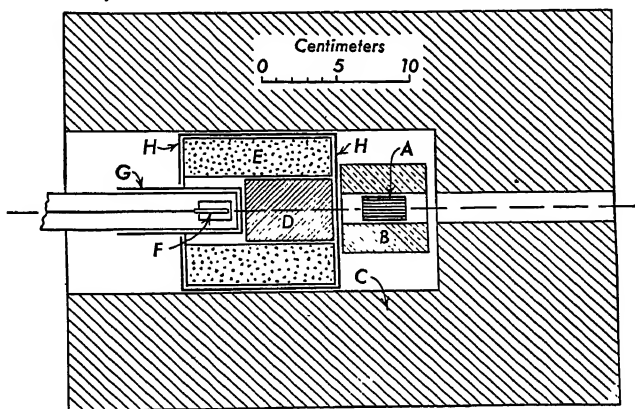


FIG. 169. — Arrangement of the apparatus for the observation of the emission of fast neutrons from uranium bombarded by slow neutrons. *A*, radium; *B*, beryllium block; *C*, paraffin wax; *D*, lead block; *E*, box filled with uranium oxide; *F*, ionization chamber; *G*, cap of cadmium sheet; *H*, shield of cadmium sheet.

trons from the beryllium *B* were slowed down by the paraffin *C*, and then bombarded the uranium oxide contained in the cylindrical box *E*. When desired, the uranium oxide could be shielded from the slow neutrons by interposing a sheet of cadmium *H*. A cadmium sheet *G* was also used to shield the ionization chamber from slow neutrons.

When the uranium oxide was exposed to the action of slow neutrons by the removal of the shield *H*, they observed 50 pulses per minute in the helium ionization chamber. When the cadmium shield was in place, only 5 pulses per minute were obtained. The difference of 45 pulses per minute must therefore be due to fast neutrons emitted from the uranium under the action of the thermal neutrons.

In order to estimate the number of fast neutrons emitted per fission under the action of slow or thermal neutrons, the helium ionization chamber was replaced by another chamber which was lined with a layer of uranium oxide of known area. The fast neutrons which entered this ionization chamber produced fission of

some of the uranium, and the number of fissions per minute was counted. Making some reasonable assumptions concerning the range of fission particles in uranium oxide, they then were able to estimate the number of fissions per minute produced in the large amount of uranium oxide in the cylinder *E*. Combining this result with the count of the number of fast neutrons which were recorded by the helium ionization chamber, Szilard and Zinn estimated that two fast neutrons were emitted per fission of uranium by slow neutrons. They also made an estimate of the time delay involved in the emission of fast neutrons after fission; they concluded that this was less than one second.

## 142. Release of Nuclear Energy

The fact that several neutrons are released in the fission of uranium 235 by the action of slow neutrons immediately suggested the idea to many physicists that a chain of nuclear reactions might be initiated by the fission of uranium which would release large amounts of energy. Each fission process releases 200 Mev or  $200 \times 1.60 \times 10^{-6}$  ergs. The fission of all the nuclei in a gram atomic weight of uranium would release about

$$6 \times 10^{23} \times 3.2 \times 10^{-4} \text{ ergs} = 19.2 \times 10^{19} \text{ ergs.}$$

This is equivalent to about  $5.3 \times 10^6$  kilowatt-hours of energy.

The discovery of nuclear fission occurred a few months before the outbreak of the second World War in Europe. The military usefulness of such a tremendous source of energy was quickly recognized and work on it began immediately. When the war spread to the United States, all work on nuclear energy was placed under government control and cloaked in military secrecy. No new information on it became available until the explosion of the first atomic bomb over Hiroshima in August, 1945. After our victory in this war, some information was released by way of the vivid and dramatic report, *Atomic Energy for Military Purposes*, prepared by Professor H. D. Smyth. The reader is urged to study this report to see how the skills of science and industry were used in the task of solving the problem of the release of nuclear energy. The following discussion is based on this report.

### 143. The Fission Chain Reaction

The principle involved in a fission chain reaction is very simple: if one or more new neutrons are produced as a result of a nuclear fission induced by a neutron, the number of fissions may increase tremendously with the consequent release of enormous amounts of energy. Two types of chain reactions are of interest: one a controlled reaction in which the number of neutrons builds up to a certain level and then remains constant; the other is an explosive reaction in which the number of neutrons multiplies indefinitely. Both of these types of fission chain reactions have been produced in the Atomic Bomb Project.

As we have seen, slow neutrons are effective in producing fission in uranium 235, and this fission process is accompanied by the emission of from one to three fast neutrons. Fast neutrons can produce fission in all three uranium isotopes, 234, 235, and 238. It has also been found that both fast and thermal neutrons can produce fission in plutonium 239 as well.

The time delay in the emission of neutrons as a result of bombarding uranium with slow neutrons has been measured accurately. It has been found that about 1.0 per cent of the neutrons emitted in uranium fission are delayed by at least 0.01 second and that about 0.7 per cent are delayed by as much as one minute. This delay is very useful in a controlled reaction.

For a chain reaction to proceed successfully, that is, to be self-sustaining, the ratio of the number of new neutrons produced by fission at any place in the substance to the number of free neutrons originally present at that place must be at least equal to 1. This ratio is called the multiplication factor  $k$ . In any given system containing a large mass of uranium, all three isotopes will be present. Each fission capture of a neutron will result in the emission of several new fast neutrons. However, not all of these neutrons will produce fission. Some may be lost by escaping from the system. The relative number of neutrons which escape from the system may be reduced by changing its size and shape; for example, by using a larger amount of uranium and making it approximately spherical in shape. Fission is a volume effect, while the escape of neutrons is a surface effect and hence is determined by its area. Some neutrons of moderate speed, corre-

sponding to about 38 ev energy, may be captured by uranium without producing fission; this is the resonance capture of neutrons. Other neutrons may be captured by impurities in the material. These are both volume effects. There is a *critical size* for any device containing uranium for producing a self-sustaining chain reaction; this is the size for which the production of free neutrons by fission is just equal to their loss by escape and by nonfission capture both in uranium and in the impurities.

To reduce the critical size to a reasonable value and make the chain reaction possible it is necessary to reduce the number of nonfission processes. One method is to purify the materials very carefully. Another method is to slow down the neutrons by the use of material containing hydrogen, deuterium, or carbon, below the speeds at which nonfission capture occurs. Material used in this way is called a *moderator*. Both methods have been used.

The first successful self-sustaining chain reaction system was constructed at Chicago in the fall of 1942. Graphite cut into bricks was used as the moderator; these graphite bricks were built up in layers, alternate ones of which contained lumps of uranium or uranium oxide at the corners of squares, forming a type of lattice. These layers were built up into a pile which had the shape of an oblate spheroid flattened at the top. For purposes of control and experiment there were ten slots passing completely through the pile. Three of those near the center were used for control and safety rods. The chain reaction could be started by any stray neutrons, such as cosmic ray neutrons or neutrons from some spontaneous fission. During the building up of this pile some cadmium strips were inserted in suitable slots to absorb the neutrons. They were removed once every day in order to check the approach to critical conditions as the pile was being built up to its critical size.

Once the critical size was reached, the reaction was controlled by inserting in the pile some strips of neutron-absorbing material, either cadmium or boron steel. When the pile was not in operation, several such cadmium strips were inserted in a number of slots, bringing the effective multiplication factor considerably below 1. In fact, any one of the cadmium strips was sufficient to bring the pile below the critical condition. To operate the pile, all but one of the cadmium strips were taken out. The remaining one was then slowly pulled out. As the critical conditions were ap-

proached, the intensity of the neutrons emitted by the pile began to increase rapidly. When this last strip of cadmium was so far inside the pile that the effective multiplication factor was just below 1, it took a rather long time for the intensity to reach the saturation value. Similarly, if the cadmium strip was just far enough out to make the effective multiplication factor greater than 1, the intensity rose at a rather slow rate. For example, if one rod is only 1 cm out from the critical position, the "relaxation time," that is, the time for the intensity to double, is about four hours. These long relaxation times were the result of the small percentage of delayed neutrons and made it relatively easy to keep the pile operating at a constant level of intensity.

The pile was first operated on December 2, 1942, at a maximum energy production of about 0.5 watt. On December 12, the intensity was run up to about 200 watts, but it was not felt safe to go higher because of the danger of the radiation to personnel in and around the building. This experiment, using normal uranium in a self-sustaining chain reaction, was performed under the general direction of E. Fermi, assisted principally by groups headed by W. H. Zinn and H. L. Anderson.

One of the important results of the operation of this pile was the production of plutonium, one of the major objectives of the project. Plutonium, as we have seen, is formed as the result of the resonance capture of neutrons by uranium 238 with the subsequent emission of two beta particles. The formation of plutonium is constantly proceeding during the operation of the pile. Plutonium was at least as valuable as uranium 235 for the Atomic Bomb Project. It was found that plutonium could be separated chemically from uranium. On the basis of the experience gained from the operation of the first pile, a gigantic plant was set up at Hanford, Washington, for the production of plutonium, a metal whose existence was unknown before 1940. The production of plutonium meant the construction of a pile developing thousands of kilowatts, and a chemical separation plant to extract the product.

A chain-reacting pile using graphite as a moderator is evidently very large. It is possible to build a much smaller pile by replacing the graphite with a better moderator such as heavy water, that is, deuterium oxide, which is more effective in slowing down neutrons. A pile using heavy water as a moderator was

constructed at the Argonne laboratory and Zinn reported that it was operating satisfactorily at a power level of 300 kilowatts.

### 144. An Atomic Bomb

The self-sustaining, chain reaction pile described above is not suitable for an atomic bomb since the energy is released comparatively slowly and also because of the tremendous size of the pile. What is desired in an atomic bomb is an explosive type of reaction; this means a sudden and violent release of a large amount of energy in a small region. This involves fast neutron fission processes almost exclusively. Ordinary metallic uranium, containing the normal proportions of the isotopes of mass numbers 234, 235, and 238, while suitable for a controlled chain reaction, is not suitable for an explosive type of reaction. To understand the reason for this let us consider what would happen to the neutrons released in fission processes which occur at the center of a large mass of uranium. Joliot and his co-workers showed that the average value of the energy of these neutrons is slightly less than 1 Mev. We have also seen that uranium 238 is fissionable by fast neutrons only, that is, neutrons of more than 1 Mev energy. Stated in other words, the probability of the fission capture by uranium 238 is very small for neutrons of less than 1 Mev energy. Hence only a very small fraction of these neutrons will take part in the fission capture process. Most of the neutrons will collide with uranium nuclei and give up their energy slowly during these collisions. Any neutron capture that occurs at these lower energies is a radiative capture with a resonance value at 38 ev, and such capture, as we have seen, leads ultimately to the production of plutonium.

To insure that an explosive chain reaction occurs, it is necessary to reduce the probability of radiative capture of neutrons by uranium 238. This can be done either by reducing the proportion of uranium 238 and increasing the proportion of uranium 235 in the metal, or else by using plutonium instead of uranium. Both methods have probably been used. Uranium 235 and plutonium are fissionable by the capture of neutrons of all energies; the probability of fission capture by these substances is very great for slow neutrons and decreases as the neutron velocity is increased. For the successful operation of an atomic bomb, the



amount of fissionable material must be at least equal to the critical mass, and it must be held together for a sufficient time (very short, of course, of the order of microseconds) for most of the available nuclear energy to be released in the explosion of the bomb. The value of the critical mass will depend upon the shape of the bomb and the nature of the material in which it is placed. This envelope or *tamper* around it scatters those neutrons which escape from the fissionable material. It has been found that the best material for a tamper is a very dense substance. Such a tamper has two interesting properties: (1) it "reflects" or scatters many neutrons back into the bomb and (2) it delays the expansion of the bomb and thus helps in building up the temperature and pressure.

A mass of fissionable material which is smaller than the critical mass for the given shape is perfectly stable. If two such masses are brought together very rapidly, and if a neutron source is activated inside the system, a violent reaction will occur in a very short time interval provided that the total mass is equal to or greater than the critical mass. It has been estimated that energy released in the nuclear fission processes which can occur in a couple of microseconds is sufficient to raise the temperature of this mass to several million degrees and to produce a pressure of hundreds of thousands or perhaps millions of atmospheres. The destructive effects of such high temperatures and pressures can be observed in the ruins of Hiroshima and Nagasaki. A large quantity of radioactive material is also released in the explosion of an atomic bomb. When this is exploded in the atmosphere, these radioactive substances are carried away by air currents, and since the half-life periods of these substances are comparatively short, see Tables XXII and XXIII, they will decay to insignificant amounts in a relatively short time.

## REFERENCES

- OLIPHANT, M. L., "The Release of Atomic Energy." *Nature* CLVII (1946), 50.
- POLLARD, E., and W. L. DAVIDSON, JR., *Applied Nuclear Physics*. New York: John Wiley and Sons, Inc., 1942, Chap. 10.
- SMYTH, H. D., *Atomic Energy for Military Purposes*. Princeton: Princeton University Press, 1945.



# APPENDIXES



## APPENDIX I

### Values of Some Physical Constants

Velocity of light	$c = 2.99776 \times 10^{10}$ cm/sec
Specific electronic charge	$e/m = 1.7592 \times 10^7$ e.m.u./gm
Electronic charge	$e = 4.8021 \times 10^{-10}$ e.s.u.
Planck constant	$h = 6.624 \times 10^{-27}$ erg sec
Avogadro number	$N = 6.0234 \times 10^{23}$ atoms/gm at wt
Faraday constant	
on Physical scale	$F = 9651.4$ e.m.u./gm equivalent
on Chemical scale	$F = 9648.77$ e.m.u./gm equivalent
Rydberg constant for infinite mass	$R_{\infty} = 109737.303$ per cm

## APPENDIX II

### Table of Atomic Weights

From the Report of the Committee on Atomic Weights of the International Union of Chemistry

J.A.C.S. 1941

At. No.	Element	Symbol	At. Weight
13	Aluminum	Al	26.97
51	Antimony	Sb	121.76
18	Argon	A	39.944
33	Arsenic	As	74.91
56	Barium	Ba	137.36
4	Beryllium	Be	9.02
83	Bismuth	Bi	209.00
5	Boron	B	10.82
35	Bromine	Br	79.916
48	Cadmium	Cd	112.41
20	Calcium	Ca	40.08
6	Carbon	C	12.01
58	Cerium	Ce	140.13
55	Cesium	Cs	132.91
17	Chlorine	Cl	35.457
24	Chromium	Cr	52.01
27	Cobalt	Co	58.94
41	Columbium	Cb	92.91
29	Copper	Cu	63.57
66	Dysprosium	Dy	162.46
68	Erbium	Er	167.2
63	Europium	Eu	152.0
9	Fluorine	F	19.00
64	Gadolinium	Gd	156.9
31	Gallium	Ga	69.72
32	Germanium	Ge	72.60
79	Gold	Au	197.2
72	Hafnium	Hf	178.6
2	Helium	He	4.003
67	Holmium	Ho	164.94
1	Hydrogen	H	1.0080
49	Indium	In	114.76
53	Iodine	I	126.92
77	Iridium	Ir	193.1
26	Iron	Fe	55.85
36	Krypton	Kr	83.7
57	Lanthanum	La	138.92
82	Lead	Pb	207.21
3	Lithium	Li	6.940
71	Lutecium	Lu	174.99
12	Magnesium	Mg	24.32
25	Manganese	Mn	54.93
80	Mercury	Hg	200.61

Table of Atomic Weights (Concluded)

At. No.	Element	Symbol	At. Weight
42	Molybdenum	Mo	95.95
60	Neodymium	Nd	144.27
10	Neon	Ne	20.183
28	Nickel	Ni	58.69
7	Nitrogen	N	14.008
76	Osmium	Os	190.2
8	Oxygen	O	16.0000
46	Palladium	Pd	106.7
15	Phosphorus	P	30.98
78	Platinum	Pt	195.23
19	Potassium	K	39.096
59	Praseodymium	Pr	140.92
91	Protactinium	Pa	231
88	Radium	Ra	226.05
86	Radon	Rn	222
75	Rhenium	Re	186.31
45	Rhodium	Rh	102.91
37	Rubidium	Rb	85.48
44	Ruthenium	Ru	101.7
62	Samarium	Sm	150.43
21	Scandium	Sc	45.10
34	Selenium	Se	78.96
14	Silicon	Si	28.06
47	Silver	Ag	107.880
11	Sodium	Na	22.997
38	Strontium	Sr	87.63
16	Sulphur	S	32.06
73	Tantalum	Ta	180.88
52	Tellurium	Te	127.61
65	Terbium	Tb	159.2
81	Thallium	Tl	204.39
90	Thorium	Th	232.12
69	Thulium	Tm	169.4
50	Tin	Sn	118.70
22	Titanium	Ti	47.90
74	Tungsten	W	183.92
92	Uranium	U	238.07
23	Vanadium	V	50.95
54	Xenon	Xe	131.3
70	Ytterbium	Yb	173.04
39	Yttrium	Y	88.92
30	Zinc	Zn	65.38
40	Zirconium	Zr	91.22

# APPENDIX III

## Periodic Table of the Elements

Atomic Weights from the Report of the Committee on Atomic Weights of the International Union of Chemistry  
J.A.C.S. 63, 845, 1941

	I	II	III	IV	V	VI	VII	VIII
1	1 H 1.0080							2 He 4.003
2	3 Li 6.940	4 Be 9.02	5 B 10.82	6 C 12.01	7 N 14.008	8 O 16.0000	9 F 19.00	10 Ne 20.183
3	11 Na 22.997	12 Mg 24.32	13 Al 26.97	14 Si 28.06	15 P 30.98	16 S 32.06	17 Cl 35.457	18 A 39.944
4	19 K 39.096	20 Ca 40.08	21 Sc 45.10	22 Ti 47.90	23 V 50.95	24 Cr 52.01	25 Mn 54.93	26 Fe 55.85
	29 Cu 63.57	30 Zn 65.38	31 Ga 69.72	32 Ge 72.60	33 As 74.91	34 Se 78.96	35 Br 79.916	36 Kr 83.7
5	37 Rb 85.48	38 Sr 87.63	39 Y 88.92	40 Zr 91.22	41 Nb 92.91	42 Mo 95.95	43 Tc —	44 Ru 101.7
	47 Ag 107.880	48 Cd 112.41	49 In 114.76	50 Sn 118.70	51 Sb 121.76	52 Te 127.61	53 I 126.92	54 Xe 131.3
6	55 Cs 132.91	56 Ba 137.36	57-71 Rare earths*	72 Hf 178.6	73 Ta 180.88	74 W 183.92	75 Re 186.31	76 Os 190.2
	79 Au 197.2	80 Hg 200.61	81 Tl 204.39	82 Pb 207.21	83 Bi 209.00	84 Po (210)	85 At —	86 Rn 222
7	87 Fr —	88 Ra 226.05	89-96 actinides†					



## \*THE RARE EARTHS

57 <sup>*</sup> La 138.92	58 Ce 140.13	59 Pr 140.92	60 Nd 144.27	61 Pm —
62 Sm 150.43	63 Eu 152.0	64 Gd 156.9	65 Tb 159.2	66 Dy 162.46
67 Ho 164.94	68 Er 167.64	69 Tm 169.4	70 Yb 173.04	71 Lu 174.99

## † ACTINIDE SERIES

89 Ac (227)	90 Th 232.04	91 Pa 231	92 U 238.07
93 Np 237	94 Pu —	95 Am —	96 Cm —

Note added in 1948: Element  $Z = 43$ , previously called masurium, has recently been renamed *technetium*, Tc; element  $Z = 85$  has been named *astatine*, At, and element  $Z = 87$ , first called actinium K, has been renamed *francium*, Fr. The transuranic elements  $Z = 95$  and  $Z = 96$  have been named *americium*, Am, and *curium*, Cm, respectively.

# APPENDIX IV

## Table of Isotopic Masses

Atomic No.	Atom	Mass No.	Mass	Atomic No.	Atom	Mass No.	Mass
1	H	1	1.00813	15	P	30	29.9885
	H	2	2.01473		P	31	30.98441
	H	3	3.01700		P	32	31.98436
2	He	3	3.01699	16	S	31	30.98965
	He	4	4.00386		S	32	31.98252
	He	5	5.01543		S	33	32.98200
3	He	6	6.0209		S	34	33.97981
	Li	6	6.01692	17	Cl	33	32.9875
	Li	7	7.01816		Cl	34	33.981
4	Li	8	8.02497		Cl	35	34.9807
	Be	7	7.01909	18	Cl	36	35.9799
	Be	8	8.00781		Cl	37	36.9777
5	Be	9	9.01496		Cl	38	37.9800
	Be	10	10.01662	19	A	35	34.9865
	B	9	9.01610		A	36	35.9792
6	B	10	10.01617		A	38	37.97473
	B	11	11.01290	20	A	40	39.97459
	B	12	12.0168		A	41	40.97740
7	C	10	10.02086		K	41	40.9731
	C	11	11.01502	21	Ca	45	44.97075
	C	12	12.00388		Sc	45	44.96977
8	C	13	13.00756		Sc	46	45.96909
	C	14	14.00774	22	Ti	48	47.96580
	N	13	13.00990		Va	51	50.96035
9	N	14	14.00753		Va	52	51.95857
	N	15	15.00487	23	Cr	52	51.948
	N	16	16.00645		Fe	56	55.9571
10	O	15	15.0078		Ni	58	57.942
	O	16	16.000000	24	Zn	64	63.935
	O	17	17.00450		As	75	74.934
11	O	18	18.00485		Se	80	79.941
	F	17	17.00758	26	Br	79	78.929
	F	18	18.00670		Br	81	80.926
12	F	19	19.00454		Kr	78	77.926
	F	20	20.00654	36	Kr	80	79.926
	Ne	19	19.00798		Kr	82	81.927
13	Ne	20	19.99889		Kr	83	82.927
	Ne	21	21.00002	41	Kr	84	83.928
	Ne	22	21.99858		Kr	86	85.929
14	Na	22	22.00032		Cb	93	92.926
	Na	23	22.99644	42	Mo	98	97.946
	Na	24	23.99774		Mo	100	99.945
15	Mg	23	23.00055		Sn	120	119.912
	Mg	24	23.99300	50	Te	126	125.937
	Mg	25	24.99462		Te	128	127.936
16	Mg	26	25.99012		I	127	126.932
	Mg	27	26.99256	53	Xe	134	133.929
	Al	26	25.99446		Cs	133	132.933
17	Al	27	26.99069		Ba	138	137.916
	Al	28	27.99077	73	Ta	181	180.927
	Al	29	28.9890		W	184	184.00
18	Si	27	26.99711		Re	187	186.981
	Si	28	27.98727	76	Os	190	189.981
	Si	29	28.98635		Os	192	191.981
19	Si	30	29.98399		Hg	200	200.016
	Si	31	30.9866	80	Tl	203	203.036
	P	29	28.9135		Tl	205	205.037

**APPENDIX V**  
**Table of Stable Isotopes**

Atomic No.	Atom	Mass No.	Relative Abundance (%)	Atomic No.	Atom	Mass No.	Relative Abundance (%)
1	H	1	99.98	16	S	32	95.1
1	H	2	0.02	16	S	33	0.74
2	He	4	100.	16	S	34	4.2
3	Li	6	7.5	17	Cl	35	75.4
3	Li	7	92.5	17	Cl	37	24.6
4	Be	9	100.	18	A	36	0.307
5	B	10	18.4	18	A	38	0.061
5	B	11	81.6	18	A	40	99.632
6	C	12	98.9	19	K	39	93.38
6	C	13	1.1	19	K	40	0.012
7	N	14	99.62	19	K	41	6.61
7	N	15	0.38	20	Ca	40	96.96
8	O	16	99.76	20	Ca	42	0.64
8	O	17	0.04	20	Ca	43	0.15
8	O	18	0.20	20	Ca	44	2.06
9	F	19	100.	21	Sc	45	100.
10	Ne	20	90.00	22	Ti	46	7.95
10	Ne	21	0.27	22	Ti	47	7.75
10	Ne	22	9.73	22	Ti	48	73.45
11	Na	23	100.	22	Ti	49	5.51
12	Mg	24	77.4	22	Ti	50	5.34
12	Mg	25	11.5	23	V	51	100.
12	Mg	26	11.1	24	Cr	50	4.49
13	Al	27	100.	24	Cr	52	83.78
14	Si	28	89.6	24	Cr	53	9.43
14	Si	29	6.2	24	Cr	54	2.30
14	Si	30	4.2	25	Mn	55	100.
15	P	31	100.	26	Fe	54	6.04
				26	Fe	56	91.57
				26	Fe	57	2.11
				26	Fe	58	0.28

Table of Stable Isotopes (Continued)

Atomic No.	Atom	Mass No.	Relative Abundance (%)	Atomic No.	Atom	Mass No.	Relative Abundance (%)
27	Co	59	100.	38	Sr	86	9.86
28	Ni	58	67.4	38	Sr	87	7.02
28	Ni	60	26.7	38	Sr	88	82.56
28	Ni	61	1.2	39	Y	89	100.
28	Ni	62	3.8	40	Zr	90	48.
28	Ni	64	0.9	40	Zr	91	11.5
29	Cu	63	70.13	40	Zr	92	22.
29	Cu	65	29.87	40	Zr	94	17.
30	Zn	64	50.9	40	Zr	96	1.5
30	Zn	66	27.3	41	Cb	93	100.
30	Zn	67	3.9	42	Mo	92	14.9
30	Zn	68	17.4	42	Mo	94	9.4
30	Zn	70	0.5	42	Mo	95	16.1
31	Ga	69	61.2	42	Mo	96	16.6
31	Ga	71	38.8	42	Mo	97	9.65
32	Ge	70	21.2	42	Mo	98	24.1
32	Ge	72	27.3	42	Mo	100	9.25
32	Ge	73	7.9	44	Ru	95	5.68
32	Ge	74	37.1	44	Ru	98	2.22
32	Ge	76	6.5	44	Ru	99	12.81
33	As	75	100.	44	Ru	100	12.70
34	Se	74	0.9	44	Ru	101	16.98
34	Se	76	9.5	44	Ru	102	31.34
34	Se	77	8.3	44	Ru	104	18.27
34	Se	78	24.0	45	Rh	103	100.
34	Se	80	48.0	46	Pd	102	0.8
34	Se	82	9.3	46	Pd	104	9.3
35	Br	79	50.6	46	Pd	105	22.6
35	Br	81	49.4	46	Pd	106	27.2
36	Kr	78	0.35	46	Pd	108	26.8
36	Kr	80	2.01	46	Pd	110	13.5
36	Kr	82	11.53	47	Ag	107	51.9
36	Kr	83	11.53	47	Ag	109	48.1
36	Kr	84	57.11	48	Cd	106	1.4
36	Kr	86	17.47	48	Cd	108	1.0
37	Rb	85	72.8	48	Cd	110	12.8
37	Rb	87	27.2	48	Cd	111	13.0
38	Sr	84	0.56	48	Cd	112	24.2
				48	Cd	113	12.3
				48	Cd	114	28.0

Table of Stable Isotopes (Continued)

Atomic No.	Atom	Mass No.	Relative Abundance (%)	Atomic No.	Atom	Mass No.	Relative Abundance (%)
48	Cd	116	7.3	57	La	139	100.
49	In	113	4.5	58	Ce	136	< 1.
49	In	115	95.5	58	Ce	138	< 1.
				58	Ce	140	89.
50	Sn	112	1.1	58	Ce	142	11.
50	Sn	114	0.8				
50	Sn	115	0.4	59	Pr	141	100.
50	Sn	116	15.5				
50	Sn	117	9.1	60	Nd	142	26.95
50	Sn	118	22.5	60	Nd	143	13.0
50	Sn	119	9.8	60	Nd	144	22.6
50	Sn	120	28.5	60	Nd	145	9.2
50	Sn	122	5.5	60	Nd	146	16.5
50	Sn	124	6.8	60	Nd	148	6.8
				60	Nd	150	5.95
51	Sb	121	56.				
51	Sb	123	44.	62	Sm	144	3.
				62	Sm	147	17.
52	Te	120	< 1.	62	Sm	148	14.
52	Te	122	2.9	62	Sm	149	15.
52	Te	123	1.6	62	Sm	150	5.
52	Te	124	4.5	62	Sm	152	26.
52	Te	125	6.0	62	Sm	154	20.
52	Te	126	19.0				
52	Te	128	32.8	63	Eu	151	49.1
52	Te	130	33.1	63	Eu	153	50.9
53	I	127	100.	64	Gd	152	0.2
				64	Gd	154	2.86
54	Xe	124	0.094	64	Gd	155	15.61
54	Xe	126	0.088	64	Gd	156	20.59
54	Xe	128	1.90	64	Gd	157	16.42
54	Xe	129	26.23	64	Gd	158	23.45
54	Xe	130	4.07	64	Gd	160	20.87
54	Xe	131	21.17				
54	Xe	132	26.96	65	Tb	159	100.
54	Xe	134	10.54				
54	Xe	136	8.95	66	Dy	158	0.1
				66	Dy	160	1.5
55	Cs	133	100.	66	Dy	161	22.
				66	Dy	162	24.
56	Ba	130	0.101	66	Dy	163	24.
56	Ba	132	0.097	66	Dy	164	28.
56	Ba	134	2.42				
56	Ba	135	6.59	67	Hf	165	100.
56	Ba	136	7.81				
56	Ba	137	11.32	68	Er	162	0.1
56	Ba	138	71.66	68	Er	164	1.5

Table of Stable Isotopes (Concluded)

Atomic No.	Atom	Mass No.	Relative Abundance (%)	Atomic No.	Atom	Mass No.	Relative Abundance (%)
68	Er	166	32.9	76	Os	188	13.3
68	Er	167	24.4	76	Os	189	16.1
68	Er	168	26.9	76	Os	190	26.4
68	Er	170	14.2	76	Os	192	41.0
69	Tm	169	100.	77	Ir	191	38.5
70	Yb	168	0.06	77	Ir	193	61.5
70	Yb	170	4.21	78	Pt	192	0.8
70	Yb	171	14.26	78	Pt	194	30.2
70	Yb	172	21.49	78	Pt	195	35.3
70	Yb	173	17.02	78	Pt	196	26.6
70	Yb	174	29.58	78	Pt	198	7.2
70	Yb	176	13.38	79	Au	197	100.
71	Lu	175	97.5	80	Hg	196	0.15
71	Lu	176	2.5	80	Hg	198	10.1
72	Hf	174	0.18	80	Hg	199	17.0
72	Hf	176	5.30	80	Hg	200	23.3
72	Hf	177	18.47	80	Hg	201	13.2
72	Hf	178	27.13	80	Hg	202	29.6
72	Hf	179	13.85	80	Hg	204	6.7
72	Hf	180	35.14	81	Tl	203	29.1
73	Ta	181	100.	81	Tl	205	70.9
74	W	180	0.2	82	Pb	204	1.5
74	W	182	22.6	82	Pb	206	23.6
74	W	183	17.3	82	Pb	207	22.6
74	W	184	30.1	82	Pb	208	52.3
74	W	186	29.8	83	Bi	209	100.
75	Re	185	38.2	90	Th	232	100.
75	Re	187	61.8	92	U	234	0.006
76	Os	184	0.018	92	U	235	0.71
76	Os	186	1.59	92	U	238	99.28
76	Os	187	1.64				

## APPENDIX VI

### Displacement Equation for Brownian Motion

The second type of experiment performed by Perrin for the determination of Avogadro's number consisted in observing the displacement of a particle in a given time interval. The fundamental assumption used in the derivation of the equation for the displacement of such particles is that the particles suspended in the fluid have a mean kinetic energy equal to the mean kinetic energy of gas molecules at the same temperature. The equation of state for one mole of an ideal gas is

$$Pv = RT, \quad (1)$$

and on the basis of the kinetic theory of gases it can be shown that this equation takes the form

$$Pv = \frac{1}{3}Nmc^2, \quad (2)$$

where  $\bar{c}^2$  is the average of the squares of the velocities of the molecules of the gas at temperature  $T$ . Thus the mean kinetic energy of a gas molecule is

$$\mathcal{E} = \frac{1}{2}m\bar{c}^2 = \frac{3}{2} \frac{R}{N} T. \quad (3)$$

In general, a particle has three degrees of freedom of translatory motion; but if the observations are confined to a single direction, say the  $x$  direction, the average kinetic energy due to the motion in this direction will be one third of its total kinetic energy, or

$$\frac{1}{2}m \overline{\left(\frac{dx}{dt}\right)^2} = \frac{\mathcal{E}}{3} = \frac{1}{2} \frac{R}{N} T, \quad (4)$$

where  $\frac{dx}{dt}$  is the instantaneous velocity of the molecule in the  $x$  direction and  $\overline{\left(\frac{dx}{dt}\right)^2}$  is the average of the squares of its velocity in the  $x$  direction.

The motion of a Brownian particle in a horizontal plane is

determined by two forces: (1) that due to the bombardment of the molecules of the medium giving an unbalanced force whose component in the  $x$  direction is  $X$ , and (2) the resistance to the motion due to the viscosity of the medium. From Stokes' law, the resistance to the motion is proportional to the velocity; hence the force on the particle in the  $x$  direction at any instant is, from Newton's second law,

$$F_x = X - K \frac{dx}{dt} = m \frac{d^2x}{dt^2}, \quad (5)$$

where  $K$  is a factor of proportionality determined by the viscosity of the medium, and is given by

$$K = 6\pi\eta a, \quad (6)$$

where  $\eta$  is the coefficient of viscosity of the fluid and  $a$  is radius of the particle. In studying Brownian motion it is easier to consider the magnitude only of the displacement; hence the equation of motion is modified to yield  $x^2$  instead of  $x$ . Multiplying through by  $x$ , we get

$$Xx - Kx \frac{dx}{dt} = mx \frac{d^2x}{dt^2}.$$

Now

$$x \frac{d^2x}{dt^2} = \frac{1}{2} \frac{d^2}{dt^2} (x^2) - \left( \frac{dx}{dt} \right)^2,$$

and

$$x \frac{dx}{dt} = \frac{1}{2} \frac{d}{dt} (x^2),$$

so that

$$Xx - \frac{1}{2}K \frac{d(x^2)}{dt} = \frac{m}{2} \frac{d^2(x^2)}{dt^2} - m \left( \frac{dx}{dt} \right)^2. \quad (7)$$

We are interested only in average values of these quantities which can be observed in a time interval  $t$ . A bar over a symbol will represent its average value. Let  $z = \frac{d(\overline{x^2})}{dt}$  and note that  $\overline{Xx} = 0$  since  $Xx$  is probably positive as often as it is negative; then equation (7) becomes

$$-\frac{Kz}{2} = \frac{m}{2} \frac{dz}{dt} - m \overline{\left( \frac{dx}{dt} \right)^2} \quad (8)$$



or

$$-\frac{Kz}{2} = \frac{m}{2} \frac{dz}{dt} - \frac{RT}{N} \quad (9)$$

from equation (4).

Separating variables we get

$$\frac{dz}{z - \frac{2RT}{KN}} = -\frac{K}{m} dt; \quad (10)$$

and integrating from 0 to  $t$ , this yields

$$z - \frac{2RT}{NK} = A e^{-\frac{K}{m}t}, \quad (11)$$

where  $A$  is a constant of integration. For any reasonable time interval required for observation, the exponential term becomes negligible so that

$$z = \frac{2RT}{NK} = \frac{d(\overline{x^2})}{dt} \quad (12)$$

and

$$\overline{x^2} = \frac{2RT}{NK} t, \quad (13)$$

where  $t$  is the time interval for observation. This equation states that the average square of the displacements of a particle depends upon the time interval  $t$  and upon the temperature of the medium. This equation was derived by Einstein (1905).

## APPENDIX VII

### Path of an Alpha Particle in a Coulomb Field of Force

Consider a nucleus of charge  $Ze$  stationary at point  $C$  and an alpha particle of mass  $M$  and charge  $E$  approaching it along the line  $AB$ , Figure 38. The original velocity of the alpha particle in

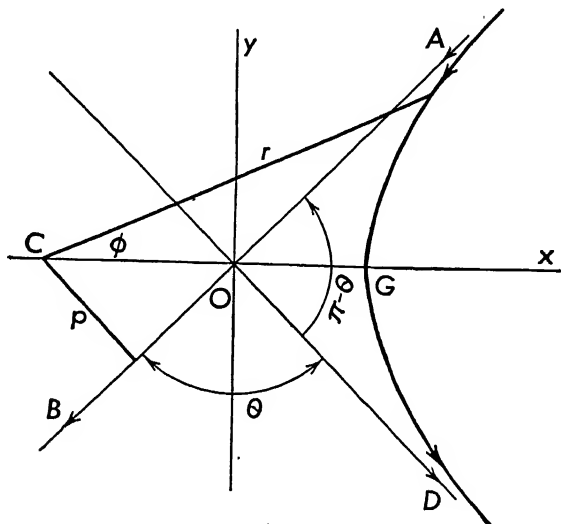


FIG. 38. — The hyperbolic path of an alpha particle in the field of force of a nucleus. the direction of  $AB$  is  $V$ . There will be a force of repulsion between the two charges given by Coulomb's law

$$F = \frac{ZeE}{r^2}, \quad (1)$$

where  $r$  is the distance of the alpha particle from the nucleus. The alpha particle will be deflected from its original direction of motion by this force of repulsion and its path will be a conic section since the motion is governed by an inverse square law of force. This conic section will be one branch of a hyperbola with the nucleus at the focus on the convex side of this branch.

To derive the expression for the path of the alpha particle, let us choose polar coordinates with the nucleus at the pole. The ac-

celeration of the particle may be resolved into two components, one along the radius,  $a_r$ , and the other transverse to the radius  $a_\phi$ . In texts on Mechanics, it is shown that these components are given by the equations

$$a_r = \frac{d^2r}{dt^2} - r \left( \frac{d\phi}{dt} \right)^2 \quad (2)$$

$$a_\phi = \frac{1}{r} \frac{d}{dt} \left( r^2 \frac{d\phi}{dt} \right). \quad (3)$$

Since the force of repulsion is along the radius vector  $r$ , the radial component of the acceleration is

$$a_r = \frac{F}{M} = \frac{ZeE}{Mr^2} = \frac{J}{r^2}, \quad (4)$$

where

$$J = \frac{ZeE}{M}.$$

Since there is no force transverse to the radius vector,

$$a_\phi = 0 = \frac{1}{r} \frac{d}{dt} \left( r^2 \frac{d\phi}{dt} \right). \quad (5)$$

Integrating equation (5) yields

$$r^2 \frac{d\phi}{dt} = K. \quad (6)$$

Equation (6) is a statement of Kepler's law of areas, and also expresses the principle of conservation of angular momentum, for, multiplying both sides by  $M$ , we get

$$Mr^2 \frac{d\phi}{dt} = MK = M V p, \quad (7)$$

where  $Mr^2$  is the moment of inertia of the alpha particle with respect to an axis through  $C$ ,  $d\phi/dt$  is the angular velocity of the particle and  $M V p$  is the initial angular momentum of the particle. The distance  $p$  from the nucleus to  $AB$  is called the *impact parameter*.

The differential equation of the path of the particle may be obtained by combining equations (2) and (4); this yields

$$\frac{d^2r}{dt^2} - r \left( \frac{d\phi}{dt} \right)^2 = \frac{J}{r^2}. \quad (8)$$

Before integrating this equation, let us change the independent variable from  $t$  to  $\phi$ , and also, for convenience, let  $u = \frac{1}{r}$ . To carry out this transformation, note that

$$\frac{dr}{dt} = \frac{dr}{d\phi} \frac{d\phi}{dt} = -\frac{1}{u^2} \kappa \omega^2 \frac{du}{d\phi} = -\kappa \frac{du}{d\phi},$$

$$\frac{dr}{d\phi} = -\frac{1}{u^2} \frac{du}{d\phi},$$

and from equation (6)

$$\frac{d\phi}{dt} = \frac{K}{r^2} = Ku^2$$

and

$$\frac{d^2r}{dt^2} = -Ku^2 \frac{d^2u}{d\phi^2}.$$

Equation (8) now becomes

$$\frac{d^2u}{d\phi^2} + u = -\frac{J}{K^2}$$

or

$$\frac{d^2}{d\phi^2} \left( u + \frac{J}{K^2} \right) = - \left( u + \frac{J}{K^2} \right). \quad (9)$$

This is a well-known differential equation and its solution is

$$u + \frac{J}{K^2} = A \cos(\phi - \delta), \quad (10)$$

where  $A$  and  $\delta$  are constants of integration. To verify that this is the solution of the differential equation, one needs only to differentiate equation (10) twice.

By the proper choice of the  $x$  axis, the phase angle  $\delta$  can be set equal to zero. Further, by setting

$$\epsilon = \frac{AK^2}{J} \quad (11)$$

equation (10) becomes

$$u + \frac{J}{K^2} = \frac{\epsilon J}{K^2} \cos \phi,$$

from which

$$u = \frac{1}{r} = -\frac{J}{K^2}(1 - \epsilon \cos \phi). \quad (12)$$

Equation (12) is one form of the equation of a conic section in polar coordinates;  $\epsilon$  is the eccentricity of this conic section. When  $\epsilon$  is greater than unity, the conic section is a hyperbola. The eccentricity of this path can be determined with the aid of the principle of conservation of energy which yields

$$\frac{1}{2}MV^2 = \frac{1}{2}Mv^2 + \frac{ZeE}{r} = \frac{1}{2}Mv^2 + \frac{JM}{r} \quad (13)$$

where  $ZeE/r$  is the potential energy of the particle at any point in its path. Resolving the velocity  $v$  into two components, one along the radius and one transverse to the radius, we get

$$v^2 = \left(\frac{dr}{dt}\right)^2 + \left(r\frac{d\phi}{dt}\right)^2 = \left[\left(\frac{dr}{d\phi}\right)^2 + r^2\right]\left(\frac{d\phi}{dt}\right)^2. \quad (14)$$

From equation (12) we get

$$\left(\frac{dr}{d\phi}\right)^2 = \frac{J^2\epsilon^2r^4\sin^2\phi}{K^4},$$

and since

$$\left(\frac{d\phi}{dt}\right)^2 = \frac{K^2}{r^4},$$

equation (14) becomes

$$v^2 = \frac{J^2\epsilon^2\sin^2\phi}{K^2} + \frac{J^2}{K^2}(1 - \epsilon \cos \phi)^2. \quad (15)$$

Substituting this value of  $v^2$  in equation (13) and the value for  $r$  from equation (12) and simplifying, we get

$$V^2 = \frac{J^2\epsilon^2}{K^2} - \frac{J^2}{K^2},$$

from which

$$\epsilon^2 - 1 = \frac{K^2}{J^2} V^2$$

or

$$\epsilon^2 - 1 = \left(\frac{MV^2p}{ZeE}\right)^2. \quad (16)$$

The eccentricity of the orbit is greater than unity and is expressed in terms of the initial energy of the alpha particle, the impact parameter  $p$ , and the nuclear charge  $Ze$ , thus

$$\epsilon = \sqrt{1 + \left( \frac{MV^2 p}{ZeE} \right)^2}. \quad (17)$$

The orbit is therefore an hyperbola with the nucleus at the focus outside the branch of the curve followed by the alpha particle. The asymptote  $AB$  represents the direction of the initial velocity of the alpha particle, while the second asymptote  $OD$  represents the direction of the final velocity of the alpha particle. The angle  $\theta$  between the two asymptotes is the angle through which the particle has been deflected and is the angle of scattering. This angle can be expressed in terms of the eccentricity from a consideration of the properties of the hyperbola.

The equation of the hyperbola in rectangular coordinates is

$$\frac{x^2}{a^2} - \frac{y^2}{b^2} = 1, \quad (18)$$

where

$$a\epsilon = OC$$

and

$$b^2 = a^2(\epsilon^2 - 1).$$

The equations of the asymptotes are obtained by setting the left-hand side of equation (18) equal to zero, yielding

$$y = \pm \frac{b}{a} x.$$

From the figure

$$\frac{b}{a} = \tan \frac{\pi - \theta}{2} = \cot \frac{\theta}{2};$$

hence

$$\epsilon^2 - 1 = \cot^2 \frac{\theta}{2}. \quad (19)$$

Using equation (16), we get

$$\cot \frac{\theta}{2} = \frac{MV^2}{ZeE} p \quad (20)$$

## APPENDIX VIII

### Derivation of the Equations for the Compton Effect

The three equations derived in § 64 are

$$h\nu = h\nu' + m_0c^2(K - 1) \quad (1)$$

$$\frac{h\nu}{c} = \frac{h\nu'}{c} \cos \phi + Km_0v \cos \theta \quad (2)$$

$$0 = \frac{h\nu'}{c} \sin \phi - Km_0v \sin \theta, \quad (3)$$

where

$$K = \frac{1}{\left(1 - \frac{v^2}{c^2}\right)^{1/2}}.$$

To solve these equations, let

$$\alpha = \frac{h\nu}{m_0c^2} = \frac{h}{m_0c\lambda}$$

$$\alpha' = \frac{h\nu'}{m_0c^2} = \frac{h}{m_0c\lambda'}$$

$$b = \sqrt{K^2 - 1} = \frac{Kv}{c}$$

or

$$K = \sqrt{1 + b^2}$$

$$l_1 = \cos \phi$$

$$n_1 = \sin \phi$$

$$l_2 = \cos \theta$$

$$n_2 = \sin \theta.$$

By dividing equation (1) by  $m_0c^2$  we get

$$\alpha = \alpha' + \sqrt{1 + b^2} - 1, \quad (4)$$

and by dividing equations (2) and (3) by  $m_0c$ , we get

$$\alpha = \alpha' l_1 + b l_2 \quad (5)$$

and

$$0 = \alpha' n_1 - b n_2. \quad (6)$$

From equation (5)

$$b^2 l_2^2 = \alpha^2 - 2\alpha\alpha' l_1 + \alpha'^2 l_1^2, \quad (7)$$

and from equation (6)

$$b^2 n_2^2 = \alpha'^2 n_1^2. \quad (8)$$

Adding equations (7) and (8), we get

$$b^2 (l_2^2 + n_2^2) = \alpha^2 - 2\alpha\alpha' l_1 + \alpha'^2 (l_1^2 + n_1^2)$$

or

$$b^2 = \alpha^2 - 2\alpha\alpha' l_1 + \alpha'^2, \quad (9)$$

since

$$l_2^2 + n_2^2 = 1 = l_1^2 + n_1^2.$$

From equation (4)

$$b^2 = \alpha^2 - 2\alpha\alpha' + \alpha'^2 + 2\alpha - 2\alpha'. \quad (10)$$

Subtracting (10) from (9), we get

$$0 = 2\alpha\alpha'(1 - l_1) - 2\alpha + 2\alpha',$$

from which

$$0 = \alpha(1 - l_1) - \left(\frac{\alpha}{\alpha'} - 1\right)$$

or

$$\frac{\alpha}{\alpha'} - 1 = \alpha(1 - l_1), \quad (11)$$

from which

$$\frac{\lambda'}{\lambda} - 1 = \frac{h}{m_0 c \lambda} (1 - \cos \phi)$$

or

$$\lambda' - \lambda = \frac{h}{m_0 c} (1 - \cos \phi), \quad (12)$$

which is the same as equation (55) in the text. To get the expres-



sion for the kinetic energy of the recoil electron, solve equation (11) for  $\alpha'$ , obtaining

$$\alpha' = \frac{\alpha}{1 + \alpha(1 - l_1)}. \quad (13)$$

Substitute this value in equation (4), obtaining

$$\begin{aligned} \sqrt{1 + b^2} - 1 &= \alpha - \frac{\alpha}{1 + \alpha(1 - l_1)} \\ &= \frac{\alpha^2(1 - l_1)}{1 + \alpha(1 - l_1)}. \end{aligned}$$

Now the kinetic energy  $\mathcal{E}$  is given by

$$\begin{aligned} \mathcal{E} &= m_0 c^2 (K - 1) = m_0 c^2 (\sqrt{1 + b^2} - 1) \\ &= m_0 c^2 \frac{\alpha^2(1 - \cos \phi)}{1 + \alpha(1 - \cos \phi)}. \end{aligned}$$

But

$$m_0 c^2 = \frac{h\nu}{\alpha};$$

therefore

$$\mathcal{E} = h\nu \frac{\alpha(1 - \cos \phi)}{1 + \alpha(1 - \cos \phi)}. \quad (14)$$

The energy of the recoil electron can also be put in terms of the angle  $\theta$  by noting that, from equations (5) and (6)

$$\frac{l_2}{n_2} = - \frac{\alpha - \alpha' l_1}{\alpha' n_1} = - \frac{1}{n_1} \left( \frac{\alpha}{\alpha'} - l_1 \right), \quad (15)$$

and eliminating  $\alpha'$  with the aid of equation (11), we get

$$\frac{l_2}{n_2} = - \frac{1}{n_1} (1 + \alpha)(1 - l_1). \quad (16)$$

Substituting the values of  $l_1$ ,  $l_2$ ,  $n_1$ , and  $n_2$ , we get

$$\cot \theta = - (1 + \alpha) \frac{1 - \cos \phi}{\sin \phi}. \quad (17)$$

Now

$$\frac{1 - \cos \phi}{\sin \phi} = \tan \frac{\phi}{2};$$

therefore

$$\cot \theta = -(1 + \alpha) \tan \frac{\phi}{2} \quad (18)$$

also

$$\tan \theta = -\frac{\cot \frac{\phi}{2}}{1 + \alpha}, \quad (19)$$

which is equation (56) in the text.

By dividing equation (18) by equation (19), we get

$$\frac{\cos^2 \theta}{\sin^2 \theta} = \frac{\cos^2 \theta}{1 - \cos^2 \theta} = (1 + \alpha)^2 \tan^2 \frac{\phi}{2}.$$

Now

$$\tan^2 \frac{\phi}{2} = \frac{1 - \cos \phi}{1 + \cos \phi};$$

hence

$$\frac{\cos^2 \theta}{1 - \cos^2 \theta} = (1 + \alpha)^2 \frac{1 - \cos \phi}{1 + \cos \phi}. \quad (20)$$

Solving equation (20) for  $\cos \phi$  and then for  $(1 - \cos \phi)$ , we get

$$1 - \cos \phi = \frac{2 \cos^2 \theta}{(1 + \alpha)^2 - 2\alpha \cos^2 \theta - \alpha^2 \cos^2 \theta}. \quad (21)$$

Substituting this value in equation (14), yields

$$\mathcal{E} = h\nu \frac{2\alpha \cos^2 \theta}{(1 + \alpha)^2 - \alpha^2 \cos^2 \theta}, \quad (22)$$

which is equation (57) in the text.

## APPENDIX IX

Evaluation of

$$\oint p_r dr = n_r h. \quad (1)$$

Now

$$p_r = m \frac{dr}{dt} \quad (2)$$

is the momentum along the radius. Changing the independent variable from  $t$  to  $\phi$ , by the relationship

$$\frac{dr}{dt} = \frac{dr}{d\phi} \frac{d\phi}{dt}, \quad (3)$$

we get

$$p_r = m \frac{d\phi}{dt} \frac{dr}{d\phi}; \quad (4)$$

and noting that

$$p_\phi = m r^2 \frac{d\phi}{dt} \quad (5)$$

and

$$dr = \frac{dr}{d\phi} d\phi, \quad (6)$$

we may write the integral as

$$\oint \frac{p_\phi}{r^2} \frac{dr}{d\phi} \cdot \frac{dr}{d\phi} \cdot d\phi = n_r h \quad (7)$$

or

$$p_\phi \oint \frac{1}{r^2} \left( \frac{dr}{d\phi} \right)^2 d\phi = n_r h. \quad (8)$$

The equation of the ellipse may be written as

$$\frac{1}{r} = \frac{1 + \epsilon \cos \phi}{a(1 - \epsilon^2)}, \quad (9)$$

where  $a$  is the semimajor axis and  $\epsilon$  is the eccentricity.

Therefore 
$$\frac{dr}{d\phi} = \frac{a(1 - \epsilon^2)\epsilon \sin \phi}{(1 + \epsilon \cos \phi)^2} \quad (10)$$

and

$$\frac{1}{r} \frac{dr}{d\phi} = \frac{\epsilon \sin \phi}{1 + \epsilon \cos \phi} \quad (11)$$

The integral equation now becomes

$$p_\phi \int_0^{2\pi} \frac{\epsilon^2 \sin^2 \phi}{(1 + \epsilon \cos \phi)^2} d\phi = n_r h. \quad (12)$$

The integral 
$$I = \int_0^{2\pi} \frac{\epsilon^2 \sin^2 \phi}{(1 + \epsilon \cos \phi)^2} d\phi \quad (13)$$

can be integrated by parts. In the usual standard form

$$\int u dv = uv - \int v du; \quad (14)$$

let

$$\begin{aligned} u &= \epsilon \sin \phi \\ du &= \epsilon \cos \phi d\phi \\ dv &= \frac{\epsilon \sin \phi}{(1 + \epsilon \cos \phi)^2} d\phi, \end{aligned}$$

so that

$$v = \frac{1}{1 + \epsilon \cos \phi};$$

then

$$I = \left[ \frac{\epsilon \sin \phi}{1 + \epsilon \cos \phi} \right]_0^{2\pi} - \int_0^{2\pi} \frac{\epsilon \cos \phi}{1 + \epsilon \cos \phi} d\phi. \quad (15)$$

Upon substitution of the limits of integration, the first term on the right-hand side becomes zero. The value of the integral is

$$I = - \int_0^{2\pi} \frac{\epsilon \cos \phi}{1 + \epsilon \cos \phi} d\phi, \quad (16)$$

which may be written in the form

$$I = \int_0^{2\pi} \left( \frac{1}{1 + \epsilon \cos \phi} - 1 \right) d\phi, \quad (17)$$

yielding

$$I = \frac{2\pi}{(1 - \epsilon^2)^{1/2}} - 2\pi. \quad (18)$$

(See Peirce's *Table of integrals*, page 41.)

Putting this back in the integral equation, we get

$$\frac{2\pi p_\phi}{(1 - \epsilon^2)^{1/2}} - 2\pi p_\phi = n_r h, \quad (19)$$

or

$$\frac{kh}{(1 - \epsilon^2)^{1/2}} - kh = n_r h \quad (20)$$

since

$$p_\phi = \frac{kh}{2\pi};$$

hence

$$(n_r + k) = \frac{k}{(1 - \epsilon^2)^{1/2}}; \quad (21)$$

so that

$$\epsilon = \sqrt{1 - \left(\frac{k}{k + n_r}\right)^2}, \quad (22)$$

which is the expression for the eccentricity of the ellipse in terms of the azimuthal and radial quantum numbers.

Of great interest is the expression for the total energy  $\mathcal{E}$  of an elliptic orbit. The potential energy is  $-Ze^2/r$ . The kinetic energy can be written as

$$\frac{1}{2}m\left[\left(\frac{dr}{dt}\right)^2 + \left(r\frac{d\phi}{dt}\right)^2\right]$$

where  $\frac{dr}{dt}$  is the radial component of the velocity and  $r\frac{d\phi}{dt}$  is the transverse component of the velocity. Now using equations (3 and 5), we get

$$\frac{dr}{dt} = \frac{p_\phi}{mr^2} \frac{dr}{d\phi} \quad (23)$$

and

$$\left(r \frac{d\phi}{dt}\right)^2 = \frac{p_\phi^2}{m^2 r^2}. \quad (24)$$

The expression for the total energy then becomes

$$\begin{aligned} \mathcal{E} &= \frac{1}{2}m \left[ \frac{p_\phi^2}{m^2 r^4} \left(\frac{dr}{d\phi}\right)^2 + \frac{p_\phi^2}{m^2 r^2} \right] - \frac{Ze^2}{r} \\ &= \frac{p_\phi^2}{2mr^2} \left[ \left(\frac{1}{r} \frac{dr}{d\phi}\right)^2 + 1 \right] - \frac{Ze^2}{r}. \end{aligned} \quad (25)$$

Solving this for  $\left(\frac{1}{r} \frac{dr}{d\phi}\right)^2$  yields

$$\left(\frac{1}{r} \frac{dr}{d\phi}\right)^2 = \frac{2m\mathcal{E}r^2}{p_\phi^2} + \frac{2mZe^2r}{p_\phi^2} - 1. \quad (26)$$

From equation (11) we get

$$\left(\frac{1}{r} \frac{dr}{d\phi}\right)^2 = \frac{\epsilon^2 \sin^2 \phi}{(1 + \epsilon \cos \phi)^2}. \quad (27)$$

Eliminating the angle  $\phi$  between this equation and the equation of the ellipse (9) yields

$$\left(\frac{1}{r} \frac{dr}{d\phi}\right)^2 = -\frac{r^2}{a^2(1 - \epsilon^2)} + \frac{2r}{a(1 - \epsilon^2)} - 1. \quad (28)$$

By equating coefficients of like powers of  $r$  in equations (26) and (28), we get

$$\frac{2m\mathcal{E}}{p_\phi^2} = -\frac{1}{a^2(1 - \epsilon^2)} \quad (29)$$

and

$$\frac{mZe^2}{p_\phi^2} = \frac{1}{a(1 - \epsilon^2)}, \quad (30)$$

from which

$$\mathcal{E} = -\frac{Ze^2}{2a}. \quad (31)$$

The total energy depends only upon the major axis of the ellipse and is the same as that for a circle of radius  $a$ . Eliminating  $a$  from equations (29) and (30) yields

$$\mathcal{E} = -\frac{mZ^2e^4(1 - \epsilon^2)}{2p_\phi^2}. \quad (32)$$

# Index

- Abelson, P. H., 360
- Absorption coefficient of X rays, 133, 263
- Absorption of energy, 237
- Absorption limit, 264
- Absorption spectrum, 237
- Absorption of X rays, 132
- Actinium K, 352
- Actinium series, 280
- $\alpha$ - $n$  reaction, 308
- $\alpha$ - $p$  reaction, 302
- Alpha particle, charge of an, 71
  - mass of an, 71
  - path of, in a Coulomb field, 392
  - probability of emission of an, 335
  - velocity of an, 72
- Alpha particles, 64, 70
  - counting of, 70
  - $E/M$  of, 68
  - ionization along path of, 285
  - nature of the, 70
  - range of, 283
  - scattered from gold foil, 79
  - single scattering of, 74
  - velocity spectrum of, 74
- Alpha rays, 64
- Alvarez, L. W., 342
- Ampère, 23
- Ampere, the, 15
- Anderson, C. D., 309
- Anderson, H. L., 373
- Andrade, 121
- Angular momentum, orbital, 215
  - total, 215
- Angular quantum number, 196
- Annihilation of charged particles, 348
- Annihilation of matter, 348
- Anomalous Zeeman effect, 92, 246
- Arago, 86
- Artificial radioactivity. *See* Induced radioactivity
- Artificially produced projectiles for nuclear experiments, 312
- Aston, F. W., 50, 60, 194
- Aston's mass spectrograph, 50
- Atomic bomb, 374
- Atomic mass unit, 61
- Atomic masses. *See* Isotopic masses
- Atomic number, 58
- Atomic weights, 23
  - chemical system of, 24
  - table of, 380
- Average lifetime of an atom, 279
- Avogadro, 23
- Avogadro number, 24, 27, 31, 34, 41, 131, 379
- Avogadro's hypothesis, 24
- Azimuthal quantum number, 196
- Bainbridge, K. T., 55
- Bainbridge's mass spectrograph, 55
- Bainbridge and Jordan's mass spectrograph, 56
- Baldwin, 323, 368
- Baldwin, D. C., 353
- Balmer, J. J., 183
- Balmer series, 184
- Barkla, C. G., 103, 137, 138
- Becker, H., 305
- Becquerel, H., 3, 62
- Bergmann series, 214
- Beta particles, 64
  - emission of, 335
- Beta-ray spectra, 287
- Beta-ray spectrum, continuous, 200
  - end-point energy of, 290
- Beta rays, 64
  - variation of mass with velocity of, 65
- Betatron, 105, 322, 353
- Bethe, H., 357
- Binding energy, 61
- Biot, 14
- Birge, R. T., 33, 41, 132, 194
- Blackett, P. M. S., 299
- Bloch, F., 342
- Björgild, J. K., 363
- Bohr, N., 168, 184, 300, 324, 364
- Bohr magneton, 221, 249, 338
- Bohr's frequency condition, 212
- Bohr's two fundamental postulates, 186
- Booth, E. T., 365
- Bothe, W., 305
- Brackett series, 190
- Bragg, W. L., 112
- Bragg's law, 113, 162
  - modified form of, 125, 162
- Bretsher, E., 282

- Brickwedde, F. G., 194  
 Brøstrom, K. J., 363  
 Brown, 28  
 Brownian motion, 27  
     displacement equation for, 389  
     displacement of particles in, 32  
     vertical distribution of particles in, 28  
 Bucherer, A. H., 65  
  
 Calcite, grating space of, 117, 131  
 Calcium, energy level diagram of, 252  
 Capacitance, 8  
     of a parallel plate capacitor, 12  
 Capacitor, 8  
 Capture of an alpha particle, and ejection  
     of a proton, 302  
     and emission of a neutron, 308  
 Cathode ray tube, 44  
 Cathode rays, 43  
     determination of  $e/m$  for, 43  
 Chadwick, J., 74, 81, 298, 305, 322  
 Chain reaction, 357, 371  
     critical size for, 372  
 Characteristic X-ray spectra, 256  
 Charge of an alpha particle, 71  
 Charge of the electron, 31, 33, 34, 37, 41,  
     132, 379  
     determination of the, 34  
 Charge, electrostatic unit of, 4  
     radiation from accelerated, 89  
 Chemical equivalent, 26  
 Chemical system of atomic weights, 24  
 Cleavage planes, 112  
 Cloud chamber, Wilson, 283, 288  
 Cockroft, J. D., 317  
 Coefficient of viscosity of air, 37  
 Compound nucleus, 300  
 Compton, A. H., 139, 141  
 Compton effect, 141, 169, 291  
     derivation of equations for the, 397  
 Conservation of energy principle, 141  
 Conservation of momentum principle,  
     141  
 Continuous beta-ray spectrum, 290  
 Continuous spectrum of hydrogen, 205  
 Continuous X-ray spectrum, 118  
     short wave length, limit of, 118  
 Corson, D. R., 351  
 Cosmic rays, 309, 352  
 Coulomb, C. A., 4, 9  
 Coulomb, a unit of charge, 5  
 Coulomb's law, 74, 185  
 Coulomb's law of force for electric  
     charges, 4  
     for magnetic poles, 9  
 Counting of alpha particles, 70  
  
 Crane, H. R., 289, 336, 345, 348  
 Critical size for chain reaction, 372  
 Critical voltage, X-ray, 265  
 Curie, I., 359  
 Curie, M., 64  
 Curie, P., 64  
 Curie-Joliot, M. and Mme, 305, 311  
 Current, electric, 13  
 Cyclotron, 314  
  
 Dalton, J., 23, 46  
 Davisson, C., 158  
 Debye, P., 124, 141  
 De Broglie, L., 153  
 De Broglie's hypothesis, 152  
     and quantization of orbits, 206  
 Debye, P., 124, 141  
 Dee, P. I., 317  
 Dempster, A. J., 52  
 Dempster's mass spectrograph, 52  
 Determination of  $E/M$  for alpha parti-  
     cles, 68  
 Determination of  $e/m$  for electrons, 43,  
     66, 95  
 Determination of nuclear charge, 81  
 Deuterium, 194  
     discovery of, 194  
 Deuteron, 195  
     magnetic moment of the, 342  
 Deuterons, disintegrations produced by,  
     318  
 Dielectric constant, 4, 129  
 Diffraction of electrons, 156  
     by a crystal, 157  
     by a slit, 170  
 Diffraction of helium atoms, 165  
 Diffraction of hydrogen molecules, 165  
 Diffraction of X rays, 110  
     powder crystal method, 122  
 Diffuse series, 214  
 Discovery, of artificial radioactivity, 311  
     of deuterium, 194  
     of induced radioactivity, 311  
     of natural radioactivity, 62  
     of the neutron, 304  
     of nuclear fission, 358  
     of the positron, 309  
     of X rays, 102  
 Disintegration by deuterons, 318  
 Disintegration energy, 301  
 Disintegration by neutrons, 324  
 Disintegration of nitrogen by alpha-  
     particle bombardment, 298  
 Disintegration of nuclei by photons, 322  
 Disintegration by protons, 317  
 Disintegration yield, 303, 333



- Dispersion of X rays, 127  
 Distribution of electrons in an atom, 227  
 Distribution-in-range of protons, 304  
 Dorsey, 16  
 Duane, W., 118  
 Dunning, J. R., 365
- Einstein, A., 3, 28, 32, 61, 65, 101, 391  
 Einstein's photoelectric equation, 101  
 Einstein's special theory of relativity, 65  
 Electric current, 13  
   magnetic effect of, 13  
 Electric discharge through gases, 41  
 Electric field, energy in, 12  
 Electric field intensity, 5  
 Electrochemical equivalent, 26  
 Electrolysis, 25  
 Electromagnetic induction, 18  
   Faraday's law of, 19  
 Electromagnetic theory of light, 86  
 Electromagnetic unit of current, 15  
 Electromagnetic wave, energy per unit  
   volume of, 88  
   intensity of, 88  
   linearly polarized, 89  
 Electron, 25, 43  
   magnetic moment of orbital, 220  
   reduced mass of the, 192  
   state of the, 225  
 Electron diffraction, 156  
   experiments of Davisson and Germer,  
   156  
   experiments of G. P. Thomson, 163  
 Electron mass, ratio of, to mass of proton,  
   194  
 Electron microscope, 175  
 Electron optics, 175  
 Electron spin, 216  
   magnetic moment due to, 222  
   Stern-Gerlach experiment and, 248  
 Electron volt, 61  
 Electron waves, 156  
   diffraction of, 156  
   wave length of, 157  
 Electronic charge, 31, 33, 34, 37, 41, 132,  
   379  
 Electronic cloud, 209  
 Electrons, emission of, by nuclei, 335  
   recoil, 141, 144  
   refraction of, 160  
 Electrostatic generator, 313  
 Elements, 23  
 Elliptic orbits for hydrogen, 196
- e/m*, 95  
   of beta rays, 66  
   of cathode rays, 43
- e/m*  
   determination of, from Zeeman effect,  
   95  
   of electrons, 43  
*E/M* of alpha particles, 68  
 Emission of beta particles, 335  
 Emission of electrons by nuclei, 335  
 Emission of positrons, 335  
 Energy, in electric field, 12  
   in magnetic field, 12  
   materialization of, 348  
   quantum of, 101, 141  
   released in nuclear fission, 363  
 Energy level, 225  
 Energy level diagram, of calcium, 252  
   of hydrogen, 202  
   nuclear, 295  
   of sodium, 235  
   X-ray, 259, 269  
 Euler, H., 353  
 Evans, G. R., 343  
 Excited state, 233  
 Exclusion principle, Pauli's, 224
- Faraday, M., 18, 91  
 Faraday constant, the, 26, 34, 41, 132, 379  
 Faraday's laws of electrolysis, 26  
 Faraday's law of electromagnetic induc-  
   tion, 19  
 Feather, N., 282  
 Feder, 121  
 Fermi, E., 358, 373  
 Fine structure, 234  
 Fine structure constant, 201  
 Fission. *See* Nuclear fission  
 Fission chain reaction, 371  
 Fizeau, 86, 152  
 Fletcher, H., 33  
 Fluorescent radiation, 205  
 Fluorescent transformation coefficient of  
   X rays, 133  
 Force on a moving charge in a magnetic  
   field, 17  
 Force on a wire carrying current in a  
   magnetic field, 16  
 Foucault, 86, 152  
 Fresnel, 86  
 Friedrich, W., 111  
 Fundamental series, 214
- Gamma-ray microscope experiment, 169  
 Gamma-ray spectra, 291  
 Gamma rays, 64  
   from alpha-particle emitters, 294  
   from beta-particle emitters, 292  
   wave lengths of, 121

- Gauss, the, 19  
 Geiger, H., 70, 74, 78  
 Geiger counter, 70  
 Geiger-Nuttall law, 286, 335  
 Geiger's rule, 80, 286  
 Genetically related nuclear isomers, 330  
 Gerlach, W., 248  
 Germer, L. H., 158  
*g*-factor, 243  
   nuclear, 338  
 Ghiorso, A., 362  
 Goldhaber, M., 322  
 Goudsmit, S., 217  
 Gram molecular volume, 24  
 Grating space, of calcite, 117, 131  
   of rock salt, 116, 131  
 Grosse, A. V., 365
- Haga, H., 103  
 Hagenow, C. F., 139  
 Hahn, O., 282, 359  
 Half-life period, 278  
 Hallwachs, W., 97  
 Halpern, J., 336  
 Hamilton, 352  
 Hamilton, J. G., 362  
 Hartzler, A. J., 353  
 Haxby, R. O., 368  
 Heisenberg, W., 168, 256, 353  
 Heisenberg's uncertainty principle, 167  
 Henry, J., 18  
 Hertz, H., 86, 97  
 Hewlett, C. W., 137  
 Holloway, M. G., 286  
 Honigschmidt, O., 64  
 Hopper, V. D., 38  
 Hull, A. W., 123  
 Hunt, F. L., 118  
 Huygens, C., 86  
 Hydrogen, 183  
   continuous spectrum of, 205  
   energy level diagram for, 202  
   ionization potential of, 204  
   multiplicity of orbits of, 198  
   Schrödinger's equation for, 207  
   spectrum of, 183  
   wave mechanics applied to, 207  
 Hydrogen atom, 59, 183  
   Bohr's theory of the, 184  
   normal state of, 190  
 Hydrogen nucleus, motion of the, 190  
 Hyperfine structure, 253
- Index of refraction, for particles, 149  
   for waves, 151  
   for X rays, 124
- Induced radioactivity, 311  
 Intensity, of an electromagnetic wave, 88  
   of a magnetic field, 10  
   of scattered X rays, 136, 140  
   of X rays, 109  
 Intercombination lines, 251  
 Internal conversion, 294  
 Ionization chamber, 109  
 Ionization potential, 204  
   of sodium, 236  
 Ions, 25  
 Isomers, nuclear, 281, 321, 328  
 Isotopes, 46, 57  
   stable, table of, 385  
 Isotopic masses and nuclear constitution, 57  
 Isotopic masses, table of, 384
- James, R. A., 362  
 Johnson, T. H., 167  
 Joliot, F., 374  
 Jordan, E. B., 56
- Kamen, M. D., 325  
 Kaufmann, W., 65  
*K*-electron capture, 342  
 Kellogg, J. M. B., 342  
 Kennedy, J. W., 361  
 Kepler's law, 196  
 Kepler's law of areas, 393  
 Kerst, D. W., 105  
 Klaiber, G. S., 353  
 Knipping, P., 111  
 Koch, 323, 368  
 Kruger, P. G., 346  
 Kusch, P., 342
- Laby, T. H., 38  
 Landé *g*-factor, 243  
 Larmor, J., 240  
 Larmor theorem, 240, 338  
 Laue, M., 103, 111  
 Laue diffraction pattern, 111  
 Lauritsen, C. C., 348  
 Lauritsen, T., 363  
 Law of definite proportions, 23  
 Law of multiple proportions, 23  
 Lawrence, E. O., 314  
 Lenz, 20  
 Light, circularly polarized, 91  
   electromagnetic theory of, 86  
   linearly polarized, 90  
   nature of, 86  
 Livingston, M. S., 286, 314  
 Lorentz, H. A., 92  
 Lorentz unit, 246

- Lyman series, 189  
 MacKenzie, K. R., 351  
 Magnet, magnetic moment of a, 11  
 Magnetic effect of an electric current, 13  
 Magnetic field, energy in, 12  
     intensity of, 10  
 Magnetic flux, 19  
 Magnetic lines of force, 10  
 Magnetic moment, of a Bohr magneton, 221, 249  
     of the deuteron, 342  
     due to electron spin, 222  
     of the neutron, 342  
     of a nucleus, 337  
     of an orbital electron, 220  
     of a plane circuit carrying current, 18  
     of the proton, 342  
 Magnetic orbital quantum number, 223  
 Magnetic quantum numbers, 222  
 Magnetic resonance method, 337  
 Magnetic spectrograph, 73, 267  
 Magnetic spectrum analysis, 266  
 Magnetic spin quantum number, 224  
 Magnetron, 221, 249  
     magnetic moment of a Bohr, 221, 249  
     nuclear, 337  
 Marsden, E., 74, 78  
 Mass absorption coefficient, 263  
     of X rays, 133  
 Mass of an alpha particle, 71  
 Mass defect, 59  
 Mass of an electron, 46, 62  
 Mass and energy, 60  
     principle of equivalence of, 60  
 Mass of a hydrogen atom, 46  
 Mass of nucleus, dependence of Rydberg constant on, 193  
 Mass number, 58  
 Mass spectrograph, 50  
 Masurium, 350  
 Materialization of energy, 348  
 Maxwell, J. C., 16, 86, 129  
 Maxwell, the, 19  
 McMillan, E. M., 360, 361  
 Meitner, L., 359  
 Menzel, D. H., 194  
 Meson, 352  
 Metastable state, 251  
     of a nucleus, 329  
 Millikan, R. A., 27, 33, 35, 100, 132  
 Millman, S., 341  
 Moderator, 372  
 Modified form of Bragg's law, 125  
 Modified X-ray line, 144  
 Mole, 24  
 Momentum of a photon, 141  
 Morgan, L. O., 362  
 Moseley, H. G. J., 81, 256  
 Moseley diagram, 257  
 Motion of the hydrogen nucleus, 190  
 Multiplication factor  $k$ , 371  
 Multiplicity of orbits, 196  
 Multiply periodic systems, 199  
 Murphy, G. M., 194  
  
*n*- $\alpha$  reaction, 324  
*n*- $\gamma$  reaction, 327  
*n*- $p$  reaction, 326  
*n*-2*n* reaction, 327  
 Natural radioactive transformations, 277  
 Neptunium, 360  
 Neutrino, 335  
 Neutron, 58  
     discovery of the, 304  
     magnetic moment of the, 342  
     mass of the, 308, 322  
 Neutrons, delay in emission of, 371  
     disintegrations produced by, 324  
     released in fission, 368  
     resonance capture, 360  
 Newton, I., 16, 86  
 Newton's third law, 16  
 Nier, A. O., 365  
 Normal state of hydrogen, 190  
 Normal Zeeman effect, 92, 240  
     and the vector model, 240  
 Nuclear charge, determination of the, 81  
 Nuclear energy level diagram, 295  
 Nuclear energy, release of, 370  
 Nuclear fission, 358, 360  
     discovery of, 358  
     energy released in, 363  
     neutrons released in, 368  
     products of, 365  
 Nuclear  $g$ -factor, 338  
 Nuclear isomers, 281, 321, 328  
     genetically related, 330  
 Nuclear  $K$ -electron capture, 342  
 Nuclear magnetic moments, 337  
 Nuclear magneton, 337  
 Nuclear model, 331  
 Nuclear particles, 253  
 Nuclear processes and model of the nucleus, 331  
 Nuclear reaction energy, 301  
 Nuclear reaction equation, 300  
 Nuclear reactions,  $\alpha$ - $n$  type, 308  
      $\alpha$ - $p$  type, 302  
     *n*- $\alpha$  type, 324  
     *n*- $\gamma$  type, 327  
     *n*- $p$  type, 326

- Nuclear reactions
  - n-2n* type, 327
  - p- $\alpha$*  type, 317
- Nuclear resonance energy, 334
- Nuclear sizes, 82
- Nuclear spin, 253
  - and nuclear particles, 253
  - quantum number, 254
- Nucleus, 25
  - potential barrier of the, 332
  - radius of the, 82
- Number of electrons per atom, 136
- Oersted, H. C., 13
- Oersted, the, 10, 19
- Ogle, W. E., 346
- Optical spectral series, 213
- Orbital angular momentum, 215
- Orthohelium, 253
- Packing fraction, 60
- Pair production, 314
- p- $\alpha$*  reaction, 317
- Parhelium, 253
- Particles, refraction of, 149
- Paschen series, 190
- Pauli, W., 335
- Pauli's exclusion principle, 224
- Period, half-life, 278
- Periodic table of the elements, 382
- Perlman, M. L., 362
- Permeability, 9
- Perrier, 350
- Perrin, J., 27, 32
- Pfund series, 190
- Photodisintegration, 322
  - threshold for, 323
- Photoelectric effect, 97
- Photoelectrons, velocity of, 98
- Photofission of nuclei, 368
- Photon, 101, 141
  - momentum of a, 141
- Photons, disintegrations produced by, 322
- Physical constants, table of, 379
- Pile, chain reacting, 372
- Planck, M., 3, 100, 101
- Planck constant, the, 100, 379
  - from X-ray spectra, 120
- Plutonium, 361
- Polarization of X rays, 138
- Positive ray analysis, 47
- Positron, discovery of the, 309
- Positrons, emission of, 335
- Potential, 6
  - difference of, 7
  - zero level of, 7
- Potential barrier, 332
- Principal quantum number, 197, 216, 225
- Principal series, 214
  - of sodium, 236
- Principle of equivalence of mass and energy, 60
- Probability concept, 171
- Production of new elements, 349
  - of pairs of charged particles, 344
  - of X rays, 103
- Proper functions, 208
- Proton, 58
  - magnetic moment of the, 342
  - mass of, 59
- Protons, disintegrations produced by, 317
  - distribution-in-range of, 304
- Prout, 46
- Quanta, 101, 141
- Quantum of energy, 101, 141
- Quantum number, angular, 196
  - azimuthal, 196
  - magnetic orbital, 223
  - magnetic spin, 224
  - nuclear spin, 254
  - principal, 197, 216
  - radial, 196
  - spin, 217
- Rabi, I. I., 337, 342
- Radial quantum number, 196
- Radiation from an accelerated charge, 89
- Radiations emitted by radioactive substances, 64
- Radiative capture of neutrons, 361
- Radioactive series, 280
- Radioactive transformations, 277
- Radioactivity, induced, 311
- Radium, 64
- Ramsey, 342
- Range of alpha particles, 283
- Recoil electrons, 141, 144
- Reduced electronic mass, 192
- Refraction, of electrons, 160
  - of particles, 149
  - of particles and waves, 149
  - of waves, 151
  - of X-rays, 124
- Relativity correction, 201
- Relativity theory, 65, 154
- Release of nuclear energy, 370
- Resonance capture of neutrons, 360
- Resonance energy, nuclear, 334
- Resonance potential, 239
- Resonance radiation, 238
- Robinson, H. R., 68, 267, 288

- Rock salt, 116, 131  
   grating space of, 116, 131  
 Röntgen, W. C., 3, 62, 102  
 Rosa, 16  
 Rosenblum, S., 72  
 Rowland, H. A., 13  
 Royds, T., 72  
 Ruled gratings for X rays, 130  
 Russell-Saunders coupling, 219  
 Rutherford, E., 68, 72, 74, 121, 298  
 Rutherford's nuclear theory of the atom,  
   74  
   experimental verification of, 78  
 Rydberg, J. R., 183, 213  
 Rydberg constant, 213, 258  
   dependence of, on mass of nucleus, 193  
   for hydrogen, 183  
  
 Savart, 14  
 Scattered X rays, wave length of, 142  
 Scattering coefficient of X rays, 133, 137  
 Scattering of X rays, 134, 137  
 Schein, M., 353  
 Scherrer, P., 124  
 Schrödinger, E., 173  
 Schrödinger's equation, 173  
   for hydrogen, 207  
 Scintillation method of counting, 70  
 Seaborg, G. T., 350, 361, 362  
 Secondary radiation, 134  
 Segré, E., 350, 351, 367  
 Selection principle, 201  
 Selection rules, 210, 236, 242, 270  
 Sharp series, 214  
   of sodium, 236  
 Shiba, K., 37  
 Shoupp, W. E., 368  
 Single crystal X-ray spectrometer, 115  
 Single scattering of alpha particles, 74  
 Smoluchowski, M., 28  
 Smyth, H. D., 370  
 Snell's law, 149  
 Soddy, F., 47, 281  
 Sodium, energy level diagram for, 235  
   ionization potential of, 236  
   principal series of, 236  
   sharp series of, 236  
   spectrum of, 233  
 Soley, 352  
 Sommerfeld, A., 196, 200  
 Sommerfeld's fine structure constant, 201  
 Source of stellar energy, 357  
 Space quantization, 224  
 Spectra, absorption X-ray, 262  
   characteristic X-ray, 256  
   of two-electron atoms, 250  
  
 Spectral notation, 232  
 Spectral series, optical, 213  
   X-ray, 256  
 Spectrograph, magnetic, 267  
 Spectrum of hydrogen, 183  
   of sodium, 233  
 Spin quantum number, 217  
 Stable isotopes, table of, 385  
 State of the electron, 225  
 Stationary orbits, 186  
 Stellar energy, source of, 357  
 Stenstrom, W., 124  
 Stephens, W. E., 368  
 Stern, O., 165, 248  
 Stern-Gerlach experiment, 248  
 Stokes' law, 37  
 Stopping potential, 99  
 Strassman, F., 359  
 Szilard, L., 368  
  
 Thibaud, J., 348  
 Thomson, G. P., 163  
 Thomson, J. J., 3, 34, 43, 47  
 Thorium series, 280  
 Threshold frequency, 100  
 Threshold for photodisintegration, 323  
 Tolman, R. C., 14  
 Total angular momentum vector, 218  
 Total reflection of X rays, 127  
 Townsend, J. S., 34  
 Tracers, 328, 361  
 Transuranic elements, 359, 360  
  
 Uhlenbeck, G. E., 217  
 Ulrey, C. T., 118  
 Uncertainty principle, 168  
 Unit magnetic pole, 10  
 Units, electrostatic system of, 4  
 Uranium series, 280  
 Urey, H. C., 194  
  
 Van de Graff, R. J., 313  
 Variation of mass with velocity, 65  
 Vector model of the atom, 215  
 Velocities of alpha particles, 72  
 Velocity of photoelectrons, 98  
 Velocity selector, 55  
 Velocity spectrum of alpha particles, 74  
  
 Wahl, A. C., 361, 362  
 Walke, H., 343  
 Walton, E. T. S., 317  
 Wave function, 174  
 Wave length of scattered X rays, 142  
 Wave lengths of gamma rays, 121  
 Wave mechanics applied to hydrogen, 207

Wave-particle parallelism, 154  
 Wave velocity, 155  
 Waves, refraction of, 151  
 Waves associated with matter, 165  
 Wells, W. H., 368  
 Westgren, 33  
 Wheeler, J. A., 364  
 Williams, E. J., 343  
 Wilson, C. T. R., 34  
 Wilson, H. A., 34  
 Wilson cloud chamber, 283, 288  
 Wind, C. H., 103  
 Wood, R. W., 237  
 Work function, 102  
 Wu, C. S., 367  
 Wyman, L. L., 123

X-ray absorption coefficient, 263  
 X-ray absorption limit, 264  
 X-ray critical voltage, 265  
 X-ray energy level diagram, 259  
   for a heavy element, 269  
 X-ray powder crystal diffraction, 122  
 X-ray spectra, 118  
   absorption, 262  
   characteristic, 256  
   continuous, 118  
   *K*-series, 256  
   *L*-series, 256  
 X-ray spectrometer, 115  
 X-ray terms, 268  
   and selection rules, 268  
 X-ray tube, betatron, 105

X-ray tube  
   Coolidge type, 104  
   gas-filled type, 103  
 X-ray wave lengths, measured by crystals, 112  
   measured by ruled gratings, 130  
 X rays, absorption of, 132  
   absorption coefficient of, 133  
   diffraction of, 110  
   discovery of, 102  
   dispersion of, 127  
   mass absorption, coefficient of, 133  
   measurement of intensity of, 109  
   modified line, 144  
   production of, 103  
   "reflection" of, 112  
   refraction of, 124  
   ruled gratings for, 130  
   scattering of, 134  
   total reflection of, 127  
   wave length of scattered, 142

Yield, in nuclear disintegration, 303, 333  
 Young, T., 86  
 Yukawa, H., 353

Zacharias, J. R., 342  
 Zeeman, P., 91  
 Zeeman effect, 91  
   anomalous, 92, 246  
   *e/m* determined from, 95  
   normal, 92  
 Zinn, W. H., 368, 373, 374

